THESIS
4
2007

LIBRARY
Michigan State
University

This is to certify that the
dissertation entitled

NEUROCHEMICAL CHARACTERIZATION OF NIGROSTRIATAL DOPAMINE NEURONAL FUNCTION IN THE 1-METHYL-4-PHENYL-1,2,3,6-TETRAHYDROPYRIDINE (MPTP) MODEL OF PARKINSON'S DISEASE

presented by

Robert E. Drolet

has been accepted towards fulfillment
of the requirements for the

Doctoral degree in Neuroscience

Major Professor's Signature

11/22/2006

Date

MSU is an Affirmative Action/Equal Opportunity Institution

PLACE IN RETURN BOX to remove this checkout from your record.
TO AVOID FINES return on or before date due.
MAY BE RECALLED with earlier due date if requested.

DATE DUE	DATE DUE	DATE DUE

2/05 p:/CIRC/DateDue.indd-p.1

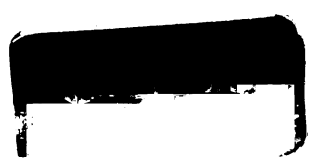

NEUROCHEMICAL CHARACTERIZATION OF NIGROSTRIATAL DOPAMINE NEURONAL FUNCTION IN THE 1-METHYL-4-PHENYL-1,2,3,6-TETRAHYDROPYRIDINE (MPTP) MODEL OF PARKINSON'S DISEASE

By

Robert Edward Drolet

A Dissertation

Submitted to
Michigan State University
in partial fulfillment of the requirements
for the degree of

Doctor of Philosophy

Neuroscience Program

2006

Abstract

NEUROCHEMICAL CHARACTERIZATION OF NIGROSTRIATAL DOPAMINE NEURONAL FUNCTION IN THE 1-METHYL-4-PHENYL-1,2,3,6-TETRAHYDROPYRIDINE (MPTP) MODEL OF PARKINSON'S DISEASE

By

Robert Edward Drolet

The gradual decline in the quality of life for Parkinson's disease (PD) patients is the result of a progressive worsening of motor function. The manifestation and gradual worsening of motor symptoms is due to the progressive loss of nigrostriatal dopamine (NSDA) neurons. Preventing the progressive loss of NSDA neurons therefore, should halt the worsening of motor symptoms. The primary goal of the research conducted in this dissertation was to identify detrimental mechanisms that may contribute to the progressive degeneration of NSDA neurons. The strategy employed was to use a neurotoxin to induce NSDA cell death similar to PD. Pharmacological approaches and neurochemical and immunohistochemical techniques were then used to identify detrimental mechanisms that may cause degeneration of the neurons that survive the initial neurotoxic insult.

The compensatory increase in the activity of neurons that survive neurotoxic insult is one potential mechanism that is likely to contribute to the progressive loss of NSDA neurons because of the consequential increase in exposure to the toxic byproducts derived from DA metabolism. Dissection of the neurochemical events at the axon terminal revealed the dysfunctional regulation of the DA biosynthetic pathway was responsible for the increased metabolism of DA that occurs during compensatory

activation. The rate of DA synthesis was accelerated as a result of increased expression of the rate limiting enzyme tyrosine hydroxylase (TH). The over-activation of DA synthesis, coupled with decreased storage capability, results in increased metabolism of the newly synthesized DA.

The findings from this research suggested that therapeutic strategies that enhance vesicular packaging capability in NSDA axon terminals may not only enhance the release of newly synthesized DA but also protect these neurons from the toxic byproducts that result from DA metabolism. Manipulating the expression of the α-synuclein protein may be one such therapeutic target. In the absence of this protein, NSDA axon terminals are less susceptible to neurotoxic lesion and have enhanced vesicular packaging capability that results in increased storage of the newly synthesized DA and decreased metabolism following a neurotoxic lesion. Taken together, the results from the studies described in this dissertation have: 1) identified and characterized the dysfunctional regulation of the DA biosynthetic pathway as a potential mechanism responsible for the progressive loss of NSDA neurons in PD, 2) clarified the role that the α-synuclein protein in NSDA neuronal demise and 3) identified a number of potential therapeutic targets that may ultimately slow or halt the progressive nature of PD.

This dissertation and all of the work that it is comprised of, is dedicated to my wife Alexis, without your continual support, guidance and encouragement this would not have been possible,

and to my daughter Laynie, I look forward to the day I make you to read this.

Acknowledgements

Mom and Dad, I could not have accomplished this without you. Thank you for the support and encouragement throughout the years.

I sincerely thank my advisors Drs. John L. Goudreau and Keith J. Lookingland for their help and guidance. I cannot convey how much I appreciate your dedication, constructive criticism and motivation regarding my scientific training over the past few years. I look forward to the years of collaboration in the future.

I would also like to thank the members of my guidance committee, Drs. Kathleen Gallo, Puliyur MohanKumar, and Hongbing Wang for their thoughtful advice and critique in the preparation of this work.

I wish to thank the Neuroscience program faculty and students for guiding my scientific development and providing an excellent training atmosphere here at MSU.

Last, but certainly not least, to the members of the lab, I hope you realize how important your friendship and scientific feedback has been over the past few years. All of you have made this a truly amazing graduate school experience. What a long, strange trip it has been.

Table of Contents

List of Tables

List of Figures

List of Abbreviations

6-OHDA	6-hydroxydopamine
AADC	L-Aromatic amino acid decarboxylase
AD	Aldehyde dehydrogenase
AMT	Alpha-methylparatyrosine
Ca^{+2}	Calcium
CamPKII	Ca2+–calmodulin-dependent protein kinase
Complex I	Nicotinamide adenine dinucleotide (NADH)-ubiquinone reductase
DAT	Dopamine transporter
DOPA	Dihydroxyphenylalanine
DOPAC	Dihydroxyphenylacetic acid
DOPAL	Dihydroxyphenylacetaldehyde
GPe	Globus pallidus external segment
GPi	Globus pallidus internal segment
GSH	Glutathione
H_2O_2	Hydrogen peroxide
HPLC-EC	High performance liquid chromatography with electrochemical detection
LNAA	Large neutral amino-acid transporter
MAO	Monoamine oxidase
Mito	Mitochondria
MLDA	Mesolimbic dopamine
MPDP	1-Methyl-4-phenyl-2,3-dihydropyridinium
MPP^+	1-Methyl-4-phenyl pyridinium

MPTP	1-Methyl-4 phenyl-1,2,3,6 tetrahydropyridine
NADH	Nicotinamide adenine dinucleotide
NSDA	Nigrostriatal dopamine
O_2^-	Superoxide
OH^-	Hydroxyl radical
$OONO^-$	Peroxinitrate
PD	Parkinsons's disease
PKA	cAMP-dependent protein kinase A
PKC	Ca2+–calmodulin-dependent protein kinase
RDU	Relative density unit
ROS	Reactive oxygen species
SEM	Standard error of the mean
SNpc	Substantia nigra pars compacta
STN	Subthalamic nucleus
TH	Tyrosine hydroxylase
TIDA	Tuberoinfundibular dopamine
UPS	Ubiquitin proteosome system
VL	Ventral lateral thalamic nucleus
VMAT-2	Vesicular monoamine transporter

Chapter 1. General Introduction

A. Statement of Purpose

Parkinson's disease (PD) is a chronic, progressive, neurodegenerative disorder that is diagnosed clinically by the development of motor abnormalities. The manifestation of motor symptoms is attributed to the primary pathological hallmark of the disease, the degeneration of nigrostriatal dopamine (NSDA) neurons. Interestingly, motor symptoms do not appear until approximately 50% of NSDA neurons have degenerated. Therefore, at the time of clinical diagnosis there is already extensive damage to the NSDA system. Throughout the disease process, the remaining 50% of these neurons will progressively degenerate causing a gradual worsening of motor symptoms ultimately resulting in patient disability and death. To this end, a primary therapeutic goal for treating PD is to halt or delay the progressive degeneration of NSDA neurons. The task has been hindered by a lack of understanding of what contributes to the progressive demise of these neurons.

The overall aim of the research that comprises this dissertation is to identify mechanisms that contribute to the progressive degeneration of NSDA neurons. The research described herein utilizes pharmacological, neurochemical and immunohistochemical approaches to test the hypothesis that the initial death of NSDA neurons causes compensatory increases in the activity of surviving neurons and the sustained increase in activity contributes to the progressive, secondary death of NSDA neurons in PD. If this hypothesis is true, then novel therapeutic targets can be identified to prevent prolonged, compensatory increases in neuronal activity to inhibit secondary, progressive NSDA death in PD.

B. Parkinson's Disease

PD is a major source of disability and death for people over the age of sixty. PD incidence rates for people under 60 are 10/100,000, but rise dramatically to 40/100,000 for people 60-69 years of age and over 100/100,000 for people seventy and over (Mayeux et al., 1995; Fall et al., 1996; Bower et al., 1999; Chen et al., 2001). The prevalence rates (or number of people affected by the disease) also dramatically increase from 99/100,000 under the age of 60 to 1193/100,000 for people seventy and older (Mayeux et al., 1995). The cause of PD is unknown and currently there is no preventative or curative therapy available for the millions of people living with the disorder. Taken together, it is not surprising that there is a tremendous research effort to understand the pathogenesis of PD and develop effective therapeutic strategies for the treatment of this disorder.

The clinical symptoms of PD were originally described in 1817 by James Parkinson in his essay "The Shaking Palsy" (Parkinson, 1817). The disease is characterized clinically by the development of cardinal motor symptoms that include; resting tremor in the distal limbs, bradykinesia, rigidity, and postural instability. Disturbances in facial expression, sleep, speech, chewing and gut motility are also common(Borek et al., 2006). Traditionally, symptoms are initially mild and more of an inconvenience for the patient rather than a significant source of disability. However, over time, the symptoms will gradually become more severe, affect greater areas of the body and become a major source of disability, eventually resulting in death. The average life-span of a patient from time of diagnosis to time of death is 11 ± 2 years (Birkmayer, 1974). The progressive worsening of PD symptoms is a distinguishing feature of the

disease that warrants additional research in order to identify the underlying pathogenic mechanisms responsible for the disability and death of millions of people.

C. Pathophysiology of PD Motor Symptoms

The Loss of Nigrostriatal Dopamine Neurons is the Pathological Hallmark of PD

The earliest report of a distinct pathological hallmark to accompany the clinical features of PD came in 1895 when Blocq and Marinesco described the loss of pigmented cells in the substantia nigra pars compacta (SNpc) of human PD patients (Alvord, 1987). Subsequently, neuroanatomical track tracing studies identified projections from the pigmented cells in the SNpc to the corpus striatum (Rosegay, 1944). Dopamine (DA) was determined to be a neurotransmitter proper, and moreover, the principle neurotransmitter of nigrostriatal projections (Bertler, 1959a, 1959b; Carlsson, 1959). In PD patients the loss of pigmented SNpc cells corresponds to a dramatic loss of striatal DA (Ehringer, 1960; Hornykiewicz, 1963). Moreover, there is a strong correlation between NSDA neuronal loss and severity of PD symptoms (Hornykiewicz, 1972). Finally, the motor complications associated with the disease can be alleviated by strategies that restore brain DA concentrations (Hornykiewicz, 1975). It is now well accepted that the specific loss of NSDA neurons is the primary pathology responsible for the development of PD motor symptoms.

NSDA Neurons are a part of the Basal Ganglia Motor System

As depicted in Figure 1-1, NSDA neurons (A8/A9) reside in the midbrain (Figure 1-1) and project axons to through the medial forebrain bundle to the forebrain where they

terminate in the striatum (Figure 1-2) (Rosegay, 1944; Anden, 1964; Dahlstrom and Fuxe, 1964; Moore et al., 1987). The release of DA into the striatum plays a critical role in regulating the activity of the basal ganglia. The basal ganglia are comprised of subcortical nuclei including the striatum (caudate nucleus and putamen), globus pallidus (internal and external segments) and subthalamic nucleus (Bergman, 1998). Connections between these subcortical nuclei serve as a critical processing loop for signals relayed from the motor cortex to the ventral lateral thalamus (VL) and back to the motor cortex that allows descending output from the primary motor cortex to be focused onto a particular set of muscles required to perform a specific task (Kaji, 2001). Primary output neurons in the motor cortex descend in the corticospinal tract and synapse directly onto motor neurons in the spinal cord that reside in layers VIII and IX of the ventral horn. Motor neurons that innervate proximal muscles are located in the medial portion of the ventral horn, while motor neurons that innervate distal muscles that control limb movement are located in the lateral portion of the ventral horn (Kandel, 1991).

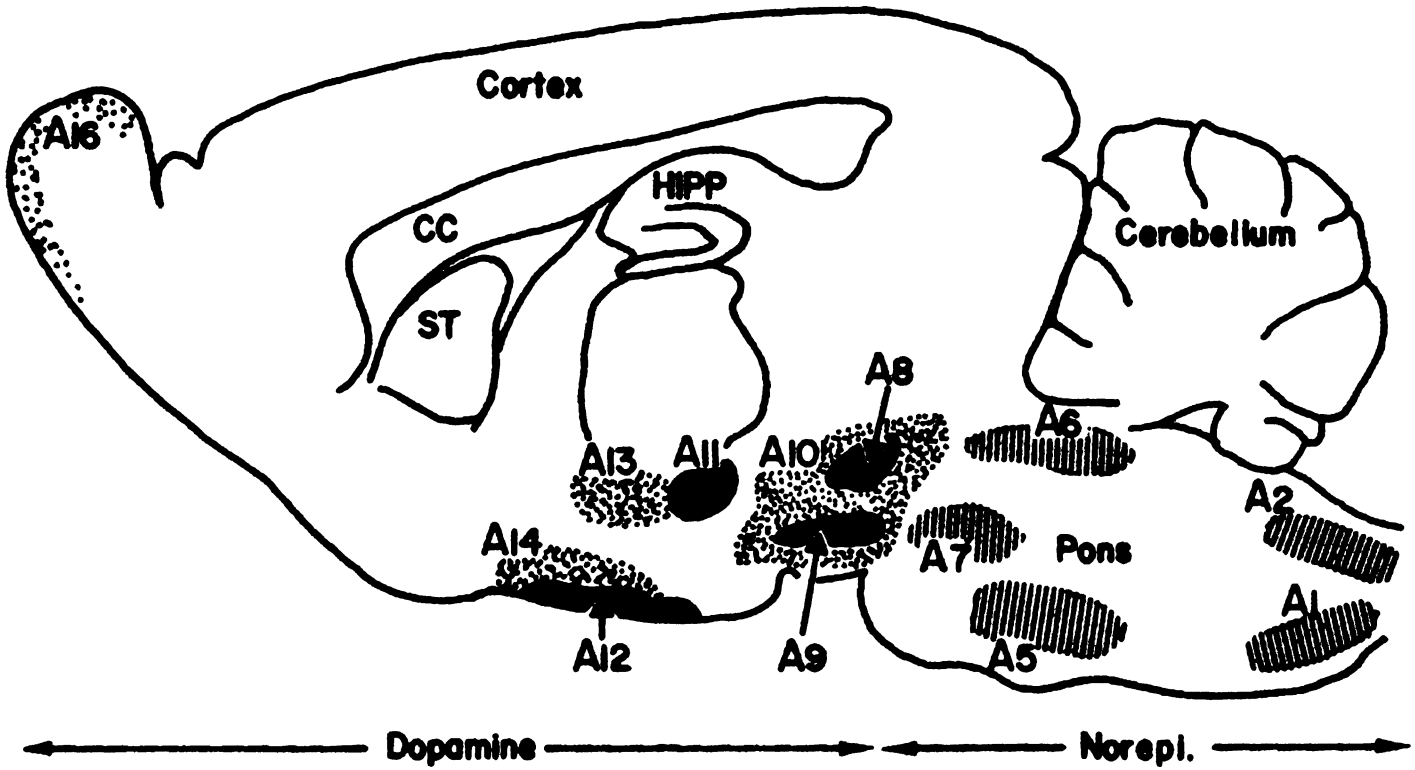

Figure 1-1. Schematic sagittal view of the rat brain depicting catecholamine nuclei distribution. A1-A7 are norepinehrine neurons, A8-A16 are dopaminergic neurons. Abbreviations: CC corpus collosum; HIPP hippocampus; ST striatum; Norepi norepinephrine (Dahlstrom and Fuxe 1964; Moore et al. 1987).

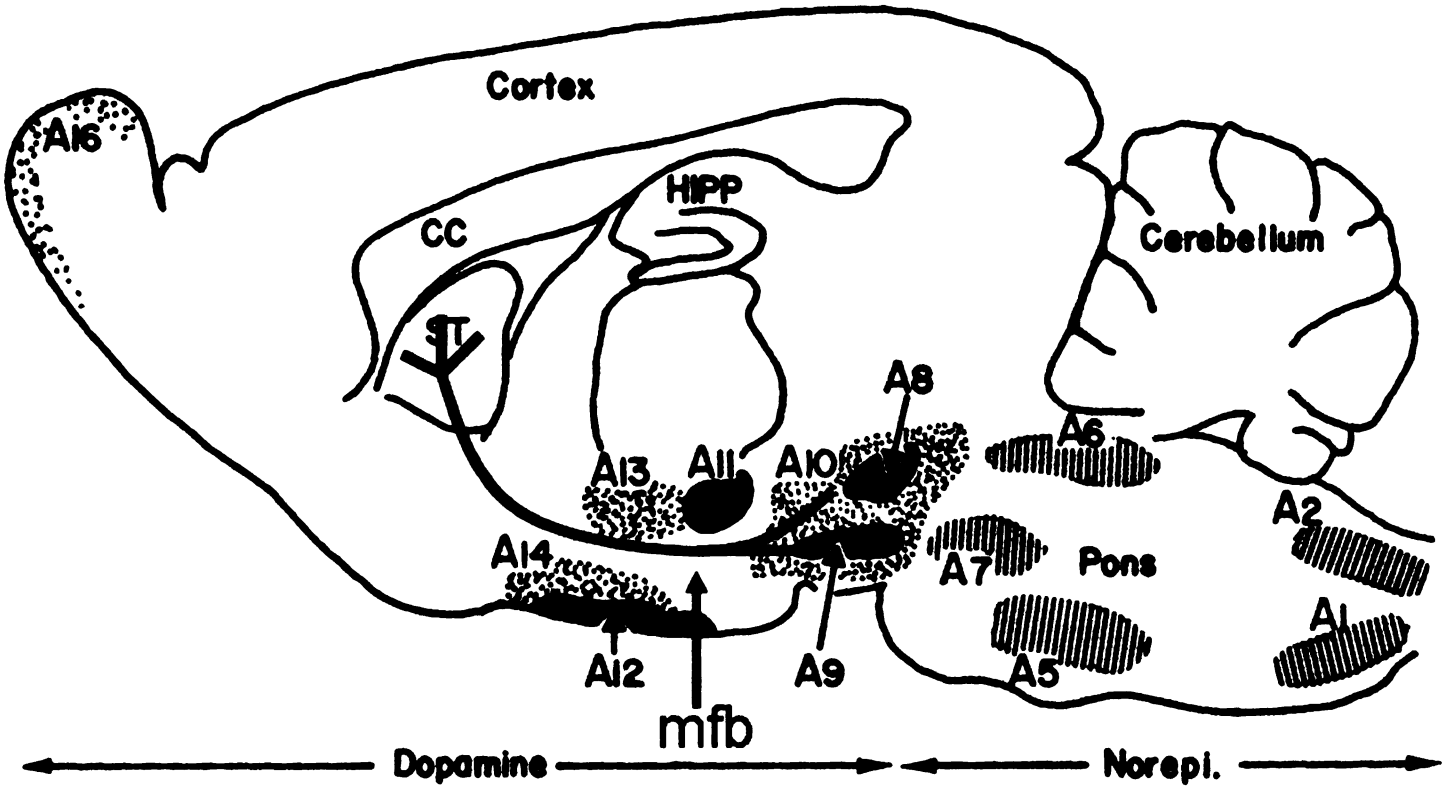

Figure 1-2. Schematic sagittal view of the rat brain depicting A8/A9 DA neuron projections. Abbreviations: mfb medial forebrain bundle (Dahlstrom and Fuxe 1964; Moore et al. 1987).

Cortical input to the basal ganglia can be processed through one of two primary basal ganglia circuits before being relayed to the VL thalamic nucleus, the direct or the indirect pathway (Figure 1-3). In the direct pathway, excitatory cortical input to the striatum increases firing of striatal medium spiny GABA neurons. Increased firing of striatal GABA neurons inhibits the firing of GABA neurons in the globus pallidus internal segment (GPi). Decreased GPi firing results in a disinhibition of glutamate neurons in the VL thalamic nucleus. Increased firing of neurons in the VL thalamic nucleus increases excitatory input back to the motor cortex (Parent and Hazrati, 1993; Herrero et al., 2002). Excitation of motor cortex neurons increases excitatory corticospinal output to primary motor neurons in the spinal cord, which facilitates muscle movement. Thus, excitation of the direct pathway reinforces subsequent cortical activity and facilitates the execution of voluntary movement.

In contrast to the direct pathway, cortical signals projected to indirect pathway medium spiny GABA neurons are first relayed to GABA neurons in the globus pallidus external segment (GPe) and then to glutamate neurons in the subthalamic nucleus (STN) before being sent to the GPi. The shunting of information from the striatum through the GPe and STN changes the net effect of basal ganglia output such that diminished STN firing decreases the firing of glutamate neurons in the VL thalamic nucleus. Inhibition of VL neuronal firing diminishes excitatory input back to the motor cortex and decreases the activity of neurons in the motor cortex, thus, reducing corticospinal output to primary motor neurons in the spinal cord and prohibiting muscle movement (Parent and Hazrati, 1993; Herrero et al., 2002). Therefore, the direct and indirect pathways have opposing

actions and balance between these pathways is critical for coordinating muscle movement.

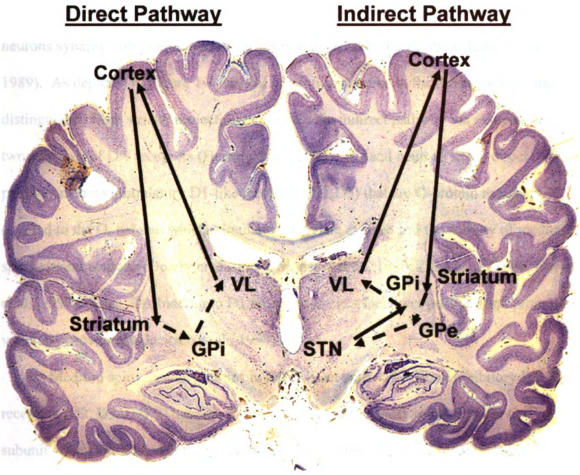

Figure 1-3. (Left side of brain) Coronal section of a human brain depicting the circuitry of the basal ganglia direct pathway. (Right side of brain) Coronal section of a human brain depicting the circuitry of the basal ganglia indirect pathway. Glutatmatergic excitatory connections are shown as solid lines. GABAergic inhibitory connections are shown as dashed lines. Abbreviations: VL ventral lateral thalamic nucleus, GPi globus pallidus internal segment, GPe globus pallidus external segment, STN subthalamic nucleus. Images in this thesis/dissertation are presented in color.

NSDA Neurons Regulate Basal Ganglia Motor Processing

Both the direct and indirect pathways are regulated by NSDA neurons. NSDA neurons synapse onto medium-spiny projection neurons in the striatum (Lavoie et al., 1989). As depicted in Figure 1-4, striatal projection neurons in the direct pathway are distinguished from striatal projection neurons in the indirect pathway via expression of two subtypes of DA receptors (Herrero et al., 2002). Striatal neurons in the direct pathway express stimulatory D1-like receptors (D1,D5) that are G-protein receptors coupled to the G_s subunit which stimulates adenylate cyclase and the activity of medium spiny striatal neurons (Dearry et al., 1990; Monsma et al., 1990; Zhou et al., 1990; Herve et al., 1993). Thus, DA binding to D1 receptors excites the direct pathway and promotes voluntary movement (Jackson et al., 1994).

Medium spiny striatal neurons in the indirect pathway express inhibitory D2-like receptors (D2, D3, D4). These are G-protein coupled receptors coupled to the $G_{i/o}$ subunit which inhibits adenylate cyclase activity and the activity of medium spiny projection neurons (Onali et al., 1985). Thus, DA binding to D2 receptors inhibits the indirect pathway. Since the indirect pathway inhibits voluntary movement, DA binding to D2 receptors in effect promotes voluntary movement (Jackson and Westlind-Danielsson, 1994). Therefore, DA released by NSDA neurons terminating in the striatum promotes voluntary movement regardless of which DA receptor it binds (Wooten, 1997).

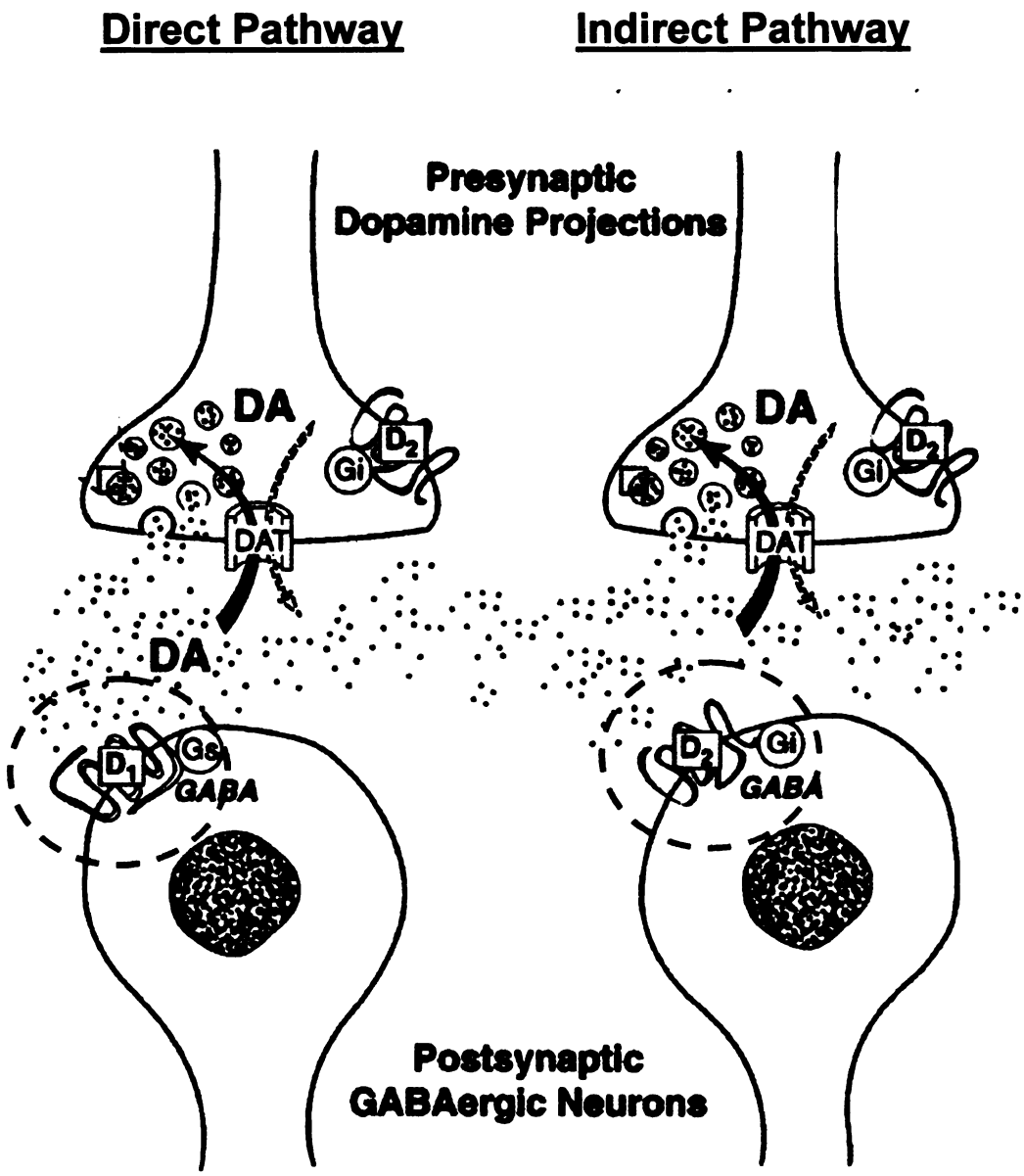

Figure 1-4. Expression of DA receptor subtypes distinguishes post-synaptic medium spiny GABAergic neurons in the direct pathway (Left Panel) from the indirect pathway (Right Panel). Striatal neurons in the direct pathway express stimulatory (Gs-coupled) D1-like receptors. Medium spiny striatal neurons in the indirect pathway express inhibitory (Gi-coupled) D2-like receptors. D2 receptors are also expressed by the pre-synaptic NSDA neurons. Abbreviations: DAT=dopamine transporter. (Missale et al., 1998).

Basal Ganglia Dysfunction in PD

In a simplified model of basal ganglia function, the loss of NSDA neurons decreases DA binding to D1 and D2 receptors on medium spiny GABA neuron in the striatum. This results in decreased direct pathway activation and increased activation of the indirect pathway. The effect of the imbalance between these pathways is a reduction in excitatory thalamic-cortical neurotransmission and diminished firing of motor cortex output neurons. Inhibition of motor cortex projections inhibits firing of primary motor neurons found in the spinal cord, thus reducing activation of peripheral muscles and prohibiting voluntary movement. Decreased voluntary movement in the limbs can explain the characteristic slowness of movement (bradykinesia) and loss of movement fluidity (rigidity) that are hallmarks of PD. Postural instability is thought to reflect inhibition of primary motor neurons in the medial ventral horn of the spinal cord which innervate proximal muscles that stabilize the trunk against unwanted directional movement. The manifestation of resting tremor is more complex.

Tremor is defined as the involuntary rhythmic oscillation of a body region that is produced by alternating contractions of reciprocally innervated muscles (Zesiewicz and Hauser, 2001). Interestingly, resting tremor in PD patients poorly correlates with NSDA damage (Otsuka et al., 1996), suggesting that tremor is not the direct result of DA cell loss. However, recent evidence suggests that abnormal activity of the STN and globus pallidus due to NSDA neuron loss is responsible for tremor manifestation. Under normal conditions, when there is sufficient DA input into the basal ganglia, STN and the pallidal firing rates fire at approximately 70 Hz. However, in untreated PD patients firing rates between these nuclei synchronize at much lower frequencies (4-8 Hz). Synchronization

directly corresponds to the very uniform 4-8 Hz limb tremor that occurs in PD patients (Brown, 2001). In fact, 4-8 Hz STN discharge is time-locked to the EMG-determined 4-8 Hz tremor in the hand (Krack et al., 1998; Rodriguez et al., 1998).

L-DOPA therapy, that restores brain DA concentrations, or deep brain stimulation of the STN or GPi eliminates low frequency STN-globus pallidus synchronization and alleviates tremor (Lozano et al., 1995; Burchiel et al., 1999). Additionally, lesions of the non-human primate SNpc results in a dramatic shift to 4-8 Hz synchronization between GPi and STN and tremor manifestation (Bergman, 1994). Thus, a critical role for NSDA neurons may be preventing low-frequency synchronization between basal ganglia nuclei. In the absence of NSDA neuronal function rhythmic low frequency (4-8 Hz) firing of the motor cortex output neurons would cause activation of primary motor neurons in the spinal cord, rhythmic excitation of reciprocally innervated muscles in the hand, and tremor.

NSDA neuronal loss can cause dysfunction of basal ganglia motor information processing which accounts for the manifestation of the cardinal motor complications associated with PD. Therefore, it is reasonable to conclude that preventing the progressive degeneration of NSDA neurons will avert the continued decline in basal ganglia function and the gradual worsening of PD symptoms.

D. Progressive Loss of NSDA Neurons in PD

The gradual worsening of PD symptoms closely corresponds to the progressive loss of NSDA neurons (Hornykiewicz, 1972; Bernheimer et al., 1973). The rate of NSDA cell loss in a PD patient is approximately 4.5% per year (Fearnley and Lees, 1991). Accordingly, the rate of NSDA axon terminal loss has been estimated at approximately 5-10% per year using several different indices to quantify axon terminal number (Riederer and Wuketich, 1976; Morrish et al., 1998; Pirker et al., 2003; Au et al., 2005; Hilker et al., 2005). As depicted in Figure 1-5, the rate of NSDA neuronal loss in a PD patient over the 11 year average time course of the disease (Birkmayer, 1974), is greatly accelerated when compared to the 0.45% per year rate of NSDA neuronal loss observed in healthy age-matched controls (Riederer and Wuketich, 1976).

NSDA neuronal number is depleted to approximately 50% of controls at the time of symptom onset (Fearnley and Lees, 1991). It is not known if the initial 50% loss of NSDA neurons follows a similar linear progression, however if a linear slope is assumed then a pre-clinical period of 5-10 years can be predicted. Regardless, the progressive nature of PD can be attributed to an exponential loss of NSDA neurons that appears to begin several years before motor abnormalities arise. Symptom onset likely occurs when DA input to the basal ganglia decreases below a threshold point, when activation of the inhibitory indirect pathway outweighs activation of the excitatory direct pathway. This would decrease excitation of the VL thalamic nucleus and inhibit motor cortical activity. Thus, cortical output to the corticospinal tract would decrease, ultimately reducing voluntary movement in the peripheral muscles. The research described in this dissertation was conducted to identify mechanisms that contribute to the progressive

degeneration of NSDA neurons. The research strategy employed was to utilize neurochemical, immunohistochemical, and pharmacological techniques to compare NSDA neurophysiology under basal conditions and during conditions that recapitulate PD to identify pathogenic mechanisms that could contribute to the progressive loss of these neurons.

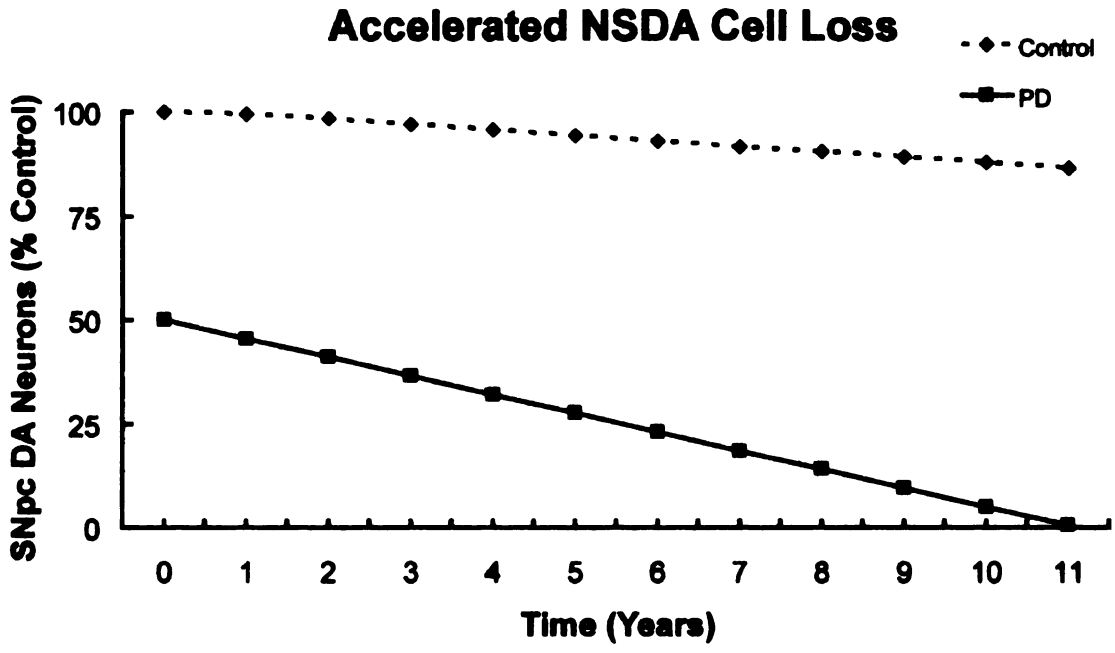

Figure 1-5. The rate of NSDA neuronal loss in the general population and PD patients shown as a percentage of age-matched controls. The loss of NSDA neurons over time in healthy controls (dashed line) is approximately 0.45% per year as determined by numbers of SNpc dopamine neurons at autopsy. In PD patients (solid line) there is an accelerated loss of NSDA neurons of approximately 4.5% per year (Fearnley and Lees, 1991).

E. NSDA Neurophysiology

NSDA Neurochemistry

The primary function of NSDA neurons is to regulate the activity of the basal ganglia. This function is depenent upon maintenance of DA synthesis, storage, release, reuptake and metabolism (Figure 1-6). DA synthesis begins with the uptake of dietary tyrosine into the axon terminal via the large neutral amino-acid transporter (Oxender and Christensen, 1963; Oldendorf and Szabo, 1976; Palacin et al., 1998). Cytoplasmic tyrosine in the axon terminal is then converted to dihydroxyphenylalanine (DOPA) by cytoplasmic tyrosine hydroxylase (TH), the rate limiting enzyme in catecholamine synthesis (Levitt et al., 1965; Kumer and Vrana, 1996). DOPA is decarboxylated to DA by L-aromatic amino acid decarboxylase (AADC) (Kumer and Vrana, 1996). Newly synthesized DA is packaged into synaptic vesicles by the vesicular monoamine transporter-2 (VMAT-2). Additionally, newly synthesized DA that is not packaged into vesicles, can be degraded to dihydroxyphenylacetic acid (DOPAC) through a two-step reaction catalyzed by mitochondrial monoamine oxidase (MAO). Cytoplasmic DA inhibits the activity of TH via end-product inhibition (Okuno and Fujisawa, 1985; Andersson et al., 1988; Haavik et al., 1991).

Action potential-induced Ca^{+2} entry into the axon terminal triggers the release of vesicular DA into the synaptic cleft. DA released into the synapse can bind to either post-synaptic D1 or D2 receptors, or pre-synaptic D2 autoreceptors. Activation of pre-synaptic D2 autoreceptors inhibits further DA synthesis and release (Christiansen and Squires, 1974; Roth, 1975). Synaptic DA is removed via the high-affinity reuptake DA transporter (DAT) which recaptures a vast majority of synaptic DA (Kilty et al., 1991).

Recaptured DA can either be repackaged into synaptic vesicles for reuse, or metabolized to DOPAC by mitochondrial MAO and aldehyde dehydrogenase (AD).

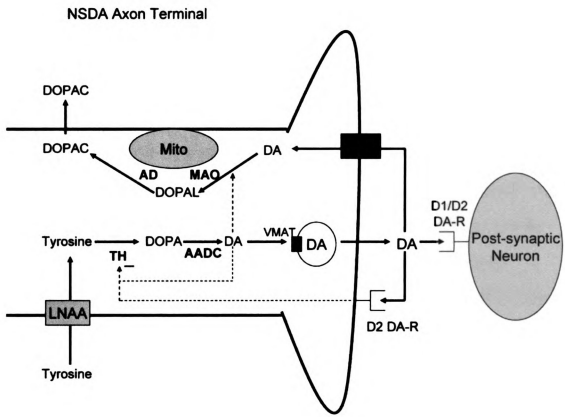

Figure 1-6. Schematic diagram depicting the neurochemical events in a NSDA axon terminal. Tyrosine is taken up into the axon terminal by the large neutral amino-acid transporter (LNAA). Tyrosine is then converted to DOPA by tyrosine hydroxylase (TH). DOPA is decarboxylated to DA by L-aromatic amino-acid decarboxylase (AADC). Newly synthesized DA is packaged by vesicular monoamine transporter-2 (VMAT) into synaptic vesicles for release. Alternatively, newly synthesized DA can be degraded by mitochondrial (Mito) MAO or feedback to inhibit TH activity. DA released into the synapse can bind to post-synaptic D1 or D2 receptors (DA-R) or D2 autoreceptors (D2-R). Synaptic DA is removed via the DAT. Recaptured DA can be repackaged into synaptic vesicles or degraded by MAO and aldehyde dehydrogenase (AD) to DOPAC. DOPAC is removed from the axon terminal through diffusion.

The Role of DA Metabolism in NSDA Neurons

It is critical that NSDA neurons tightly regulate DA synthesis, storage, release and reuptake because byproducts of DA metabolism are toxic to neurons and may contribute to the progressive degeneration of NSDA neurons in PD (Graham, 1978; Graham et al., 1978; LaVoie and Hastings, 1999b, 1999a; Perez and Hastings, 2004). As depicted in Figure 1-7, DA oxidation by mitochondrial MAO results in the formation of dihydroxyphenylacetaldehyde (DOPAL) which is a highly toxic metabolite (Burke et al., 2004; Legros et al., 2004; Ebadi et al., 2005). As such, the activity of AD is normally sufficient to quickly convert DOPAL to DOPAC, a less toxic species. However, mitochondrial impairment or AD inhibition leads to the accumulation of DOPAL in DA neurons. Also, AD inhibition exacerbates neurotoxicity induced by mitochondrial inhibition in DA neurons (Lamensdorf et al., 2000), suggesting that this DA metabolite can directly decrease neuronal viability.

The enzymatic conversion of DOPAL to DOPAC also produces reactive oxygen species (ROS, Figure 1-6). ROS can cause oxidative damage to neurons by reacting with lipids, protein or DNA, and ultimately causing cell death. The conversion of DOPAL to DOPAC by AD results in the formation of a hydrogen peroxide molecule (H_2O_2). H_2O_2 can react with Fe^{+2} to produce the neurotoxic hydroxyl radical (OH^-) through a reaction known as the Fenton reaction.

Cytoplasmic DA can also undergo non-enzymatic auto-oxidation which produces ROS. In this case, the catecholamine ring of DA is oxidized resulting in the formation of a DA-quinone molecule, superoxide (O_2^-) and H_2O_2 radicals. In addition to the H_2O_2-mediated OH^- generation, the O_2^- radical can interact with nitric oxide to form

peroxynitrite ($OONO^-$) a free radical that causes substantial oxidative damage to intracellular proteins and lipids. The DA-quinone molecule, formed from DA auto-oxidation, can also cause neuronal dysfunction. DA-quinones have an affinity for cysteine residues on proteins, and bind to these residues causing covalent protein modification and loss of function of intracellular proteins (LaVoie and Hastings, 1999b).

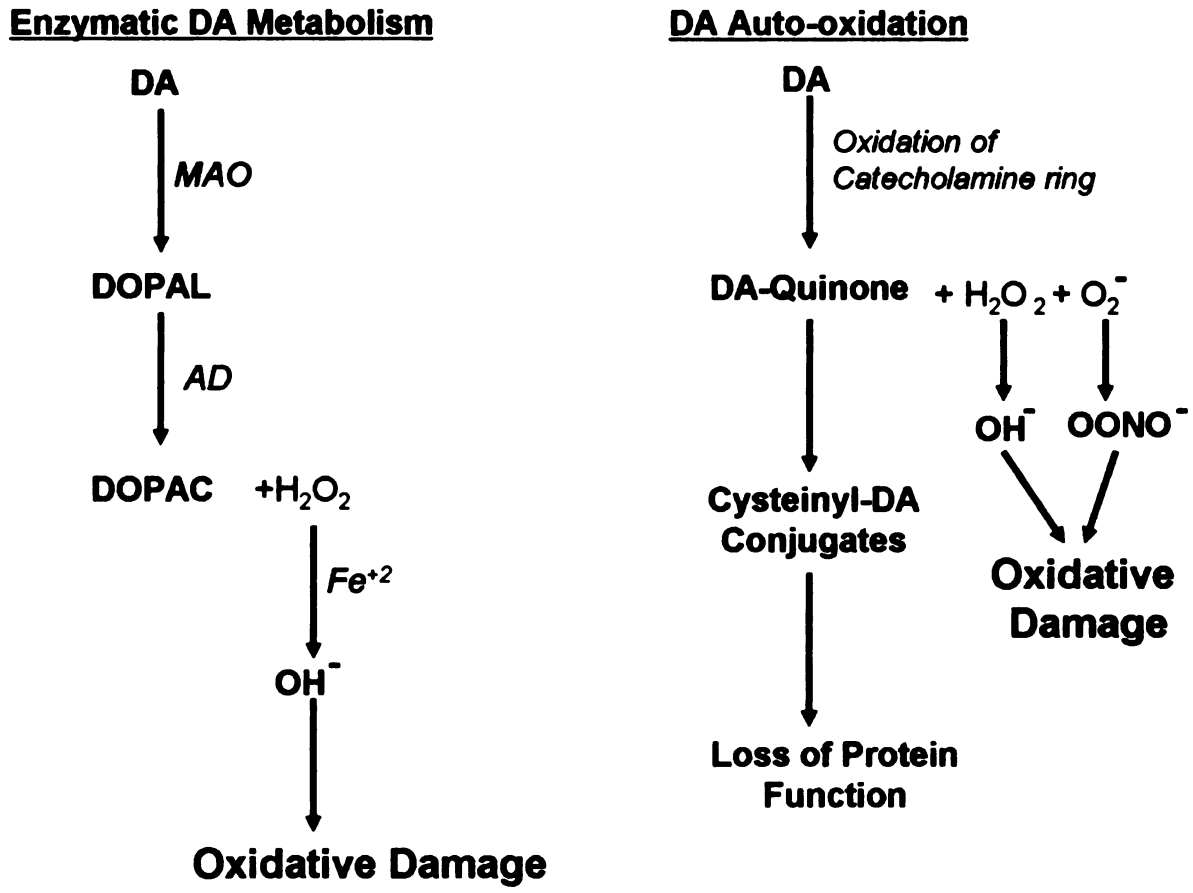

Figure 1-7. DA enzymatic (left) and non-enzymatic (right) metabolic pathways. The enzymatic metabolism of DA results in the formation of DOPAC and a hydrogen peroxide (H_2O_2) molecule. H_2O_2 can be scavenged by glutathione (GSH) or react with iron to form hydroxyl radical (OH^-) through the Fenton reaction (Dringen et al., 2000). DA auto-oxidation results in the formation of DA-quinone molecules and the reactive oxygen species H_2O_2 and superoxide (O_2^-). H_2O_2 can produce OH^- while O_2^- can react with nitric oxide to form peroxynitrite ($OONO^-$). ROS cause oxidative damage by reacting with lipids, DNA and proteins, and may ultimately result in neuronal death.

intrac

antiox

donat

less to

Gluta

al., 20

GSH r

requir

capaci

form o

oxidati

of PD.

their ab

either e

DOPAL

neurons

release a

byprodu

Neurons are protected from ROS-induced oxidative damage by endogenous intracellular antioxidant proteins that scavenge free radicals. Glutathione is the primary antioxidant defense protein in neurons (Cooper and Kristal, 1997). Glutathione (GSH) donates an electron to free radicals (O_2^-, OH^-, $OONO^-$ and H_2O_2) reducing the ROS to a less toxic molecule, but consequently oxidizing glutathione to glutathione disulfide. Glutathione disulfide can be converted back to GSH by glutathione reductase (Dringen et al., 2000). However, GSH also participates in non-enzymatic reactions, whereby the GSH molecule is consumed in the reaction. In this case, *de novo* protein synthesis is required to replenish depleted levels of GSH.

If ROS formation increases and overwhelms antioxidant proteins or if antioxidant capacity decreases, ROS can accumulate in neurons and cause oxidative damage in the form of lipid peroxidation, macromolecular damage and protein dysfunction. If the oxidative damage is severe, it can cause neuronal death. This is important in the context of PD, because GSH levels are depleted in NSDA neurons of PD patients, suggesting their ability to manage ROS is compromised (Jenner and Olanow, 1996). Taken together, either enzymatic or non-enzymatic DA metabolism can produce ROS, the toxic aldehyde DOPAL, and DA-quinone molecules that can cause intracellular damage to NSDA neurons through a number of mechanisms. Thus, the regulation of DA synthesis, storage, release and reuptake is critical to controlling DA metabolism and formation of toxic byproducts.

F. NSDA Physiology in PD

There is considerable evidence to suggest that the regulation of DA homeostasis is dysfunctional in early PD. At the time of clinical diagnosis there is a loss of approximately 50% of SNpc neurons and 70-80% of striatal DA axon terminals (Bernheimer et al., 1973; Hornykiewicz, 1975; Fearnley and Lees, 1991; Hornykiewicz, 1998). Interestingly, the clinical symptoms of the disease do not appear until there is already an extensive loss of NSDA neurons. The delayed appearance of motor complications is thought to reflect compensatory changes in the activity of surviving neurons that maintains DA output at the near control levels, thus upholding the balance between direct and indirect basal ganglia pathways (Zigmond, 1997). Evidence from both human PD patients and animal models of NSDA damage support this hypothesis.

Positron emission tomography (PET) using 6-[^{18}F]-fluoro-L-dopa (F-DOPA) provides an *in vivo* index of the rate of DA synthesis and release in patients with PD. F-DOPA imaging can be used as a reliable estimate of the rate of DA synthesis by quantifying the conversion of F-DOPA to [^{18}F]-DA by AADC and its subsequent storage into synaptic vesicles (Patlak et al., 1983; Vingerhoets et al., 1994; Vingerhoets et al., 1996). Measuring the rate of decline in striatal [^{18}F]-DA is an index of the rate of DA release and thus NSDA neuronal activity (Barrio et al., 1990; Pate et al., 1993; Yee et al., 2001). F-DOPA imaging studies have demonstrated that early in PD, there is a compensatory increase in the rate of DA synthesis and release in residual NSDA neurons (Ribeiro et al., 2002; Sossi et al., 2002). Post-mortem neurochemical studies have supported this hypothesis. DA neuronal activity is defined neurochemically by the ratio of the DA metabolite, DOPAC to stored DA and is a reliable index of the rate of DA,

release, reuptake and metabolism (Westerink and Spaan, 1982; Gopalan et al., 1993). There is an increase in NSDA neuron activity, as defined by the DOPAC to DA ratio in post-mortem PD patients that died during the early stages of the disease (Hornykiewicz, 1975; Lloyd et al., 1975; Ribeiro et al., 2002; Sossi et al., 2002; Sossi et al., 2004).

Animal studies have supported *in vivo* imaging and post-mortem neurochemical data obtained in humans. Neurotoxin-induced partial lesions of the NSDA pathway increase the activity of surviving neurons, as reflected by an increased DOPAC to DA ratio (Hornykiewicz, 1975; Zigmond and Stricker, 1984; Zigmond et al., 1990; Hornykiewicz, 1998; Thiffault et al., 2000). Microdialysis experiments, which provide a more direct measurement of DA release demonstrate that synaptic DA concentrations are maintained at near normal levels despite the loss of axon terminals (Zigmond and Stricker, 1984; Stachowiak et al., 1987; Snyder et al., 1990). While decreased DA clearance may be partially responsible for increased synaptic DA, pre-synaptic changes that enhanced stimulus-evoked DA release also occur (McCallum et al., 2006). Thus, partial lesions of the NSDA pathway cause compensatory changes that increase DA synthesis, release, reuptake and metabolism in surviving neurons that is associated with delaying the onset of PD motor symptoms.

Compensatory increases in DA synthesis and release are likely beneficial in delaying symptom onset in PD, however, due to the toxic nature of DA metabolism, it is also possible that prolonged increases in DA synthesis, release, reuptake and metabolism results in increased exposure to DOPAL, $OH^{\cdot}$, $O_2^{\cdot}$ and DA-quinone molecules (Figure 1-7). Thus, ROS-induced oxidative stress and DA-quinone-induced covalent protein modification, derived from sustained increases in DA metabolism, may contribute to the

progressive degeneration of NSDA neurons in PD. Consistent with this hypothesis, several studies suggest that ROS damage, decreased antioxidant defense, and mitochondrial impairment play key roles in the pathogenesis of PD. There is extensive ROS-mediated damage in the striatum of post-mortem PD brains, reflected by high levels of lipid peroxidation and protein carbonyls, an index of oxidative damage (Dexter et al., 1989; Dexter et al., 1994; Yoritaka et al., 1996). Additionally, there is a specific decrease in GSH content in the SNpc of PD patients, suggesting the ability of NSDA neurons to scavenge the free radicals generated by DA metabolism is compromised (Sofic et al., 1992; Sian et al., 1994). Finally, mitochondrial complex I deficits have been reported in the SNpc of PD patients (Schapira et al., 1990; Swerdlow et al., 1996). Mitochondrial deficits could result in NSDA damage due to bioenergetic deficits, generation of ROS, or accumulation of the highly toxic metabolite DOPAL (Lamensdorf et al., 2000). Pathological hallmarks found in the post-mortem PD brain suggest DA metabolism may contribute to NSDA neuron loss. Yet, the neurochemical changes that underlie the acceleration in DA release, reuptake and metabolism remain unclear.

The goal of the research described herein is to identify and characterize the biochemical mechanisms that are responsible for compensatory changes in DA neuron function in response to partial lesions of the NSDA pathway. Accomplishing this task could lead to the development of novel therapeutic targets that can be exploited to slow or halt the progressive loss of NSDA neurons. To this end, the regulation of DA release, reuptake and metabolism in surviving neurons, will be studied using animal models of PD that recapitulate damage to the NSDA pathway that occurs in PD.

G. PD Animal Models

The cause(s) of idiopathic PD remain unknown. As such, there is no perfect animal model of PD that is able to recapitulate every aspect of the disorder. There exists however, a variety of animal models that are used for reproducing different features of the disease. Animal models are evaluated based on their ability to reproduce the cardinal clinical and pathological hallmarks of the disease. For the purposes of the research described in this dissertation, selection of an animal model of PD will be based on the ability to produce reliable, reproducible lesions of the NSDA pathway that are in keeping with the severity of NSDA loss observed in PD.

A number of genetic mutations are associated with heritable/familial PD. While familial PD only accounts for approximately 10% of all reported cases (Payami and Zareparsi, 1998), the identification of genes that are associated with PD pathogenesis has been instrumental to understanding the neurodegenerative process that occurs in the disease. In particular, mutations, duplications, or triplications in the gene encoding the α-synuclein protein are reported to result in heritable PD and cause degeneration of NSDA neurons (Polymeropoulos et al., 1997; Kruger et al., 1998; Singleton et al., 2003).

α-Synuclein is also important in idiopathic PD. Abnormal aggregation of α-synuclein into Lewy-bodies is a primary pathological hallmark of PD (Spillantini et al., 1997). As such, several transgenic mouse animal models have been developed that incorporate known α-synuclein mutations into the genome (Feany and Bender, 2000; Masliah et al., 2000; van der Putten et al., 2000; Matsuoka et al., 2001; Giasson et al., 2002; Lee et al., 2002). These studies have provided insight into the molecular events that lead to Lewy-body formation and cell death in PD. However, the α-synuclein

transgenic models, as well as transgenic mice expressing mutations in other genes linked to PD, fail to reproduce the primary pathological hallmark of PD, the loss of NSDA neurons (Matsuoka et al., 2001; Greene et al., 2003; Pesah et al., 2004; Goldberg et al., 2005; Park et al., 2005). As such, these models are not ideal for studying compensatory changes that occur in NSDA neurons in response to neurodegeneration.

Alternatively, a number of neurotoxin-based animal models of PD have been developed that produce specific NSDA neuron loss. The most commonly used neurotoxins for this purpose are 6-hydroxydopamine (6-OHDA), N,N'-dimethyl-4-4'-bipiridinium (paraquat), rotenone, and 1-methyl-4-phenyl-1,2,3,6-tetrahydropyridine (MPTP). Paraquat, rotenone and MPTP were identified as risk factors for PD in humans and subsequently developed for use in animals to recapitulate the disease in the laboratory. Epidemiology studies have highlighted the importance of human exposure to pesticides and herbicides in increasing risk for PD (Tanner, 1992). These studies provided a basis for the development of animal models of PD using rotenone, a widely used pesticide, and paraquat, a naturally occurring herbicide. The unintentional use of MPTP, which caused a syndrome that was clinically indistinguishable from idiopathic PD in a number of people in the 1980's, provided the basis for development of MPTP as an animal model of PD (Langston et al., 1983). The use of these neurotoxin-based animal models of PD has advanced the understanding of PD etiology and pathogenesis. However, there are a number of advantages and disadvantages to each neurotoxin-based animal model of PD and selection of the proper animal model is critical to experimental design and data interpretation.

6-OHDA

6-OHDA was the first neurotoxin used to produce a specific loss of NSDA neurons (Ungerstedt, 1968). 6-OHDA cannot cross the blood-brain barrier, and thus must be directly injected into the substantia nigra, medial forebrain bundle or striatum, the sites of NSDA neuronal cell bodies, axon projections and axon terminals, respectively. 6-OHDA is a hydroxylated analogue of DA (Blum et al., 2001) and as such, following its injection 6-OHDA is transported into DA neurons through the DAT where it accumulates in the cytoplasm.

ROS and reactive quinone molecules are primarily responsible for the toxicity of cytoplasmic 6-OHDA. 6-OHDA can be directly oxidized to H_2O_2 and para-quinone in the presence of molecular oxygen and transition metals (Przedborski and Ischiropoulos, 2005). As depicted in Figure 1-8, 6-OHDA can react with molecular oxygen to yield semi-quinone and $O_2^{\cdot}$. The $O_2^{\cdot}$ molecule formed from this reaction can react with additional 6-OHDA molecules to produce semi-quinone and H_2O_2. Semi-quinone can react with molecular oxygen to produce para-quinone and $O_2^{\cdot}$. The $O_2^{\cdot}$ formed in this reaction can react with additional semi-quinone producing more para-quionone and H_2O_2. The ROS and quinones generated from these four reactions can cause oxidative damage to lipids, proteins and DNA and are responsible for the toxicity induced by 6-OHDA (Heikkila and Cohen, 1973). Additionally, 6-OHDA may also directly inhibit mitochondrial complex I (Betarbet et al., 2002; Schober, 2004), suggesting neurotoxicity may be due in part, to a bioenergetic defect. However, it is not clear if complex I inhibition is due to a direct binding of 6-OHDA to the enzyme, or indirect effect of macromolecular damage to mitochondria due to ROS-generated from the intracellular

oxidation of the neurotoxin. The latter may be the case, since inhibition of MAO activity provides almost complete protection from 6-OHDA toxicity (Knoll, 1986).

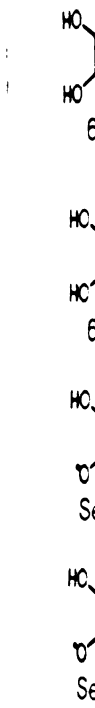

Figure 1
molecul
in the fir
H2O2. S
oxygen c
isotropo

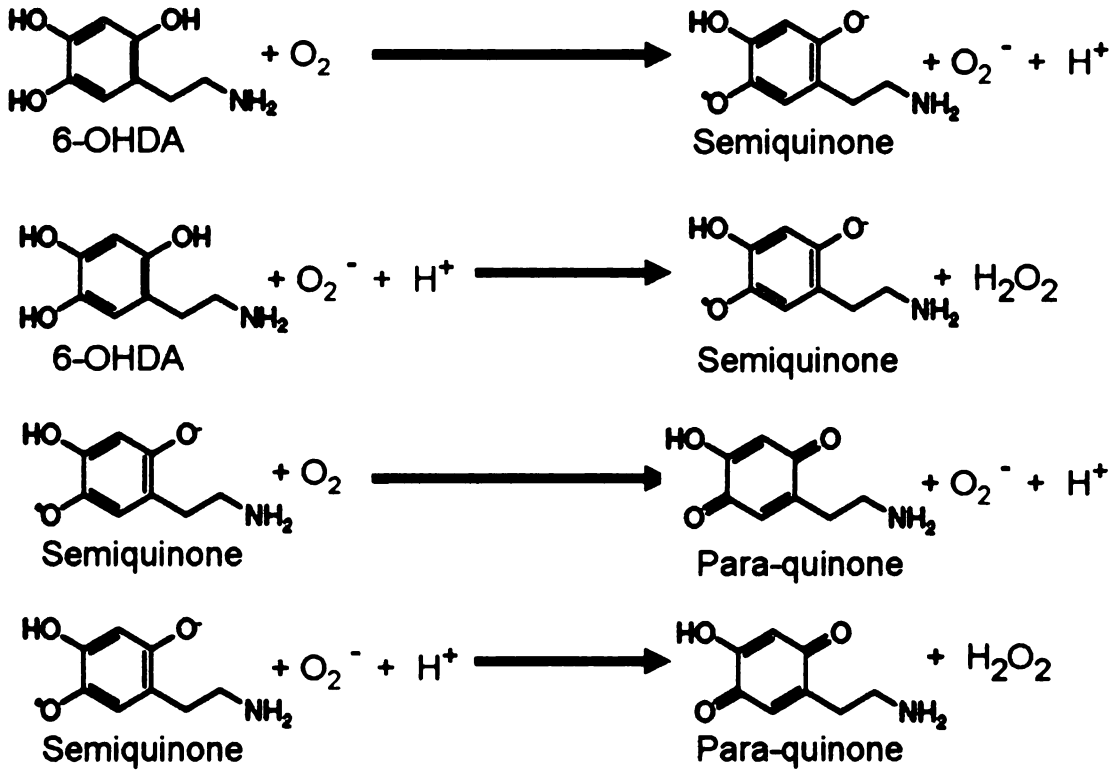

Figure 1-8. The oxidation reaction for two molecules of 6-OHDA. The first 6-OHDA molecule reacts with molecular oxygen to form semi-quinone and O2-. The O2- formed in the first reaction reacts with the second 6-OHDA molecule to form semi-quinone and H2O2. Semi-quinones generated from the first two reactions can react with molecular oxygen or O2- to form para-quinone and either O2- or H2O2 (Przedborski and Ischiropoulos, 2005).

6-OHDA injection produces a reliable, rapid and severe loss of NSDA neurons (Jeon et al., 1995). The extent of the lesion is dependent on the amount of 6-OHDA injected. The advantage of the 6-OHDA model is that the neurotoxin can be injected unilaterally to destroy SNpc neurons on one side of the brain, while sparing contralateral neurons to be used as a control. Moreover, a unilateral NSDA lesion produces asymmetric turning behavior to the contralateral side of the lesion. The contralateral turns are the result of an imbalance between the lesioned and unlesioned striatum that causes basal ganglia dysfunction on one side of the brain and decreases motor cortex output to the opposite side of the body. The degree of the circling behavior directly corresponds with the extent of the lesion (Ungerstedt, 1968). As such, quantification of the circling provides an *in vivo* index of the NSDA lesion severity.

The disadvantages of the 6-OHDA model is the specificity, time-course and mechanism of cell death are not similar to what is observed in PD. 6-OHDA enters cells via active transport mediated by the DAT and once inside the cell, the neurotoxin causes ROS formation, oxidative damage and neuron death. However, the neurotoxicity induced by 6-OHDA injection is not selective to NSDA neurons. 6-OHDA can be taken up into other DA neurons or be transported into norepinepherine neurons via the norepinepherine transporter and causes the destruction of these neurons (Luthman et al., 1989). Thus, NSDA neurons are not more vulnerable to 6-OHDA, the selective loss of these neurons is a function of the location of toxin administration. Additionally, the time-course of cell death induced by 6-OHDA is very rapid (within 24 hours), which does not match the slow progressive loss of NSDA neurons in PD. Neuronal cell death following 6-OHDA is primarily necrotic with no evidence of apoptotic cell death as seen in PD (Jeon et al.,

1995). Due to a lack of selectivity, and rapid necrotic cell death induced by 6-OHDA, this neurotoxin is not ideal for identifying mechanisms that may contribute to the progressive cell death of NSDA neurons in PD.

Paraquat

Paraquat is an herbicide that is naturally found in the environment and is associated with increased risk for PD (Liou et al., 1997). Paraquat enters DA neurons via the DAT (Shimizu et al., 2001; Shimizu et al., 2003), however, non-DAT-mediated transport may also occur (Richardson et al., 2005). Once inside the neuron paraquat reacts with nicotinamide adenine dinucleotide (NADPH, NADH) in a reaction catalyzed by diaphorases to form reactive paraquat and $NADP^+$ (Figure 1-9). Diaphorases are enzymes that transfer electrons from electron donors (NADH, NADPH) to other molecules (Dicker and Cederbaum, 1991; Liochev and Fridovich, 1994; Liochev et al., 1994; Shimada et al., 1998). The reactive paraquat formed in the first reaction can then react with molecular oxygen to form O_2^- radicals (Day et al., 1999; Przedborski and Ischiropoulos, 2005).

Paraquat-induced O_2^- generation leads to oxidative stress, the destruction of NSDA neurons, and the formation of neuronal inclusions in the frontal cortex reminiscent of Lewy-bodies (Manning-Bog et al., 2002; McCormack et al., 2002). However, the degeneration of cortical neurons has not been reported. The advantage of the paraquat model is that it causes the formation of protein inclusions in neurons similar to Lewy-bodies, allowing the molecular mechanisms that result in the formation of Lewy-bodies to be investigated. The disadvantage of this model is that NSDA cell loss has not been

consistently reported and it is not known if NSDA neurons are particularly vulnerable to paraquat toxicity (Thiruchelvam et al., 2000).

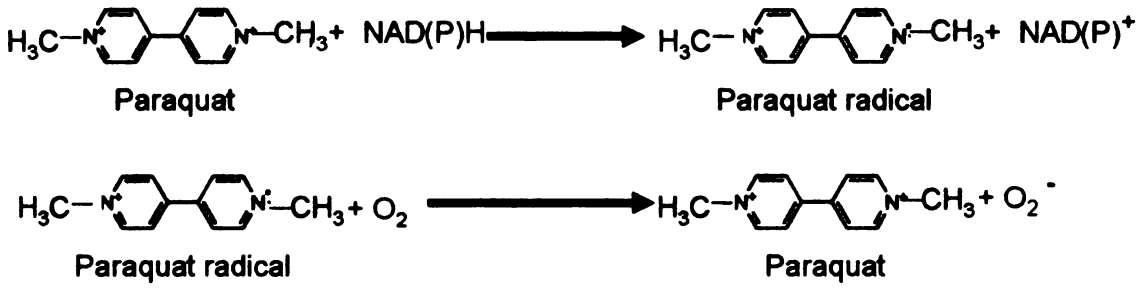

Figure 1-9. Generation of O2- radicals following the oxidation of paraquat. Paraquat reacts with NADPH to form paraquat radical and NADP+. The paraquat radical generated in the first reaction can react with molecular oxygen to form paraquat and O2-.

Rotenone

Rotenone is a naturally occurring mitochondrial complex I inhibitor developed for use as an insecticide. Rotenone is highly lipophillic and can easily cross the blood-brain barrier and gain access to all cells. Following systemic injection, rotenone is found evenly distributed throughout the brain and highest concentrations are achieved within 15 minutes (Talpade et al., 2000). As shown in Figure 1-10, once rotenone enters cells it accumulates in mitochondria where it binds to nicotinamide adenine dinucleotide (NADH)-ubiquinone reductase (complex I) and inhibits the transfer of electrons, thus inhibiting mitochondrial respiration and ATP production. Additionally, binding to complex I inhibits the transfer of electrons and allows these electrons to leak out of the mitochondria which can then react with molecular oxygen to form ROS (Betarbet et al., 2002).

Cellular toxicity following rotenone is due to ROS generation and ATP depletion. Despite the ability of rotenone to enter all cell types, chronic (28 day) intravenous administration of the drug produces a relatively selective degeneration of NSDA neurons and intraneuronal inclusions similar to Lewy-bodies (Betarbet et al., 2000; Thiffault et al., 2000). These results suggest that the primary pathological hallmarks of PD, the unique vulnerability of NSDA neurons and Lewy-body formation, can be produced as a result of systemic inhibition of mitochondrial complex I. Also, the chronic nature of NSDA cell loss induced by rotenone more accurately reflects the progressive nature of PD and causes motor dysfunctions including; abnormal animal posture and decreased spontaneous movement. Thus, rotenone recapitulates the primary aspects of idiopathic PD, however, the use of rotenone has a number of disadvantages as well. While rotenone

induces a relatively selective loss of NSDA neurons, other brain regions that are not damaged in PD (i.e. post-synaptic striatal neurons), show pathology following chronic rotenone treatment. Moreover, NSDA lesions only occurred in approximately 50% of the animals that received rotenone and the lesion severity was highly variable (Hoglinger et al., 2003). Thus, rotenone requires further investigation and characterization before being used as a reliable animal model of PD.

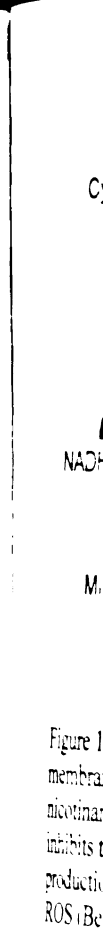

Figure 1
membra
nicotinar
inhibits t
productio
ROS (Be

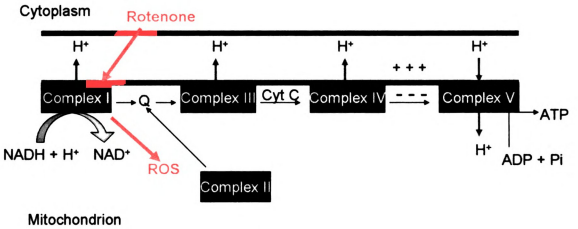

Figure 1-10. The highly lipophillic rotenone molecule can freely pass through cellular membranes. Once inside the cell, it accumulates in mitochondria where it binds to nicotinamide adenine dinucleotide (NADH)-ubiquinone reductase (complex I) and inhibits the transfer of electrons, inhibiting mitochondrial respiration and decreasing ATP production. Additionally, binding to complex I causes electron leak and the formation of ROS (Betarbet et al., 2002).

MPTP

MPTP was discovered to be a neurotoxin in the 1980's when a number of people developed a syndrome clinically indistinguishable from idiopathic PD as a result of inadvertent administration of the compound (Langston et al., 1983). Since then, administration of MPTP to non-human primates and mice has been the most widely used animal models of PD. However, for the purposes and aims of this dissertation, only MPTP mouse models will be discussed.

As depicted in Figure 1-11, following systemic administration of MPTP, the lipophillic MPTP molecule crosses the blood brain barrier. Once inside the central nervous system, MPTP is able to gain access to all cells, but the majority of the toxin is taken up by glial cells due to a much greater number of these cells compared to neurons (Markey et al., 1984). Inside glial cells MPTP is converted to 1-methyl-4-phenyl-2,3-dihydropyridinium (MPDP) by mitochondrial MAO-B and then oxidized to the toxic metabolite 1-methyl-4-phenyl pyridinium (MPP^+). MPP^+ is released from glial cells through unknown mechanisms (Dauer and Przedborski, 2003). The positively charged MPP^+ ion has an affinity for the DAT and is actively transported into DA neurons.

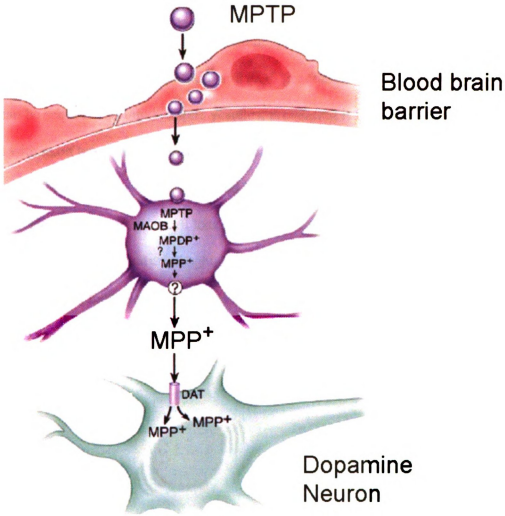

Figure 1-11. MPTP transport into the brain, conversion to MPP^+ and transport into DA neurons. MPTP readily crosses the blood brain barrier and is taken up predominantly by glial cells and converted though a two-step reaction to MPP^+ that is catalyzed by MAO-B. MPP^+ is then released from glial cells and is taken up primarily by DA neurons due to its affinity for the DAT. (Panel B) The axon terminal effects of MPP^+. MPP^+ enters the axon terminals of DA neurons and can either; bind to mitochondrial complex I, interfere with cytosolic enzyme function, or be sequestered into synaptic vesicles (Dauer and Przedborski, 2003).

As depicted in Figure 1-12 , once inside DA neurons, MPP^+ can bind to mitochondrial complex I and similar to rotenone, produce DA neuron death through impairment of mitochondrial respiration and ROS generation. Alternatively, cytoplasmic MPP^+ can be sequestered into synaptic vesicles, preventing it from binding to complex I or react with axon terminal proteins. MPP^+-induced toxicity is not restricted to the DA neurons. MPTP also causes toxicity in glial cells that bio-activate the toxin (Di Monte et al., 1999). However, overt glial cell loss is not observed because glial cells that take up the toxin are distributed evenly throughout the brain, and as such, there is not a concentrated loss of these cells in any region and, unlike neurons, new glial cells may be produced to replace lost cells.

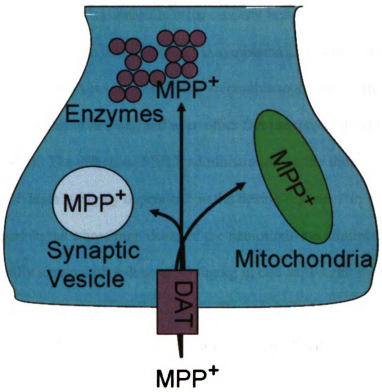

Figure 1-12. The effects of MPP^+ on the axon terminal of NSDA neurons. MPP^+ enters the axon terminals of DA neurons and can either; bind to mitochondrial complex I, interfere with cytosolic enzyme function, or be sequestered into synaptic vesicles (Dauer and Przedborski, 2003). Binding to mitochondrial complex I and cytosolic proteins results in the neurotoxic effects of MPP^+. Sequestration into synaptic vesicles protects the axon terminals from the neurotoxicity of MPP^+.

Systemic MPTP administration in mice causes a loss of NSDA neurons and the development of motor deficits that resemble PD symptoms (Jackson-Lewis et al., 1995; Sedelis et al., 2001). NSDA neurons are more vulnerable to the toxic effects of MPTP, compared to norepinephrine neurons and even other DA neurons that express the DAT (Chiueh et al., 1985). The effects of MPTP administration on the time course, extent, and mechanism of cell death is highly dependent on the dosing regimen. In general, acute administration paradigms where high doses of the neurotoxin are administered over a brief period (usually a cumulative dose of 80 mg/kg in one day) result in very rapid and severe NSDA cell loss that is primarily necrotic (Bezard et al., 1997; Smeyne and Jackson-Lewis, 2005). However, the rapidity and severity of cell loss in the acute treatment model does not match the slowly progressive nature of early PD where apoptotic cell death is known to occur (Mochizuki et al., 1996; Anglade et al., 1997).

Sub-chronic dosing regimens (25 mg/kg per day for five consecutive days) and prolonged-chronic regimens (20 mg/kg, twice a week for five consecutive weeks) have been developed that distribute the total dose of MPTP over several days, causing a prolonged impairment of mitochondrial function and chronic exposure to ROS. Using these dosing regimens cell death occurs from both apoptotic and necrotic mechanisms, which more accurately reflects cell death in PD (Bezard et al., 1997; Tatton and Kish, 1997; Novikova et al., 2006). Also, despite a higher cumulative dose of MPTP the lesion produced by the neurotoxin is less severe than in the acute model and more reminiscent of the extent of NSDA neuron loss observed in early PD.

Sub-chronic or prolonged-chronic MPTP dosing regimens both produce reliable and reproducible lesions of NSDA neurons (Petroske et al., 2001). NSDA neurons are

more vulnerable to degeneration in PD, and the time course and mechanisms of cell death closely resemble what occurs in PD. Taken together, chronic administration regimens of MPTP recapitulate the key pathological features of idiopathic PD, and as such, are ideal for studying NSDA neuronal function during conditions that are similar to PD.

H. **Thesis Objective**

The studies described herein are designed to test the hypothesis that increased DA metabolism secondary to compensatory increases in DA synthesis, release and reuptake contributes to the progressive degeneration of NSDA neurons in PD. To test this hypothesis, pharmacological, neurochemical and immunohistochemical techniques will be used to address the following Specific Aims: 1) determine if chronic MPTP administration regimens cause compensatory increases in the activity of surviving unlesioned neurons, 2) characterize the neurochemical changes that allow NSDA neurons to maintain the increased neuronal activity, 3) determine if sustained increases in DA metabolism can cause a progressive loss of NSDA neurons. Identification of the mechanisms that underlie compensatory changes in NSDA neuron function should lead to the development of therapeutic strategies that can halt or delay the progressive loss of these neurons in PD.

Chapter 2. Materials and Methods

A. Animals

Generation of wild-type and homozygous α-synuclein knock-out mice

Homozygous α-synuclein knock-out mice were obtained in breeding pairs from Jackson Labs (B6;129X-SncatmlRosl, stock #3692, Bar Harbor, MA). The generation, viability, fertility and basic biochemical features of this strain have been previously described (Abeliovich et al., 2000). α-Synuclein knock-out mice were crossed with the inbred strain (C57/Bl6) used as the host for the blastocyst during the original generation of the α-synuclein knock-out mice (Abeliovich et al., 2000) to yield heterozygous mice (F1). Heterozygous mice were then crossed and the offspring of this cross (F2) were used to maintain a stable breeding colony. Additional heterozygous (F2 x F2 and F3 x F3) crosses were performed to expand and maintain the colony for the experiments described herein. University-trained technicians maintained the breeding colony.

Determining Animal Genotype

Animal genotype was confirmed by PCR analysis of genomic DNA (isolated from tail samples) using primers specific for Exon 2 of the α-synuclein gene to identify native α-synuclein, and the neomycin resistance gene insert to identify the knock-out sequence (Abeliovich et al., 2000). Mouse tail snips were dissolved in 600 μl of nuclei lysis buffer with proteinase K (25 mM EDTA, 50 mM NaCl, 0.8 mg/ml proteinase K) at 55°C for 4 hours. Following digestion, RNase (0.05 mg/ml) was added to the lysate and incubated for 30 min. Subsequently, 200μl protein precipitation solution (4.2 M NaCl, 0.63 M KCL, 10 mM Tris base, pH 8.0) was added to the mixture, incubated on ice for 5 minutes, and centrifuged (15,000 x g 10 min) to pellet protein. The supernatant was

placed into a fresh microcentrifuge tube containing 600 µl room temperature isopropanol. The solution was gently mixed by inversion until white strands of DNA appeared. The insoluble DNA strands were isolated by centrifugation at 15,000 x g 60 sec. The supernatant was removed, and the DNA-containing pellet was washed in ethanol and resuspended in 100 µl of DNA rehydration solution (10 mM tris-HCL, 1 mM EDTA, pH 7.4).

The concentration of DNA in each sample was determined by measuring the absorbance at 260/280 nm with a nanodrop ND-1000 spectrophotometer (Nanodrop, Wilmington, DE). The concentration of each sample was adjusted to 50 ng/µl by adding the appropriate amount of DNA rehydration solution. For the PCR reaction, 5 µl of the DNA sample (50 ng/µl) was added to 20 µl of PCR reaction solution (1 mM PCR buffer, 200 mM dNTP, 2 mM MgCl, 0.18 pm/µl oligo primers, 0.4 u/µl taq polymerase, Invitrogen Carlsbad, CA). Primers were selected to bracket exon 2 of the α-synuclein gene, or the neomycin resistance gene sequences, as described previously (Drolet et al., 2004). Samples were vortexed and placed into the PCR machine. PCR run parameters were 94°C x 5 min, then 30 cycles of 94°C, 65°C, 72°C x one minute each, followed by 72°C x 5 min. Subsequently, gel electrophoresis (75 mV, one hour) on a 3.0% agarose gel was used to separate amplified DNA (10 µl) from each sample. As depicted in Figure 2-1, animal genotype was confirmed for all animals through visualization of the amplified DNA using a UV transilluminator (UVC co., San Gabriel, CA). Only homozygous α-synuclein knock-out mice or homozygous wild-type mice were used in the experiments described herein.

Figure
hetero
gel fol
gene (3

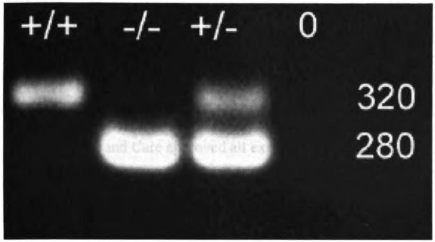

Figure 2-1. Genotyping of Wild-type (+/+), homozygous α-synuclein knock-out (-/-), heterozygous (+/-) mice, and control blanks (0). Ethidium bromide stained 3% agarose gel following electrophoresis of PCR amplification products of exon 2 of the α-synuclein gene (320 base pairs) and the neomycin resistance construct (280 base pairs).

Animal Housing

Animals were housed two to four per cage, maintained in a temperature- (22 ± 1°C) and light-controlled (12-h light–dark cycle, lights on at 0600 hr) room, and provided with food and tap water *ad libitum*. The Michigan State University, All University Committee on Animal Use and Care approved all experiments using live animals.

B. Drugs

All drugs were purchased from Sigma-Aldrich (St. Louis, MO). Concentrations were calculated from the free base of the respective drug.

Prolonged Chronic MPTP Administration

MPTP was dissolved in 0.9% sterile saline. For dose-response experiments, dipropylsulfamoyl-benzoic acid (probenecid) was dissolved in dimethyl sulfoxide (DMSO). To improve solubility of the probenecid, for time-course experiments, probenecid was dissolved in 0.1 N NaOH and the pH was adjusted to 7.4 using HCL. Male 8–12 week old mice received s.c. injections of either vehicle (1 ml/kg) or MPTP (1, 5, 10, or 20 mg/kg) twice a week, alternating morning and afternoon every 3.5 days, for a total of 10 total injections over 5 weeks. Probenecid (250 mg/kg; i.p.) was co-administered with each dose of MPTP to increase the plasma and central nervous system half-life of MPTP and MPP^+, respectively (Petroske et al., 2001). Neither DMSO nor probenecid produces an effect per se on NSDA neurons (Lau et al., 1990). All experiments using MPTP were performed using previously published safety guidelines (Przedborski et al., 2001). Experiments were terminated three weeks following the last injection of MPTP.

Sub-chronic MPTP Administration

MPTP was dissolved in 0.9% sterile saline. Male 8–12 weeks old mice received s.c. injections of vehicle (1 ml/kg) or MPTP (1, 5, or 25 mg/kg) once daily for five consecutive days. Experiments were terminated three days following the last MPTP.

Acute m-Hydroxybenzylhydrazine (NSD-1015) Administration

NSD-1015 was dissolved in 0.9% saline. For determining TH catalytic activity in NSDA neurons, mice were injected with the L-AADC inhibitor NSD-1015 (100 mg/kg, i.p.) thirty min prior to decapitation and striatal DOPA concentrations were measured (Figure 2-4). The accumulation of DOPA following blockade of L-AADC with NSD-1015 is an *in vivo* assay for TH catalytic activity (Carlsson et al., 1972).

Acute Raclopride Administration

Raclopride was dissolved in 0.9% saline. Mice were injected with raclopride (1.0 mg/kg, i.p.) and killed by decapitation either 30, 60, or 120 min later.

Acute Gamma-butyrolactone (GBL) Administration

GBL was diluted in 0.9% saline. Mice were injected with GBL (750 mg/kg, i.p.) and killed by decapitation either 1, 2, or 3 h later.

Acute Tyrosine Administration

L-tyrosine dihydrochloride was dissolved in 0.1 N HCL diluted in 0.9% saline. Mice were injected with tyrosine-HCL (100 mg/kg, i.p.) and killed by decapitation 1 h after administration. In some experiments, mice were injected with L-tyrosine disodium salt, since it dissolves in 0.9% saline. Mice were injected with tyrosine disodium salt and killed by decapitation 1 h after administration.

Chronic Raclopride and Quinelorane Administration

Alzet osmotic minipumps (#2004, Durect Corporation, Cupertino, CA) were filled with either raclopride hydrochloride (Sigma) dissolved in sterile saline (2.5 mg/ml) or quinelorane hydrochloride (Sigma) dissolved in sterile saline (2.5 mg/ml). Mice received 0.015 mg/day (0.5 mg/kg/day) of either raclopride or quinelorane based on the pump delivery rate (0.25 µl/hr, 28 days) and the average weight of a mouse (0.030 kg).

C. Preparation and Implantation of Alzet Osmotic Mini-pumps

Prior to implantation, Alzet osmotic mini-pumps were filled with saline, raclopride or quinelorane, and primed by placing the pumps in saline at 37°C for 24 h. On the day of implantation, mice were anesthetized with ketamine:xylazine cocktail (10:2 mg/kg, i.p.). The incision site was shaved and cleaned with 10% povidone iodine solution. An incision (3 mm) was made across the width of the animals back. Forceps were used to prepare a s.c. pocket for the pump. Pumps were placed under the skin in the prepared pocket and the wound was sealed with wound-clips. The animals were placed on a heating pad and monitored until fully recovered from anesthesia (approximately 2-3 h).

Alzet pumps (#2004) deliver drugs at a constant rate of 6 µl/day for 28 days. Pumps were left in mice for 21 days to prevent any loss of drug delivery due to improper pump filling or decreased diffusion rate. For a 21 day experiment, 126 µl is the ideal volume delivered. The actual volume delivered was determined by removing residual fluid from the inner chamber of the pumps following completion of the experiment and

subtracting the value from the 220 µl mean filling volume. If the actual and ideal volume delivered differed by greater than 50 µl, the sample was not used for analysis.

D. Neurochemistry

Tissue Preparation

Following drug administration, mice were decapitated and their brains were rapidly removed and placed on a glass dissecting surface (4°C) on its dorsal surface. The median eminence was microdissected with the aid of a dissecting microscope and placed into ice-cold tissue buffer (0.1M phosphate-citrate buffer pH 2.5) for neurochemical analysis. The brain was then quickly frozen over dry ice. Consecutive 500 µm thick coronal sections were prepared from the frozen brains using a cryostat set at -10 °C (CTD-Model Harris, International Equipment Co., Needham, MA). Sections were collected through the rostro-caudal extent of the forebrain beginning approximately 2.5 mM anterior to bregma (Paxinos and Watson 1986). Sections were thaw-mounted onto glass slides, refrozen and the nucleus accumbens and striatum were dissected using a modification of the method described by Palkovits (Palkovits, 1973, 1978).

As depicted in Figure 2-2, using a dissecting microscope the nucleus accumbens was removed using a 22-gauge punch tool fashioned from a 22-gauge hypodermic needle. Sections located approximately 1.8 mm anterior to bregma were collected for dissection. The nucleus accumbens was dissected bilaterally and samples were placed into ice-cold tissue buffer and stored at -20°C until neurochemical analysis.

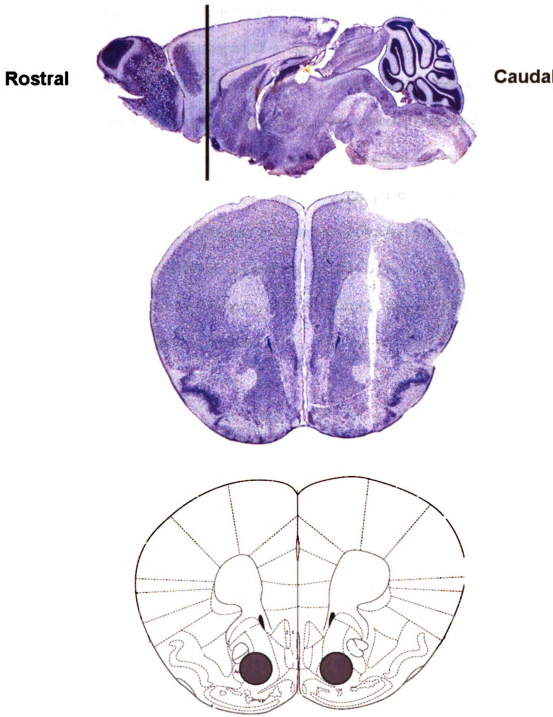

Figure 2-2. A. Sagittal view of a Nissl stained mouse brain depicting the rostro-caudal location of the sections used to dissect the nucleus accumbens. B. Coronal brain sections stained for Nissl that depicts the section used to dissect the nucleus accumbens. C. Diagram of the location and size of the Palkovits micropunch (approximately 0.5 mm i.d.) used to dissect the nucleus accumbens (Paxinos and Watson, 1986).

As depicted in Figure 2-3, using a dissecting microscope the striatum from the left side of the brain was removed using an 18-gauge punch tool, fashioned from an 18 gauge hypodermic needle. Striata from two consecutive sections, located approximately 1.1 mm and 0.6 mM anterior to bregma, respectively, were dissected and placed into 100 µl of ice-cold tissue buffer and stored at -20°C until neurochemical analysis. Striata from the right side of the brain were dissected using a 12-gauge punch tool and placed into ice-cold homogenization buffer for Western blot analysis, described in further detail below. This method discretely isolates the terminal regions of NSDA, mesolimbic dopamine (MLDA) and tuberinfundibular dopamine (TIDA) neurons that can be used for neurochemical and Western blot analysis.

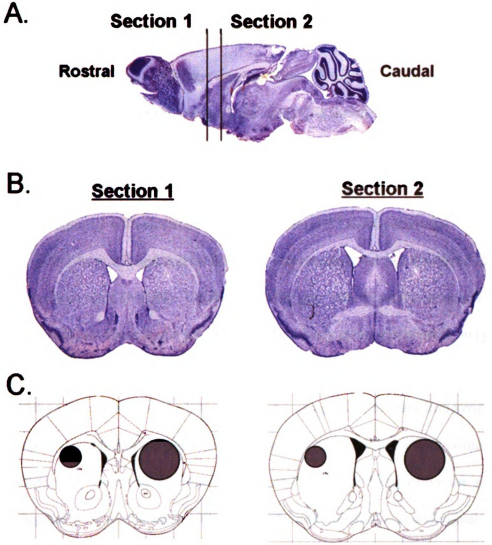

Figure 2-3. A. Sagittal view of a Nissl stained mouse brain depicting the rostro-caudal location of the sections used to dissect the striatum. B. Coronal brain sections stained for Nissl that depicts the first section (left) and second section (right) used to dissect the striatum. C. Diagram of the location and size of the Palkovits micropunch (approximately 1 mm i.d.) used to dissect the striatum for neurochemistry (Left Side of Brain) and Western blot analysis (approximately 1.5 mm i.d., Right Side of Brain) (Paxinos and Watson, 1986).

Neurochemical Analysis

On the day of assay, samples were thawed and sonicated (Heat Systems Ultrasonics, Plainview NY) using three one sec bursts. Samples were then centrifuged at 18,000 x g (Beckman Coulter microfuge, Palo Alto, CA) for one min. The supernatant was removed using a 100 µl Hamilton syringe and the final volume of the supernatant was adjusted to 100 µl and placed into a fresh microcentrifuge tube for high pressure liquid chromatography with electrochemical detection (HPLC-EC) analysis.

The pellet from the initial centrifugation was resuspended and dissolved in 100 µl of 1N sodium hydroxide (NaOH). On the following day, striatal protein concentrations were determined from these tissue pellets using the Lowry protein method (Lowry et al., 1951). Aliquots of striatal protein samples (50 µl) were transferred from the microcentrifuge tube to a 12 x 75 glass culture tube using a 100 µl Hamilton syringe. NaOH (50 µl) was added to the protein sample in each tube yielding a final volume of 100 µl/culture tube. Standard solutions with either 12.5, 25, or 50 µg of bovine serum albumin (Sigma) were dissolved in 100 µl of NaOH and transferred to individual 12 x 75 culture tubes. For colorimetric determination of protein concentrations in the culture tubes, 1.0 ml of reagent A (0.2 M sodium carbonate, 40 mM cupric sulfate, 70 mM sodium potassium tartrate) was added to each tube and allowed to incubate for 10 min. Subsequently, 100 µl of reagent B (folin reagent diluted 1:2 with dH_2O) was added to the culture tubes and incubated for 30 min. Following incubation, protein concentrations were determined by normalizing the absorbance of each sample, read at 700 nm on a Gilford spectrophotometer (Gilford Instruments, Oberlin, OH) to the absorbance of the

known protein standards assayed concurrently. A single 18-gauge striatal punch yields an average of 40 μg of protein.

Striatal DA, DOPAC and DOPA was determined with HPLC-EC using a Waters 515 HPLC pump (Waters) with a flow rate of 1.0 ml/min and a ESA Coulochem 5100A electrochemical detector with an oxidation potential of +0.4V. Neurochemical standards containing 1.0 ng of DOPAC, DA and DOPA and striatal supernatant samples were injected onto a C18 reverse phase analytical column (Bioanalytical systems, West Lafayette, IN). The HPLC-EC mobile phase (0.5M sodium phosphate, 0.03M citrate, 0.1 mM EDTA, sodium octylsulfate, 15-20% methanol, pH 2.5) was adjusted by varying the amounts of sodium octylsulfate and the methanol concentration to optimize DA, DOPAC, and DOPA separation.

DA, DOPAC, and DOPA content was quantified by normalizing the peak heights of each sample to the peak heights of these compounds measured in the known 1.0 ng standards (Figure 2-4). The linear range for measuring DA content in the striatum is approximately 0.15-4.0 ng using this HPLC-EC technique (Figure 2-5). A single 18-gauge striatal punch yields approximately 3,000 pg of striatal DA. The broad range of this technique allows for an approximately 200-fold increases or decreases from baseline to be detected while remaining within the linear range of the curve. The DA, DOPAC and DOPA content of each sample was normalized to the amount of striatal protein dissected to yield a concentration of striatal DA, DOPAC, and DOPA per striatal protein (ng/mg protein).

Fig
hei
Rep
of
Rep
of
(-N

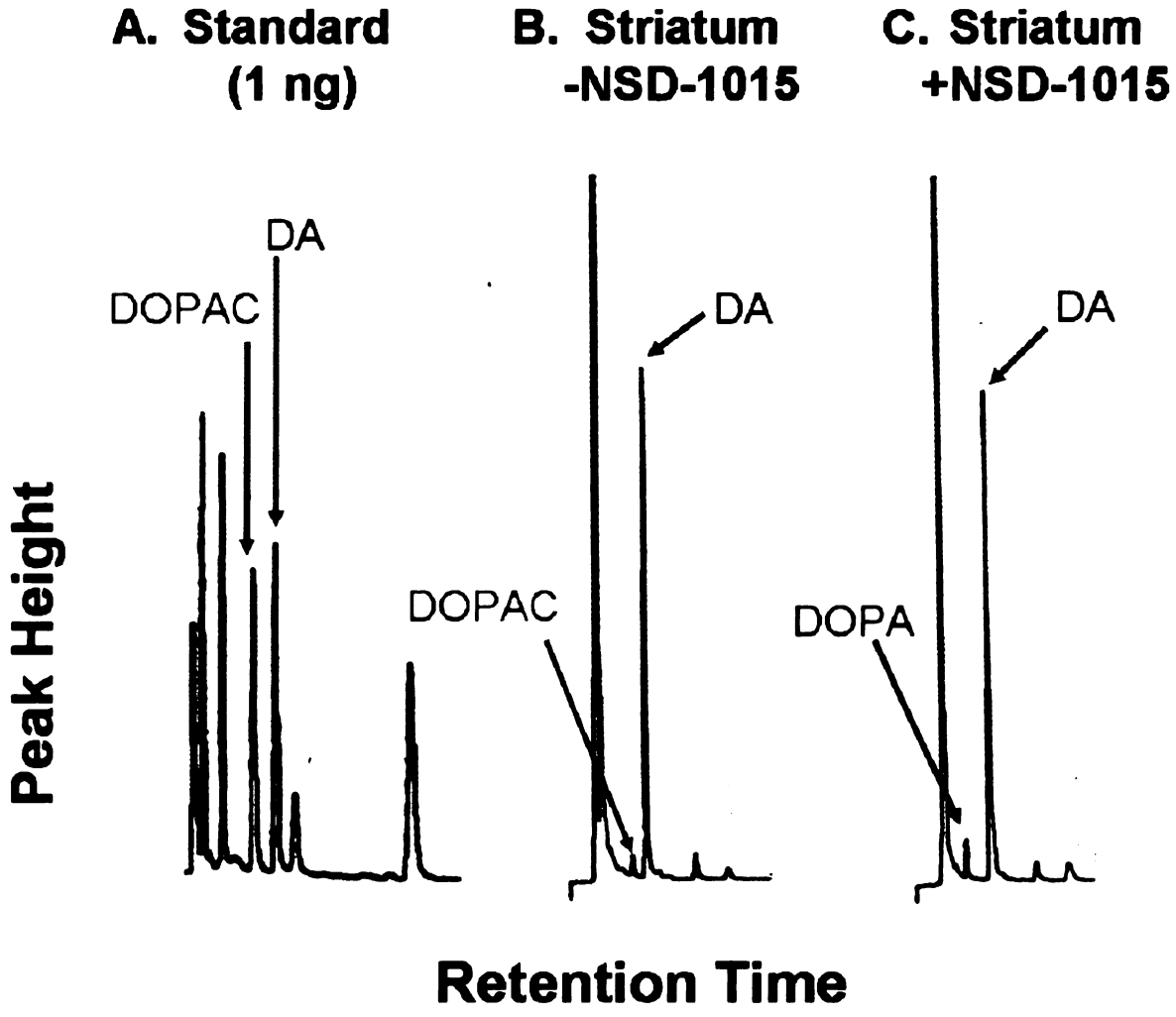

Figure 2-4. A. HPLC-EC chromatogram depicting the retention times (x-axis) and peak heights (y-axis) for a standard mixture containing 1 ng of DOPAC and DA (B) Representative HPLC-EC chromatogram depicting the peak heights and retention times of DOPAC and DA from a striatal sample from un-treated (-NSD-1015). (C) Representative HPLC-EC chromatogram depicting the retention times and peak heights of DOPA and DA from striatal sample taken from a mouse injected with NSD-1015 (+NSD-1015) 30 min prior to sacrifice.

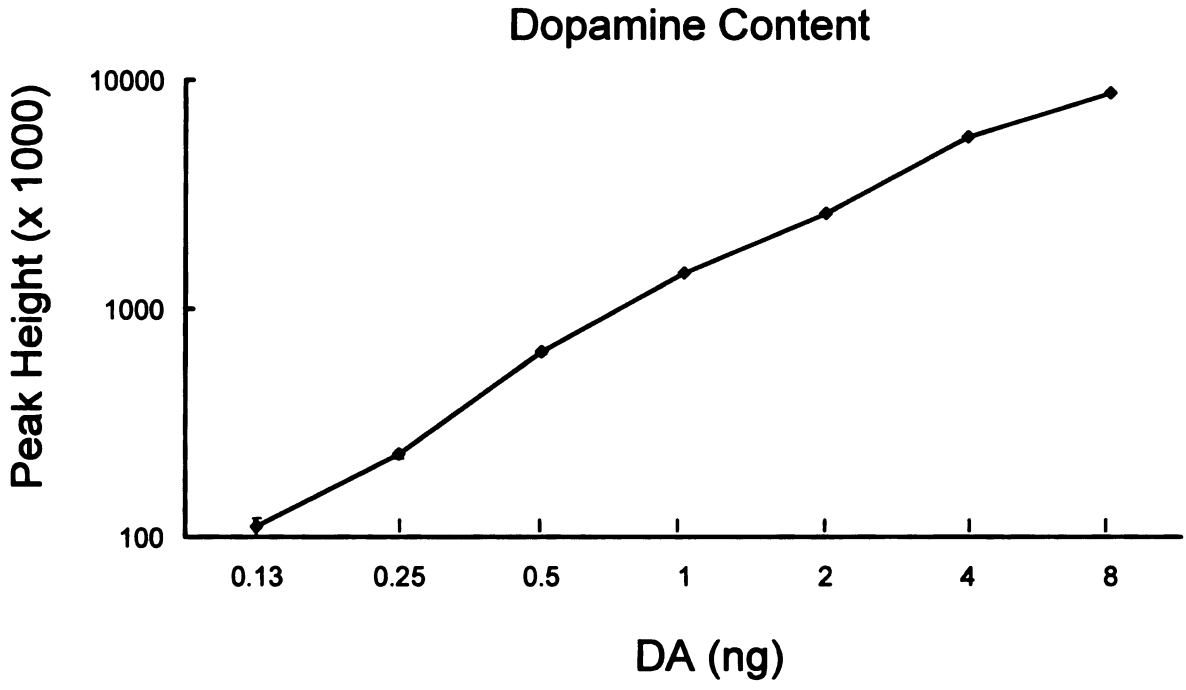

Figure 2-5. Logarithmic scale plot demonstrating the linear range for determining DA content using HPLC-EC. DA content was determined by comparing peak heights in samples with increasing known DA concentrations (ng). Peak height was determined at an oxidation potential of +0.4 V, and gain of 500 with a constant flow rate of 1.0 ml/min.

E. Western Blot Analysis

Tissue Preparation

Striata to be used for Western blotting were dissected from the contralateral side of section 1 and section 2 (Figure 2-3) using a 12-gauge punch tool approximately 1.5 mm i.d., and were placed into ice-cold homogenization buffer (320 mM sucrose, 5.0 mM HEPES, with Complete Mini Protease Inhibitor Cocktail Tablets, Roche Diagnostics, Mannheim, Germany, pH 7.4).

Protein Extraction/Isolation/Determination

Striata were homogenized by sonication and centrifuged (1000 x g 10 min). Nuclear and plasma membrane containing pellets (P1) were saved for further analysis. Supernatants (S1) were removed, placed into a fresh microcentrifuge tubes, and centrifuged (22,000 x g 30 min). Supernatants from this second high-speed centrifugation (S2) were removed, placed into a fresh microcentrifuge tubes, and assayed for protein content using the bicinchoninic acid protein method (BCA, Sigma). 12-gauge striatal punches yield approximately 100 μg of protein. Following determination of protein concentrations, 10 μl of loading buffer (250 mM tris base pH 6.8, 20% glycerol, 5% SDS, 0.01% bromophenol blue) were added to samples. Samples were vortexed, boiled at 95°C for 10 min, and cooled to 4°C.

Electrophoresis/Transfer Conditions

Two precast polyacrylamide gels (7.5-12%; Bio-Rad, Hercules, CA, USA) were snapped into the inner chamber of a mini-protean-3 electrophoresis cell (BioRad). The inner chamber was filled with 125 ml of Laemli running buffer (25 mM Tris base, 192 mM glycine, 0.1% SDS). Isolated striatal protein samples were loaded into 9 of 10 lanes

within the gel. The volume of each sample loaded was adjusted to ensure loading of equal concentrations of protein. A standard containing proteins of known molecular weights was loaded into the tenth lane. The inner chamber was then placed into the outer chamber containing 350 ml of Laemli running buffer. Striatal protein was separated by applying a 200 mV current for approximately 45 min. Electrophoresis was stopped when the lightest band of the protein standard reached the bottom of the gel. Proteins were then transferred to 0.45-μm nitrocellulose membranes (Fisher Scientific, Pittsburgh, PA, USA) by electrophoresis at 30 mV for 12 h.

Immunoblot Detection of Striatal Protein

Following protein transfer, nitrocellulose membranes were washed in 25 mM TBS (4 x 5 min) and incubated in blocking buffer (Li Cor, Inc., Lincoln, NE, USA) for one h. Membranes were reacted with primary antiserum overnight. Primary antiserum consisted of blocking buffer containing the primary antibody to the protein of interest as well as a loading control primary antibody, i.e. a protein not affected by experimental conditions. The dilution and source of each primary antibody used in the studies described in this dissertation is listed in Table 2-1.

Antigen	Species	Dilution	Source
α-Synuclein	Mouse	1:3000	BD Transduction Laboratories San Jose, CA(610786)
B-III Tubulin	Mouse	1:5000	Chemicon (MAB1637)
Dopamine transporter (DAT)	Rabbit	1:2000	Chemicon (MAB369)
Early Endosomal Antigen-1	Rabbit	1:3000	Affinity Bioreagents Golden, CO (PA1-063)
SNAP-25	Mouse	1:4000	Chemicon (MAB331)
Synaptophysin	Mouse	1:4000	Chemicon (MAB368)
Tyrosine hydroxylase (TH)	Rabbit	1:2000	Chemicon, Temecula, CA (#AB152)
Serine-40 phospho-TH	Rabbit	1:1500	Cell Signaling Technology, Beverly, MA (#2791)
Serine-31 phospho-TH	Rabbit	1:1500	Chemicon (AB5423)
Serine-19 phospho-TH	Rabbit	1:1500	Chemicon (AB5425)
Vesicular Monoamine Transporter-2 (VMAT-2)	Rabbit	1:1000	Chemicon (AB1767)

Table 2-1. Description of each primary antibody (antigen) used in the studies described in this dissertation. Antigen characterization is based on the animal used to generate the antibody (species), the standard dilution used for Western blotting and the company the antibody was purchased from (source).

Following incubation with primary antibodies, membranes were washed in TBS (4 x 5 min). Subsequently, membranes were incubated with both IRDye 800-conjugated goat anti-rabbit (Rockland, Gilbertsville, PA, USA) and Alexa Fluor 680-labeled goat anti-mouse (Molecular Probes, Eugene, OR, USA) secondary antibodies diluted 1:20,000 in blocking buffer for 1 h. Membranes were then washed in TBS (4 x 5 min) and bound antibodies were visualized using the Odyssey infrared imager. Band density was quantified by measuring the infrared absorbance of each band using an Odyssey infrared imager and Odyssey software (Li-Cor). In order to determine if band density increased proportionally to increasing concentrations of striatal protein, TH and β-III tubulin were measured with increasing concentrations of post-nuclear striatal protein (Figure 2-6). TH band density is linear when 10-320 μg of striatal protein is loaded per lane. However, when 160 or 320 μg of protein is loaded, band smearing and non-specific immunoreactivity is observed. B-III tubulin detection and visualization is linear when 10-80 μg of striatal protein is loaded, with band smearing and non-specific band formation becoming apparent when 160 or 320 μg of protein is loaded. Therefore, using this Western blot technique changes in band density can be interpreted as linear changes in the amount of protein in each sample.

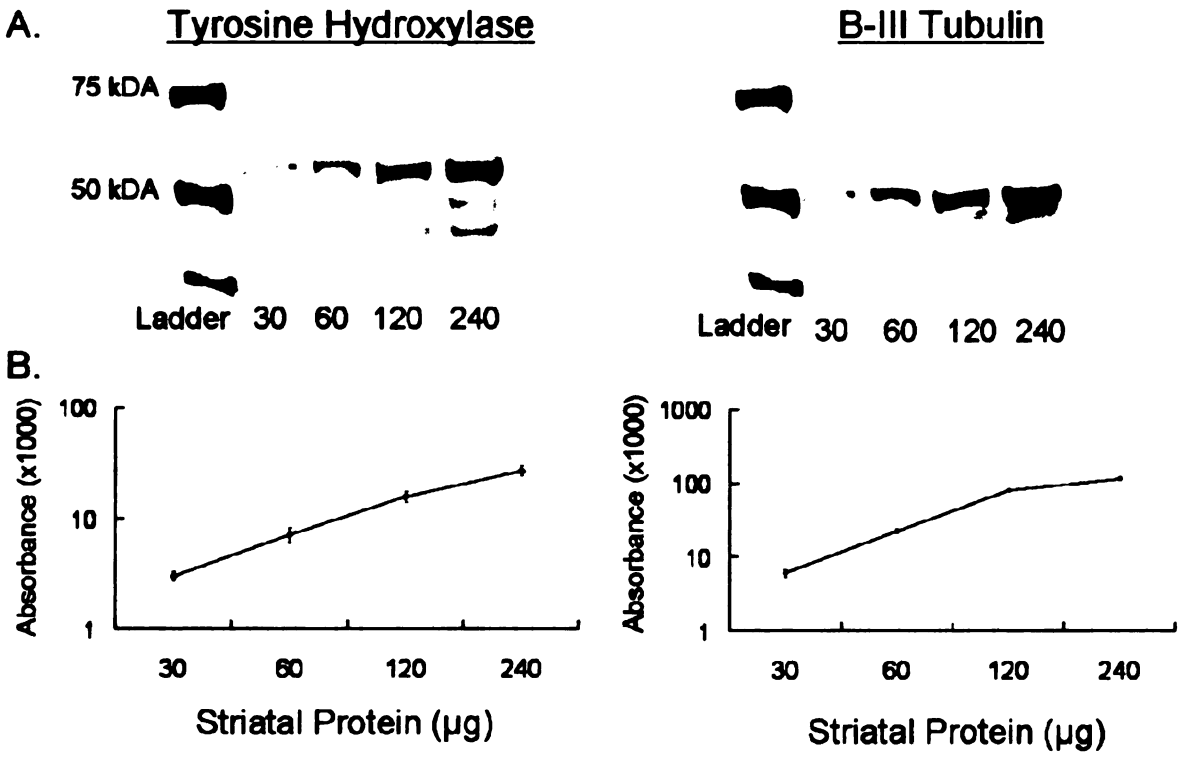

Figure 2-6. (A). Immunoreactivity of TH (~60 kDA, Left Panel) and β-III tubulin (~50 kDA, Right Panel) with either 30, 60, 120 or 240 µg of striatal protein separated on 10% polyacrylamide gels. (B) Quantification of TH (left) and β-III tubulin (right) band density using the Odyssey Imaging software and shown in absorbance units (x 1000).

Quantification of Protein Immunoreactivity

Relative density units (RDU) are obtained by normalizing the band density (absorbance) of the protein of interest to the band density of the control protein. Each nitrocellulose membrane contains samples that represent all experimental condition such that, only samples run at the same time, transferred onto the same nitrocellulose membrane, exposed to the same primary and secondary conditions, and visualized at the same time can be compared.

F. *In vitro* Monoamine Oxidase Activity Assay

MAO catalyzes the enzymatic conversion of DA to DOPAL. Therefore, the enzymatic activity of MAO can be determined by incubating MAO enzyme with known concentrations of DA and measuring the rate of the DOPAL product formed using HPLC-EC (Legros et al., 2004). DA was dissolved in phosphate buffer (140 mM NaCl, 8.1 mM Na_2HPO_4, 1.4 mM KH_2PO_4, pH 7.5) to a final concentration of 5 μM. Phosphate buffered DA (500 μl) was incubated in 12x75 culture tubes at 37 C for 15 min. The reaction was started by adding 11.25U of MAO to the culture tube and gently mixing. The reaction was stopped at either 15, 30, 45 or 60 min by adding 1 ml of tissue buffer to the culture tube and placing the tube on ice. Samples were transferred to a 1.5 ml centrifuge tube and centrifuged at 12,000 x g for 10 min. Supernatants were removed and placed into a fresh tube for HPLC-EC analysis of DA and DOPAL. Concentrations of DA were compared to 1ng standards of DA. Since DOPAL is not available commercially for the preparation of standards, concentrations of DOPAL were

determined by normalizing the DOPAL peak height to the amount of DA lost at each time point (Figure 2-7).

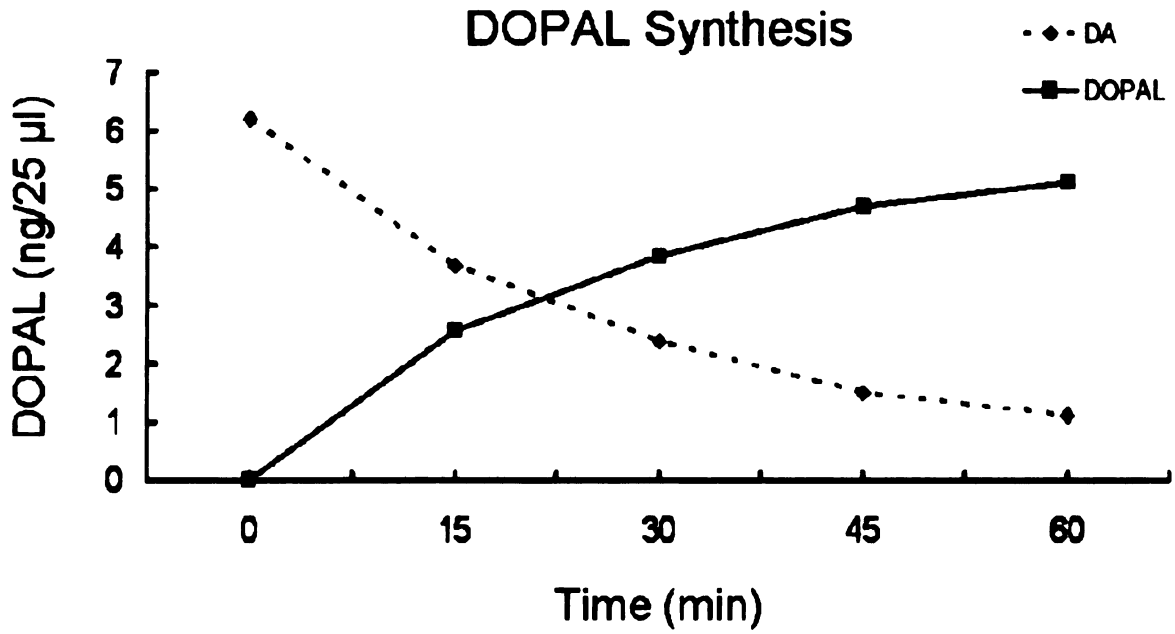

Figure 2-7. The rate of DOPAL formation (solid line) and DA depletion (dashed line) after incubating DA (5µM) with MAO (11.25 U). DA and DOPAL were measured using HPLC-EC. Concentrations of DA were determined by comparing to 1 ng DA standards. Concentrations of DOPAL were determined by comparing DOPAL peak heights to the amount of DA decreased at each time point.

G. Subcellular Fractionation of TH

Tissue Preparation

Striatal protein used for subcellular fractionation was dissected from fresh tissue. Following decapitation, the brain was rapidly removed and placed ventral side up in TBS (4°C). A 1 mm coronal section containing the striatum was made with a razor blade. The striatal section was then placed flat in the ice-cold TBS and a 12-gauge punch tool was used to bilaterally dissect the striatum. The dissected striata from two mice were placed into a 1.5 ml microcentrifuge tube containing ice-cold homogenization buffer with protease inhibitors and phosphatase inhibitor (1 mM sodium orthovanadate). Tissue was then homogenized in the 1.5 ml tube with 20 strokes with a plastic pestle. Homogenized striatal tissue was centrifuged at 1,000 x g for 10 min (4°C Beckman Coulter microfuge).

Isolation of Plasma Membrane Protein

The pellet from this initial centrifugation (P1) was resuspended in 500 µl of homogenization buffer. A sucrose gradient was created by adding 830 µl of high sucrose homogenization buffer (2.5 M sucrose, 5.0 mM HEPES, Protease Inhibitor Cocktail, pH 7.4) to P1. Samples were vortexed and the sucrose gradient was centrifuged at 20,000 x g for 5 h (4°C Beckman Coulter microfuge). Nuclear protein will pellet in the high-density sucrose buffer. Plasma membrane protein will pellet in the low density sucrose but not in the high-density sucrose buffer such that membrane protein locates at the interface between the two buffers. Low molecular weight proteins such as microsomes remain in the upper portion of the low density sucrose buffer. Plasma membrane protein (200 µl) was extracted and placed into a fresh tube and frozen (-80°C).

Isolation of Cytosolic, Synaptic Vesicle and Endosomal Protein

As depicted in Figure 2-8, the supernatant from the initial low-speed centrifugation (S1) was removed and placed into a fresh tube and centrifuged at 20,000 x g for 20 min at 4°C. The supernatant from this high-speed centrifugation (S2) was placed into ultracentrifuge tubes and centrifuged at 100,000 x g for 60 min using a Sorvall ULTRA PRO 80 Ultracentrifuge with a swinging-bucket rotor (#TH-660). The supernatant from this ultracentrifugation (S3) was removed and placed into a fresh tube. The pellet from this ultracentrifugation (P3) was resuspended in 50 µl of homogenization buffer and frozen on dry ice. The S3 supernatant was then centrifuged at 200,000 x g for 90 min. The supernatant from this centrifugation (S4) was removed and frozen on dry ice. The pellet (P4) was resuspended in 50 µl of homogenization buffer and frozen on dry ice. This method has previously been used to produce fractions enriched in plasma membrane (P1), synaptic vesicle (P3), endosomal (P4), and cytosolic (S4) protein (Bennett 2003).

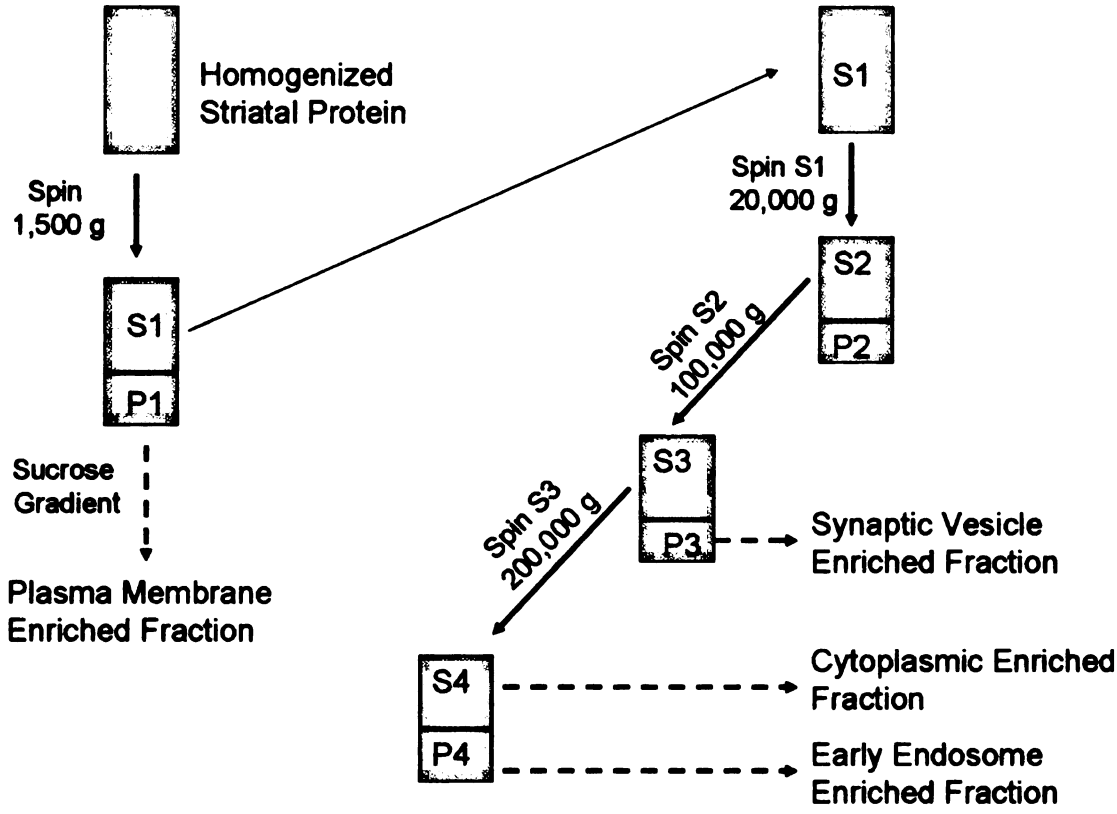

Figure 2-8. Subcellular fractionation of striatal tissue using differential centrifugation. Homogenized striatal tissue was centrifuged at 1,500 g. The pellet (P1) from this low-speed centrifugation was separated using a sucrose gradient into plasma membrane and nuclear enriched fractions. The supernatant (S1) from the initial low-speed centrifugation was centrifuged at 20,000 g. The supernatant (S2) from this high-speed centrifugation was centrifuged at 100,000 g. The pellet (P3) from this ultracentrifugation was isolated and used as the synaptic vesicle enriched fraction. The supernatant (S3) from the ultracentrifugation was centrifuged at 200,000 g to pellet light vesicles (P4). The supernatant (S4) from the second ultracentrifugation was isolated as the cytoplasmic enriched fraction.

Protein Detection/Quantification

Protein concentrations in each fraction were determined using the BCA protein method using 10 μl from each sample. Equal concentrations of protein from each fraction were separated using Western blot technique as described above. TH subcellular fractionation was determined by normalizing TH protein to the following fraction specific proteins; SNAP-25 (plasma membrane), synaptophysin (synaptic vesicle), early endosomal antigen 1 (early endosome), and monomeric β-III tubulin (cytosolic). The efficiency of subcellular fractionation was determined by measuring the immunoreactivity of fraction specific proteins in each subcellular compartment (Table 2-2). B-III tubulin, EEA1, and synaptophysin were enriched in the S4, P4, and P3 fractions, respectively, suggesting differentential centrifugation successfully isolated fractions enriched in cytosolic, early endosomal and synaptic vesicle protein. SNAP-25 however, was enriched in both P1 and P3, fractions indicative of incomplete separation of the plasma membrane fraction. Data obtained from the plasma membrane sub-cellular compartment should therefore be interpreted cautiously.

	Tubulin	EEA1	Synaptophysin	SNAP-25
Cytosol	140 ± 2	5.0 ± 0.3	n.d.	n.d.
Endosome	124 ± 1	41 ± 1	n.d.	5.5 ± 0.5
Synaptic Vesicle	71 ± 2	1.5 ± 0.1	137 ± 2	66 ± 2
Membrane	60 ± 2	3.0 ± 0.1	105 ± 5	56 ± 3

Table 2-2. Efficiency of sub-cellular fractionation using differential centrifugation. Protein immunoreactivity is shown in absorbance units (x 1000) determined using Odyssey imagining software. Results demonstrated B-III tubulin and EEA1, and synaptophysin proteins were enriched in the cytosolic, endosomal, and synaptic vesicle fractions, respectively, indicative of a good sub-cellular fractionation. SNAP-25 was enriched in both S.V. and membrane fractions, indicative of incomplete separation of the plasma membrane fraction. Values represent means of groups of 5-7 determinants ± SEM.

H. Statistical Analysis

Power analyses were conducted to determine optimal sample size required for each experiment. For experiments that involve Western blot analysis, a minimum sample size of 7 mice per group was determined to be necessary to obtain 80% power to detect a 25 % difference in means using a standard deviation of 10% that was determined from preliminary studies. One-way analysis of variance (ANOVA) tests were used to detect statistical significance between two or more groups on a single independent variable. Two-way ANOVA's were used to detect statistical significance between two or more groups when there were two independent variables in the study. An alpha value of less than or equal to 0.05 was considered statistically significant. If the two-way ANOVA revealed an interaction of statistical significance a one-way ANOVA was used for multiple comparisons among groups.

Chapter 3. The Effects of Prolonged-Chronic MPTP Administration on NSDA Neurons

A. Introduction

It is unknown why NSDA neurons progressively degenerate in PD. It is hypothesized that the loss of NSDA neurons triggers compensatory increases in the activity of surviving neurons in order to maintain sufficient levels of DA release in the striatum. The compensatory increase in activity likely contributes to the progressive demise of NSDA neurons due to increased exposure to ROS derived from enzymatic or non-enzymatic DA metabolism. To test this hypothesis, the studies described in this chapter utilized the prolonged-chronic MPTP administration to induce NSDA cell death similar to what is observed in PD. The activity of surviving neurons was assessed using pharmacological, neurochemical and immunohistochemical techniques. If this hypothesis is true then: A) MPTP will cause a compensatory increase in the activity of surviving NSDA neurons; B) changes in neuronal activity should be long-term, such that surviving neurons are chronically exposed to ROS; and C) compensatory changes in DA neuron activity should be more pronounced in NSDA neurons, as compared to other central DA neurons systems, since these neurons progressively degenerate in PD.

B. Experimental Design

To determine if MPTP-induced loss of NSDA neurons causes a compensatory increase in the activity of residual neurons a dose-response experiment was designed to identify the MPTP dose that causes axon terminal loss similar to PD. As depicted in Table 3-1, mice were injected with either MPTP (1, 5, 10, or 20, mg/kg, s.c.) or saline (1.0 ml/kg, s.c.) every 3.5 days for 5 consecutive weeks. Probenecid (250 mg/kg; i.p.) was co-administered with each MPTP injection. Probenecid inhibits the transport of organic acids across epithelial membranes, thus preventing the excretion of MPP^+ from the central nervous system (Petroske et al., 2001). Mice were killed by decapitation three weeks following the last injection and their brains were processed for neurochemical and Western blot analysis.

	MPTP Dose (mg/kg, s.c.)				
	0	1	5	10	20
Male Mice (age 10-12 weeks)	n=8	n=8	n=8	n=8	n=8

Table 3-1. Prolonged-chronic MPTP dose-response experimental design. Male mice (8 per group) were injected with either MPTP (1, 5, 10, or 20 mg/kg, s.c.) or saline (1.0 ml/kg, s.c.) every 3.5 days for 5 consecutive weeks for a total of 10 injections. Probenecid (250 mg/kg, i.p.) was co-administered with each injection of saline or MPTP. Mice were killed by decapitation three weeks following the last injection.

As depicted in Table 3-2, the primary endpoint used to determine NSDA axon terminal loss was striatal DA concentrations. Striatal DA concentrations reflect vesicular stored DA at the axon terminal, which represents greater than 99% of striatal DA as compared to extracellular DA measured by microdialysis and can be eliminated by the vesicular depletor, reserpine (Carlsson, 1975; Carboni et al., 1992; Di Chiara et al., 1996). Vesicular DA concentrations are used as an index of NSDA axon terminal integrity that reflects the ability of the axon terminal to synthesize and store DA. Additionally, striatal VMAT-2 protein was measured using Western blot analysis. VMAT-2 is a vesicular protein unique to catecholamine neurons in the brain. VMAT-2 protein levels are a reliable indicator of vesicular concentrations and provide an additional measure of axon terminal density (Wilson et al., 1996; Kilbourn et al., 2000; Reveron et al., 2002). The activity of surviving neurons was assessed by measuring striatal DOPAC concentrations and the ratio of DOPAC to DA. DOPAC is the primary metabolite of DA, and concentrations of DOPAC are an index of DA metabolism. The ratio of DOPAC to DA reflects the ratio of DA metabolism to stored DA and is an index of DA neuron activity that reflects the rate of DA release, reuptake and metabolism in NSDA neurons (Westerink and Spaan, 1982; DeMaria et al., 1999).

End-point Indices of NSDA Axon Terminal Neurotoxicity

Measurement	Reflects	Index of
DA	Vesicular DA	Axon terminal integrity
DOPAC	DA metabolism	Axon terminal function
DOPAC / DA ratio	DA release, reuptake and metabolism	NSDA activity
VMAT-2	Vesicle content	DA storage capacity
TH	TH protein	DA synthesis capacity
DAT	DAT protein	DA reuptake capacity
TH / DA ratio	TH expression	Amount of protein per axon terminals
DAT / DA ratio	DATexpression	Amount of protein per axon terminals

Table 3-2. The primary experimental end-points used for indices of NSDA neuron function. Striatal DA and DOPAC concentrations and the DOPAC to DA ratio were determined by HPLC-EC. Striatal VMAT-2, TH and DAT protein levels were determined by Western blot analysis.

If the compensatory increase in NSDA activity (and consequently accelerated DA metabolism) contributes to NSDA cell death in PD, then prolonged-chronic MPTP should cause a sustained increase in the activity of surviving neurons. If the increase in neuronal activity is sustained, then it is likely that chronic exposure to the toxic by-products of DA metabolism contribute to progressive neuron death in PD. To determine if this is the case, time-course experiments were performed to measure the activity of surviving NSDA axon terminals either 0.5, 1, 3, or 8 weeks following the last MPTP injection. As depicted in Figure 3-1, male mice (age 10-12 weeks) were injected with either MPTP (20 mg/kg, s.c.) or saline (1.0 ml/kg, s.c.), and probenecid (250 mg/kg, i.p.) twice a week for 5 consecutive weeks. Mice were killed by decapitation at 0.5, 1, 3, or 8 weeks following the last MPTP injection and their brains were processed for neurochemical and Western blot analysis. Saline-treated mice were used as 0 time controls and were sacrificed 3 weeks after the 10^{th} saline injection. The time of the first MPTP injection was staggered so that all mice were killed on the same day. NSDA activity in surviving neurons was determined by measuring the DOPAC to DA ratio.

In order to determine what neurochemical changes occur in NSDA neurons that permits prolonged accelerations in activity, the present study measured the expression of TH and DAT protein in surviving neurons using Western blot analysis. TH and DAT regulate DA synthesis and reuptake at the axon terminal, respectively, the two primary sources of cytoplasmic DA that can be metabolized to produce ROS. Thus, changes in the expression of TH or DAT may reflect compensatory changes in DA synthesis or reuptake, respectively that underlies the compensatory increase in activity. TH and DAT protein content were determined in the striatum by normalizing protein expression,

determined through Western blot analysis, to striatal DA concentrations to account for the loss of axon terminals following MPTP. TH and DAT protein content are an index of the relative amount of these proteins expressed in the axon terminals of NSDA neurons.

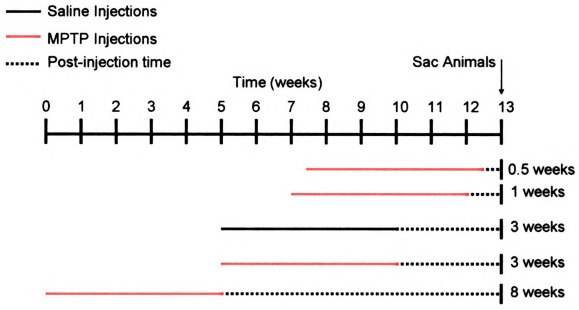

Figure 3-1. Experimental design for MPTP time-course experiments. Mice were injected with either MPTP (red, 20 mg/kg, s.c.) or saline (blue, 1.0 ml/kg, s.c.) and killed by decapitation at 0.5, 1, 3, or 8 weeks (dashed line, n=8 per group) following the last injection. Probenecid (250 mg/kg, i.p.) was co-administered with each injection of saline or MPTP. The day of the first MPTP injection was staggered so that all animals were killed on the same day.

It is unknown why NSDA neurons are more vulnerable than other populations of DA neurons in PD. One strategy used to answer this question is to compare NSDA neurons to other populations of DA neurons that are less vulnerable in PD. Thus, the compensatory increase in activity may be an attribute that is unique to NSDA neurons that renders them vulnerable in PD. In this case, axon terminal loss induced by MPTP should only cause a compensatory increase in the activity of these neurons as compared to other DA neuron populations. To test this, the effect of prolonged-chronic MPTP administration on DA neuron activity was compared between NSDA, mesolimbic (MLDA) and tuberoinfundibular (TIDA) neurons.

MLDA neurons reside in the ventral tegmental nucleus in the midbrain and project axons through the medial forebrain bundle to terminate primarily in the limbic structures including the nucleus accumbens, amygdala, olfactory tubercles, and septum. Similar to NSDA neurons, MLDA neurons synthesize and release DA at the axon terminal and are regulated by D2 autoreceptors. The synaptic action of DA is terminated via reuptake at the DAT (Lookingland, 2005). There is evidence that MLDA neurons also degenerate in PD, however to a lesser extent than NSDA neurons (German et al., 1989). Thus, it is hypothesized that MPTP will cause a less severe loss of MLDA axon terminals and a less robust increase in neuronal activity compared to NSDA neurons.

TIDA neurons are distinct from NSDA and MLDA neurons in several respects. TIDA neurons reside in the arcuate nucleus (A12) and project ventrally a short distance to the median eminence. Median eminence DA is released into the hypophysial portal vasculature and is transported to the anterior lobe of the pituitary where it binds to DA receptors on lactotrophs and tonically inhibits prolactin secretion (Ben-Jonathan, 1985).

TIDA neurons do not express D2 autoreceptors and as such, DA synthesis and release are not controlled at the axon terminal by autoreceptors (Gudelsky and Moore, 1976; Demarest and Moore, 1979b; Lookingland and Moore, 1984). Since DA released from TIDA neurons travels through the hypophysial portal system to the anterior pituitary, the relevance of DAT-mediated reuptake in these neurons is questionable since DA is transporter away (Demarest and Moore, 1979a). Cell bodies in the arcuate nucleus stain very weakly for DAT protein, while axon projections to the external layer of the median eminence have relatively strong immunoreactivity (Revay et al., 1996). Tritiated-DA uptake occurs in the median eminence, however it has a much lower affinity for the DAT in these neurons. Taken together, these results suggest that these neurons express the DAT but it is less functional than in other DA neurons (Cuello and Iversen, 1973; Demarest and Moore, 1979b; Annunziato et al., 1980). Thus, in the axon terminals of TIDA neurons, the metabolism of newly synthesized, un-released DA is the primary source of DOPAC (Lindley et al., 1990). Unlike NSDA and MLDA neurons, TIDA neurons are spared in PD (Langston and Forno, 1978; Braak and Braak, 2000). Therefore, it is hypothesized that MPTP will not cause TIDA axon terminal loss and subsequently, no change in the activity of these neurons.

B. Results

The Effects of Prolonged-Chronic MPTP on NSDA Neurons

Prolonged-chronic MPTP treatment produced a dose-dependent decrease in striatal DA concentrations in mice (Figure 3-2). Administration of 10 mg/kg and 20 mg/kg of MPTP decreased striatal DA concentrations by approximately 50% and 90%, respectively, when compared to saline-treated control mice. There was also a dose-dependent decrease in DOPAC concentrations in the striatum of mice treated with MPTP (Figure 3-3, A). Administration of 10 and 20 mg/kg of MPTP decreased striatal DOPAC concentrations by 30% and 80%, respectively. In both the 10 and 20 mg/kg MPTP groups the loss of DOPAC was less severe than the loss of DA. As such, there was an increase in the DOPAC to DA ratio in these mice (Figure 3-3, B). The increased DOPAC to DA ratio was significantly correlated (0.72) with the MPTP-induced decrease in striatal DA (Figure 3-4). Prolonged-chronic MPTP also produced a dose-dependent decrease in striatal VMAT-2 immunoreactivity (Figure 3-5)

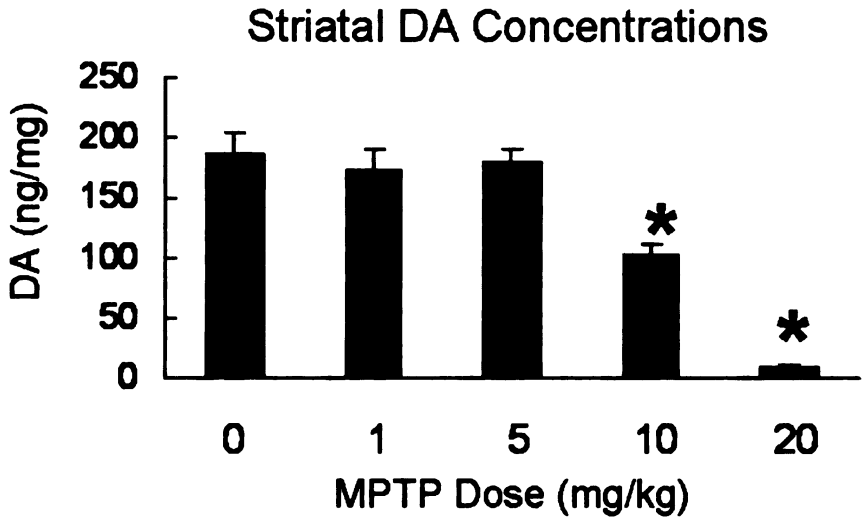

Figure 3-2. Dose response effect of prolonged-chronic MPTP administration on DA concentrations in the striatum. Mice were treated with either MPTP (1, 5, 10 or 20 mg/kg, s.c.) or its saline vehicle (1 ml/kg, s.c.) every 3.5 days for 5 consecutive weeks and killed by decapitation 3 weeks following the last injection. Probenecid (250 mg/kg, i.p.) was co-administered with each injection of saline or MPTP. Columns represent means of groups, vertical lines represent 1 S.E.M. of six to eight determinants. (*) indicate a significant difference from saline treatment group. ($p \leq 0.05$).

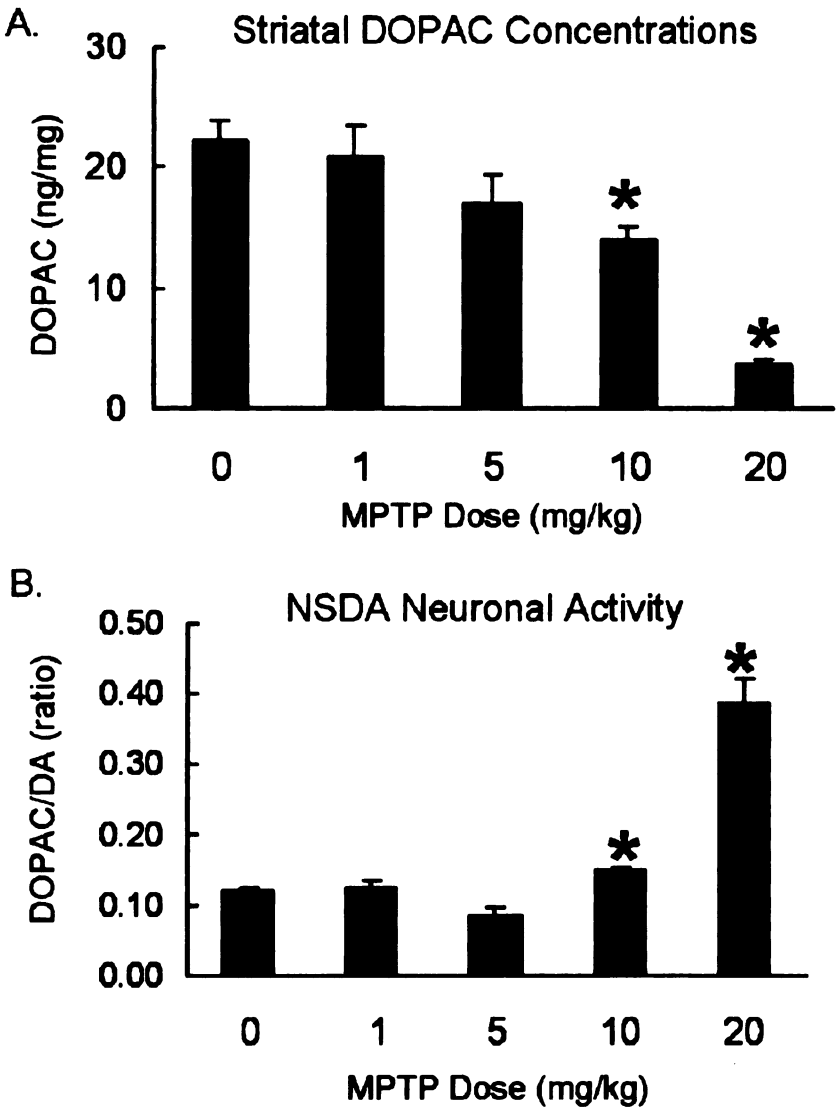

Figure 3-3. Dose response effect of prolonged-chronic MPTP administration on striatal DOPAC concentrations (A) and the DOPAC/DA ratio (B). Mice were injected with either MPTP (1, 5, 10, or 20 mg/kg, s.c.) or its saline vehicle (1 ml/kg, s.c.) and killed by decapitation 3 weeks following the last injection. Probenecid (250 mg/kg, i.p.) was co-administered with each injection of saline or MPTP. Columns represent means of groups, vertical lines represent 1 S.E.M. of six to eight determinants. (*) indicate a significant difference from saline treatment group. ($p \leq 0.05$).

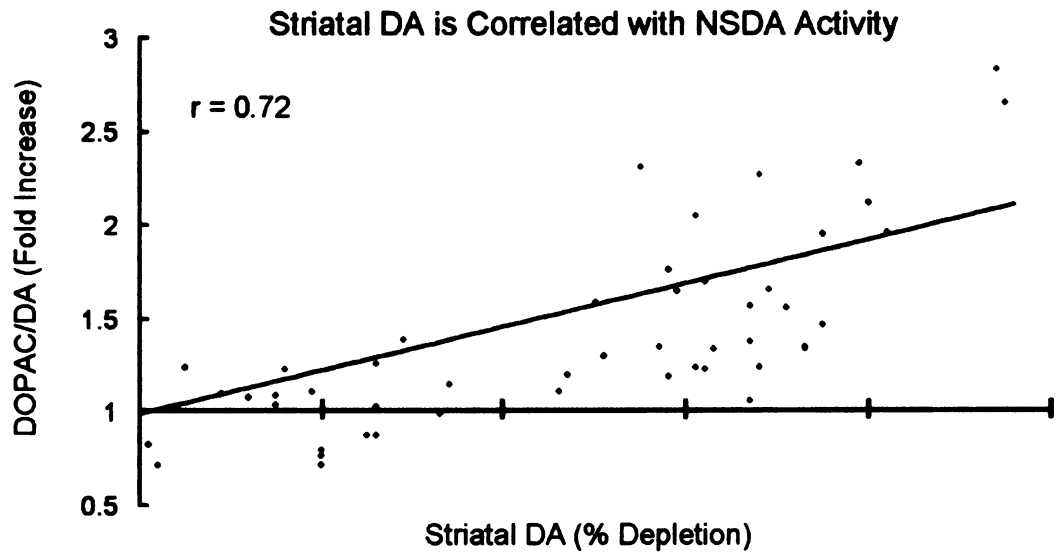

Figure 3-4. Correlation between the DOPAC/DA ratio (shown as fold increases over saline-treated controls) and striatal DA concentrations (shown as a percent depletion of control mice) in response to prolonged-chronic MPTP (1, 5, 10, or 20 mg/kg, s.c.). There was a significant correlation between the DOPAC/DA ratio and DA concentrations. $r = 0.72$. $p \leq 0.001$.

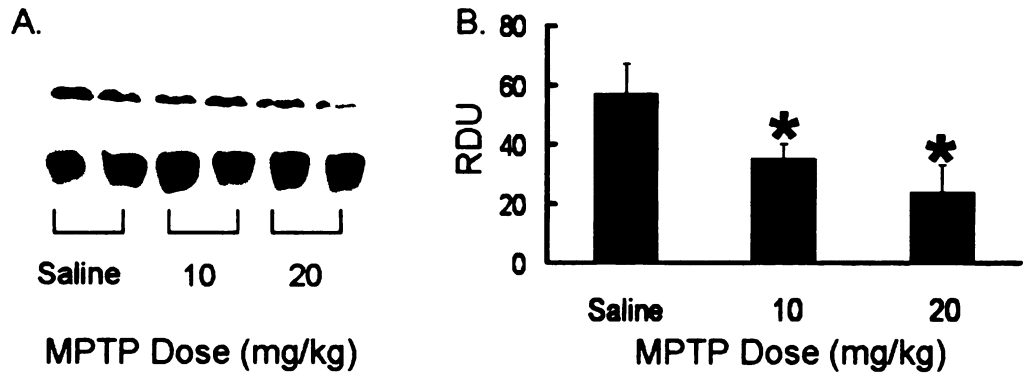

Figure 3-5. Dose response effect of prolonged-chronic MPTP administration on striatum VMAT-2 immunoreactivity. Mice were injected with either MPTP (10 or 20 mg/kg, s.c.) or its saline vehicle (1.0 ml/kg, s.c.) every 3.5 days for 5 consecutive weeks and killed by decapitation 3 weeks following the last injection. Probenecid (250 mg/kg, i.p.) was co-administered with each injection of saline or MPTP. (A) Two representative immunoblot samples of striatal VMAT-2 (80 kDa) and b-III-Tubulin (50 kDa) protein following prolonged, chronic MPTP or saline treatment. (B) Quantification of striatal VMAT-2 protein. Relative density units (RDU) were obtained by normalizing the β-III tubulin signal from the VMAT-2 protein signal. Columns represent means of groups, vertical lines represent 1 S.E.M. of six to eight determinants. (*) indicate a significant difference from saline treatment group. ($p \leq 0.05$).

Prolonged-Chronic MPTP Time-Course

Compared to saline-treated mice, DA concentrations were significantly reduced in all mice treated with prolonged-chronic MPTP (20 mg/kg, s.c.), however, the degree of DA loss was different depending on whether mice were killed 0.5, 1, 3 or 8 weeks after the last MPTP injection (Figure 3-6). In the group of mice killed 0.5 weeks after the last MPTP injection, DA concentrations were decreased to approximately 90% of saline-treated controls. This degree of loss was similar in mice killed at 1 or 3 weeks after the last MPTP injection (90% and 80%, respectively). However, DA concentrations were significantly increased in mice killed 8 weeks after the last MPTP injection compared to mice killed 3 weeks after the last MPTP treatment.

The MPTP-induced loss of striatal DOPAC concentrations was similar to the loss of DA, but less severe. In mice killed 0.5 weeks after the last MPTP injection, striatal DOPAC concentrations were reduced to approximately 40% of saline-treated mice. These levels were similar to mice killed 1and 3 weeks after the last MPTP treatment (Figure 3-7, A). However, there was a significant increase in DOPAC concentrations between the 3 and 8 week MPTP treatment groups. Due to the less severe loss of DOPAC compared to DA, the DOPAC to DA ratio was increased in all mice that were treated with MPTP (Figure 3-7, B).

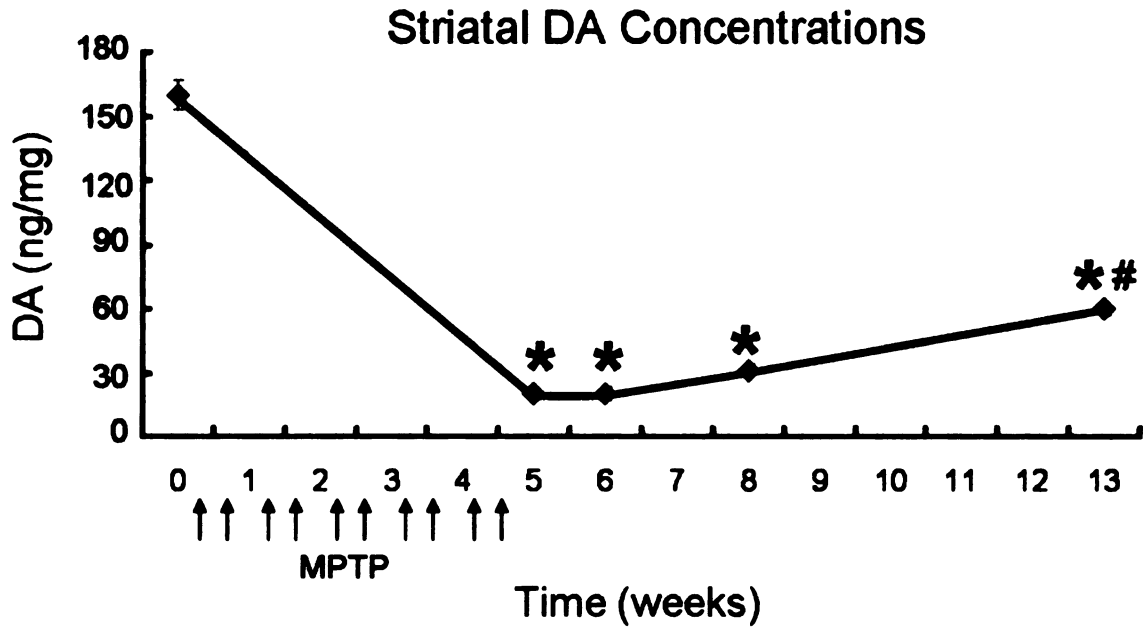

Figure 3-6. Time-course of striatal DA concentrations in mice treated with prolonged-chronic MPTP (20 mg/kg, s.c.) or its saline vehicle (1.0 ml/kg, s.c.). DA concentrations were measured 0.5, 1, 3 or 8 weeks following the last MPTP injection. Saline-treated mice were used as zero time controls and killed 3 weeks following the last injection. Data points represent means of groups, vertical lines represent 1 S.E.M. of six to eight determinants. Arrows represent MPTP injections. (*) indicate a significant difference from saline treatment group. # indicate a significant difference from mice killed 0.5, 1 or 3 weeks following MPTP treatment. $p \leq 0.05$.

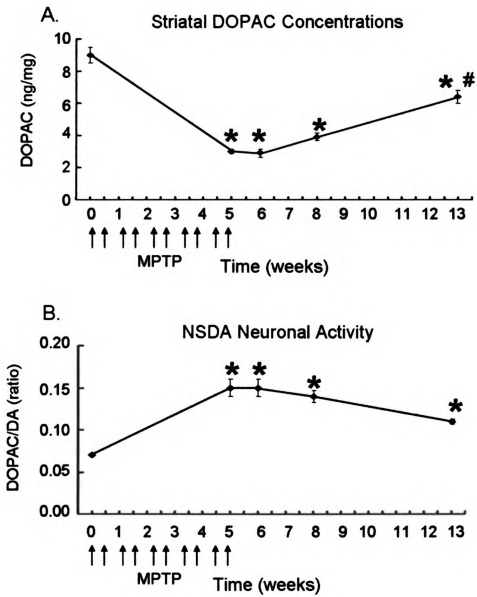

Figure 3-7. Time-course of striatal DOPAC concentrations (A) and the DOPAC/DA ratio (B) in mice treated with prolonged-chronic MPTP (20 mg/kg, s.c.) or its vehicle (1.0 ml/kg, s.c.). DOPAC concentrations and DOPAC/DA ratios were measured 0.5, 1, 3 or 8 weeks following the last MPTP injection. Saline-treated mice were used as zero time controls and killed 3 weeks following the last injection. Data points represent means of groups, vertical lines represent 1 S.E.M. of six to eight determinants. Arrows indicate MPTP injections. (*) indicates a significant difference from saline treatment group. # indicate a significant difference from mice killed 3 weeks following MPTP. $p \leq 0.05$.

B. TH and DAT Expression Following MPTP

Striatal TH protein expression was significantly decreased in all mice that were treated with prolonged-chronic MPTP (Figure 3-8). TH was decreased 50% in mice killed 0.5 weeks after the last MPTP injection (Figure 3-8, B). The degree of TH loss was consistent in mice killed at 1, 3 or 8 weeks following MPTP treatment. When compared to the loss of striatal DA concentrations, there was an increase in the ratio of TH to DA in mice killed 3 weeks after the last MPTP injection (Figure 3-8, C). Striatal DAT protein was also significantly decreased in mice that were treated with prolonged-chronic MPTP. However, the degree of DAT loss was different depending on whether mice were killed 0.5, 1, 3 or 8 weeks after drug treatment (Figure 3-9, B). In mice killed 0.5 weeks after MPTP, DAT was decreased by approximately 50%. DAT protein levels were consistent between the 0.5 and 1 week groups. However, in mice killed 3 weeks after MPTP, DAT was significantly decreased as compared to mice killed at 0.5 and 1 week after MPTP. DAT expression was increased in mice killed 8 weeks after MPTP to levels comparable with the 3 week groups. In contrast, to TH, the ratio of DAT protein to striatal DA concentrations did not change in mice killed 3 weeks after the last MPTP injection (Figure 3-9, C).

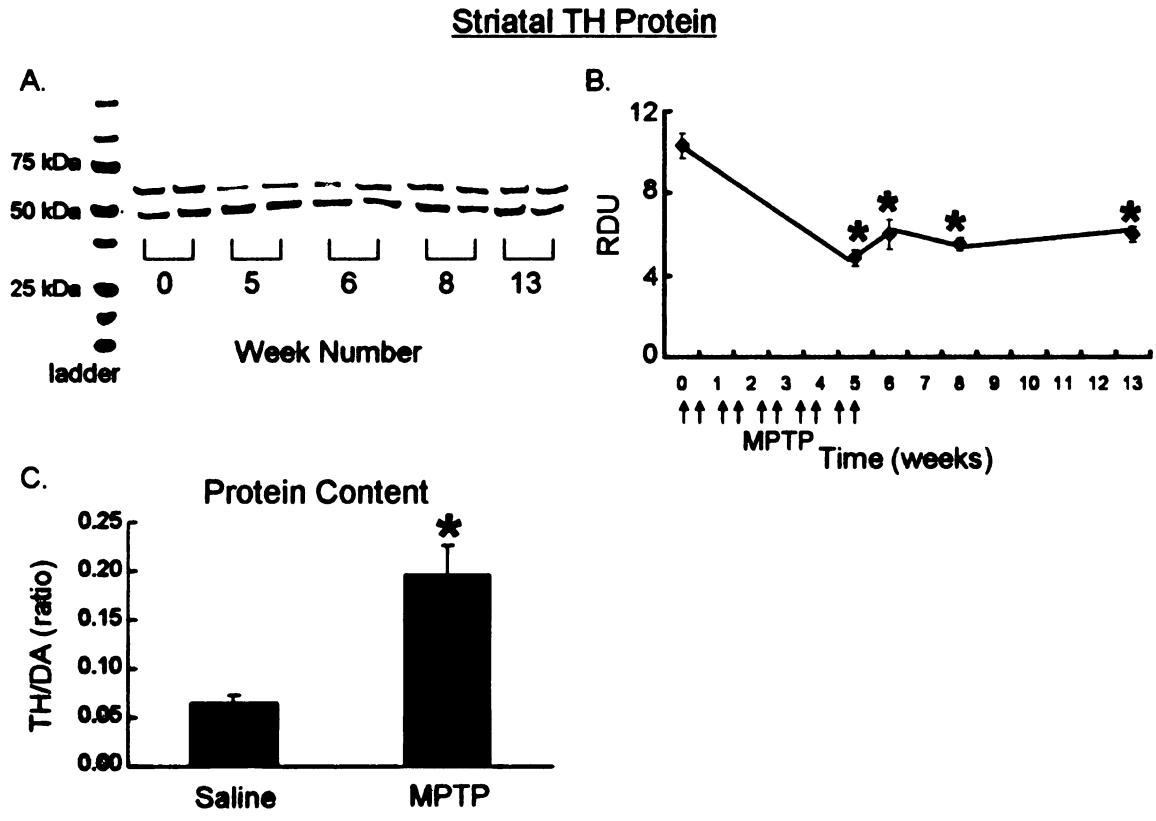

Figure 3-8. (A) Representative immuno-blot demonstrating the effects of prolonged-chronic MPTP (20 mg/kg, s.c.) or its saline vehicle (1.0 ml/kg, s.c.) on striatal TH (~55 kDa), and β-III tubulin (~50 kDa) protein expression. Striatal TH and β-III tubulin protein are shown for two mice per group. (B) Quantification of TH immunoreactive bands following prolonged-chronic MPTP administration. TH was measured in mice sacrificed 0.5, 1, 3 or 8 weeks following the last MPTP injection. Saline-treated mice were used as zero time controls and killed 3 weeks after the last injection. Relative density units (RDU) for TH were obtained by normalizing band density of the TH signal to the band density of β-III tubulin. (C) TH protein content in the striatum of mice treated with either saline or MPTP and killed 3 weeks after the last MPTP injection. TH protein content was determined by normalizing TH RDU to striatal DA concentrations for each mouse. Values represent means of groups (n=6-8) ± 1 S.E.M. of six to eight determinants. (*) indicate a significant difference from saline treatment group. $p \leq 0.05$.

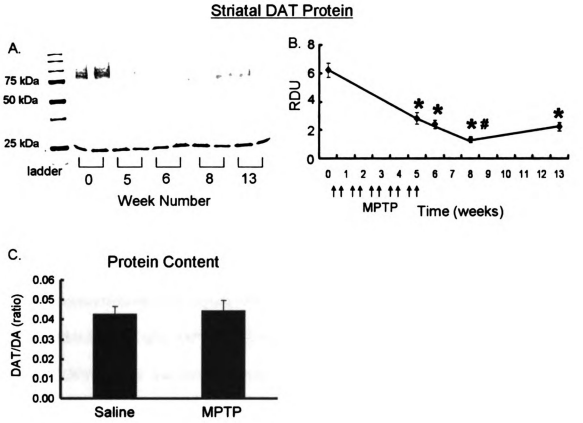

Figure 3-9. (A) Representative immuno-blot demonstrating the effects of prolonged-chronic MPTP (20 mg/kg, s.c.) or its saline vehicle (1.0 ml/kg, s.c.) on striatal DAT (~80 kDa), and SNAP-25 (~25 kDa) protein expression. Striatal DAT and SNAP-25protein are shown for two mice per group. (B) Quantification of DAT immunoreactive bands following prolonged-chronic MPTP administration. DAT was measured in mice sacrificed 0.5, 1, 3 or 8 weeks following the last MPTP injection. Saline-treated mice were used as zero time controls and killed 3 weeks after the last injection. Relative density units (RDU) for DAT were obtained by normalizing band density of the DAT signal to the band density of SNAP-25. (C) DAT protein content in the striatum of mice treated with either saline or MPTP and killed 3 weeks after the last MPTP injection. DAT protein content was determined by normalizing DAT RDU to striatal DA concentrations for each mouse. Values represent means of groups ± 1 S.E.M. of six to eight determinants. (*) indicate a significant difference from saline treatment group. # indicate a significant difference from mice killed at 6 weeks, 1 week after the last MPTP injection. $p \leq 0.05$.

C. The Effect of Prolonged-Chronic MPTP on MLDA and TIDA Neurons

As depicted in Table 3-3, prolonged-chronic MPTP administration produced a less severe loss of DA concentrations in the nucleus accumbens than in the striatum. In mice killed 0.5 weeks after MPTP administration, nucleus accumbens DA concentrations were reduced to approximately 40% of saline-treated controls. This degree of nucleus accumbens DA loss was similar in all mice treated with MPTP. In contrast, prolonged-chronic MPTP administration had no effect on DA concentrations in the median eminence of mice killed at any time point (Table 3-3).

As depicted in Table 3-4, compared to saline-treated mice, nucleus accumbens DOPAC concentrations were significantly decreased in all mice treated with MPTP. In mice killed 0.5 weeks after MPTP, DOPAC was decreased by approximately 50%. The degree of DOPAC loss was similar in mice killed 1 and 3 weeks following MPTP. However, DOPAC concentrations were significantly increased in mice killed 8 weeks after MPTP compared to the 0.5, 1, or 3 week groups. There was no change in DOPAC concentrations in the median eminence in mice treated with MPTP and sacrificed at any time point (Table 3-4). As shown in Figure 3-10, the DOPAC to DA ratio was significantly increased in the nucleus accumbens of mice killed 0.5, 3, and 8 weeks following MPTP, however, there was no effect in the median eminence.

	Time after MPTP (weeks)				
	0	0.5	1	3	8
Nucleus Accumbens	99 ± 5	37 ± 3*	44 ± 6*	45 ± 4*	45 ± 5*
Median Eminence	100 ± 6	98 ± 7	109 ± 9	103 ± 8	113 ± 11

Table 3-3. Nucleus accumbens and median eminence DA concentrations in mice treated with prolonged-chronic MPTP (20 mg/kg, s.c.) or its saline vehicle (1.0 ml/kg, s.c.). DA concentrations were measured 0.5, 1, 3 or 8 weeks following the last injection. Saline-treated mice were used as zero time controls and were killed 3 weeks after the last injection. Values represent means of groups ± 1 S.E.M.. (*) indicate a significant difference from saline treatment group. $p \leq 0.05$.

	Time after MPTP (weeks)				
	0	0.5	1	3	8
Nucleus Accumbens	13.4 ± 0.6	6.7 ± 0.3*	6.4 ± 0.7*	7.1 ± 0.6*	8.3 ± 0.7*#
Median Eminence	3.2 ± 0.4	2.2 ± 0.4	3.1 ± 0.4	3.1 ± 0.2	3.1 ± 0.3

Table 3-4. Nucleus accumbens and median eminence DOPAC concentrations in mice treated with prolonged-chronic MPTP (20 mg/kg, s.c.) or its saline vehicle (1.0 ml/kg, s.c.). DOPAC concentrations were measured 0.5, 1, 3 or 8 weeks following the last MPTP injection. Saline-treated mice were used as zero time controls and were killed 3 weeks after the last injection. Values represent means of groups ± 1 SE.M. (*) indicate a significant difference from saline treatment group. # indicate a significant difference from mice killed 3 weeks after the last MPTP injection. $p \leq 0.05$.

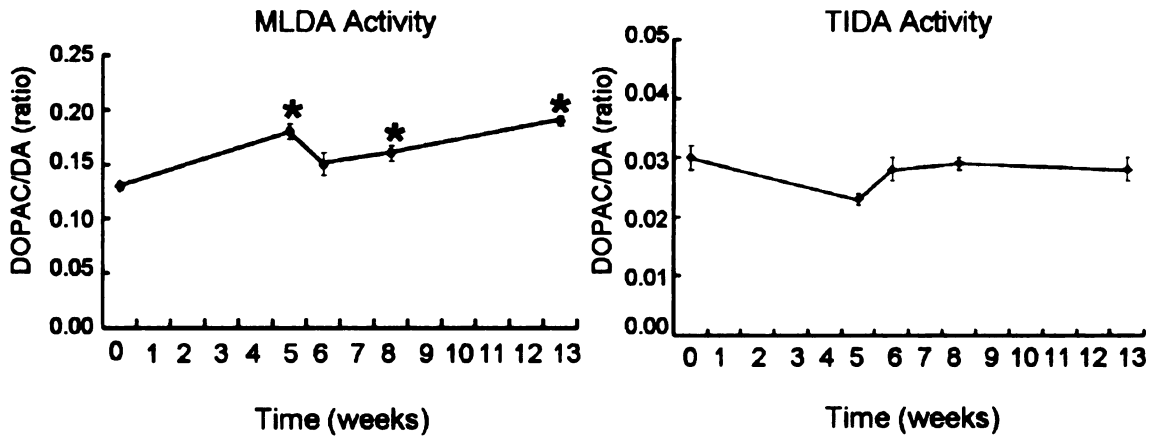

Figure 3-10. The DOPAC to DA ratio in the nucleus accumbens and median eminence in mice treated with prolonged-chronic MPTP (20 mg/kg, s.c.) or its saline vehicle (1.0 ml/kg, s.c.). DOPAC to DA ratios were measured 0.5, 1, 3 or 8 weeks following the last MPTP injection. Saline-treated mice were used as zero time controls and were killed 3 weeks after the last injection. Values represent means of groups ± 1 S.E.M. (*) indicate a significant difference from saline treatment group. $p \leq 0.05$.

C. Discussion

The present studies have demonstrated that prolonged-chronic MPTP administration causes a loss of NSDA axon terminals that is similar to what is observed in PD. The loss of NSDA axon terminals was associated with an increase in DA metabolism in surviving neurons. MPTP induced long-term changes in the activity of surviving neurons and this effect was not restricted to NSDA neurons. The results from these studies are consistent with the finding that in PD, the loss of NSDA neurons triggers a compensatory increase in the activity of NSDA neurons (Ribeiro et al., 2002; Sossi et al., 2002). Due to the toxic nature of DA metabolism, the increased activity may contribute to the progressive degeneration of NSDA neurons in PD.

The Effects of Prolonged-Chronic MPTP on NSDA Axon Terminal Loss

Following systemic administration of MPTP, the lipophillic molecule crosses the blood brain barrier and is absorbed primarily by glial cells, where it is converted to its active metabolite MPP^+ and released. MPP^+ is primarily taken into the axon terminals of DA neurons, due to its affinity for the DAT, where it accumulates in mitochondria and binds to and inhibits complex I of the electron transport chain. Axon terminal death was originally believed to result from ATP depletion and overproduction of ROS (Nicklas et al., 1985). Recently it was determined that MPP^+ is a weak inhibitor of mitochondrial complex I (Ramsay et al., 1991) and furthermore, greater than 72% reductions in complex I activity are required before mitochondrial function and ATP levels are compromised (Davey and Clark, 1996). These results suggest that MPTP toxicity is not the result of compromised mitochondrial function. The primary mechanism of MPTP

toxicity is believed to be due to ROS and DA-quinones generated from DA oxidation. Following MPP^+ uptake into the axon terminal there is a robust displacement of vesicular DA into the cytoplasm and this is associated with an increase in ROS. If DA stores are depleted prior to MPTP administration, there is no increase in ROS and cellular toxicity is completely blocked (Lotharius and O'Malley, 2000). Once the ROS generated from DA oxidation exceeds the capability of intracellular antioxidant proteins, oxidative damage to the axon terminals occurs. If the oxidative damage is severe enough it may destroy the axon terminals.

In the present study, the effects of repeated MPTP injections was assessed by measuring NSDA axon terminal loss. NSDA axon terminal loss in the striatum was determined by measuring concentrations of striatal DA three weeks following the last injection of MPTP. DA concentrations reflect DA storage at the axon terminal and are used as an index of axon terminal integrity. MPTP caused a dose-dependent decrease in NS DA concentrations, which is indicative of a dose-dependent destruction of NSDA axon terminals. Alternatively, since MPTP displaces vesicular DA, the decreased DA concentrations could reflect a deficit in DA storage as opposed to loss of terminals. However, this is unlikely because DA concentrations were measured 3 weeks after the last MPTP injection, long after the neurotoxin has been excreted from the body and direct effects on vesicular storage have subsided (Przedborski et al., 2001). Repeated MPTP injections (20 mg/kg) caused NSDA axon terminal loss similar to what is observed in PD (Hornykiewicz, 1975), suggesting that prolonged, exposure to ROS derived from DA oxidation likely plays a key role in PD pathogenesis. This hypothesis is strengthened by

severe oxidative damage found in the striatum of post-mortem PD brains (Dexter et al., 1989; Schapira et al., 1990; Dexter et al., 1994).

Prolonged administration of MPTP caused severe damage to NSDA axon terminals that persisted for several weeks after the last insult. In mice treated with 20 mg/kg, of MPTP there was a significant loss of NSDA axon terminals up to 8 weeks following the last injection. Thus, prolonged complex I inhibition in mice causes a robust, chronic loss of axon terminals, similar to what is observed in PD. Axon terminal recovery, as reflected by an increase in striatal DA concentrations, was observed between mice killed 3 and 8 weeks after the last MPTP injection, suggesting that in those 5 weeks, new axon terminals sprouted from existing NSDA neurons and re-innervated the striatum. It is unlikely that the recovery was the result of neurogenesis, since under basal conditions and following toxic insult there are no cells in the substantia nigra that co-label with TH and bromodeoxyuridine a marker for proliferating cells (Frielingsdorf et al., 2004).

Interestingly, sprouting of new axon terminals and recovery does not occur in PD, or in non-human primates treated with MPTP. Thus, recovery is a phenomenon that is specific to the mouse MPTP model of PD. Identifying the mechanisms in the mouse that facilitate recovery has become an interesting area of PD research that may lead to new therapeutic targets for human PD. However, in mice killed at either 0.5, 1 or 3 weeks following MPTP administration, NSDA axon terminals loss is severe and long lasting and there is no evidence of axonal sprouting. Thus, prolonged-chronic MPTP administration recapitulates the key pathological features of idiopathic PD at these time points.

The Effect of Prolonged-Chronic MPTP on the Activity of Surviving NSDA Neurons

The purpose of these studies was to determine if a lesion of the NSDA pathway similar to what occurs in PD causes a compensatory increase in the activity of un-lesioned neurons. The activity of surviving neurons was assessed by measuring the ratio of DOPAC to DA in the striatum of mice treated with MPTP. The ratio of DOPAC to DA reflects the rate of DA release, reuptake and metabolism, and is used as an index of DA neuron activity (Westerink and Spaan, 1982; DeMaria et al., 1999). Chronic exposure to ROS derived from DA oxidation produced a robust lesion of the NSDA pathway and a dose-dependent increase in the activity of surviving neurons. The degree of the lesion was significantly correlated with activity of residual, un-lesioned neurons. These results suggest that as NSDA axon terminals are destroyed by MPTP, surviving neurons compensate by increasing DA release in order to maintain sufficient synaptic concentrations of DA capable of activating post-synaptic D1 and D2 receptors. This is particularly relevant in the context of PD because during the early stages of the disease there is a compensatory increase in the rate of DA release in surviving NSDA neurons (Ribeiro et al., 2002; Sossi et al., 2002).

PD symptom onset likely reflects a balance between NSDA loss and the ability of remaining neurons to compensate. When neuronal compensation is not sufficient to activate post-synaptic D1 and D2 receptors and regulate the direct and indirect pathways the onset of motor symptoms occurs. Unfortunately, the compensatory increase in DA release, reuptake and metabolism likely contributes to the gradual, progressive loss of NSDA neurons as a result of the toxic nature of DA oxidation. Increased DA oxidation is associated with an increased exposure to the ROS; $OH^{\cdot}$, $O_2^{\cdot-}$, $ONOO^{-}$ and DA-quinone

molecules. If the increase in neuronal activity is prolonged, exposure to ROS becomes chronic and macromolecular damage and lipid peroxidation may become severe enough to cause axon terminal death. However, if the increase in activity is only transient, neuronal antioxidant defense mechanisms are likely capable of scavenging the ROS and there would be very little adverse consequences on neuron survival.

To determine if axon terminal loss induced by prolonged-chronic MPTP causes a long-term change in the activity of surviving NSDA neurons, a time-course experiment was designed to measure NSDA activity from 3 days to 8 weeks following the last MPTP injection. The results from this experiment demonstrated that NSDA activity was accelerated for at least 8 weeks following MPTP administration. Therefore, as a result of the compensatory activation, surviving NSDA neurons are chronically exposed to ROS derived from DA oxidation. The chronic exposure to ROS is likely detrimental to neuronal survival and may ultimately be responsible for the progressive loss of NSDA neurons in PD.

It is unknown what neurochemical changes occur in NSDA neurons that permits them to sustain a prolonged increase in activity. Likely, increased DA synthesis is necessary to supply the increased demand for release, and increased reuptake is likely occurs as a result of more DA being released. To determine what neurochemical changes underlie the compensatory increase in NSDA activity, TH and DAT protein expression were measured in the striatum of mice treated with prolonged-chronic MPTP using Western blot analysis. TH and DAT are responsible for regulating the rate of DA synthesis and reuptake, respectively.

The MPTP-induced loss of NSDA axon terminals was associated with decreased striatal TH protein expression. In mice treated with prolonged-chronic MPTP and killed 0.5, 1, 3 or 8 weeks following MPTP, TH was decreased by approximately 50%. However, the loss of TH was attenuated when compared to the loss of axon terminals as indicated by DA concentrations. As such, TH protein content, an index of the amount of TH per axon terminal, was increased following MPTP. Consistent with this, there is an increase in TH mRNA in NSDA neurons following MPTP administration (Jakowec et al., 2004). Thus, one mechanism surviving neurons use to increase neuronal activity is inducing expression of the rate limiting enzyme responsible for synthesizing the neurotransmitter. Presumably, this allows the rate of DA synthesis to be accelerated to supply the increased demand for release.

Interestingly, the loss of striatal DAT protein was not as uniform as TH. Initially, in mice killed 0.5 weeks following MPTP the loss of DAT was approximately 50%, similar to TH. However, in mice killed 3 weeks following the last injection of MPTP, DAT protein levels were decreased by approximately 85%. This is consistent with previous reports describing a more robust loss of DAT compared to TH protein, and no change in DAT mRNA following MPTP (Jakowec et al., 2004). The loss of DAT at this time point was consistent with the loss of striatal DA concentrations. As such, DAT protein content, an index of the amount of transporter at the axon terminal, did not change in surviving neurons. These results suggest that unlike DA synthesis, there is no change in reuptake in NSDA neurons that survive chronic MPTP administration. However, it is also possible that the expression of TH and DAT protein do not reflect the actual rate of DA synthesis and reuptake, respectively. Further experimentation is

required to determine if changes in protein expression correspond with functional changes in the rate of DA synthesis and reuptake.

The Effects of MPTP on MLDA and TIDA Neurons

PD is characterized by a more pronounced loss of NSDA neurons compared to other populations of DA neurons in the brain. The vulnerability of central DA neurons to ROS derived from DA oxidation was assessed by comparing axon terminal loss in the terminal fields of NSDA, MLDA and TI DA neurons following MPTP administration. Chronic exposure to MPTP caused a differential effect on DA neuronal populations, with NSDA neurons being the most vulnerable (~80% loss), MLDA neurons being moderately (~60% loss) affected, and TIDA neurons being completely spared. Interestingly, the differential susceptibility to neurotoxic insult was similar to the degree of DA neuronal loss observed in the populations of neurons in PD (Hornykiewicz, 1975; Langston and Forno, 1978; German et al., 1989). Therefore, these results suggest that inherent differences in the susceptibility to ROS-mediated oxidative damage are responsible for the vulnerability of NSDA neurons in PD.

Differential DAT expression, between NSDA, MLDA, and TIDA neurons could also account for the differential susceptibility to MPTP as a consequence of altered neurotoxin uptake. DAT expression is higher in NSDA neurons compared to MLDA or TIDA neurons (Shimada et al., 1992; Lorang et al., 1994; Freed et al., 1995). However, this is not the case, since these neuronal populations are also differentially sensitive to the neurotoxic effects of rotenone, a complex I inhibitor that is not dependent on DAT uptake

(Betarbet et al., 2000). Therefore, it is more likely that NSDA neurons are more vulnerable to oxidative stress-induced cell death than MLDA or TIDA neurons.

A number of mechanisms may account for the vulnerability of NSDA neurons to oxidative stress induced cell death. NSDA neurons may have higher concentrations of stored DA capable of being oxidized to ROS following displacement by MPP^+. MLDA or TIDA neurons may express higher levels of antioxidant defense proteins (such as glutathione), or proteins that prevent apoptosis (such as BCL-2). Alternatively, MLDA or TIDA neurons may react differently than NSDA neurons following exposure to ROS and oxidative damage. For example, the compensatory increase in NSDA activity may render these neurons more vulnerable

To determine if compensatory increases in activity is a phenomenon specific to NSDA neurons, the activity of MLDA and TIDA neurons was assessed following MPTP administration. Results demonstrated that the loss of approximately 60% of MLDA axon terminals was associated with increased neuronal activity in surviving, un-lesioned neurons. No change in TIDA activity was observed, supporting the hypothesis that neuronal activity increases as a compensatory mechanism in response to axon terminal loss, rather than a direct effect of MPTP. These results suggest that similar to NSDA neurons, MLDA neurons also respond to axon terminal loss by increasing DA release, reuptake and metabolism. Therefore, compensatory increases in neuronal activity may contribute to the progressive loss of NSDA neurons in PD, but they are not unique to NSDA neurons and thus, are unlikely to be responsible for the enhanced vulnerability of these neurons to ROS-mediated cell death. Future studies will have to determine if

differences in DA storage or expression of protective proteins determines the vulnerability of central DA neurons to MPTP-induced cell death.

Interestingly, as the time from the last MPTP injection increased, MLDA activity also gradually increased. Whereas NSDA activity peaked in mice killed 0.5 weeks after MPTP and continued to decline. Although compensatory changes in neuronal activity occurred in both NSDA and MLDA neurons, the time-course was different between the two populations of neurons. This may be due to differential regulation of proteins responsible for synthesizing DA at the axon terminal. Studies have demonstrated several key differences in TH gene regulation between NSDA and MLDA neurons (Pasinetti et al., 1990; Leviel et al., 1991; Sturtz et al., 1994) that may highlight the importance of increasing expression of TH protein to permit the compensatory increase in activity. It is unknown what functional consequence this has on MLDA neurons but it may affect axon terminal recovery from neurotoxic insult.

In NSDA neurons there was a recovery of axon terminals between 3 and 8 weeks after the last MPTP injection and this likely reflected axon terminal sprouting from existing neurons (Bezard et al., 2000). Recovery was associated with a decrease in the activity of surviving neurons. However; it is difficult to interpret cause and effect from these results. One possibility is that, as new axon terminals sprouted from surviving and/or lesioned neurons, the burden on individual axon terminals was lessened and activity gradually declined. Alternatively, the decrease in neuronal activity may have facilitated neuronal recovery by decreasing exposure to ROS and alleviating oxidative stress in surviving neurons. The present study cannot distinguish between these two alternatives, yet it was interesting that in MLDA neurons no axon terminal recovery was

observed, and neuronal activity gradually increased. It is possible that MPTP did not cause a sufficient lesion in MLDA neurons to induce recovery mechanisms or there may be inherent differences in NSDA versus MLDA axon terminal sprouting. The latter seems more likely since a 60% decrease in NSDA axon terminals induces recovery in NSDA neurons (Petroske et al., 2001). Taken together, the results from the present experiments highlight differences between NSDA and MLDA neurons in axonal sprouting and neuronal activity in response to a neurotoxic lesion. While the present studies are not sufficient to explain the precise mechanisms that underlie differences between NSDA and MLDA neurons, they propose a link between neuronal recovery and activity that highlight a need for additional research.

Summary

The results from the studies described in this chapter have demonstrated that chronic exposure to MPTP (and presumably ROS derived from DA oxidation), causes NSDA and MLDA axon terminal loss similar to what is observed in PD. Moreover, in response to the loss of axon terminals, surviving NSDA and MLDA neurons compensate by increasing DA release, reuptake and metabolism. As a result of ROS generated by DA oxidation, it is likely the sustained acceleration in NSDA activity causes oxidative damage and contributes to the progressive loss of NSDA neurons. Thus, preventing the compensatory activation of NSDA neurons or inhibiting DA oxidation may protect these neurons in PD. However, the neurochemical mechanisms that underlie the sustained activation of NSDA neurons are unclear. Western blot analysis of protein expression suggested changes in the DA biosynthetic pathway occur in surviving neurons. However,

further experimentation is required in order to understand the neurochemical changes that occur in NSDA neurons that permit a prolonged acceleration in DA release, reuptake and metabolism.

Chapter 4. Identification of the Neurochemical Changes that Underlie the Compensatory Activation of NSDA Axon terminals

A. Introduction

The results from Chapter 3 demonstrated that NSDA axon terminal loss causes a sustained increase in the activity of surviving axon terminals that maintains sufficient concentrations of released DA in the striatum. The accelerated activity was associated with increased DA metabolism in surviving axon terminals, reflected by an increase in the ratio of DOPAC to DA. DOPAC is an index of the enzymatic metabolism of cytoplasmic DA, thus, these results are indicative of an increase in cytoplasmic DA concentrations in surviving axon terminals. Alternatively, the increased in DA metabolism may reflect an increase in MAO activity, however this is unlikely since MAO activity is decreased following MPTP administration (Johannessen et al., 1991). Excess cytoplasmic DA can increase ROS formation in axon terminals due to enzymatic or non-enzymatic DA oxidation, suggesting that there is increased ROS exposure in surviving axon terminals. If the ROS are not scavenged by intracellular antioxidant proteins, oxidative damage to the axon terminal will occur. If oxidative damage is severe, it may cause axon terminal death. Identifying the mechanisms that are responsible for the compensatory changes that occur in NSDA axon terminals that culminate in neurotoxic levels of cytoplasmic DA levels should provide novel therapeutic targets to protect NSDA axon terminals in PD. To this end, the purpose of the experiments described in this chapter is to identify the source of the cytoplasmic DA that is metabolized in surviving NSDA axon terminals following MPTP.

As depicted in Figure 4-1, newly synthesized and recaptured DA are the two primary sources of cytoplasmic DA, and thus DA metabolism in axon terminals. An increase in the rate of either DA synthesis or reuptake could account for the increased metabolism of DA in NSDA axon terminals that survive MPTP treatment. Results from Chapter 3 showed there was an increase in TH protein expression in surviving axon terminals, suggesting an increase in newly synthesized DA may be largely responsible for the excess cytoplasmic DA and accelerated metabolism in NSDA axon terminals that survive MPTP administration. Therefore, it was hypothesized that DA synthesis is the primary source of cytoplasmic DA and increased metabolism. To test this hypothesis, pharmacological, neurochemical and immunohistochemical techniques were used to distinguish between the metabolism of newly synthesized versus recaptured DA in NSDA axon terminals under basal conditions and following activation induced by MPTP administration.

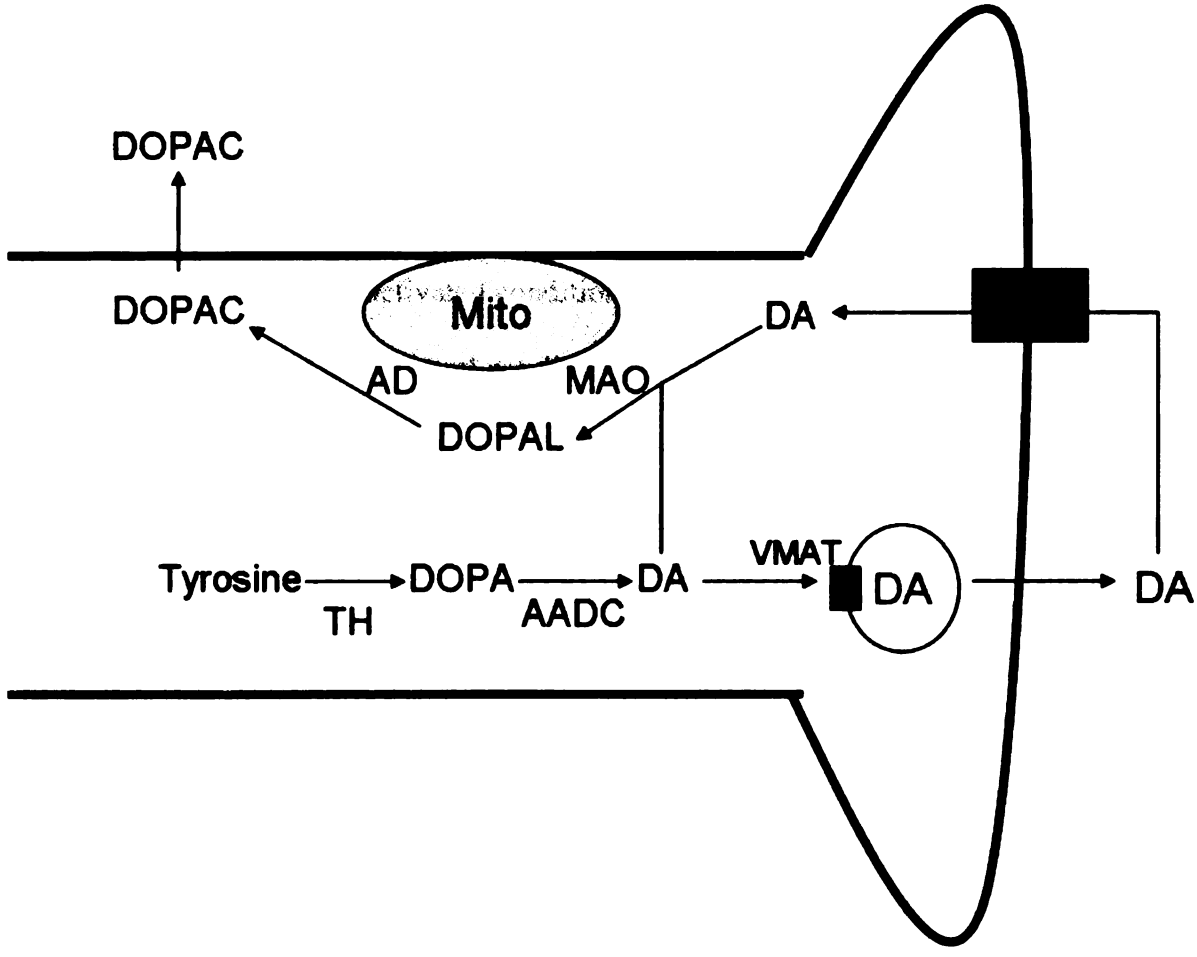

Figure 4-1. Schematic diagram of a NSDA axon terminal depicting the two primary sources of cytoplasmic DA (synthesis and reuptake). Both newly synthesized and recaptured DA can be metabolized by mitochondrial (mito) MAO to DOPAL. DOPAL is then converted to DOPAC by aldehyde dehydrogenase (AD).

B. Experimental Design and Results

Determining the Contribution of DAT-Mediated Reuptake to DA Metabolism under Basal and Activated Conditions

Blocking DAT-mediated reuptake of synaptic DA and measuring the change in striatal DOPAC concentrations provides an index of the proportion of recaptured DA that is metabolized (Figure 4-2 A,B). The contribution of recaptured DA to metabolism was compared under basal and activated conditions. To determine the amount of recaptured DA that is metabolized under basal conditions, mice were injected with either saline (1.0 ml/kg, i.p.) or the DAT blocker GBR-12909 (GBR, 10 mg/kg, i.p.) and killed 30 min later (Figure 4-2, C). This GBR administration regimen maximally inhibits DA reuptake in NSDA axon terminals (Camarero et al., 2002). Striatal DOPAC concentrations in GBR-treated mice were compared to saline-treated mice and the difference between these groups was used as an index of the proportion of recaptured DA that is metabolized.

The amount of recaptured DA metabolized under basal conditions was compared to activated conditions. Activated conditions were induced by injecting mice with MPTP in a sub-chronic regimen which consisted of MPTP injections (25 mg/kg, s.c.) once a day for 5 consecutive days. Mice were killed 3 days after the last injection. The effects of MPTP on NSDA neuron axon terminal loss were determined by measuring striatal DA concentrations. The effect of sub-chronic MPTP on the activity of surviving axon terminals was determined by measuring the ratio of DOPAC to DA, and TH and DAT protein expression. The sub-chronic MPTP model was chosen because it produces a similar loss of NSDA axon terminals as the prolonged-chronic administration regimen (but in a much shorter time frame), allowing several neurochemical experiments to be

conducted simultaneously. Control and MPTP-treated mice were then injected with either saline or GBR-12909 (10 mg/kg, i.p.) 30 min prior to sacrifice (Figure 4-2, C). Striatal DOPAC concentrations in GBR-treated mice were compared to saline-treated controls and the difference between these groups was used as a measure of the amount of recaptured DA that is metabolized under activated conditions.

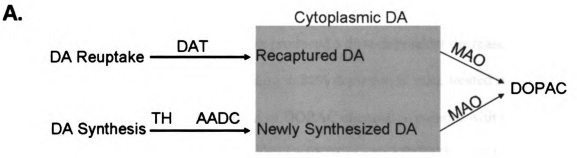

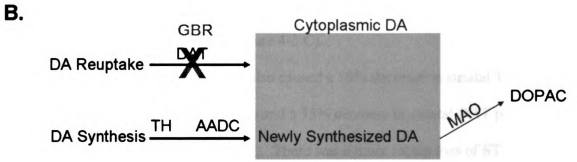

C.

Basal Conditions		Compensatory Activation	
Saline (1.0 ml/kg, i.p.)	n=7	Saline (1.0 ml/kg, i.p.)	n=7
GBR (10 mg/kg, i.p.)	n=7	GBR (10 mg/kg, i.p.)	n=7

Figure 4-2. Strategy for determining the amount of recaptured DA metabolized under basal and activated conditions. (A,B) Blockade of DAT-mediated reuptake under basal and activated conditions allows changes in striatal DOPAC concentrations to be measured as an index of the amount of recaptured DA that is metabolized. (C) Mice were injected with either saline (1.0 ml/kg, i.p.) or GBR-12909 (GBR, 10 mg/kg, i.p.) and killed 30 min later. Activated conditions were induced by injecting mice with MPTP (25 mg/kg, s.c.) once a day for 5 consecutive days. Mice were killed by decapitation 3 days after the last injection.

The Effects of Sub-Chronic MPTP on NSDA Axon terminals

Sub-chronic MPTP administration produced a dose-dependent decrease in striatal DA concentrations (Figure 4-3 A), resulting in 80% depletion in mice treated with the highest dose (25 mg/kg). Concentrations of DOPAC changed in parallel with that of DA, with a 65% decrease observed in mice treated with 25 mg/kg MPTP (Figure 4-3 B). The DOPAC to DA ratio was two-fold higher in mice treated with the highest MPTP dose compared to saline-treated controls (Figure 4-3 C).

Sub-chronic MPTP (25 mg/kg) also caused a 50% decrease in striatal TH protein expression (Figures 4-4 A,B, Left Panel) and a 75% decrease in striatal DAT protein expression (Figure 4-4 A,B, Right Panel). There was a more robust loss of ST DA concentrations compared to striatal TH expression. As such, there was an increase in TH protein content in mice treated with MPTP (Figure 4-4 C, Left Panel). Alternatively, the loss of DA concentrations was comparable to the loss of striatal DAT expression. As such, there was no change in DAT protein content (Figure 4-4 C) in the striatum of mice treated with MPTP.

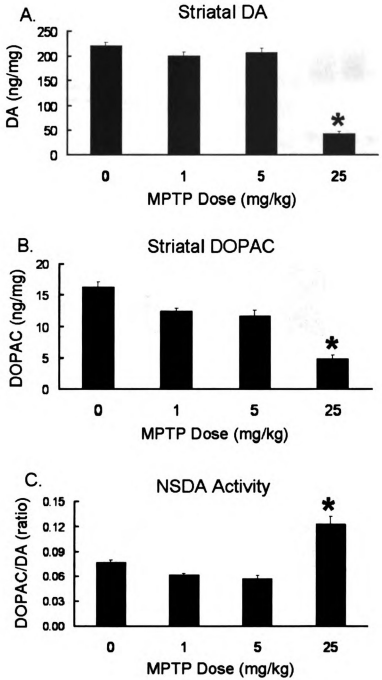

Figure 4-3. Effects of sub-chronic MPTP administration on striatal DA (A) and DOPAC (B) concentrations and DOPAC/DA ratios (C). Mice were treated with saline (1.0 ml/kg, s.c.) or MPTP (1,5, or 25 mg/kg, s.c.) once a day for five consecutive days and killed by decapitation three days following the last injection. Columns represent means of groups, vertical lines represent 1 S.E.M. of six to eight determinants. (*) indicate a significant difference from saline treatment group. ($P \leq 0.05$).

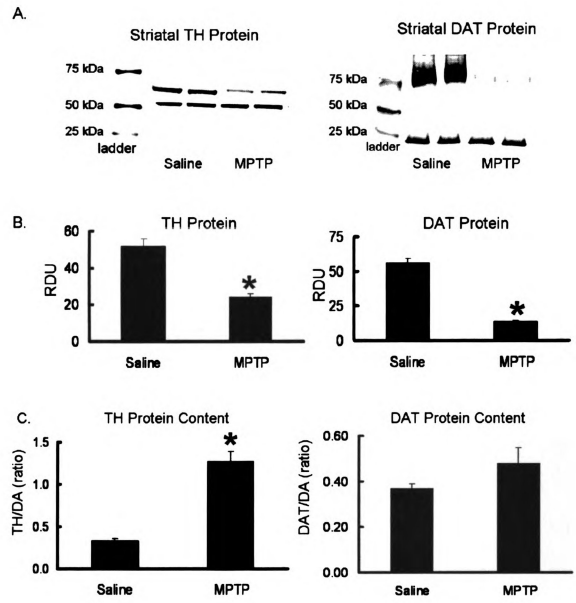

Figure 4-4. (A, LEFT PANEL) Representative immuno-blot demonstrating the effects of sub-chronic MPTP (25 mg/kg, s.c.) or saline (1.0 ml/kg, s.c.) on striatal TH (~55 kDa) and β-III tubulin (~50 kDa) or (RIGHT PANEL) DAT (~80 kDa) and SNAP-25 (~25 kDa) protein expression. (B) Quantification of TH (LEFT PANEL) and DAT (RIGHT PANEL) protein expression. Relative density units (RDU) were obtained by normalizing the band density of TH to β-III tubulin band density and DAT to SNAP-25 band density. (C) TH (LEFT PANEL) and DAT (RIGHT PANEL) protein content in the striatum determined by normalized TH or DAT RDU to striatal DA concentrations. Columns represent means of groups, vertical lines represent 1 S.E.M. of six to eight determinants. (*) indicate a significant difference from saline treatment group. ($P \leq 0.05$).

The Contribution of DA Reuptake to Striatal DA Metabolism

Under basal conditions, (vehicle pre-treated mice), GBR administration decreased striatal DOPAC concentrations by approximately 30% compared to saline-treated mice (Figure 4-5, Left Panel). Under activated conditions (MPTP pre-treated mice), GBR administration had a similar effect on striatal DOPAC concentrations as it did under basal conditions (Figure 4-5, Right Panel).

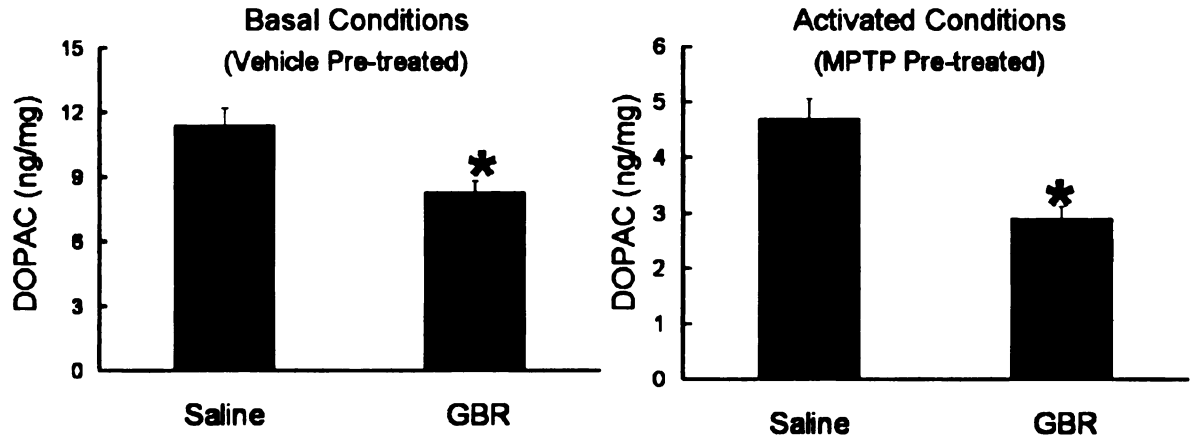

Figure 4-5. The effect of saline or GBR-12909 on striatal DOPAC concentrations under basal conditions (vehicle pre-treated, Left Panel) and activated conditions (MPTP pre-treated, Right Panel. Mice were injected with saline (1.0 ml/kg, s.c.) or MPTP (25 mg/kg, s.c.) once a day fro 5 consecutive days and killed 3 days after the last injection. Mice were injected with saline (1.0 ml/kg, i.p.) or GBR-12909 (GBR, 10 mg/kg, i.p.) 30 min prior to sacrifice. Striatal DOPAC was determined by HPLC-EC. Columns represent means of groups, vertical lines represent 1 S.E.M. of seven determinants. (*) indicate a significant difference from saline treatment group. ($P \leq 0.05$).

Determining the Contribution of DA Synthesis to Metabolism of DA

The amount of newly synthesized DA that is metabolized under basal and activated conditions was determined by blocking DA synthesis and measuring the change in striatal DOPAC concentrations. Unlike DA reuptake, synthesis is a two-step reaction that occurs within the axon terminal, the location of MAO. DA synthesis can be blocked by inhibiting TH catalytic activity with α-methylparatyrosine (AMT). AMT competes with the normal substrate tyrosine for binding to TH and decreases the conversion of tyrosine to DOPA. Alternatively, DA synthesis can be blocked by inhibiting the catalytic activity of AADC with m-hydroxybenzylhydrazine (NSD-1015) (Carlsson et al., 1972). In order to use DOPAC concentrations as an index of the rate of DA metabolism, AMT or NSD-1015 must not directly alter the enzymatic activity of MAO.

To determine if AMT or NSD-1015 alters MAO catalytic activity, purified MAO enzyme (11.5 U) was incubated with its substrate DA (5 μM) along with either; vehicle, AMT (10 μM, or 25 μM) or NSD-1015 (5 μM, 10 μM). Doses of AMT and NSD-1015 were chosen based on the expected brain concentrations of the drug following systemic injection that maximally inhibit TH and AADC activity, respectively (Widerlov and Lewander, 1978; Bongiovanni et al., 2003). MAO enzymatic activity was quantified by measuring the elimination of substrate DA, and the formation of product DOPAL using HPLC-EC. Results demonstrated that AMT had no effect on MAO activity, whereas, NSD-1015 caused a dose-dependent decrease in MAO enzymatic activity (Figure 4-6). As such, AMT was used to inhibit TH activity and DA synthesis in subsequent experiments.

Effects of AMT or NSD-1015 on MAO Activity

As depicted in Figure 4-6 (Left Panel), basal DA concentrations were determined by incubating DA with vehicle for 60 min. Incubation of DA with MAO enzyme decreased DA concentrations. The addition of AMT (10 or 25 μM) to this reaction had no effect on DA concentrations when compared to MAO and DA alone. However, incubating MAO and DA with NSD-1015 (5 or 10 μM) caused a dose-dependent increase in DA concentrations when compared to MAO and DA alone.

Consistent with DA concentrations, DOPAL concentrations were not detectable when DA was incubated in the absence of MAO. Incubation of DA with MAO enzyme dramatically increased DOPAL concentrations. The addition of AMT (10 or 25 μM) to this reaction had no effect on DOPAL concentrations. However, incubating MAO and DA with NSD-1015 (5 or 10 μM) caused a dose-dependent decrease in DOPAL concentrations compared to MAO and DA alone.

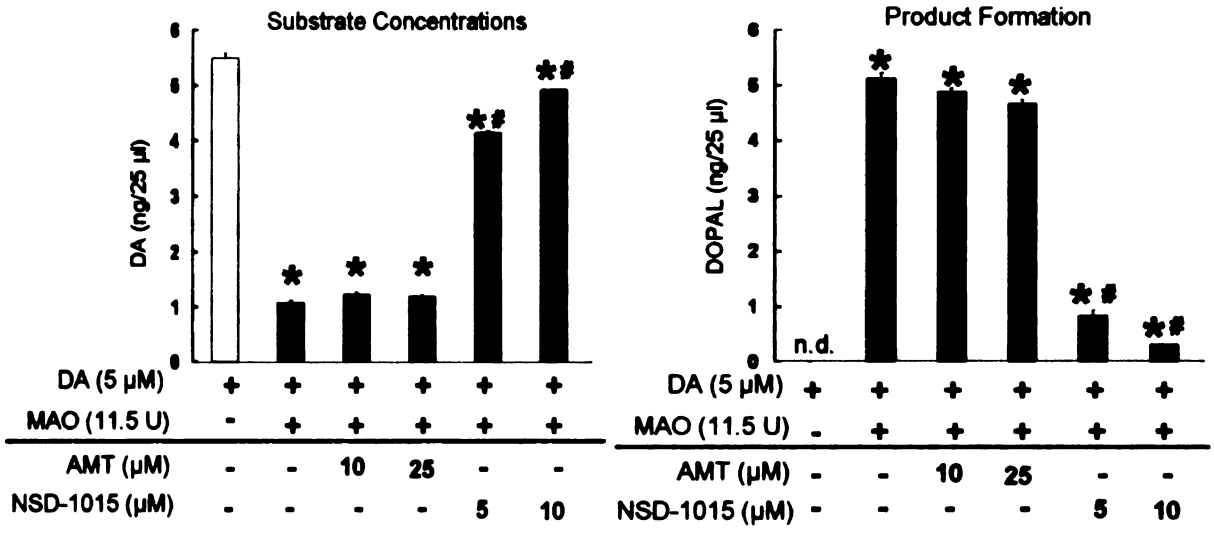

Figure 4-6. The effects of AMT and NSD-1015 on MAO enzymatic activity. DA (5 µM) was incubated with either vehicle (no MAO enzyme) or MAO (11.5 U) for 60 min. The elimination of substrate DA (LEFT PANEL) and formation of product DOPAL (RIGHT PANEL) was measured using HPLC-EC after 60 min. DA and MAO were then incubated with either AMT (10 or 25 µM) or NSD-1015 (5 or 10 µM) and DA and DOPAL concentrations were measured 60 min after the start of the reaction. Columns represent means of groups, vertical lines represent 1 S.E.M. of 4 determinants. (*) indicate a significant difference from DA -MAO group. # indicate a significant difference from DA+MAO group. ($p \leq 0.05$).

Blocking DA synthesis with AMT and measuring the decrease in striatal DOPAC concentrations should provide an index of the proportion of newly synthesized DA that is metabolized in NSDA axon terminals (Figure 4-7, AB). To determine the contribution of newly synthesized DA to metabolism under basal conditions, mice were injected with either saline (1.0 ml/kg, i.p.) or AMT (250 mg/kg, i.p.) and killed 30 min later (Figure 4-7, C). This AMT administration regimen maximally inhibits TH catalytic activity in NSDA axon terminals (Widerlov and Lewander, 1978). Striatal DOPAC concentrations in AMT-treated mice were compared to saline-treated mice and the difference between these groups was used as an index of the amount of newly synthesized DA that is metabolized under basal conditions.

To determine the proportion of newly synthesized DA that is metabolized under activated conditions mice were pre-treated with MPTP (25 mg/kg, s.c.) in a sub-chronic regimen to cause axon terminal loss and the compensatory activation of surviving axon terminals. Control and MPTP-treated mice were injected with either saline or AMT (250 mg/kg, i.p.) thirty minutes prior to sacrifice (Figure 4-7, C). Striatal DOPAC concentrations in AMT-treated mice were compared to vehicle-treated mice and the difference between these groups was used as an index of the amount of newly synthesized DA that is metabolized during the compensatory activation of NSDA axon terminals.

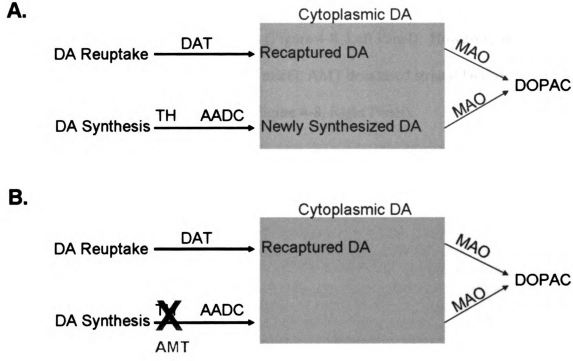

C.

Basal Conditions		Compensatory Activation	
Saline (1.0 ml/kg, i.p.)	n=7	Saline (1.0 ml/kg, i.p.)	n=7
AMT (250 mg/kg, i.p.)	n=7	AMT (250 mg/kg, i.p.)	n=7

Figure 4-7. Strategy for determining the amount of newly synthesized DA metabolized under basal and activated conditions. (A,B) TH inhibition under basal and activated conditions allows changes in striatal DOPAC concentrations to be measured as an index of the amount of newly synthesized DA that is metabolized. (C) Mice were injected with either saline (1.0 ml/kg, i.p.) or AMT (10 mg/kg, i.p.) and killed 30 min later. The decrease in striatal DOPAC concentrations was used to reflect the amount of newly synthesized DA that is metabolized under basal conditions and during the compensatory activation of NSDA axon terminals.

The Contribution of Newly Synthesized DA to Striatal DA Metabolism

Under basal conditions, (vehicle pre-treated mice), AMT administration had no effect on striatal DOPAC concentrations (Figure 4-8, Left Panel). However, under activated conditions, (MPTP pre-treated mice), AMT decreased striatal DOPAC concentrations by approximately 40% (Figure 4-8, Right Panel).

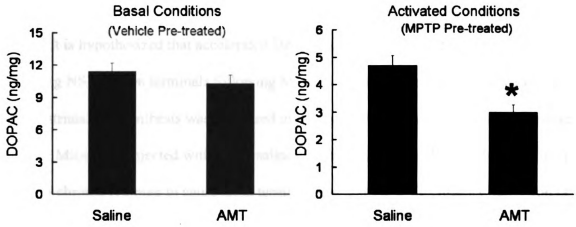

Figure 4-8. The effect of saline or α-methylparatyrosine (AMT) on striatal DOPAC concentrations under basal conditions (vehicle pre-treated, LEFT PANEL) and activated conditions (MPTP pre-treated, RIGHT PANEL). Mice were injected with saline (1.0 ml/kg, s.c.) or MPTP (25 mg/kg, s.c.) once a day fro 5 consecutive days and killed 3 days after the last injection. Mice were injected with saline (1.0 ml/kg, i.p.) or AMT (250 mg/kg, i.p.) 30 min prior to sacrifice. Striatal DOPAC was determined by HPLC-EC. Columns represent means of groups, vertical lines represent 1 S.E.M. of seven determinants. (*) indicate a significant difference from saline treatment group. ($P \leq 0.05$).

Determining the Rate of DA Synthesis in NSDA Axon terminals

It is hypothesized that accelerated DA synthesis increases cytoplasmic DA in surviving NSDA axon terminals following MPTP. To determine if this is the case, the rate of striatal DA synthesis was measured in surviving NSDA axon terminals following MPTP. Mice were injected with either saline (1.0 ml/kg, s.c.) or MPTP (25 mg/kg, s.c.) in a sub-chronic regimen to cause axon terminal loss and the compensatory activation of surviving axon terminals. NSD-1015 (100 mg/kg, i.p.) was injected 30 min prior to sacrifice and striatal DOPA concentrations were measured with HPLC-EC. The accumulation of DOPA following blockade of AADC with NSD-1015 is an *in vivo* assay for TH catalytic activity (Carlsson et al., 1972). DOPA concentrations were normalized to striatal DA concentrations to control for MPTP-induced axon terminal loss. The ratio of TH catalytic activity relative to DA concentrations is an index of the rate of DA synthesis following neurotoxic lesion (Zigmond et al., 1984).

The Rate of Striatal DA Synthesis under Basal and Activated Conditions

Sub-chronic MPTP administration caused a decrease in striatal DOPA (Figure 4-9, A) and DA concentrations (Figure 4-9, B). However, the loss of striatal DA concentrations was much more severe than the loss of DOPA concentrations. As such, MPTP caused a robust increase in the ratio of DOPA to DA in the striatum of mice treated with MPTP (Figure 4-9, C).

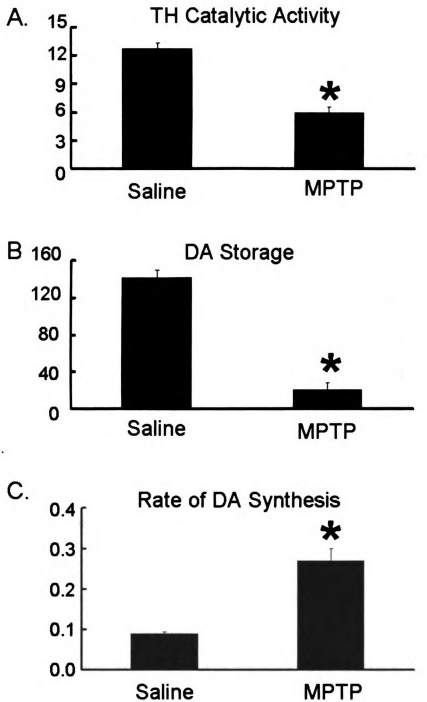

Figure 4-9. Concentrations of DOPA (A), DA (B) and the DOPA to DA ratio (C) in the striatum of mice injected with either saline (1.0 ml/kg, s.c.) or MPTP (25 mg/kg, s.c.) once a day for 5 consecutive days. DOPA concentrations were determined 30 min after NSD-1015 (100 mg/kg, i.p.) injection. Columns represent means of groups, vertical lines represent 1 S.E.M. of seven determinants. (*) indicate a significant difference from saline treatment group. ($P \leq 0.05$).

C. Discussion

The Effect of Sub-Chronic MPTP Administration on NSDA Axon terminals

Sub-chronic MPTP administration produced similar effects on NSDA axon terminals as the prolonged-chronic administration regimen despite a decreased cumulative dose and time-course. Sub-chronic MPTP caused an 80% loss of NSDA axon terminals and a compensatory increase in the activity of surviving axon terminals. Moreover, TH and DAT protein expression were decreased in the striatum by 50 and 85% respectively, which was consistent with changes in the expression of these proteins in the striatum following prolonged-chronic MPTP. A less severe decrease in TH protein expression compared to loss of axon terminals suggests there is an increase in TH expression in surviving axon terminals following MPTP. The equal loss of DAT protein and axon terminals induced by MPTP is indicative of no change in DAT protein expression in surviving axon terminals. Thus, the toxicity to NSDA axon terminals, induced by sub-chronic MPTP is comparable in extent to the prolonged-chronic administration regimen and surviving axon terminals appear to compensate through similar mechanisms.

The sub-chronic administration regimen offers several advantages over the prolonged-chronic administration regimen, including a shortened time-course which allows several neurochemical experiments to be conducted simultaneously. Also, there was no animal mortality associated with sub-chronic MPTP administration and as such, fewer animals can be used in experiments. The disadvantage of the sub-chronic regimen is that, unlike prolonged-chronic administration, axon terminals recover between 3 and 30 days after-the last MPTP injection (Petroske et al., 2001). Thus, this model is not

ideal for testing neuroprotective/restorative treatments since interpretations of results may be confounded by recovery at later time points. For experiments that are designed to test the effects of axon terminal loss on the function of surviving axon terminals, sub-chronic MPTP administration is ideal for causing a rapid, reliable and reproducible lesions of NSDA neurons and a compensatory increase in the activity of surviving axon terminals.

Contribution of DA Reuptake to Metabolism of DA

The purpose of the present experiments was to determine the contribution of recaptured DA to its enzymatic metabolism under basal conditions and during the compensatory activation of NSDA axon terminals. Under basal conditions, blocking DA reuptake decreased striatal DOPAC concentrations by approximately 30%, suggesting that roughly one third of enzymatic DA metabolism is due to DA recaptured from the synaptic cleft. The amount of recaptured DA that is metabolized to DOPAC reflects a balance between vesicular storage capabilities versus the enzymatic activity of MAO. Vesicular storage capability is determined by number of synaptic vesicles available for storage and the activity of VMAT-2 which transports cytoplasmic DA into the vesicle protecting it from metabolism. Thus under basal conditions, roughly 30% of the recaptured DA escapes repackaging and is metabolized by MAO.

It was interesting that DA metabolism only decreased by 30%, since DA release and reuptake is thought to be the primary source of metabolism in the axon terminal (Lindley et al., 1990). Several potential explanations may account for this. Residual DOPAC (due to metabolism prior to blockade of DA reuptake) may mask more robust decreases in DA metabolism. However, this is not the case since the half-life of DOPAC

is 11.3 min (Cumming et al., 1992), suggesting most DOPAC at the axon terminal prior to DAT blockade would have been eliminated in the 30 min time frame between GBR administration and animal decapitation. Also, the dose of GBR may not have been sufficient to completely block DA reuptake in NSDA axon terminals. However, this seems unlikely, because this administration regimen causes a dramatic increase in extracellular DA concentrations (as measured using microdialysis), indicative of effective blockade of DA reuptake (Camarero et al., 2002). Alternatively, there may be an additional source for cytoplasmic DA and DOPAC levels in NSDA axon terminals such as leakage from synaptic vesicles. Although the present experiments cannot rule out these alternative explanations for the degree to which DOPAC is decreased following blockade of DA reuptake, results demonstrate the relative contribution of DA reuptake to enzymatic metabolism by blocking DA transport for 30 min. The results can, therefore, be interpreted to reflect the relative amount of recaptured DA that is metabolized in this time frame and whether this relative amount changes across treatment conditions.

The amount of recaptured DA that is metabolized to DOPAC under basal conditions was compared to that metabolized under activated conditions. Activated conditions were induced by treating mice with MPTP to cause a compensatory activation of NSDA axon terminals. Under these conditions, blocking DA reuptake had a similar effect as under basal conditions. This data is consistent with the finding that there was no change in DAT protein expression levels in surviving NSDA axon terminals after MPTP administration. This was interesting because chronic elevation in neuronal activity (induced by blocking D2 receptors) decreases DAT mRNA and protein expression (Meiergerd et al., 1993; Kimmel et al., 2001). In the present study, the acceleration of

NSDA activity induced by MPTP was not associated with decreased DAT expression or the amount of recaptured DA that is metabolized to DOPAC. These results suggest the compensatory activation of NSDA neurons is not mediated by D2 receptors, although a loss of D2 receptor regulation of DAT protein expression could occur in NSDA axon terminals following MPTP. Alternatively, decreased DAT mRNA and protein expression following blockade of D2 receptors may not reflect actual changes in the rate of DA reuptake. Nevertheless, the present study utilized a functional assay to determine there is no change in the amount of recaptured DA that is metabolized in NSDA axon terminals. Therefore, altered DA reuptake does not contribute to the increased metabolism of cytoplasmic DA that is a neurochemical hallmark of the compensatory activation of NSDA axon terminals.

The Contribution of DA Synthesis to Metabolism of DA

In the present experiments, the relative amount of newly synthesized DA that is metabolized by MAO under basal and activated conditions was determined. Normally, DA synthesis is tightly coupled to release, such that as DA molecules are released, new molecules are synthesized and packaged into vesicles where they are protected from metabolism. The coupling of DA synthesis to release minimizes the metabolism of newly synthesized DA and maintains stable concentrations of vesicular DA available for release. Consistent with this, in the present experiments blockade of DA synthesis with AMT had no effect on striatal DOPAC concentrations under basal conditions. Therefore, unlike DA reuptake, synthesis does not contribute to metabolism in NSDA axon terminals under basal conditions.

The amount of newly synthesized DA metabolized under basal conditions was compared to activated conditions induced by pre-treating mice with MPTP in a sub-chronic dosing regimen to cause compensatory activation of surviving axon terminals. In contrast to basal conditions, blockade of DA synthesis in activated NSDA axon terminals decreased striatal DOPAC concentrations by approximately 40%, suggesting newly synthesized DA was a primary source for metabolism. Thus, the MPTP-induced compensatory increase in NSDA activity (reflected by an increase in the ratio of DOPAC to DA) is due in large part to increased metabolism of newly synthesized DA. These results could suggest there is no compensatory increase in DA release from surviving axon terminals. Rather the increased DOPAC to DA ratio is strictly due to increased metabolism of newly synthesized DA. However, this is not the case, since in response to MPTP administration there is an increase in the firing rate of NSDA neurons and synaptic DA concentrations are maintained at near baseline levels despite a dramatic loss of axon terminals (Albert et al., 1984; Zigmond et al., 1984; Stachowiak et al., 1987; Snyder et al., 1990; McCallum et al., 2006). More likely, the present study suggests that, while there is increased DA release from surviving NSDA axon, synthesis is accelerated to a much greater extent. The newly synthesized DA exceeds vesicular packaging capability and a great majority of the newly synthesized DA is metabolized rather than utilized.

The Rate of DA Synthesis in NSDA Axon terminals Following MPTP Treatment

The results from the previous experiments suggested that there is a dramatic increase in newly synthesized DA in NSDA axon terminals that survive MPTP treatment. The increased synthesis exceeded vesicular packaging capability and, as such, was

metabolized within axon terminals without ever being released. Therefore, accelerated synthesis is likely responsible for the increased metabolism of cytoplasmic DA that is a neurochemical hallmark of the compensatory activation of NSDA axon terminals. To verify these results, the rate of striatal DA synthesis was determined in mice treated with either saline or MPTP. Results from this experiment demonstrated that MPTP administration caused a dramatic increase in the rate of striatal DA synthesis in surviving axon terminals.

It is unclear why the rate of DA synthesis is accelerated to an extent that exceeds vesicular packaging capability. Normally, DA synthesis and release are tightly coupled, suggesting there may be a deficit in the regulatory mechanisms that govern this coupling. At the axon terminal, the rate of DA synthesis and release are controlled by D2 autoreceptors. D2 autoreceptors are G-protein coupled receptors that inhibit adenylate cyclase activity at the axon terminal (Missale et al., 1998). Adenylate cyclase regulates the cAMP levels and thus the activity of cAMP-dependent protein kinase A (PKA). D2 autoreceptor-PKA signaling cascade regulates both short and long-term changes in the rate of DA synthesis by regulating the phosphorylation state and *de novo* synthesis of TH, the rate limiting enzyme, respectively (Haycock, 1990; Leviel et al., 1991; Missale et al., 1998). Therefore the present results may indicate the rate of DA synthesis is accelerated due to a loss of D2-autoreceptor function at the axon terminal of NSDA axon terminals that survive MPTP. Consistent with this, there was an increase in TH protein expression in surviving axon terminals following MPTP administration. Further experiments are required to determine if the regulation of TH is dysfunctional and whether there is a loss

of D2 autoreceptor regulation of the rate of DA synthesis that is ultimately responsible for the uncoupling between DA synthesis and release.

The unregulated acceleration of DA synthesis is not restricted to mouse NSDA axon terminals lesioned with MPTP. Other neurotoxin-induced lesions of the NSDA pathway in the rat cause an increase in the amount of TH protein per terminal and an acceleration in the rate of DA synthesis (Zigmond et al., 1984). Thus, this phenomenon is not species or neurotoxin specific, but more likely typical of the compensatory activation of mammalian NSDA axon terminals. This is particularly relevant to the pathogenesis of PD, where there appears to be a multitude of factors that cause primary damage to the NSDA pathway, yet it is unknown what causes secondary, progressive, loss of NSDA neurons. The uncoupling of DA synthesis and release at the axon terminal (and the corresponding increase in cytoplasmic DA) may be a primary pathogenic factor that contributes to the progressive loss of NSDA neurons in PD.

Summary

The results from the experiments described in this chapter have successfully identified DA synthesis as the source of the increased cytoplasmic DA and accelerated metabolism that is typical of the compensatory activation of NSDA axon terminals. The rate of DA synthesis is accelerated to an extent that the newly synthesized DA exceeds packaging capabilities and is subsequently metabolized rather than released. The uncoupling of DA synthesis and release is likely due to dysfunctional regulation of the rate limiting enzyme, TH. It is unclear what changes in TH regulation are responsible for

the excessive rate of DA synthesis, but identification of these underlying mechanisms may lead to novel therapeutic targets to protect NSDA neurons in PD.

Chapter 5. Dysfunctional Regulation of Tyrosine Hydroxylase in NSDA Axon Terminals that Survive MPTP Administration.

A. Introduction

The results from the experiments summarized in Chapter 4 demonstrated that regulation of the DA biosynthetic pathway is dysfunctional in NSDA axon terminals that survive MPTP administration. Dysfunction in the DA synthesis pathway causes an uncoupling between synthesis and vesicular packaging capability, such that there is an increase in the metabolism of newly synthesized DA. The rate of DA synthesis is regulated by controlling the activity of TH, the rate limiting enzyme. TH catalytic activity and expression are tightly regulated at the axon terminal. Acceleration of TH catalytic activity mediates short-term changes in the rate of DA synthesis, while long-term changes in the rate of DA synthesis are achieved by increasing expression of the protein (Kumer and Vrana, 1996).

As depicted in Figure 5-1, the catalytic activity of TH is tightly regulated at the axon terminal through activation and inactivation signaling mechanisms. TH activation occurs through phosphorylation of critical serine residues (40, 31 and 19) located in the N-terminus of the enzyme (Campbell et al., 1986; Haycock, 1990). TH can be phosphorylated by cyclic AMP (cAMP)-dependent protein kinase A (Joh et al., 1978; Yamauchi and Fujisawa, 1979; Vulliet et al., 1980), Ca^{+2}–phospholipid-dependent protein kinase (Albert et al., 1984; Vulliet, 1985) and Ca^{+2}–calmodulin-dependent protein kinase (Yamauchi and Fujisawa, 1981; Vulliet et al., 1984). As such, TH enzyme activity is accelerated in response to increased neuronal activity (Ca^{+2} regulated) and

increased adenylate cyclase activity (cAMP regulated). Phosphorylation of TH decreases the Michaelis constant (Km) for the co-factor tetrahydrobiopterin and increases the inhibitory constant (Ki) for DA (Lovenberg and Bruckwick, 1975; Haavik et al., 1990; Daubner et al., 1992). These kinetic changes result in increased enzymatic efficiency, decreased susceptibility to end-product inhibition, but also lead to decreased enzyme stability (Lazar et al., 1981; Vrana and Roskoski, 1983; Gahn and Roskoski, 1995).

TH inactivation occurs through at least two activity-dependent mechanisms. Diminished NSDA firing (impulse-flow) results in reduced TH phosphorylation by activity-dependent kinases, thus allowing the enzyme to be de-phosphorylated by protein phosphatases 2A and 2C (Haavik et al., 1989). TH inactivation in this manner is reversible, such that subsequent phosphorylation can re-activate enzyme catalytic activity (Vrana et al., 1981; Vrana and Roskoski, 1983; Roskoski et al., 1990). Second, in the presence of a constant stimulus phosphorylated TH can undergo long-term inactivation through destabilization of secondary and tertiary protein structure (Lazar et al. 1981; Vrana and Roskoski 1983; Gahn and Roskoski 1995).

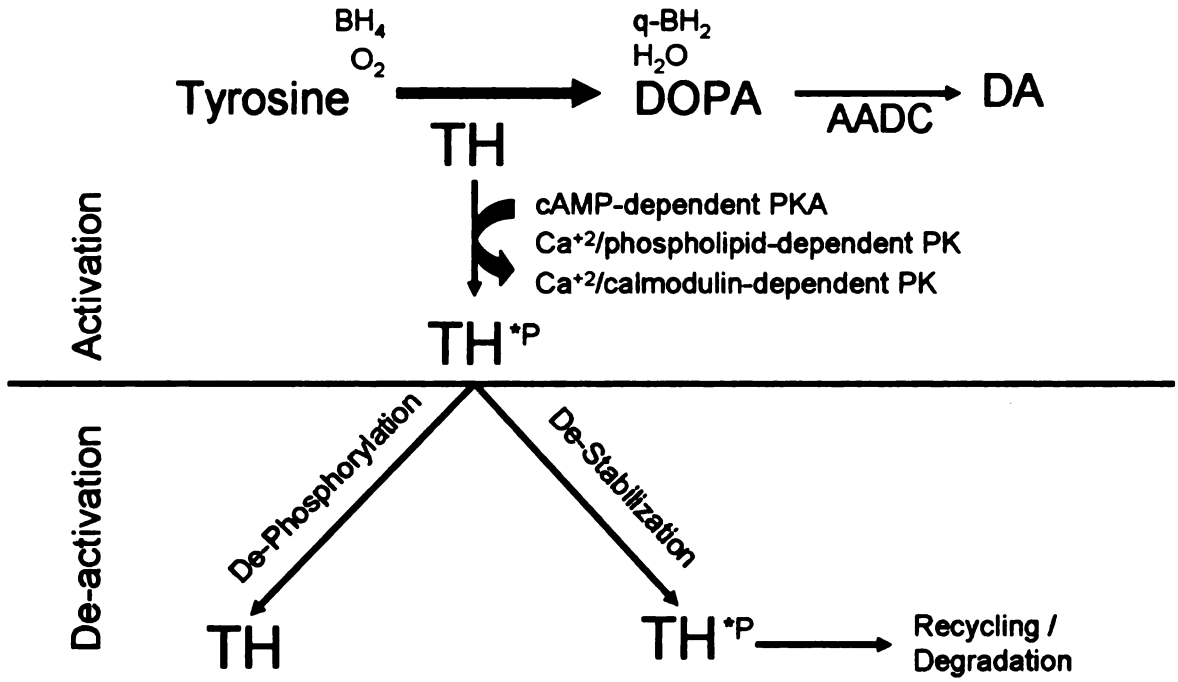

Figure 5-1. Schematic diagram depicting the DA biosynthetic pathway in the axon terminals of NSDA neurons. The activity of the rate limiting enzyme TH is controlled through activation and de-activation mechanisms. TH is activated through phosphorylation at critical serine residues within the N-terminus of the enzyme. Phosphorylation of TH increases the catalytic activity of the enzyme. De-activation of TH occurs through two mechanisms. TH can be de-phosphorylated by protein phosphatases or by destabilization which results in either recycling or degradation of the protein.

In contrast to the phosphorylation-dependent short-term acceleration in DA synthesis, long-term (stable) acceleration in synthesis is dependent on increased expression of the rate limiting enzyme, TH. Increased impulse-driven neuronal activity stimulates expression of the immediate early genes c-Fos and c-Jun (Morgan and Curran, 1989). These transcription factors bind to the promoter region of TH and induce gene transcription, protein translation, enzyme expression and accelerated DA synthesis. Thus, the increased rate of striatal DA synthesis in surviving axon terminals following MPTP administration may be due to increased TH catalytic activity (short-term), protein expression (long-term), or both (Figure 5-2). Results from Chapter 3 demonstrated there is an increase in the amount of TH protein in surviving axon terminals following MPTP. To this end, it was hypothesized that an increase in TH expression, rather than increased catalytic activity mediates the increased rate of DA synthesis. To test this hypothesis the present studies investigated the regulation of TH catalytic activity and protein content in NSDA neurons under basal and activated conditions induced by MPTP administration.

The present experiments were designed to identify changes in the regulation of TH catalytic activity and expression in NSDA axon terminals following MPTP administration. Neurochemical, Western blot and cell biological techniques were used to test the hypothesis that dysfunctional regulation of TH is responsible for the increased rate of DA synthesis that is a characteristic of the compensatory activation of NSDA neurons. Mice were treated with sub-chronic MPTP to destroy NSDA axon terminals and cause a compensatory activation of surviving neurons. The regulation of TH; phosphorylation state, enzymatic activity, substrate limitations, and sub-cellular localization were all assessed in the striatum of mice following MPTP treatment.

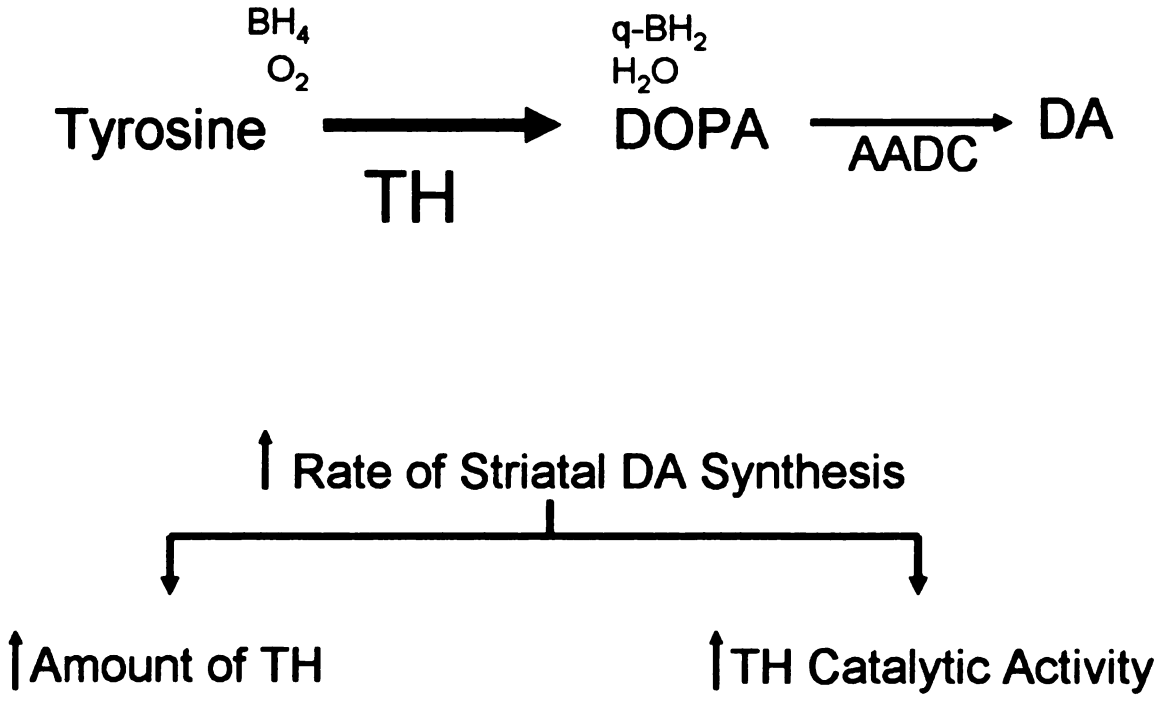

Figure 5-2. Following the compensatory activation of NSDA neurons the DA biosynthetic pathway was accelerated such that there is an increase in newly synthesized DA (TOP PANEL). Increasing the rate of this reaction requires an increase in either the amount, or catalytic activity of the rate limiting enzyme TH (BOTTOM PANEL).

B. Experimental Design and Results

Characterizing the Regulation of TH Catalytic Activity in NSDA Axon Terminals

The regulation of TH activity was assessed by measuring the phosphorylation state of the enzyme at serine-19, 31 or 40, using Western blot analysis and antibodies specific for TH phosphorylated at each specific serine residue. Phosphorylated TH protein was assessed from striatal protein isolated from mice treated with either saline (1.0 ml/kg, s.c.) or sub-chronic MPTP (25 mg/kg, s.c.). TH phosphorylated at serine-19, 31, or 40 was normalized to total striatal TH protein levels in each animal and was used as an index of the amount of enzyme phosphorylated at each residue relative to the total amount of enzyme in the axon terminal. Phosphorylated TH and total TH protein were measured from one half of the striatum (Figure 5-3).

In one experiment, MPTP-induced changes in TH phosphorylation were compared to the catalytic activity of the enzyme in the striatum. The catalytic activity of TH was determined by injecting mice with the AADC inhibitor NSD-1015 (100 mg/kg, i.p.) and measuring striatal DOPA concentrations using HPLC-EC from the contralateral striatum not used for Western blotting. The acute 30 min NSD-1015 administration regimen is unlikely to cause changes in TH protein expression during this short time frame. Striatal DOPA concentrations were normalized to the amount of TH protein, determined through Western blot analysis. The ratio of TH catalytic activity (DOPA) to TH protein was used to reflect the enzymatic activity of TH in mice treated with either saline (1.0 ml/kg, s.c.) or sub-chronic MPTP (25 mg/kg, s.c.).

Saline (1.0 ml/kg, s.c.)	n=7
MPTP (25 mg/kg, s.c.)	n=7

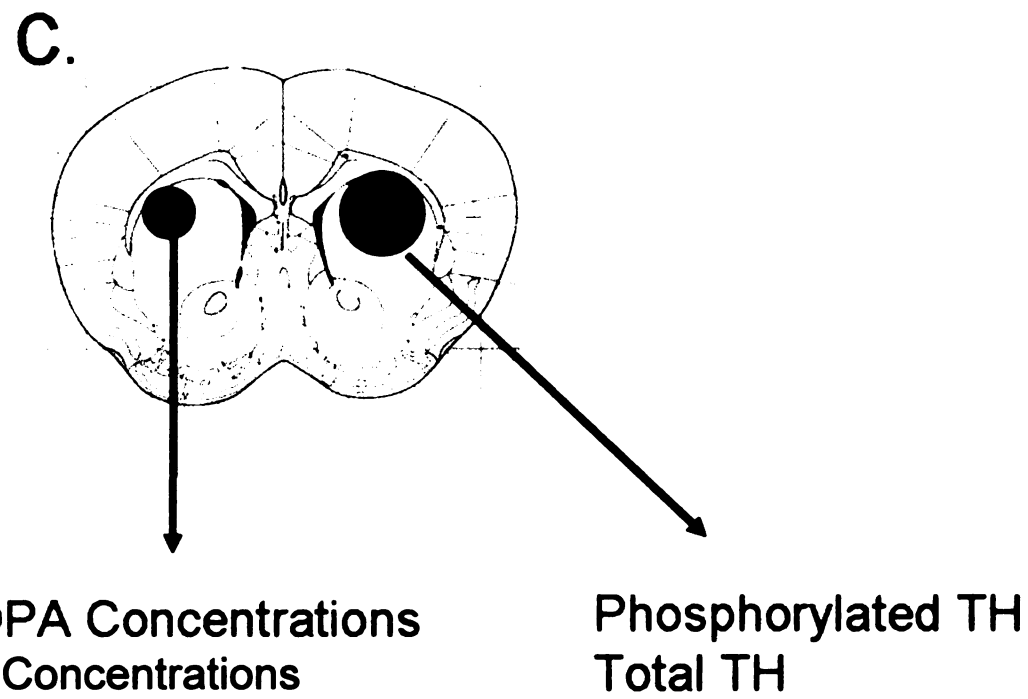

Figure 5-3. Experimental design (TOP PANEL) and isolation of NSDA axon terminals for neurochemical analysis of striatal DOPA concentrations or Western blot analysis of phosphorylated and total TH (BOTTOM PANEL). Mice were injected with either saline (1.0 ml/kg, s.c.) or MPTP (25 mg/kg, s.c.) once a day for 5 consecutive days and killed by decapitation 3 days following the last injection. The striatum was dissected from frozen brain sections and processed for HPLC-EC determination of striatal DOPA and DA concentrations or Western blot determination of phosphorylated and total striatal TH.

In a second experiment, TH catalytic activity was further evaluated by assessing the relationship between the enzyme and its substrate tyrosine under basal conditions and following MPTP administration. When TH catalytic activity is accelerated, substrate levels diminish and may become rate limiting, such that administration of tyrosine augments DOPA formation (Sved and Fernstrom, 1981). Thus, if the activity of TH is accelerated in NSDA neurons following MPTP, administration of supplemental tyrosine should enhance TH catalytic activity if substrate limiting conditions exist. To determine if this is the case, mice were injected with either saline (1.0 ml/kg, s.c.) or MPTP (25 mg/kg, s.c.) once a day for 5 consecutive days and killed 3 days following the last injection. Mice were injected with tyrosine (100 mg/kg, i.p.) 60 min prior to sacrifice and NSD-1015 (100 mg/kg, i.p.) 30 min prior to sacrifice. TH catalytic activity was determined by measuring the ratio of DOPA concentrations to TH protein as described above.

The Effects of MPTP on TH Phosphorylation and Catalytic Activity in the Striatum

Sub-chronic MPTP administration caused a differential loss of serine-19, serine-31 and serine-40 phosphorylated TH (Figure 5-4). MPTP caused a 63% decrease in serine-19 phosphorylated TH levels and 75% decrease in serine-31 phosphorylated TH levels. However, there was no change in serine-40 phosphorylated TH levels in the striatum of mice treated with MPTP as compared to saline-treated mice. Phosphorylated serine-19, serine-31, or serine-40 TH levels were normalized to total TH protein levels in the striatum, as an index of the relative proportion of TH phosphorylated at each residue (Figure 5-5). Total striatal TH protein was decreased by 50% following MPTP administration. MPTP had no effect on the amount of TH phosphorylated at serine-19 in the axon terminal and decreased the amount of serine-31 phosphorylated TH. In contrast, MPTP caused a robust increase in the proportion of serine-40 phosphorylated TH in NSDA axon terminals of mice treated with MPTP.

Sub-chronic MPTP administration caused a decrease in striatal DOPA concentrations (Figure 5-6, A) and TH protein expression (Figure 5-6, B). However, the decrease in DOPA concentrations paralleled that of TH protein. As such, MPTP administration did not alter the enzymatic activity of TH, as reflected by the ratio of DOPA to TH protein (Figure 5-6, C).

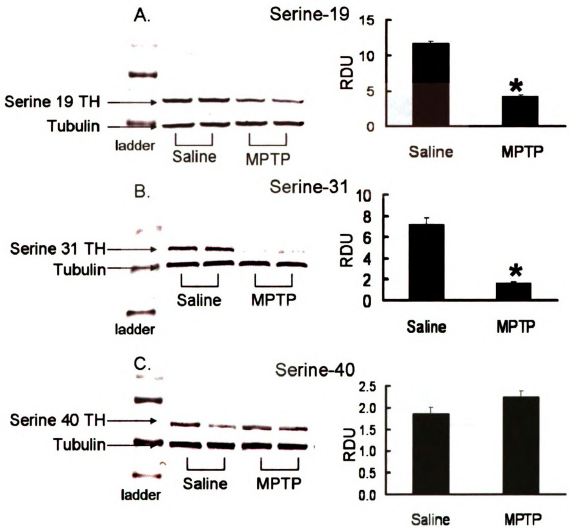

Figure 5-4. LEFT PANEL: Representative immunoblots depicting the band intensity of serine-19 (A), serine-31 (B) or serine-40 (C) (~ 55 kDA) and β-III tubulin (~ 50 kDA) of samples from two mice treated with saline and two mice treated with MPTP. RIGHT PANEL: Quantification of the effect of MPTP (25 mg/kg, i.p.) on serine-19 (A), serine-31 (B), or serine-40 (C) phosphorylated TH in the striatum. Relative density units for serine-19, 31, or 40 phosphorylated TH were obtained by normalizing the respective band intensities to β-III tubulin band intensity. Columns represent mean ± S.E.M. of seven mice/group. * indicates a significant difference from saline-treated controls. $p \leq 0.05$.

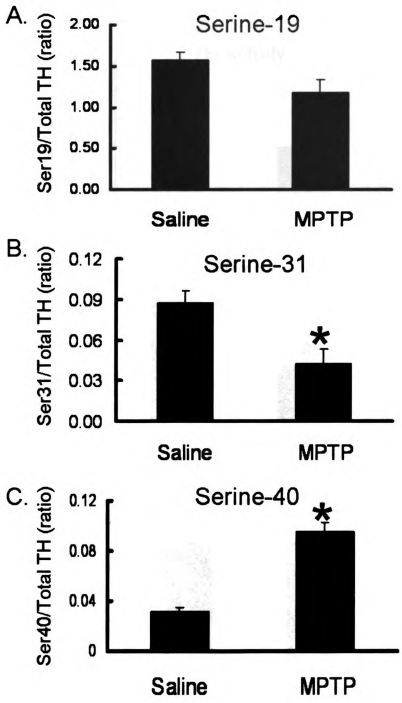

Figure 5-5. Quantification of the effect of MPTP (25 mg/kg, s.c.) on the relative proportion of serine-19 (A), serine-31 (B), or serine-40 (C) phosphorylated TH compared to total TH in the striatum. Phosphorylated serine-19, 31, or 40 phosphorylated TH relative density units were normalized to total TH relative density units. Columns represent mean ± S.E.M. of seven mice/group. * indicates a significant change from saline-treated controls. $p \leq 0.05$.

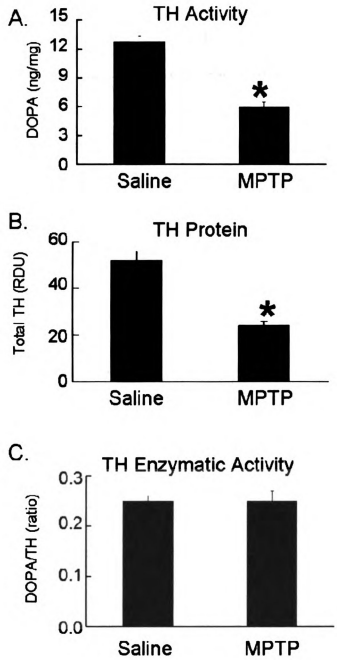

Figure 5-6. Striatal DOPA concentration (A), TH protein (B), and the ratio of DOPA to TH in the striatum of mice treated with either saline (1 ml/kg, s.c.) or MPTP (25 mg/kg, s.c.). Striatal DOPA accumulation was measured 30 min following injection of NSD-1015 (100 mg/kg, i.p.). Columns represent means ± S.E.M. of seven mice/group. * indicates a significant change from saline-treated controls. $p \leq 0.05$.

Effects of Tyrosine Administration on Striatal TH Catalytic Activity in Mice Pre-Treated with Saline or MPTP

As depicted in Figure 5-7, under basal conditions (saline-treated controls) tyrosine administration 60 min prior to decapitation had no effect striatal DOPA concentrations or TH protein. As such, tyrosine had no effect on TH enzymatic activity as reflected by the ratio of DOPA to TH. Similarly, under activated conditions (mice pre-treated with MPTP) tyrosine administration did not alter TH enzymatic activity.

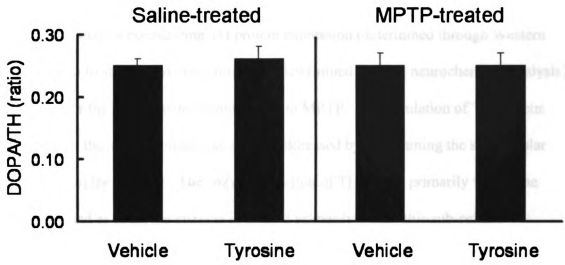

Figure 5-7. The effect of tyrosine supplementation (100 mg/kg, i.p., 60 min) on TH enzymatic activity in mice pre-treated with either saline (1 ml/kg, s.c.) or MPTP (25 mg/kg, s.c.). Striatal TH enzymatic activity was determined by normalizing striatal DOPA concentrations, determined through Western blot analysis, to striatal DA concentrations, determined through neurochemical analysis. Striatal DOPA concentrations were measured following NSD-1015 (100 mg/kg, i.p., 30 min) administration. Columns represent means ± S.E.M. of seven mice/group.

Characterizing the Regulation of TH Protein Expression in NSDA Axon Terminals

TH protein expression in NSDA axon terminals following MPTP administration were determined by normalizing TH protein expression (determined through Western blot analysis) to striatal DA concentrations (determined through neurochemical analysis) to account for the loss of axon terminals due to MPTP. The regulation of TH protein expression at the axon terminal was further addressed by determining the sub-cellular localization of the enzyme. The enzymatic action of TH occurs primarily within the cytoplasm, and as such, the enzyme is located primarily within this sub-cellular compartment. However, TH may also been suggested to be associated with synaptic vesicles and plasma membrane at the axon terminal (Kumer and Vrana, 1996). TH compartmentalization is thought to reflect segregation of functional TH at the axon terminal near the site of vesicular packaging. It is possible that a deficit in TH compartmentalization could cause an increase in cytoplasmic DA due to the synthesis without vesicular packaging. To test this, sub-cellular fractionation was performed to determine if there are changes in the localization of TH during compensatory activation of NSDA axon terminals. Differential centrifugation of striatal tissue was used to isolate sub-cellular fractions enriched in cytoplasmic, endosomal, synaptic vesicle and plasma membrane protein. The amount of TH associated with each fraction was compared under basal conditions and following MPTP administration.

Mice were injected with either saline (1.0 ml/kg, s.c., 8 mice) or MPTP (25 mg/kg, s.c., 8 mice) once a day for 5 consecutive days and killed 3 days following the last injection. In order to preserve sub-cellular compartmentalization, following decapitation striatal protein was freshly dissected rather than frozen. Striatal tissue from two mice

was pooled into a single micro-centrifuge tube resulting in 4 samples from saline-treated mice and 4 samples from MPTP-treated mice (Table 5-1). Tissue was homogenized and differentially centrifuged as depicted in Figure 5-8, and described in greater detail in Chapter 2. Centrifugation of homogenized striatal protein using this technique isolates fractions enriched in cytoplasmic protein (S4), early endosomal vesicles (P4), synaptic vesicles (P3) and plasma membrane protein (P1) (Slowiejko et al., 1996; Leng et al., 2001). Following differential centrifugation, equal protein concentrations from each fraction were loaded onto 10% PAGE gels by varying the volume loaded (10-20 μl). Resulting Western blots were probed for TH protein immunoreactivity. TH band density was normalized to the band densities of proteins enriched in each sub-cellular fraction; β-III tubulin, early endosomal antigen 1 (EEA1), synaptophysin and SNAP-25, respectively, to yield relative density units for TH. To account for axon terminal loss following MPTP, TH relative density units of in each fraction was normalized to total striatal TH relative density units to yield a relative proportion of TH in each fraction to total TH following MPTP administration.

Treatment	# of Animals	# of Samples
Saline (1.0 ml/kg, s.c.)	n=8	n=4
MPTP (25 mg/kg, s.c.)	n=8	n=4

Table 5-1. Experimental design used to determine TH sub-cellular distribution in the striatum. Mice were injected with either saline (1.0 ml/kg, s.c.) or MPTP (25 mg/kg, s.c.) once a day for 5 consecutive days and killed by decapitation 3 days following the last injection. The striatum was freshly dissected, placed into micro-centrifuge tubes, and homogenized. Striata dissected from 2 mice were pooled into a single micro-centrifuge tube for analysis, resulting a total of 4 striatal samples from mice treated with saline and 4 striatal samples from mice treated with MPTP.

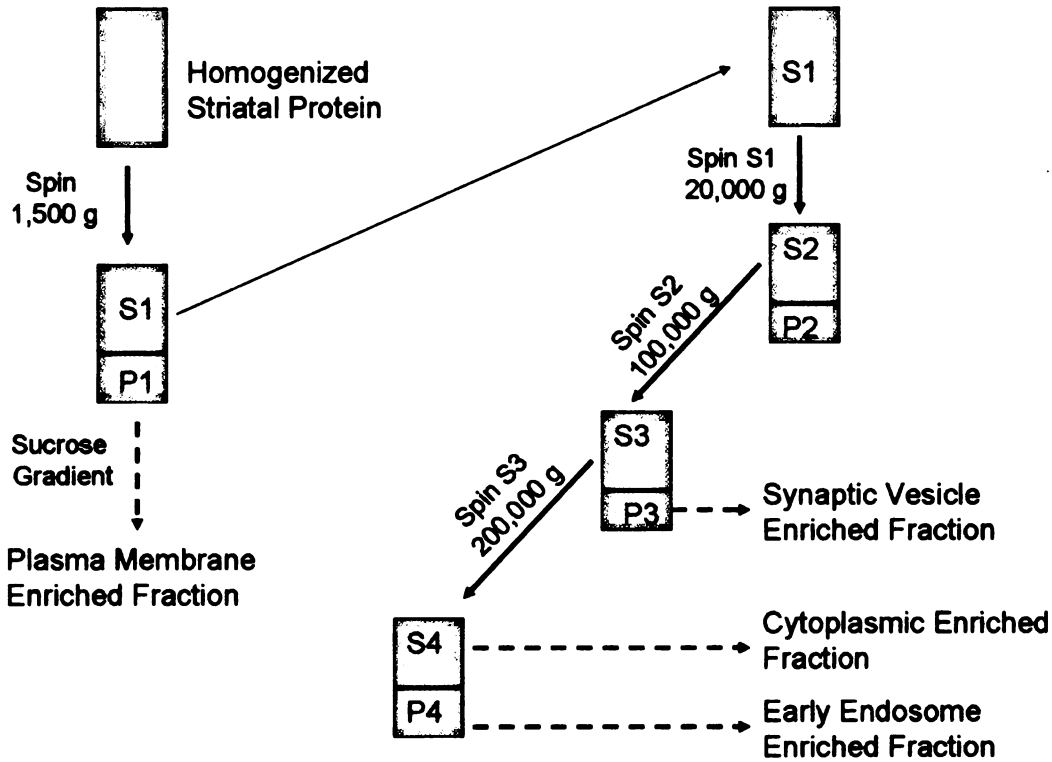

Figure 5-8. Differential centrifugation technique used to isolate plasma membrane, synaptic vesicle, endosomal and cytoplasmic enriched fractions from homogenized striatal protein. Homogenized striatal tissue was centrifuged at 1,500 g. The pellet from this low-speed centrifugation was separated using a sucrose gradient into plasma membrane and nuclear enriched fractions. The supernatant (S1) from the initial low-speed centrifugation was centrifuged at 20,000 g. The supernatant (S2) from this high-speed centrifugation was centrifuged at 100,000 g. The pellet (P3) from this ultracentrifugation was isolated and used as the synaptic vesicle enriched fraction. The supernatant (S3) from the first ultracentrifugation was centrifuged at 200,000 g to pellet early endosomal vesicles (P4). The supernatant (S4) from the second ultracentrifugation was isolated as the cytoplasmic enriched fraction.

The Effects of MPTP on TH Protein Expression in the Striatum

MPTP caused a decrease in striatal TH protein (Figure 5-9, A) and striatal DA concentration (Figure 5-9, B), however the decrease in TH protein expression was not as severe as the loss of striatal DA concentrations. As such, sub-chronic MPTP administration caused a robust increase in TH protein content, as reflected by the ratio of TH to DA (Figure 5-9, C).

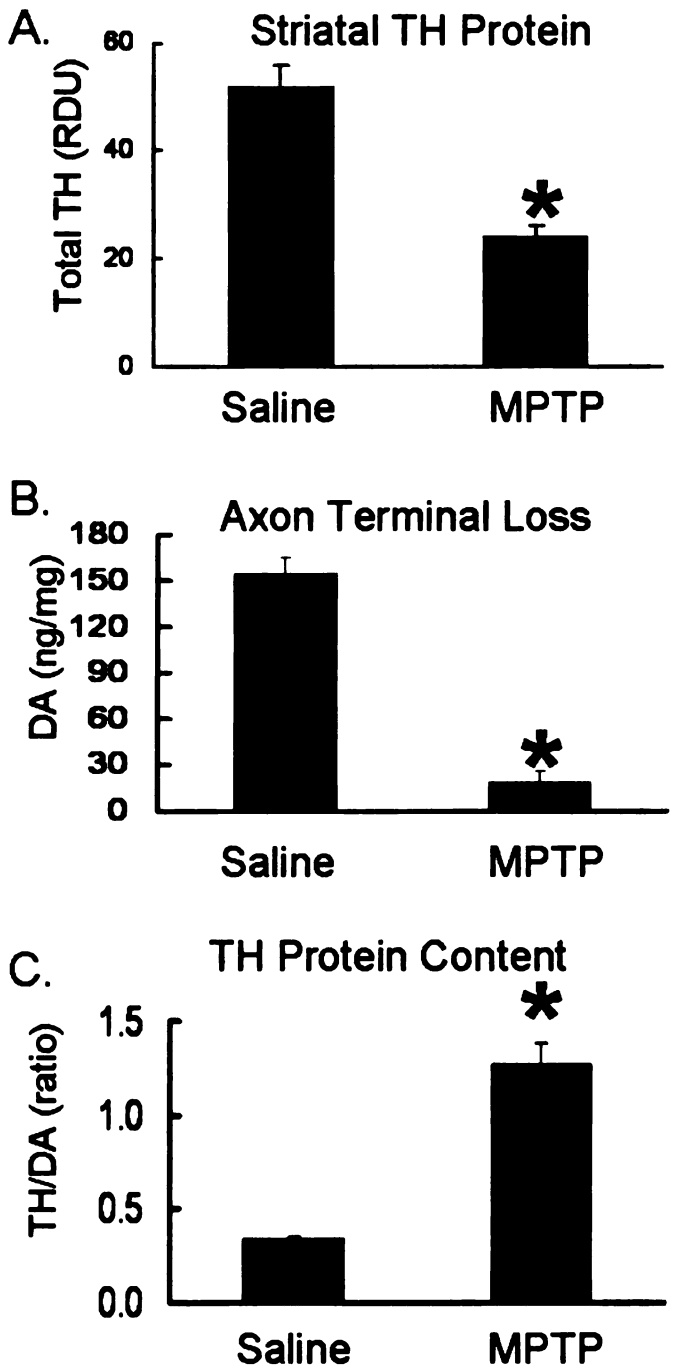

Figure 5-9. TH protein (A), DA concentrations (B), and the TH to DA ratio (C) in the striatum of mice treated with either saline (1 ml/kg, s.c.) or MPTP (25 mg/kg, s.c.). Relative density units (RDU) for TH were obtained by normalizing the TH band intensity to β-III tubulin band intensity. Columns represent means ± S.E.M. of seven mice/group. * indicate a significant difference from saline treated mice. $p \leq 0.05$.

The Effects of MPTP on the Sub-Cellular Localization of TH in the Striatum

Sub-chronic MPTP administration caused a differential loss of TH protein in the striatum depending on which sub-cellular compartment the enzyme was associated with (Figure 5-10, 5-11). MPTP caused a 35% decrease in TH protein immunoreactivity in the cytoplasmic fraction and a 29% decrease in TH protein in the early endosomal fraction. The loss of TH expression associated with the synaptic vesicle and plasma membrane enriched fractions were more severe. MPTP caused a 65 and 75% loss of TH associated with the synaptic vesicle and plasma membrane enriched fractions, respectively. To quantify the relative change in TH localization relative to total TH at the axon terminal, relative density units of TH in each fraction were normalized to relative density units for total striatal TH. Sub-chronic MPTP increased the proportion of TH associated with the cytoplasmic and early endosomal vesicle fractions, but decreased TH associated with the synaptic vesicle and plasma membrane enriched fractions (Figure 5-12).

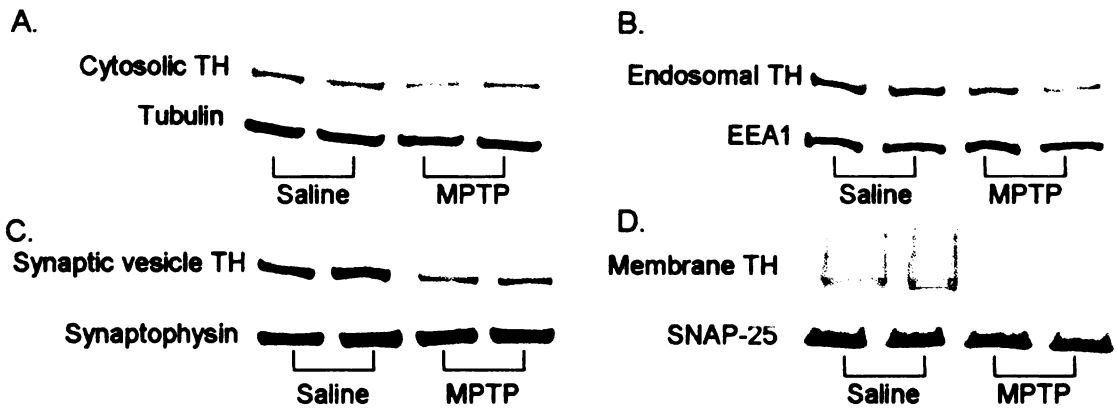

Figure 5-10. Representative Western blots of TH protein in the cytosolic (A), endosomal (B), synaptic vesicle (C), and plasma membrane (D) sub-cellular compartments from mice treated with either saline (1 ml/kg, s.c.) or MPTP (25 mg/kg, s.c.). Differential centrifugation was used to isolate TH associated with sub-cellular fractions enriched in either cytosolic (A), early endosomal vesicles (B), synaptic vesicles (C), or plasma membrane (D) protein. TH associated with each compartment was normalized to proteins enriched in each fraction β-III tubulin, early endosome antigen 1 (EEA1), synaptophysin, or Snap-25, respectively to control for variations in loading.

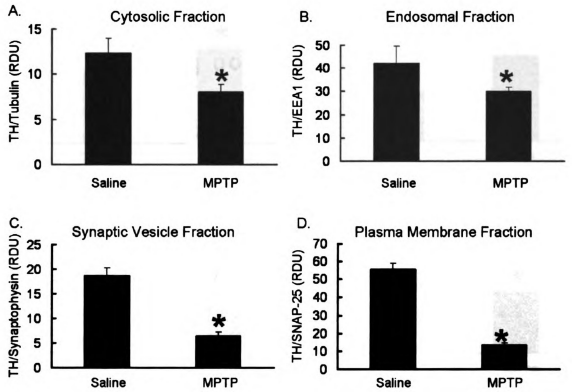

Figure 5-11. Quantification of the TH protein distribution in the striatum of mice treated with either saline (1 ml/kg, s.c.) or MPTP (25 mg/kg, s.c.). TH protein in each fraction was normalized to either β-III tubulin (A), EEA1 (B), synaptophysin (C), or SNAP-25 (D). Columns represent means ± S.E.M. of four samples per group. * indicate a significant difference from saline treated mice. $p \leq 0.05$.

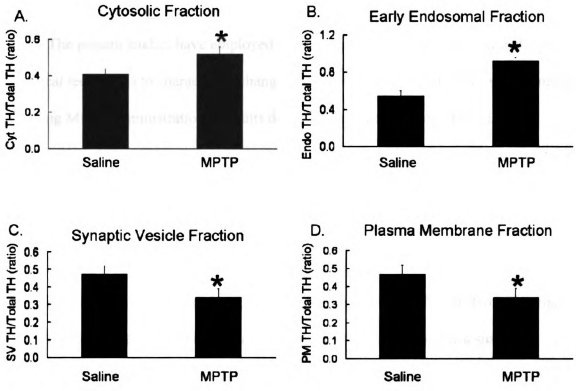

Figure 5-12. The effects of MPTP (25 mg/kg, s.c.) on the proportion of TH associated with sub-cellular fractions enriched in either cytoplasmic (A), early endosomal vesicles (B), synaptic vesicles (C) or plasma membrane (D) protein. The relative amount of TH protein associated with each sub-cellular fraction was determined by normalizing relative density units for TH in each fraction to the relative density units of total striatal TH. Columns represent means ± S.E.M. of four samples per group. * indicate a significant difference from saline treated mice. $p \leq 0.05$.

C. Discussion

The present studies have employed neurochemical, immunohistochemical and cell biological techniques to characterize changes in the regulation of TH at the axon terminal following MPTP administration. Results describe abnormal regulation of TH phosphorylation, protein expression and sub-cellular compartmentalization, suggesting that deficits in TH expression and localization underlie the uncoupling of DA synthesis and release at the axon terminal following MPTP.

The Effect of MPTP on the Regulation of TH Catalytic Activity in NSDA Axon Terminals

Following MPTP-induced loss of NSDA axon terminals there is a sustained increase in the rate of DA release from surviving axon terminals. In order to meet the increased demand for release, the rate of DA synthesis is accelerated. However, DA synthesis is accelerated to an extent that supersedes storage resulting in metabolism of the newly synthesized DA. TH is the rate limiting enzyme in the DA biosynthetic pathway. As such, over-activation of DA synthesis is likely the result of changes in the regulation of TH. The present experiments characterized the regulation of TH catalytic activity in NSDA axon terminals.

To determine if the compensatory activation of NSDA neurons causes a change in the enzymatic activity of TH, the phosphorylation state of was determined at three serine residues within the N-terminus of the enzyme. Results demonstrated that MPTP caused a differential loss of various forms of phosphorylated TH. MPTP decreased serine-19 and serine-31 phosphorylated TH, however there was no change in serine-40 phosphorylated TH. When the proportion of TH phosphorylated at each residue was compared to total

TH, the percentage of serine-40 phosphorylated TH increased at the axon terminal, while there was no change and a decrease in serine-19 and serine-31 phosphorylated TH, respectively.

Serine-40 can be phosphorylated by a number of kinase-second messenger systems, however, cAMP-dependent PKA is the primary protein kinase that phosphorylates this residue (Kumer and Vrana, 1996). Thus, increased levels of serine-40 phosphorylated TH suggest there is an increase in adenylate cyclase activity, cAMP levels and PKA activation. D2 autoreceptors inhibit adenylate cyclase activity and thus PKA-mediated phosphorylation of TH at serine-40. It is possible that there is a loss of D2 autoreceptor regulation in NSDA neurons that survive MPTP induced neurotoxicity.

Serine-40 is the primary regulatory serine residue that controls TH catalytic activity (Campbell et al., 1986; Haycock, 1990). Phosphorylation at this residue causes a conformational change in the enzyme that increases activity by increasing its affinity for substrate tyrosine and decreasing susceptibility to end-product inhibition from DA. Therefore, increased serine-40 phosphorylated TH levels predicted accelerated TH activity in surviving NSDA axon terminals following MPTP. This was not the case however, as there was no increase in TH enzymatic activity as reflected by the ratio of DOPA to TH. To confirm these results, tyrosine was administered to either saline-treated controls or MPTP-treated mice. When TH activity is accelerated, supplemental tyrosine enhances the rate of DOPA formation. Tyrosine administration did not increase product formation, suggesting that there is no increase in the enzymatic activity of TH in axon terminals that surviving MPTP neurotoxicity.

Interestingly, there was a discrepancy between increased serine-40 phosphorylated TH and a lack of increase in the enzymes catalytic activity. One potential explanation for this discrepancy is that the increase in serine-40 phosphorylated TH, which accelerates enzymatic activity, may have been compensated for by decreased phosphorylation at serine-31, such that there was no net change in the enzymes activity. The Western blot and neurochemical techniques used in the present study did not allow determination of the phosphorylation state of individual TH molecules. It is possible the activity of molecules phosphorylated at serine-40 were accelerated while the decreased phosphorylation at serine-31 decreased the activity of other molecules resulting in no net change in overall enzymatic activity. Alternatively, if the changes in serine-40 and serine-31 phosphorylation occur on the same TH molecules, the acceleration in enzymatic activity induced by serine-40 phosphorylation may be blocked by decreased phosphorylation at the serine-31 residue. Further biochemical experiments are required to determine the phosphorylation state of individual TH molecules. Site-directed mutagenesis of the key serine residues on TH or mass-spectrometry analysis of the individual phosphorylation state of the enzyme under these conditions may provide critical information regarding the role of second messenger systems involved in regulating TH at the axon terminal.

A second potential explanation for the discrepancy between increased serine-40 phosphorylated TH but no change in the enzymes activity may be that there is an increase in de-activated TH at the axon terminal. Phosphorylation of the enzyme causes an increase in catalytic activity but consequently decreases stability. Thus, the increased serine-40 phosphorylated TH may represent de-activated enzyme at the axon terminal

that is being recycled. Further co-immunoprecipitation experiments that directly measure levels of ubiquitinated TH are required to determine whether there is an increase in destabilized TH at the axon terminal following MPTP and whether TH associated with the early endosomal sub-cellular fraction is indeed de-activated enzyme.

If TH is degraded by the ubiquitin-proteosome system (UPS) (as most intracellular proteins are) the accumulation of de-activated TH may reflect deficits in protein degradation following MPTP. This is relevant to PD pathogenesis since Lewy-body formation is thought to result from dysfunctional protein degradation. Additionally, mutations in genes encoding UPS proteins are associated with inheritable PD (Kitada et al., 1998). Accordingly, there may be an important link to abnormal protein degradation and the dysfunctional regulation of TH. Nevertheless, using two separate functional assays of TH enzymatic activity the present experiments demonstrate there is no change in TH catalytic activity in NSDA axon terminals that survive MPTP treatment. Therefore, the accelerated rate of DA synthesis that occurs during the compensatory activation of NSDA axon terminals is likely due to long-term changes in the expression of TH.

The Effect of MPTP on TH Protein Expression in NSDA Axon Terminals

To determine if the loss of NSDA axon terminals induced by MPTP causes an increase in TH protein expression in surviving neurons, TH protein levels were determined in the striatum of mice treated with saline or sub-chronic MPTP. MPTP decreased total striatal TH protein but there was a more severe loss of NSDA axon terminals as reflected by striatal DA concentrations. As such, there was a robust increase

in TH protein in surviving axon terminals following MPTP. Several lines of evidence support this conclusion; 1) following the loss of axon terminals induced by MPTP there is a prolonged acceleration in NSDA activity and rate of DA synthesis, 2) long-term changes in the rate of DA synthesis are mediated by increasing protein expression rather than a change in catalytic activity (Dunkley et al., 2004), and 3) following MPTP there is an increase in TH mRNA and protein expression in surviving NSDA neurons (Jakowec et al., 2004). Taken together, these results suggest the accelerated rate of DA synthesis in NSDA axon terminals following MPTP is due to an increase in the expression of TH.

Sub-chronic MPTP caused a decrease in TH associated with the synaptic vesicle and plasma membrane sub-cellular fractions. TH is thought to associate with synaptic vesicles to localize newly synthesized DA to the site of vesicular packaging. This function presumably enhances storage and consequently decreases the metabolism of newly synthesized DA. The loss of this function therefore, may be responsible for the increased metabolism of newly synthesized DA and uncoupling between DA synthesis and storage capability in NSDA axon terminals following MPTP.

MPTP also decreased TH associated with the plasma membrane. TH associated with the membrane may reflect reserve populations of TH at the axon terminal that may be utilized to increase DA synthesis during activated conditions. The loss of plasma membrane associated TH may reflect a recruitment of reserve populations of TH to meet the increased demand for synthesis. It is unclear if this loss of function represents protein translocation to the cytosol or a dysfunction in the ability to compartmentalize protein under activated conditions.

In contrast to the synaptic vesicle and plasma membrane fractions, MPTP caused an increase in cytoplasmic and endosomal TH. The enzymatic activity of TH takes place within the cytoplasm at the axon terminal, suggesting increased expression of the enzyme in this fraction contributes to the increased rate of DA synthesis. Since the increased cytoplasmic TH is not associated with synaptic vesicles, the increase in newly synthesized DA is likely metabolized rather than released.

MPTP also increased the amount of TH associated with early endosomal vesicle fraction, suggesting there was an increase in deactivated TH being recycled through the endosomal pathway. The endosome-lysosome pathway is generally associated with recycling/degradation of macromolecules rather than cytoplasmic protein. However, α-synuclein, is also associated with endosome recycling (Leng et al., 2001), suggesting small cytoplasmic proteins at the axon terminal may also be recycled through the endosome-lysosome pathway. It is also possible that TH associated with this light vesicle fraction represents TH bound to a complex of proteins involved in recycling degradation such as the ubiquitin-proteosome system (UPS) which primarily recycles cytoplasmic protein. Nevertheless, these results suggest there is an increase in deactivated TH at the axon terminal of NSDA neurons that survive MPTP administration. Further biochemical experiments are necessary to identify the mechanisms that are responsible for TH recycling and turnover at the axon terminal and whether TH associated with the light vesicle fraction is indicative of protein being recycled.

Summary

The experiments described in this chapter demonstrate changes in the regulation of TH at axon terminals of NSDA neurons that survive MPTP neurotoxic insult. Results showed that increased cytoplasmic TH (rather than enzyme catalytic activity) causes an accelerated rate of DA synthesis that exceeds vesicular packaging and is metabolized, rather than released. Changes in the sub-cellular localization of TH at the axon terminal suggest deficits in compartmentalization of TH causes the increased metabolism of newly synthesized DA. The net effect of these compensatory changes in TH protein content and uncoupling between DA synthesis and release are not clear. Identification of the regulatory mechanisms that govern TH phosphorylation, protein expression and sub-cellular localization however, may provide targets to prevent ROS-mediated damage and the progressive loss of NSDA neurons in PD.

Chapter 6. Dopamine Receptor (D2) Regulation of Dopamine Synthesis in NSDA Neurons

A. Introduction

Results from the experiments conducted in the previous chapters have identified and characterized the neurochemical mechanisms that underlie the compensatory activation of NSDA neurons. The dysfunctional regulation of the DA biosynthetic pathway is responsible for the accelerated metabolism of cytoplasmic DA, and is likely a pathogenic factor that contributes to the progressive loss of NSDA neurons in PD. Understanding how the DA synthetic pathway and the activity of NSDA neurons are regulation will be crucial to devising strategies to protect surviving neurons from ROS-mediated oxidative damage derived from DA metabolism.

The activity of NSDA neurons is regulated by feedback inhibition which controls the firing rate of these neurons in concert with the rate of DA synthesis and release at the axon terminal. Feedback inhibition is mediated by D2 receptors that are located on post-synaptic target neurons and pre-synaptic axon terminals. The compensatory activation of NSDA neurons is the result of decreased inhibitory feedback mediated by D2 receptors. D2 receptors are G-protein receptors that are coupled to inhibitory G-proteins ($G_{i/o}$) which decrease the activity of adenylate cyclase and reduce intracellular cAMP levels (Sibley, 1999). Activation of post-synaptic D2 receptors by DA released from a NSDA axon terminal elicits long-loop, multi-synaptic, feedback inhibition to NSDA cell bodies in the substantia nigra which inhibits subsequent cell firing (Imperato and Di Chiara, 1988). Following MPTP administration, the loss of axon terminals decreases the amount

of released DA capable of activating post-synaptic D2 receptors and, as such, NSDA firing rate increases due to the loss of feedback inhibition to NSDA cell bodies.

The rate of DA synthesis and release are also regulated by short-loop feedback inhibition mediated by pre-synaptic D2 autoreceptors directly at the axon terminal. Activation of D2 autoreceptors inhibits adenylate cyclase activity and cAMP concentrations, which decreases, cAMP-dependent PKA phosphorylation of TH (Kehr et al., 1972). Phosphorylation of TH at serine-40 by PKA increases the enzymes catalytic activity (Haycock, 1990). Additionally, D2 autoreceptors modulate DA release directly at the axon terminal. Action potential-stimulated DA release activates D2 autoreceptors which inhibits DA release in response to subsequent action potentials by accelerating K+ efflux and hyperpolarizing the axon terminal (Koeltzow et al., 1998; Missale et al., 1998; Sibley, 1999). Therefore, following MPTP administration, the loss of axon terminals decreases the amount of released DA capable of activating pre-synaptic D2 autoreceptors and as such, increases TH phosphorylation and enzymatic activity as well as increases action potential-stimulated DA release.

It is clear there is a dysfunctional regulation of DA synthesis in NSDA axon terminals following MPTP administration. This may be due to the loss of D2 receptor-mediated inhibitory feedback. However, it is unclear what effect a loss of long and short-loop feedback inhibition has on the regulation of TH phosphorylation, enzymatic activity and the rate of DA synthesis at the axon terminal. To address this, the experiments described in this chapter were designed to; 1) characterize the regulation of TH following the loss of D2 receptor-mediated feedback inhibition, 2) determine if there is a loss of D2 receptor regulation of the activity of NSDA neurons following MPTP administration and

3) determine if prolonged loss of D2 receptor-mediated feedback inhibition (and the consequent chronic activation of NSDA neurons) causes the degeneration of NSDA axon terminals.

B. Experimental Design and Results

Characterizing the Effects of a Loss of Long and Short-Loop Feedback Inhibition on the Regulation of DA Synthesis in NSDA Axon Terminals

Pharmacological blockade of post- and pre-synaptic D2 receptors was used to recapitulate the loss of feedback inhibition following MPTP administration. Raclopride, a selective D2 antagonist (Hall et al., 1988), was used to block both post-synaptic D2 receptors (long-loop feedback inhibition) and pre-synaptic D2 autoreceptors (short-loop feedback inhibition). As depicted in Figure 6-1, raclopride increases NSDA cell firing, action potential generation, and Ca^{+2} entry into the axon terminal. Activation of Ca^{+2}/Calmodulin-dependent protein kinase can accelerate DA synthesis by phosphorylating TH at serine-19 (Yamauchi and Fujisawa, 1981; Vulliet et al., 1984). Raclopride blockade of pre-synaptic D2 autoreceptors increases adenylate cyclase activity, cAMP production and activation of cAMP-dependent PKA. Activation of PKA can accelerate DA synthesis by phosphorylating TH at serine-40 (Joh et al., 1978; Yamauchi and Fujisawa, 1979; Vulliet et al., 1980). Thus, the loss of both long and short-loop feedback inhibition can accelerate TH enzymatic activity. Under these conditions the enzymatic activity of TH can become limited by a lack of substrate availability (Sved and Fernstrom, 1981).

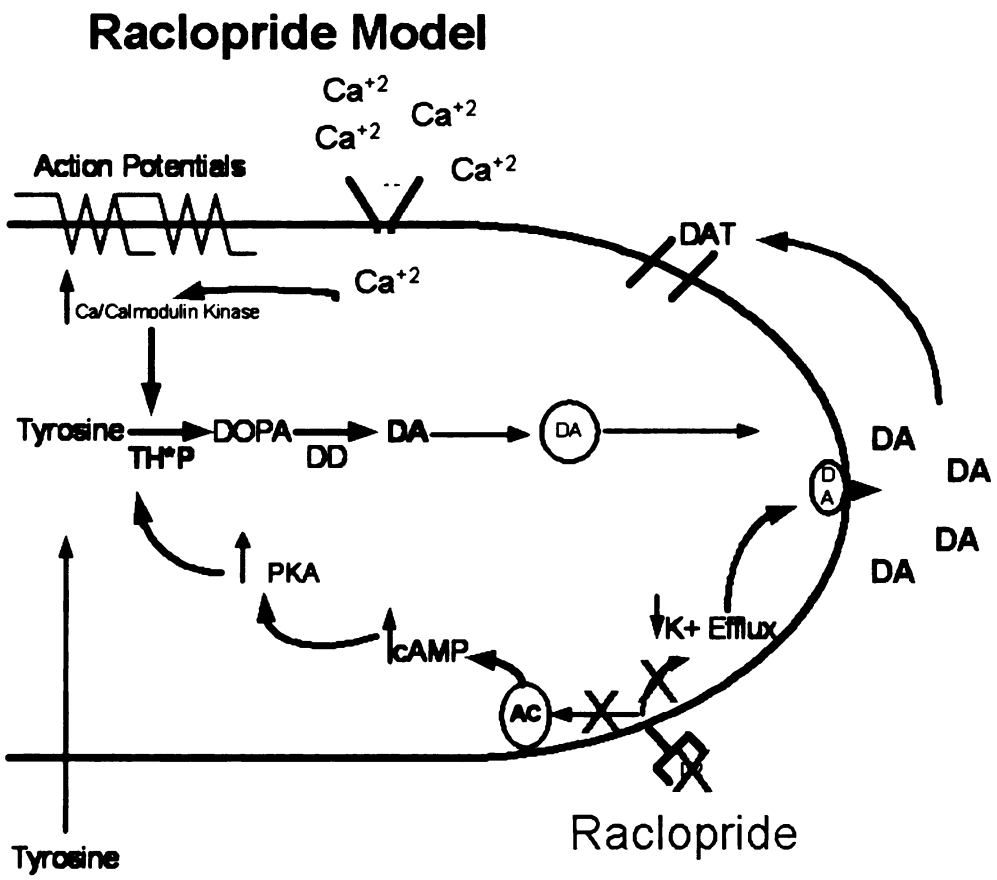

Figure 6-1 Schematic diagram depicting the neurochemical events in the axon terminal following administration of raclopride. Raclopride administration blocks both post-synaptic and pre-synaptic D2 receptors. Blockade of D2 receptors increases cell firing and disinhibits adenylate cyclase activity at the axon terminal. This results in TH phosphorylation by activity and cAMP-dependent kinases and acceleration in TH enzymatic activity.

In the first set of experiments, mice were injected with either saline (1 ml/kg, i.p.), tyrosine (100 mg/kg, i.p.), raclopride (1.0 mg/kg, i.p.), or tyrosine plus raclopride and decapitated 1 h following injection. Supplemental tyrosine was administered to prevent substrate limitations on TH activity in activated NSDA neurons. Administration of raclopride using this dose and time course maximally activates NSDA neurons (Eaton et al., 1992). The effects of raclopride on NSDA activity was assessed by measuring striatal DOPAC and DA concentrations, and the DOPAC to DA ratio. To evaluate the effects of raclopride on TH enzymatic activity, mice were injected as described above and killed 1 h after drug administration. Mice were injected with NSD-1015 30 min prior to sacrifice and striatal DOPA concentrations were measured as an index of TH catalytic activity. TH phosphorylation state, enzymatic activity and protein expression were also determined in the striatum as described previously.

The Effect of Acute Raclopride on NSDA Activity

As depicted in Figure 6-2 (A), tyrosine administration had no effect on DA metabolism, as reflected by striatal DOPAC concentrations. Raclopride administration caused a 4-fold increase in striatal DOPAC concentrations Tyrosine supplementation in raclopride-treated mice increased striatal DOPAC concentrations when compared to mice treated with raclopride alone. As depicted in Figure 6-2 (B), tyrosine administration slightly increased basal levels of striatal DA storage, as reflected by concentrations of DA. Raclopride administration decreased striatal DA concentrations by approximately 25% in both vehicle and tyrosine-treated mice. As depicted in Figure 6-2 (C), tyrosine administration had no effect on NSDA activity, as reflected by the DOPAC to DA ratio. Raclopride administration caused a 5-fold increase in the DOPAC to DA ratio and tyrosine supplementation caused a further increase over mice treated with raclopride alone.

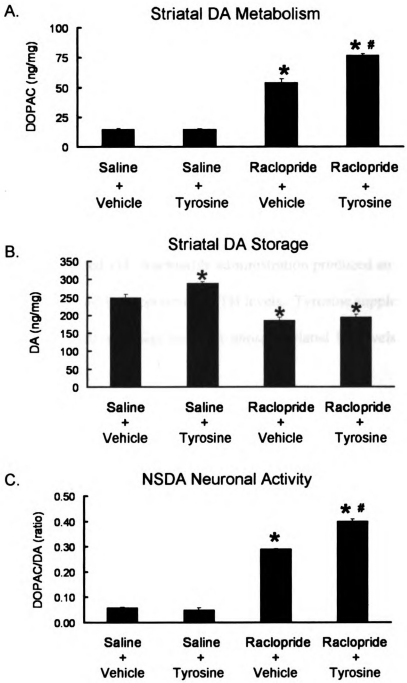

Figure 6-2. Concentrations of DOPAC (A), and DA (B), and the DOPAC/DA ratio (C) in the striatum of mice 60 min after administration of either saline (1 ml/kg, i.p.) + vehicle (saline 1 ml/kg, i.p.), saline + tyrosine (100 mg/kg, i.p.), raclopride (1.0 mg/kg, i.p.) + vehicle, or raclopride + tyrosine. Columns represent means of groups ± 1.0 SE.M. of seven mice per group. (*) Values significantly different from saline + vehicle treated controls. # Values significantly different from raclopride + vehicle-treated mice. $p \leq 0.05$.

The Effect of Acute Raclopride on TH Phosphorylation State

As depicted in Figure 6-3 (A), tyrosine administration had no effect on basal levels of serine-19 phosphorylated TH. Raclopride administration produced an approximately 1.5-fold increase in serine-19 phosphorylated TH levels. Tyrosine plus raclopride administration increased serine-19 phosphorylated TH levels over mice treated with raclopride alone.

As depicted in Figure 6-3 (B), tyrosine administration did not change basal levels of serine-31 phosphorylated TH. Raclopride administration produced an approximately 1.6-fold increase in serine-31 phosphorylated TH levels. Tyrosine supplementation in raclopride-treated mice did not affect serine-31 phosphorylated TH levels compared with raclopride treatment alone.

As depicted in Figure 6-3 (C), tyrosine administration had no effect on basal levels of serine-40 phosphorylated TH. Raclopride administration produced an approximately 6.8-fold increase in serine-40 phosphorylated TH. Tyrosine plus raclopride administration significantly increased serine-40 phosphorylated TH levels an additional 25% over mice treated with raclopride alone.

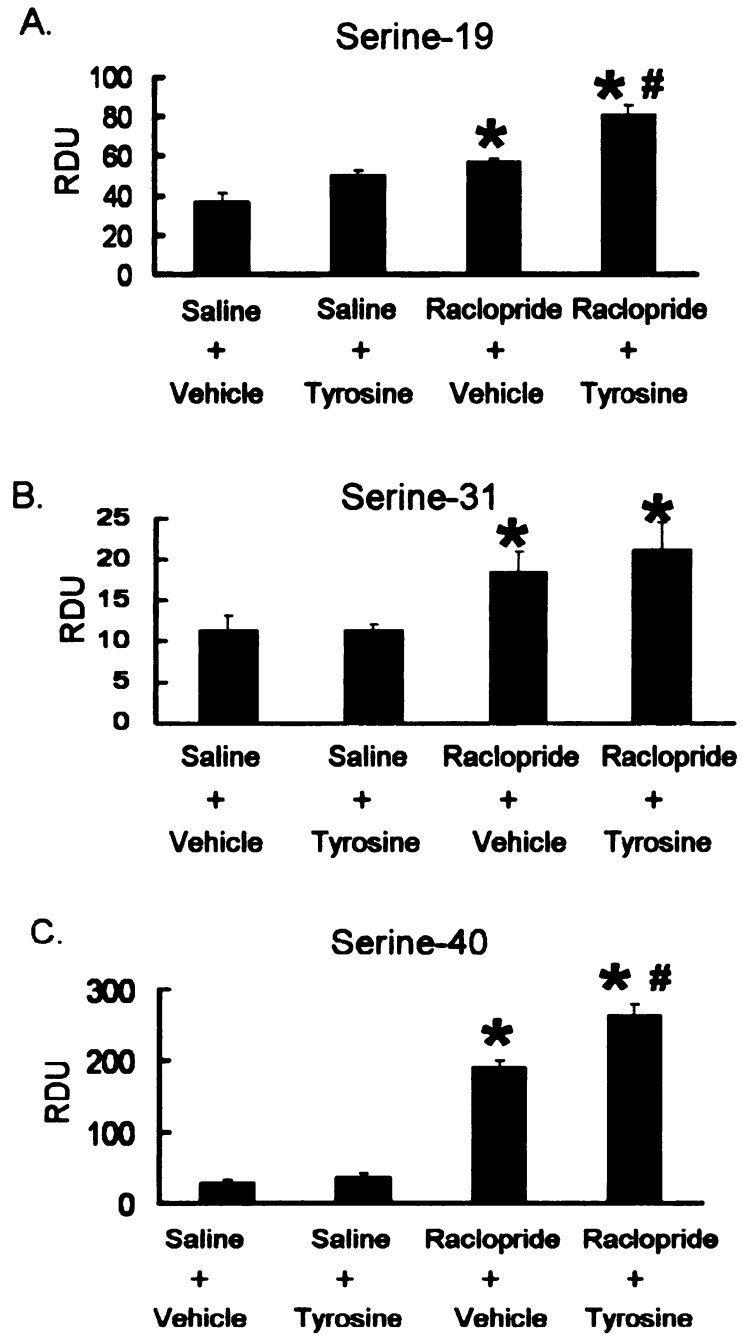

Figure 6-3. Serine-19 (A), serine-31 (B) and serine-40 (C) phosphorylated TH levels in the striatum of mice 60 min after treatment with either saline (1 ml/kg, i.p.) + vehicle (1 ml/kg, i.p.), saline + tyrosine (100 mg/kg, i.p.), raclopride (1.0 mg/kg, i.p.) + vehicle, or raclopride + tyrosine. Mice were killed 1 hr after drug administration. Relative density units (RDU) were obtained by normalizing the phosphorylated TH band density to β-III tubulin band density. Columns represent means of groups ± S.E.M. of seven mice/group. * indicate a significant difference from saline + vehicle-treated mice. # Values significantly different from raclopride + vehicle-treated mice. $p \leq 0.05$.

The Effect of Acute Raclopride on TH Enzymatic Activity and Protein Expression

The accumulation of DOPA following blockade of AADC is an *in vivo* assay for TH catalytic activity (Carlsson et al., 1972). As depicted in Figure 6-4, tyrosine administration alone did not change basal TH catalytic activity, as reflected by striatal DOPA concentrations. Raclopride administration produced an approximately 3-fold increase in TH catalytic activity and tyrosine supplementation resulted in an approximately 5-fold increase in TH catalytic activity that was significantly increased from mice treated with raclopride alone. As depicted in Table 6-1, levels of total TH did not vary in response to any treatment condition.

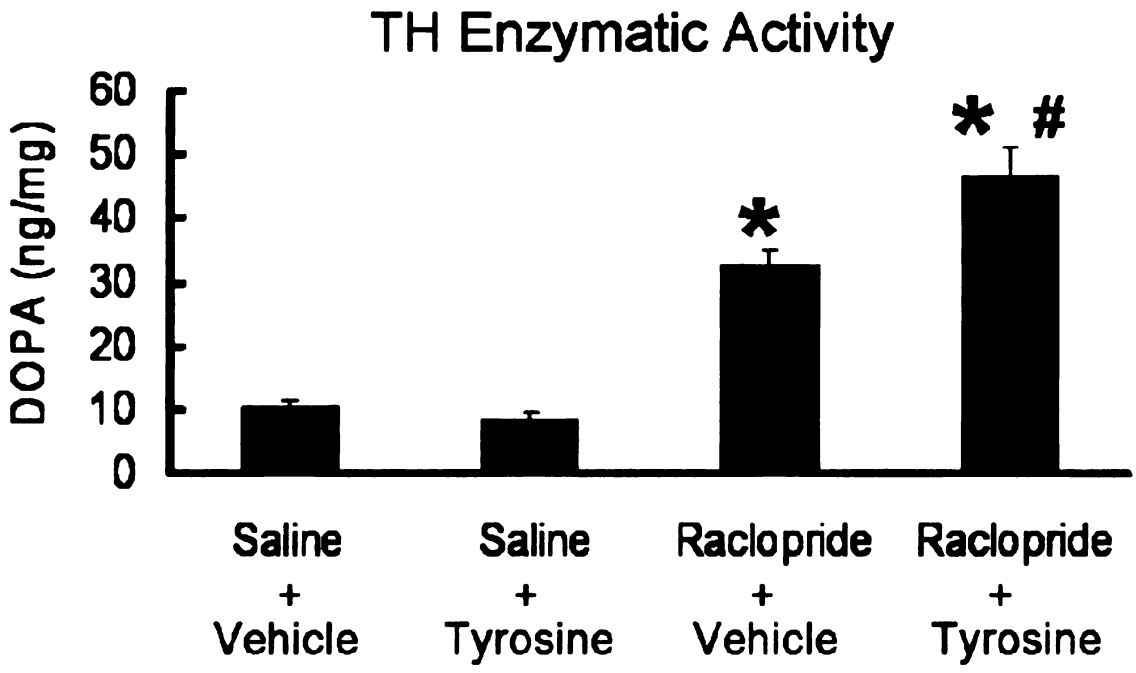

Figure 6-4. Concentrations of DOPA in the striatum of mice 60 min after administration of either saline (1 ml/kg, i.p.) + vehicle (saline, 1 ml/kg, i.p.), saline + tyrosine (100 mg/kg, i.p.), raclopride (1.0 mg/kg, i.p.) + vehicle, or raclopride + tyrosine. All mice received an injection of NSD-1015 (100 mg/kg, i.p.) 30 minutes prior to decapitation. Columns represent means of groups ± 1.0 S.E.M. of seven mice per group. (*) Values significantly different from saline + vehicle treated controls. (#) Values for tyrosine plus raclopride-treated mice significantly different from raclopride + vehicle-treated mice. $p \leq 0.05$.

	Saline + Vehicle	Saline + Tyrosine	Raclopride + Vehicle	Raclopride + Tyrosine
TH Protein (RDU)	32 ± 3	27 ± 4	24 ± 3	33 ± 3

Table 6-1. Total TH levels measured in relative density units (RDU) in the striatum of mice 60 min after administration of either saline (1 ml/kg, i.p.) + vehicle (saline, 1 ml/kg, i.p.), saline + tyrosine (100 mg/kg, i.p.), raclopride (1.0 mg/kg, i.p.) + vehicle, or raclopride + tyrosine. Relative density units were obtained by normalizing total TH band intensity to β-III tubulin band intensity. Values represent means of groups ± SEM.

Characterizing the Effects of Loss of Short-Loop Feedback Inhibition on the Regulation of DA Synthesis in NSDA Axon Terminals

Pharmacological inhibition of pre-synaptic D2 autoreceptors was used as a model to study the loss of short-loop feedback inhibition on DA synthesis. Administration of γ-butyrolactone (GBL) is a well documented pharmacological model that allows for autoreceptor-specific functions to be evaluated in the absence of activity-dependent compensation. As depicted in Figure 6-5, GBL inhibits NSDA cell firing (Howard and Feigenbaum, 1997) and impulse driven release of DA (Bettini et al., 1987; Imperato et al., 1987), which decreases DA binding to pre-synaptic and post-synaptic D2 receptors. Similar to the raclopride, inhibiting DA release functionally blocks both pre-synaptic and post-synaptic D2 receptors. The inhibition of cell firing however, prevents long-loop feedback from stimulating DA synthesis. This allows D2 autoreceptor-stimulated DA synthesis to be evaluated. GBL-induced disinhibition of pre-synaptic D2 autoreceptors increases adenylate cyclase activity, cAMP production and activation of cAMP-dependent PKA. Activation of PKA can accelerate DA synthesis by phosphorylating TH at serine-40 (Joh et al., 1978; Yamauchi and Fujisawa, 1979; Vulliet et al., 1980). Thus, the loss of short-loop feedback inhibition can accelerate DA synthesis.

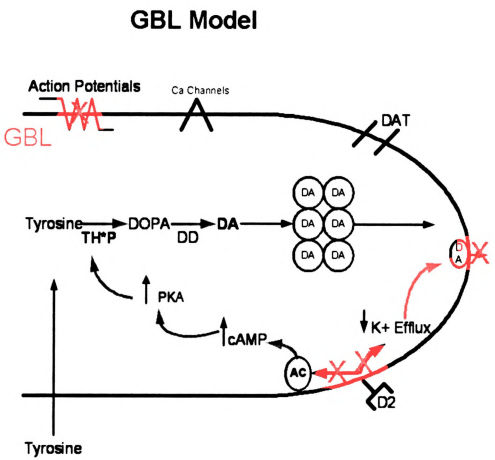

Figure 6-5. Schematic diagram depicting the neurochemical events in the axon terminal following administration of GBL. GBL administration blocks NSDA cell firing and decreases DA release and occupation of pre-synaptic D2 autoreceptors. This results in disinhibition of adenylate cyclase, TH phosphorylation by cAMP-dependent kinases and acceleration of TH enzymatic activity. Because DA release does not occur, DA stores increase in axon terminasl of NSDA neurons following GBL.

In the second set of experiment, mice were injected with either saline (1 ml/kg, i.p.) or GBL (750 mg/kg, i.p.) and decapitated 1 h following injection. Administration of GBL using this dose and time course activates DA synthesis (Demarest and Moore, 1979b). The effect of GBL on NSDA activity was assessed by measuring striatal concentrations of DOPAC and DA, and the DOPAC to DA ratio. To determine the effects of GBL on TH enzymatic activity and phosphorylation state, mice were injected with either saline (1 ml/kg, i.p.), tyrosine (100 mg/kg, i.p.), GBL (750 mg/kg, i.p.) or GBL + tyrosine and sacrificed 1 h following injection. Supplemental tyrosine was administered to prevent substrate limitations on TH activity in activated NSDA neurons (Sved and Fernstrom, 1981). Mice were then injected with NSD-1015 30 min prior to sacrifice. TH phosphorylation state was measured using Western blot analysis whereas, TH enzymatic activity was determined by measuring striatal DOPA concentration as described previously.

The Effects of GBL on DA Metabolism and Storage

GBL administration increased striatal DOPAC concentrations approximately 2-fold (Figure 6-6, A). Striatal DA concentrations were also increased by approximately 2-fold following GBL administration. Due to equivalent increases in striatal DOPAC and DA concentrations, there was no change in the ratio of DOPAC to DA in the striatum of mice treated with GBL (C).

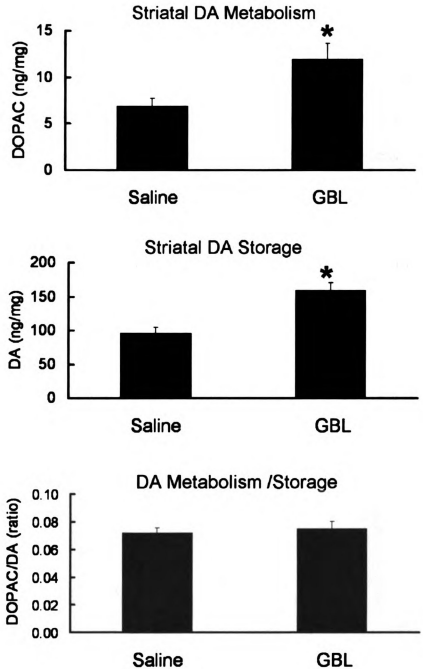

Figure 6-6. Concentrations of DOPAC (A), and DA (B), and the DOPAC/DA ratio (C) in the striatum of mice 60 min after administration of either saline (1 ml/kg, i.p.) or GBL (750 mg/kg, i.p.). Columns represent means of groups ± 1.0 S.E.M. of seven mice per group. (*) Values significantly different from saline treated controls. $p \leq 0.05$.

The Effect of Acute GBL on TH Phosphorylation State

As depicted in Figure 6-7 (A), neither tyrosine nor GBL altered basal levels of serine-19 phosphorylated TH. Administration of tyrosine plus GBL increased serine-19 phosphorylated TH levels 2-fold. As depicted in Figure 6-7 (B), there was no change in serine-31 phosphorylated TH in response to any drug treatment. As depicted in Figure 6-7 (C), tyrosine administration had no effect on basal levels of serine-40 phosphorylated TH. GBL administration produced an approximately 3-fold increase in serine-40 phosphorylated TH. Tyrosine plus GBL administration significantly increased serine-40 phosphorylated TH levels over raclopride treatment alone.

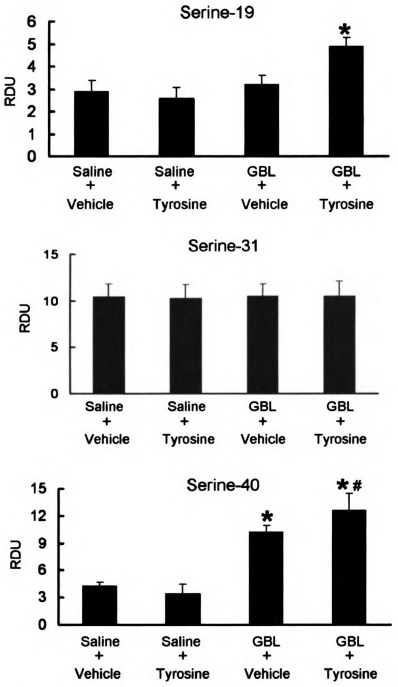

Figure 6-7. Serine-19 (A), serine-31 (B) and serine-40 (C) phosphorylated TH levels in the striatum of mice treated with either saline (1 ml/kg, i.p.) + vehicle (saline, 1 ml/kg, i.p.), saline + tyrosine (100 mg/kg, i.p.), raclopride (1.0 mg/kg, i.p.) + vehicle, or raclopride + tyrosine. Mice were killed 1 hr after drug administration. Relative density units (RDU) were obtained by normalizing the phosphorylated TH band density to β-III tubulin band density. Columns represent means of groups ± S.E.M. of seven mice/group. * indicate a significant difference from saline + vehicle-treated mice. # indicate a significant difference from GBL + vehicle-treated mice. $p \leq 0.05$.

The Effects of GBL on TH Enzymatic Activity and Expression

As depicted in Figure 6-8, tyrosine administration did not change basal TH enzymatic activity, as reflected by striatal DOPA concentrations. GBL administration produced an approximately 3-fold increase in TH catalytic activity and tyrosine supplementation resulted in an approximately 5-fold increase in TH catalytic activity that was significantly increased from mice treated with GBL alone. In contrast, levels of total TH did not vary in response to any treatment condition (Table 6-2).

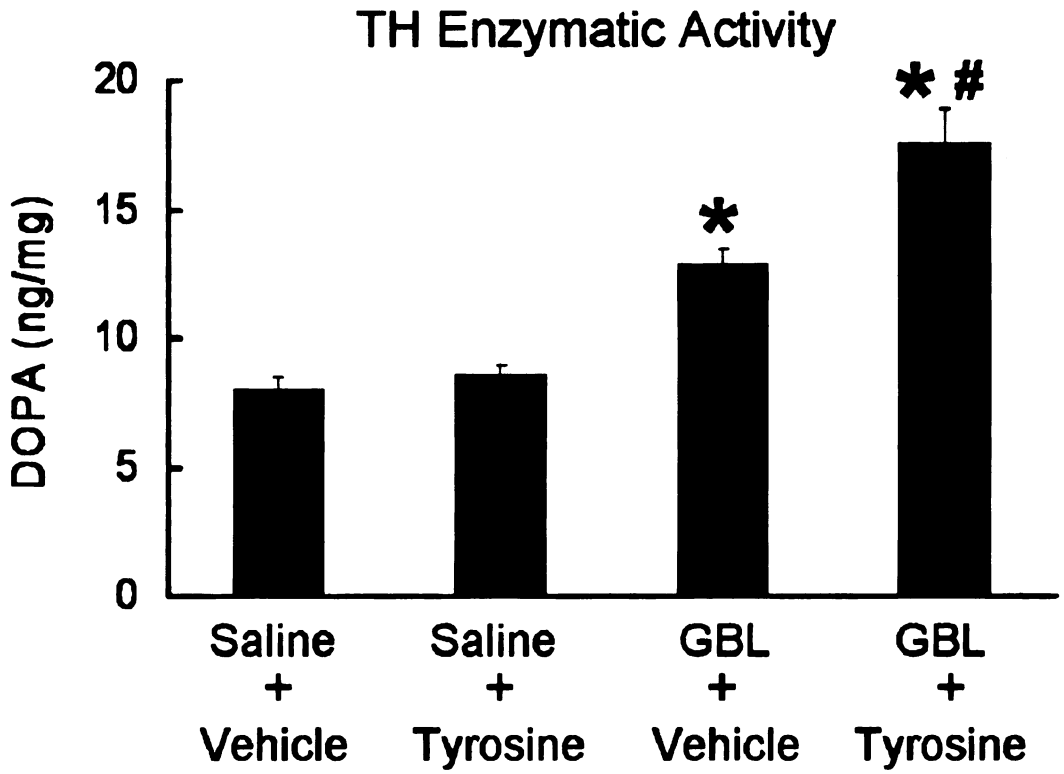

Figure 6-8. Concentrations of DOPA in the striatum of mice after administration of either saline (1 ml/kg, i.p.) + vehicle (saline 1 ml/kg, i.p.), saline + tyrosine (100 mg/kg, i.p.), GBL (750 mg/kg, i.p.) + vehicle, or GBL + tyrosine. All mice received an injection of NSD-1015 (100 mg/kg, i.p.) 30 minutes prior to decapitation. Columns represent means of groups (7 mice/group). Vertical lines represent ± 1.0 SEM. (*) Values that are significantly different from saline treated controls. (#) Values for tyrosine plus raclopride-treated animals that are significantly different from raclopride-treated animals. $p \leq 0.05$.

.

	Saline + Vehicle	Saline + Tyrosine	GBL + Vehicle	GBL + Tyrosine
TH Protein (RDU)	28 ± 4	28 ± 2	29 ± 3	33 ± 4

Table 6-2. Total TH levels measured in relative density units (RDU) in the striatum of mice after administration of either saline (1 ml/kg, i.p.) + vehicle (saline 1 ml/kg, i.p.), saline + tyrosine (100 mg/kg, i.p.), GBL (750 mg/kg, i.p.) + vehicle, or GBL + tyrosine. Relative density units were obtained by normalizing total TH band intensity to β-III tubulin band intensity. Values represent means of groups ± SEM.

Characterizing D2 Receptor Regulation of NSDA Activity Under Basal Conditions and Following MPTP Administration

The loss of D2 receptor function following MPTP could account for the dysfunctional regulation of DA synthesis in surviving axon terminals. To determine if this is the case, mice were pre-treated with either saline (basal conditions) or MPTP (compensatory activation). Subsequently, mice were treated with either raclopride, a D2 receptor antagonist, or quinelorane, a D2 receptor agonist, to determine if D2 receptors can accelerate or inhibit NSDA activity, respectively.

As depicted in Table 6-3, mice were injected with either saline (1 ml/kg, s.c.) or MPTP (20 mg/kg, s.c.) twice a week for 5 consecutive weeks. Three days following the last injection mice were anesthetized and Alzet osmotic mini-pumps filled with either saline, raclopride or quinelorane were implanted s.c. Mice were treated with either saline (150 µl/day), raclopride (0.5 mg/kg/day), or quinelorane (0.5 mg/kg/day) for 21 consecutive days. NSDA activity was assessed by measuring striatal DA metabolism, storage and activity by determining striatal concentrations of DOPAC, DA and the DOPAC to DA ratio, respectively.

Pre-Treatment	Post-Treatment: Saline (150 µl/day)	Post-Treatment: Raclopride (0.5 mg/kg/day)	Post-Treatment: Quinelorane (0.5 mg/kg/day)
Vehicle (1 ml/kg)	n=7	n=7	n=7
MPTP (20 mg/kg)	n=7	n=7	n=7

Table 6-3. Experimental design for determining whether D2 receptors regulate the activity of NSDA neurons following MPTP administration. Mice were pre-treated with either vehicle saline (1 ml/kg, s.c.) or MPTP (20 mg/kg, s.c.) twice a week for 5 consecutive weeks. Three days after the last injection osmotic mini-pumps were implanted s.c. filled with either saline, raclopride or quinelorane. Mice were treated with either saline (150 µl/day), raclopride (0.5 mg/kg/day) or quinelorane (0.5 mg/kg/day) for 21 consecutive days.

The Effects of Chronic Loss of D2 Receptor Regulation of NSDA Activity Under Basal Conditions and Following MPTP Administration

As depicted in Figure 6-9, in saline-treated mice (basal conditions), treatment with raclopride had no effect on striatal DOPAC (A) or DA (B) concentrations or the DOPAC to DA ratio (C). Under basal conditions, treatment with quinelorane decreased striatal DOPAC concentrations by approximately 25% (A), but did not alter striatal DA concentrations (B). Due to the decrease in striatal DOPAC, quinelorane decreased the DOPAC to DA ratio by approximately 25% (C).

MPTP treatment increased the DOPAC to DA ratio in all mice as compared to mice treated with saline. In MPTP-treated mice, raclopride had no effect on striatal DOPAC concentrations (A), but decreased striatal DA concentrations approximately 50% compared to MPTP + vehicle-treated mice. As such, raclopride treatment caused a dramatic increase in NSDA activity, as reflected by the DOPAC to DA ratio (C). In MPTP-treated mice, quinelorane treatment decreased striatal DOPAC (A) and DA (B) concentrations by approximately 50%. Due to the equivalent changes in DOPAC and DA concentrations, quinelorane treatment in MPTP-treated mice had no effect on the DOPAC to DA ratio (C).

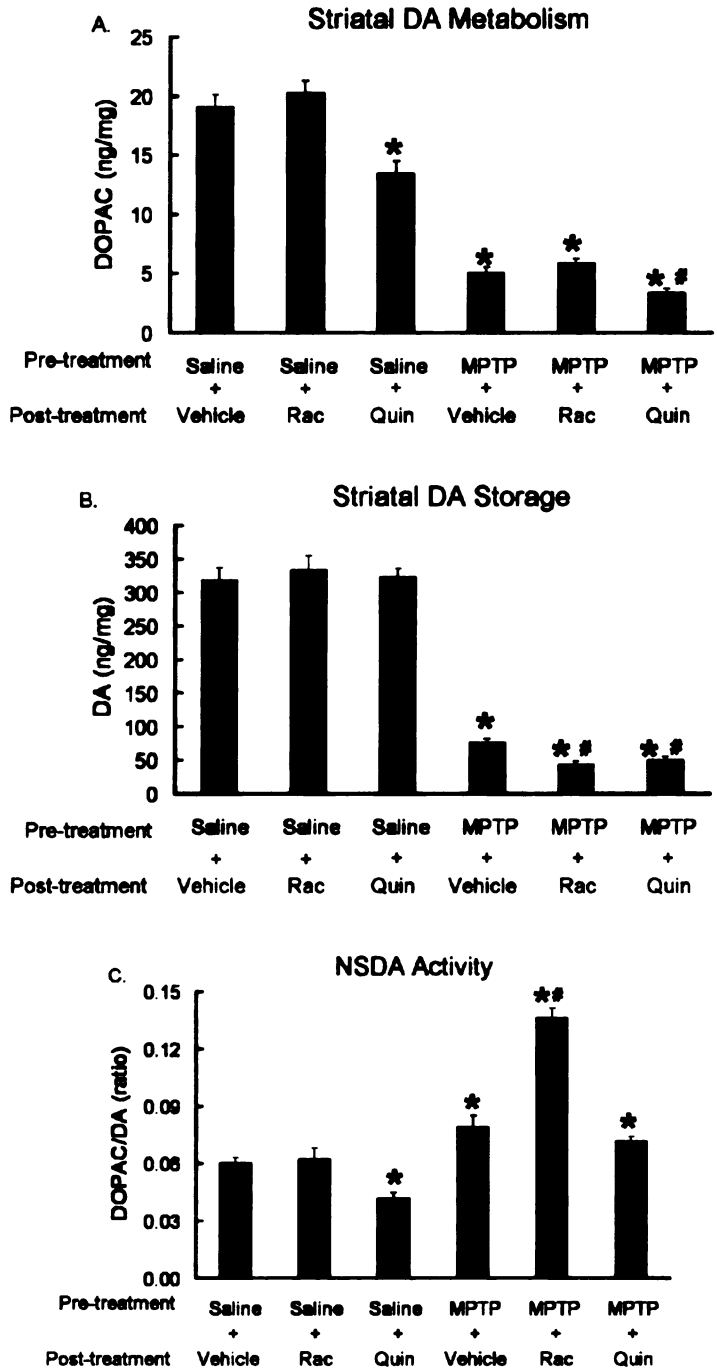

Figure 6-9. Concentrations of DOPAC (A), and DA (B), and the DOPAC/DA ratio (C) in the striatum of mice injected with either saline (1 ml/kg, s.c.) or MPTP (20 mg/kg, s.c.) twice a week for 5 consecutive weeks and post-treated with either vehicle (saline, 150 µl/day, s.c.), raclopride (Rac, 0.5 mg/kg/day, s.c.) or quinelorane (Quin 0.5 mg/kg/day, s.c.) for 21 consecutive days. Columns represent means ± SEM of seven mice/group. * indicate a significant difference from saline + vehicle treated mice. # indicate a significant difference from MPTP + vehicle treated mice. $p \leq 0.05$.

Determining if a Prolonged Loss of D2-Receptor-Mediated Feedback Inhibition and Chronic Activation is Detrimental to NSDA Neurons

To determine if a prolonged loss of D2 receptor-mediated feedback inhibition and the consequential chronic activation of NSDA neurons is detrimental, osmotic mini-pumps filled with either saline or raclopride were implanted s.c. in mice. Saline (150 μl/day) or raclopride (6 mg/kg/day) was administered to mice for 21 consecutive days. Administration of raclopride (1.0 mg/kg, i.p.) activates NSDA neurons for at least 4 h (Eaton et al., 1992). As such, the dose of raclopride was chosen to induce continual maximal activation of NSDA neurons. Mice were sacrificed on the 21st day of drug treatment. NSDA axon terminal loss was assessed by measuring striatal DA concentrations. To discriminate between the effects of raclopride on DA vesicular stores versus axon terminal loss, one group of mice was treated with raclopride for 21 days and pumps were removed 3 days prior to sacrifice to allow a drug elimination period. The half-life of raclopride following systemic administration is approximately 22 min (Volkow et al., 1996). Behavioral deficits and NSDA neuronal activity return to baseline by 4 h after systemic administration (Eaton et al., 1992; Ahlenius et al., 1997). Thus, 3 days after administration it is unlikely that raclopride is available to activate NSDA neurons.

The Effects of Chronic Raclopride on NSDA Axon Terminals

As depicted in Figure 6-10, chronic raclopride administration had no effect on striatal DOPAC concentrations (A). Chronic raclopride decreased striatal DA concentrations by approximately 50%, however this loss was transient as it was eliminated in mice following a 3 drug elimination period (B). Due to the decrease in striatal DA storage, chronic raclopride caused a 2-fold increase in the DOPAC to DA ratio (C). In mice treated with raclopride for 21 days followed with a 3 day drug elimination period, the DOPAC to DA ratio was significantly reduced compared to raclopride-treated mice.

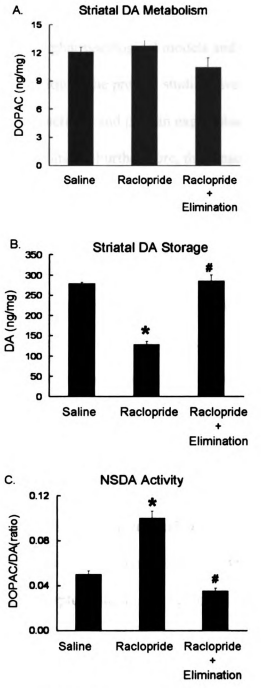

Figure 6-10. Concentrations of DOPAC (A), and DA (B), and the DOPAC/DA ratio (C) in the striatum of treated with either saline (150 µl/day) or raclopride (6 mg/kg/day, s.c.) chronically for 21 days. In the 3rd group of mice, pumps were implanted 3 days prior to the other 2 groups. Mice were treated for 21 days, and then 3 days prior to sacrifice, pumps were removed to allow a drug washout period. Columns represent means of groups ± S.E.M. of seven mice/group. * indicate a significant difference from saline + vehicle treated mice. # indicate a significant difference from raclopride-treated mice $p \leq 0.05$.

C. Discussion

Using well-characterized pharmacological models and standard neurochemical and immunohistochemical techniques, the present studies investigated the regulation of TH phosphorylation, enzymatic activity and protein expression following the loss of D2 receptor-mediated feedback inhibition. Furthermore, the present studies have characterized D2 receptor regulation of NSDA activity under basal conditions and following MPTP-induced compensatory activation of surviving NSDA neurons. The findings from these studies highlight differences in the regulation of DA metabolism following D2 receptor-mediated chronic activation of NSDA neurons and the neurotoxin-induced compensatory activation that suggest the compensatory activation of NSDA neurons is unique and may be detrimental to the survival of these neurons.

NSDA Activity Following a Loss of D2 Receptor-Mediated Long and Short-loop Feedback Inhibition

Under basal conditions, NSDA cell firing and DA release is governed at the axon terminal by feedback inhibition from post-synaptic and pre-synaptic D2 receptors. Blockade of post-synaptic D2 receptors diminishes feedback inhibition to NSDA cell bodies and increases cell firing, bursts of action potentials, and DA release at the axon terminal (Andersson et al., 1994; Andersson et al., 1995; Millan et al., 1998). Consistent with this, the present study suggests that acute raclopride-mediated blockade of D2 receptors increased NSDA neuronal activity, as reflected by the DOPAC to DA ratio. The findings from this study demonstrate that under basal conditions D2 receptors play a major role in inhibiting the activity of NSDA neurons, and that the loss of this feedback

inhibition results in a dramatic increase in DA release, reuptake and metabolism at the axon terminal.

The increased DOPAC to DA ratio was due to an increase in DA metabolism and a decrease in DA storage in the striatum. Normally, newly synthesized DA is preferentially released (Arbuthnott et al., 1990; Fairbrother et al., 1990a, 1990b; Biggs et al., 1996a; Biggs et al., 1996b), while storage pools of DA are only depleted when synthesis cannot keep up with the demand for release. The results from this experiment suggest that following blockade of long and short-loop feedback inhibition, DA synthesis cannot generate sufficient concentrations of DA to maintain the accelerated rate of release, and as a result stored vesicular DA is released to compensate.

TH Regulation Following a Loss of Long and Short-loop Feedback Inhibition

D2 receptors inhibit the activity of adenylate cyclase and thereby decrease cAMP concentrations. TH activation occurs predominantly through cAMP-dependent PKA phosphorylation of the serine-40 residue (Kumer and Vrana, 1996). Consistent with this, blockade of D2 receptors increased serine-40 phosphorylated TH levels and produced a dramatic increase in the catalytic activity of the enzyme. Additionally, as expected, there was no change in TH protein expression following acute raclopride since the 1 h time frame is too short to allow for *de novo* protein synthesis. The results from this study demonstrate that short-term (1 h) regulation of the rate of DA synthesis is achieved through D2 receptor-mediated inhibition of TH phosphorylation at serine-40.

The acceleration of NSDA neuronal activity caused by blockade of D2 receptors also resulted in increased TH phosphorylation at serine-31 and serine-19 but to a much

lesser extent than the serine-40 residue. The role of these serine residues in regulating TH activity is less well understood. Serine-31 is phosphorylated by MAP kinases, and the results from this study are consistent with previous reports that phosphorylation of this residue correlates with a 2-fold increase in TH activity (Haycock et al., 1992; Sutherland et al., 1993; Halloran and Vulliet, 1994). Serine-19 is phosphorylated predominantly by Ca^{+2} Calmodulin-dependent protein kinase II (Yamauchi and Fujisawa, 1981; Vulliet et al., 1984; Campbell et al., 1986) and this corresponded with an approximately 1.5-fold increase in enzymatic activity. Results suggest that serine-31 and serine-19 are also phosphorylated following accelerated neuronal activity and likely contribute to the increase in enzymatic activity. However, the Western blot and neurochemical techniques used in the present study do not resolve whether individual TH molecules are phosphorylated specifically at serine-40, serine-31 or serine-19, or whether multiple residues may be phosphorylated at the same time. If multiple serine residues may be simultaneously phosphorylated, the phosphorylation sequence of each residue in response to increased neuronal activity could provide important information as to the role of second messenger systems involved in TH activation and resolve the physiological consequence of phosphorylation of serine-31 and serine-19.

The present study also investigated the specific role of D2 autoreceptors in regulating TH phosphorylation and enzymatic activity. GBL administration inhibits NSDA cell firing thus decreasing action potential-mediated DA release. Decreased DA release prevents DA from binding to and activating pre-synaptic autoreceptors. The disinhibition of autoreceptors accelerates DA synthesis at the axon terminals, similar to the raclopride, but in the absence of increased neuronal activity. Acute GBL

administration caused a 2-fold increased DA metabolism and storage in the striatum. Since GBL inhibits DA release, the increased metabolism and storage of DA reflects the metabolism of newly synthesized DA, rather than recaptured DA.

Inhibition of D2 autoreceptor occupancy following GBL caused a 3-fold increase in serine-40 phosphorylated TH and a 2-fold increase in enzymatic activity. In contrast to the raclopride model, there was no change in serine-19 or serine-31 phosphorylated TH following GBL. Thus, D2 autoreceptors inhibit TH phosphorylation specifically at serine-40 and a loss of this feedback inhibition accelerates enzymatic activity. By comparing the effects of raclopride versus GBL on TH phosphorylation state and enzymatic activity we can infer that kinases activated in response to increased neuronal activity can phosphorylated TH at serine-19, serine-31 and also serine-40, whereas kinases activated in response to blockade of D2 autoreceptors can only phosphorylate TH at serine-40. Consistent with this, the induction of enzymatic activity by GBL was not as robust as following raclopride.

The specific increase in serine-40 phosphorylated TH following GBL was similar to the increase in serine-40 phosphorylated TH following MPTP administration. Thus, the dysfunctional regulation of DA synthesis following MPTP may be due to a loss of D2 autoreceptor function. However, in the present study, the increased phosphorylation was associated with a stimulation of catalytic activity. Following MPTP, there is no change in TH catalytic activity. The discrepancies between these two studies may be due to the acute GBL model versus the chronic MPTP model. D2 autoreceptor phosphorylation may increase TH enzymatic activity on a short-term basis, but lead to changes in protein expression for long-term acceleration in enzymatic activity. Thus, the increased

phosphorylation of TH following MPTP administration may reflect a loss of D2 autoreceptor function, but compensatory increases in TH protein expression which allow the rate of DA synthesis to be elevated, without increasing the activity of individual TH molecules.

The Effects of Substrate Tyrosine on TH in Activated NSDA Neurons

In the present study, administration of tyrosine had no effect on basal levels of serine-40, serine-31 or serine 19 phosphorylated TH, total TH or TH enzymatic activity. However, tyrosine supplementation to raclopride or GBL-treated mice resulted in enhanced TH catalytic activity over that seen following raclopride and GBL treatment alone. This is consistent with previous reports demonstrating that when the rate of catecholamine synthesis is increased, tyrosine administration enhances TH activity (Sved et al., 1979; Melamed et al., 1980; Sved and Fernstrom, 1981). Moreover, the effect of tyrosine on TH catalytic activity was associated with enhanced serine-40 and serine-19 phosphorylated TH. This is the first demonstration of substrate-enhanced TH activity corresponding enhanced phosphorylated TH levels at two distinct serine residues in activated NSDA neurons.

The balance of kinase activity, phosphatase activity and the amount of total TH available determine the final degree of phosphorylated TH. As such, tyrosine may have 1) facilitated TH phosphorylation, 2) hindered TH de-phosphorylation, or 3) increased the amount of available TH for phosphorylation. Tyrosine alone did not alter phosphorylated TH levels or TH catalytic activity. Therefore, it seems unlikely that the effect of substrate administration on TH occurs by enhanced kinase activity, increased

kinase access to phosphorylation sites, or interference with phosphatase activity under basal conditions. It is possible, that tyrosine is able to manipulate TH phosphorylation/de-phosphorylation only under stimulated conditions.

Another possibility is that tyrosine enhanced phosphorylated TH levels in response to raclopride and GBL by increasing the amount of TH available for phosphorylation. While striatal levels of total TH remained consistent in all treatment conditions, total TH protein may not reflect the actual amount of enzyme that is available for phosphorylation. Therefore, tyrosine may have either permitted additional TH to be phosphorylated or prevented irreversible TH inactivation. In the case of additional TH phosphorylation, sub-cellular fractionation studies have not been performed that would allow for distinguishing between TH protein available for phosphorylation, versus total TH levels in activated NSDA neurons in the presence or absence of tyrosine. The second mechanism by which tyrosine may increase the amount of TH available for phosphorylation is by preventing the irreversible inactivation of TH, such that it cannot be re-phosphorylated. In this case, tyrosine may enhance phosphorylated TH levels and TH activity in response to raclopride by preventing the long-term inactivation of TH through destabilization. The latter mechanism is supported by the observation that in rat striatal homogenates incubated with the protein kinase catalytic subunit (constant stimulus), increasing tyrosine concentrations prevents the irreversible inactivation of TH (Roskoski et al., 1990).

D2 Receptor Regulation of NSDA Activity Following MPTP Administration

D2 receptors regulate the activity of NSDA neurons and the rate of DA synthesis. As such, the compensatory activation of these neurons and dysfunctional regulation of DA synthesis following MPTP administration suggests there is a loss of D2 receptor function. To determine if this is the case, the ability of a D2 antagonist and agonist to increase or decrease NSDA activity, respectively, was assessed under basal conditions and following MPTP administration. This study was also used to determine if activation of D2 receptors could be used to decrease the activity of surviving NSDA neurons and protect them from oxidative damage due to increased DA metabolism. To this end, mice were pre-treated with either saline (basal conditions) or MPTP to recapitulate the compensatory activation of NSDA neurons. Mice were then treated with either vehicle, raclopride, or the D2 agonist quinelorane for 21 consecutive days.

The results demonstrated that under basal conditions, raclopride administration had no effect on striatal DA metabolism, storage or NSDA activity. It is possible the dose of raclopride was not sufficient to block D2 receptors and stimulate NSDA activity. However, treatment with quinelorane produced a 25% decrease in striatal DA metabolism, while having no effect on DA storage. Due to the decreased DA metabolism and no change in DA storage, quinelorane decreased the activity of NSDA neurons by approximately 25%. These findings suggest that chronic treatment with a DA agonist can cause a sustained decrease in DA metabolism in NSDA neurons. Thus, DA agonist therapy may protect NSDA neurons from oxidative damage under normal conditions. Consistent with this, chronic DA agonist administration decreases the age-related loss of NSDA neurons in rats (Felten et al., 1992).

Similar to basal conditions, in MPTP treated mice, raclopride treatment had no effect on striatal DA metabolism. However, raclopride had a very different effect on DA storage and NSDA activity compared to basal conditions. At the same dose of raclopride that had no effect under basal conditions, raclopride treatment in MPTP-treated mice caused a 50% decrease in DA storage and a robust increase in the activity of surviving NSDA axon terminals. These findings demonstrate that D2 receptors are functional in the striatum following MPTP administration. In fact, since the blockade of D2 receptors results in a more robust increase in NSDA activity in MPTP-treated mice, D2 receptors play a primary role in regulating neuronal activity under activated conditions.

Interestingly, acute raclopride administration causes an increase in DA metabolism and a decrease in DA storage. However, chronic raclopride decreased DA storage, but had no effect on DA metabolism. These results may suggest the dose of raclopride was not sufficient to increase DA metabolism, however this is unlikely because the same dose caused a 50% decrease in striatal DA storage. More likely, these results suggest there are compensatory mechanisms that occur in NSDA neurons that allow them to sustain an accelerated rate of DA release, in the absence of increased DA metabolism. This is particularly relevant, since this does not occur in NSDA neurons that have been activated in response to neurotoxic lesion. The compensatory activation of NSDA neurons is associated with a prolonged, sustained increase in DA metabolism due to over-activation of DA synthesis coupled with decreased storage capability. These results therefore suggest that DA synthesis and storage remain coupled during chronic activation of NSDA neurons induced by the loss of D2 receptor-mediated long- and

short-loop feedback inhibition. This may be due to either; increased VMAT-2 expression and activity, increased TH-synaptic vesicle association, or both.

Taken together, the results from the present experiments highlight differences between the compensatory activation of NSDA neurons following MPTP and activation of these neurons in response to a prolonged loss of D2 receptor-mediated long and short-loop feedback inhibition. Determining the mechanisms that occur in NSDA neurons that permit a prolonged acceleration in neuronal activity without increasing DA metabolism may; 1) identify targets that can be used to protect NSDA neurons from the toxic byproducts of DA metabolism, without compromising their ability to accelerate DA release and 2) delineate dysfunctional mechanisms in NSDA neurons that may contribute to the pathogenesis of PD.

In MPTP-treated mice, quinelorane treatment produced a similar decrease in DA metabolism as it did under basal conditions. However, quinelorane treatment had a different effect on DA storage and NSDA activity than it did basal conditions. The same dose of quinelorane that failed to alter DA storage under basal conditions decreased DA concentrations by approximately 50% in MPTP-treated mice. Since quinelorane decreased DA metabolism and storage there was no change in the activity of NSDA neurons compared to mice treated with MPTP and treated with vehicle. The decrease in DA storage likely reflects an inhibition of DA synthesis by D2 autoreceptors. The inhibition of DA synthesis decreased the amount of newly synthesized DA available for release and stored DA was released to compensate.

Interestingly, while the activation of D2 receptors by quinelorane did not decrease neuronal activity, it did inhibit DA metabolism. Therefore, activation of D2 receptors

may protect NSDA neurons from the toxic byproducts of DA metabolism and prevent the progressive demise of these neurons in PD. However, in the MPTP model of PD this was not the case, since quinelorane treatment did not protect NSDA axon terminals, as reflected by striatal DA concentrations. One potential explanation for this finding is that quinelorane was administered after MPTP had already caused significant damage to NSDA axon terminals. It is possible that if quinelorane was co-administered with MPTP, the inhibition of DA metabolism may slow the progressive loss of NSDA axon terminals caused by MPTP. A number of previous studies have supported this conclusion (Lange et al., 1994; Youdim et al., 2000; Schapira, 2002), however, since activation of D2 receptors can also decrease DAT expression and uptake of the MPP+ neurotoxin, these results are open to interpretation. Further experiments utilizing neurotoxins that are not dependent on the DAT (such as rotenone) or transgenic PD models may determine if DA agonists (due to their ability to decrease DA metabolism) are neuroprotective in animal models of PD.

Differences Between Acute and Chronic Activation of NSDA Neurons

Acute blockade of D2 receptors with raclopride increases DA metabolism, decreases DA storage and increases the DOPAC to DA ratio. However, chronic blockade of D2 receptors with raclopride in MPTP-treated mice had no effect on DA metabolism, but caused a decrease in DA storage and an increase in NSDA activity. These results highlight differences between short and long-term regulation of NSDA activity and suggest that long-term compensatory changes in NSDA regulation allow for an increase in neuronal activity without an increase in DA metabolism. However, these findings may

have been due to the low dose of raclopride used in the chronic dosing study compared to the relatively high dose used in the acute dosing study or the effects of MPTP pre-treatment. To determine if this is the case, mice were treated with raclopride chronically for 21 days using a dose sufficient to activate NSDA neurons for 24 consecutive h.

Results from this study demonstrated that chronic activation of NSDA neurons with raclopride has no effect on DA metabolism, but decreased DA storage and increased NSDA activity. Due to the decreased concentrations of striatal DA, these results could suggest that chronic activation of NSDA neurons caused a loss of NSDA axon terminals. However, this is not the case since the decreased DA concentrations were only transient and were eliminated in mice that had a 3 day drug elimination period. The findings from this study demonstrate critical differences between acute and chronic activation of NSDA neurons using a D2 antagonist as well as differences between chronic activation with a D2 antagonist and the compensatory activation of NSDA neurons following neurotoxin insult. Under normal conditions, the chronic activation of NSDA neurons is unlikely to cause axon terminal loss, since compensatory mechanisms prevent excessive DA metabolism. However, the MPTP-induced compensatory increase in activity results in a chronic activation of NSDA neurons that may contribute to axon terminal loss due to un-regulated accelerations in DA metabolism and induction of cytoplasmic DA-mediated oxidative stress.

Summary

The results from the present studies have characterized the regulation of TH following a loss of D2 receptor-mediated feedback inhibition. The loss of D2

autoreceptor-mediated short-loop feedback inhibition increases TH phosphorylation at the axon terminal similar to the MPTP-induced compensatory activation of NSDA neurons. These findings suggest that a loss of D2 autoreceptor regulation could underlie the dysfunctional regulation of DA synthesis following MPTP. However, further studies using the GBL and raclopride models of D2 autoreceptor regulation and evaluation of D2 autoreceptor expression will be necessary to delineate the specific role for short-loop feedback inhibition in the dysfunctional regulation of DA synthesis following MPTP.

The present studies also describe critical differences in acute versus chronic activation of NSDA neurons, induced by blockade of D2 receptor-mediated feedback inhibition. Acute loss of feedback inhibition results in activation of NSDA neurons and increased DA metabolism that is similar to the compensatory activation of these neurons following neurotoxin insult. However, prolonged activation of NSDA neurons results in compensatory mechanisms that allow DA release to remain accelerated in the absence of increased DA metabolism. Taken together, the compensatory activation of NSDA neurons in response to MPTP administration is unique from the chronic activation of these neurons induced by blockade of D2 receptor-mediated feedback inhibition. Further experiments comparing the regulation of VMAT-2 protein expression and activity as well as the coupling between DA synthesis and storage will be crucial to understanding the differential activation of NSDA neurons in response to axon terminal loss versus the loss of D2 receptor mediated feedback inhibition. These studies will be important for identifying compensatory mechanisms that allow NSDA neuronal activity to be accelerated without a corresponding increase in DA metabolism.

Chapter 7. The Role of α-Synuclein in MPTP-Induced Neurotoxicity and the Compensatory Activation of NSDA Neurons

A. Introduction

α-Synuclein is a protein that is distributed ubiquitously throughout the brain and found primarily in axon terminals (Nakajo et al., 1993; Jakes et al., 1994). α-Synuclein is a relatively small protein with 140 amino acids and a molecular weight of 19 kDa. The biochemical structure predicts that this protein may be a molecular chaperone capable of binding to other intracellular proteins. Within the first 87 residues of the 140 amino acid sequence there are repetitive amino acid motifs (KTKEGV) with a strict periodicity of 11 amino acids. These repeats are reminiscent of amphipathic helices in apolipoproteins that determine protein hydrophobicity and facilitate membrane binding (George et al., 1995). α-Synuclein exists primarily in the cytosolic fraction as a natively unfolded protein (Ostrerova et al., 1999; Takenouchi et al., 2001). However, this protein can readily associate with membranes (McLean et al., 2000) and take on a α-helical conformation upon binding to synthetic lipid membranes (Davidson et al., 1998; Jo et al., 2000).

Several lines of evidence suggest that α-synuclein is critical to NSDA neuronal function. Degeneration of NSDA neurons is associated with the clinical motor deficits of PD and inappropriate aggregation of α-synuclein likely plays a causative role in NSDA cell death. Mutations, duplications, or triplications in the α-synuclein gene occur in familial forms of PD and result in the degeneration of NSDA neurons (Polymeropoulos et al., 1997; Kruger et al., 1998; Singleton et al., 2003). Also, degenerating NSDA neurons in brain tissue from post-mortem PD patients contain cytoplasmic aggregations of protein

termed Lewy-bodies. α-Synuclein is the primary structural component of Lewy-bodies. The roles that α-synuclein aggregation and Lewy-body formation play in NSDA neuronal degeneration are not known, but it is clear these protein aggregates overlap PD pathogenesis. Taken together, it is apparent that understanding the function of normal α-synuclein in NSDA neurons will greatly enhance the relatively unknown pathology of PD.

Comparing the function of NSDA neurons that express α-synuclein to those lacking this protein provides a useful tool for determining the function of α-synuclein. To this end, our laboratory generated a stable breeding colony of homozygous α-synuclein knock-out mice. Mice originally obtained in breeding pairs from Jackson Laboratories (B6;129 X-SNCA^{tm1Rosl}) were crossed with wild type C57/Bl6 mice to obtain heterozygote mice (F1). Heterozygote mice were then crossed and the offspring were used to generate a stable breeding colony of age-matched wild-type and α-synuclein knock-out mice. The generation, viability, and anatomical characteristics of these mice have been described previously (Abeliovich et al., 2000). However, NSDA neuronal physiology in these mice has not been thoroughly studied.

α-Synuclein knock-out mice are virtually indistinguishable from wild-type mice using several indices of NSDA neuron function. α-Synuclein knock-out mice possess normal complements of NSDA cell bodies and synapses, and there is no difference in electrical stimulus-evoked DA release compared to wild-type mice (Abeliovich et al., 2000). Thus, it is unlikely that α-synuclein plays an essential role in maintaining NSDA activity under basal conditions. α-Synuclein, however, may be important in the regulation of activated NSDA neurons. Evidence suggests α-synuclein serves as an

activity dependent regulator of axon terminal function. While there is no difference electrophysiological measurements of synaptic transmission in the striatum under simple electrically stimulated conditions, following paired pulse trains of electrical stimuli, α-synuclein knock-out mice display enhanced neurotransmitter release (Abeliovich et al., 2000). This suggests that α-synuclein is important to neuronal physiology under activated conditions.

Administration of MPTP is a useful pharmacological model for evaluation of NSDA neuron function under activated conditions which results from the compensatory increase in the activity of surviving neurons. To determine if α-synuclein plays a role in regulating NSDA activity under activated conditions, α-synuclein knock-out mice were treated with prolonged-chronic MPTP and DA metabolism, storage and the activity of surviving NSDA neurons were measured in the striatum. Results from this initial experiment suggested that mice lacking α-synuclein had a deficit in NSDA neuronal response to MPTP administration. Since the compensatory activation of NSDA neurons is known to be due to dysfunctional regulation of DA synthesis, these experiments suggested α-synuclein may play a role in regulating TH. To determine if this is the case, regulation of TH phosphorylation state, enzymatic activity and expression were assessed in the striatum following either; raclopride-induced loss of D2 receptor-mediated feedback inhibition, or MPTP-induced compensatory activation of NSDA neurons.

B. Experimental Design and Results

Prolonged-Chronic MPTP Administration in α-Synuclein Knock-out Mice

To determine if α-synuclein plays a role in regulating NSDA activity under activated conditions, mice lacking α-synuclein were injected with either saline (1 ml/kg, s.c.) or MPTP (1, 5, 10 or 20 mg/kg, s.c.) twice a week for 5 consecutive weeks. Probenecid (250 mg/kg, i.p.) was co-administered with saline and MPTP injections. Mice were sacrificed 3 weeks following the last MPTP injection. Striatal DOPAC and DA concentrations were measured using HPLC-EC.

The Effects of Prolonged-Chronic MPTP Administration on NSDA Axon Terminals in α-Synuclein Knock-out Mice

In α-synuclein knock-out mice prolonged-chronic MPTP administration at the highest dose (20 mg/kg) decreased striatal DA concentrations approximately 60% compared to saline-treated mice (Figure 7-1, A). MPTP administration at this dose also caused a decrease in DOPAC concentrations in the striatum (Figure 7-1, B). The decrease in striatal DOPAC concentrations was equivalent to the loss of striatal DA following MPTP, such that there was no change in the DOPAC to DA ratio in α-synuclein knock-out mice treated with MPTP (Figure 7-1, C). Despite a loss of approximately 60% of striatal DA concentrations, there was no change in striatal VMAT-2 protein levels following MPTP (Figure 7-2).

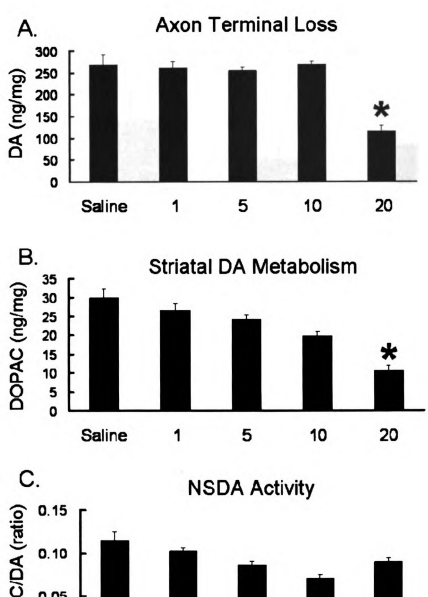

Figure 7-1. Dose response effect of prolonged-chronic MPTP administration on DA (A) and DOPAC (B) concentrations and the DOPAC to DA ratio (C) in the striatum of α-synuclein knock-out mice. Mice were treated with either MPTP (1, 5, 10 or 20 mg/kg, s.c.) or its saline vehicle (1 ml/kg, s.c.) every 3.5 days for 5 consecutive weeks and killed by decapitation 3 weeks following the last injection. Probenecid (250 mg/kg, i.p.) was co-administered with each injection of saline or MPTP. Columns represent means of groups ± S.E.M. of six to eight determinants. (*) indicate a significant difference from saline treatment group. ($p \leq 0.05$).

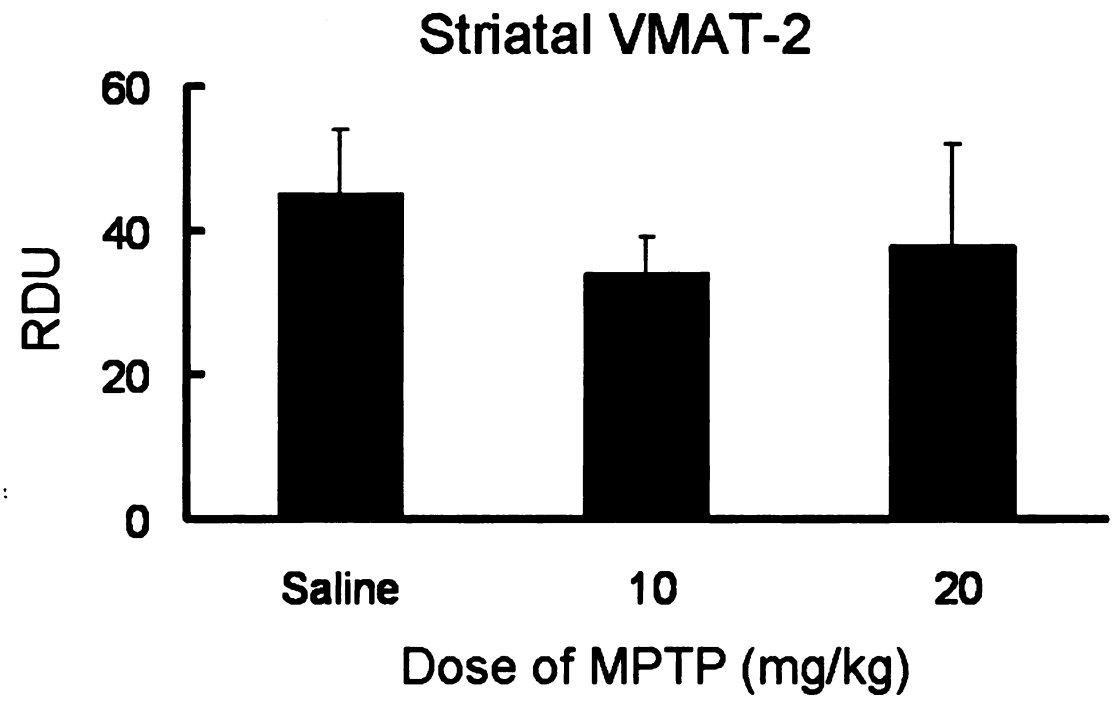

Figure 7-2. Dose-response effect of prolonged-chronic MPTP administration on striatal VMAT-2 immunoreactivity. Mice were injected with either MPTP (10 or 20 mg/kg, s.c.) or its saline vehicle (1.0 ml/kg, s.c.) every 3.5 days for 5 consecutive weeks and killed by decapitation 3 weeks following the last injection. Probenecid (250 mg/kg, i.p.) was co-administered with each injection of saline or MPTP. Striatal VMAT-2 was measured using Western blot analysis and are shown as relative density units (RDU). Columns represent means of groups ± S.E.M. of six to eight determinants.

Regulation of TH Activity in α-Synuclein Knock-out Mice Following Raclopride-Induced Loss of D2 Receptor Mediated Feedback Inhibition

To determine if α-synuclein plays a role in regulating DA synthesis under basal and/or activated conditions, α-synuclein knock-out mice were injected with either saline or raclopride, in the presence or absence of supplemental tyrosine. Mice were injected with either saline (1 ml/kg, i.p.) or saline plus tyrosine (100 mg/kg, i.p.) to simulate basal conditions. Other groups of mice were injected with either raclopride (1.0 mg/kg, i.p.) plus vehicle, or raclopride plus tyrosine to simulate activated conditions. Mice were sacrificed 60 min after drug administration. NSDA activity was determined by measuring striatal DOPAC and DA concentrations using HPLC-EC. To determine if α-synuclein regulates TH catalytic activity, a separate experiment was performed in which mice were administered either saline, tyrosine, raclopride or tyrosine plus raclopride as described above and killed 60 min following injection. All mice were injected with NSD-1015 (100 mg/kg, i.p.) 30 min prior to sacrifice. TH phosphorylation state was measured using Western blot analysis. Striatal DOPA concentrations were measured using HPLC-EC as an index of TH catalytic activity.

The Effect of Acute Raclopride on NSDA Activity in α-Synuclein Knock-out Mice

As depicted in Figure 7-3 (A), tyrosine administration alone had no effect on DA metabolism, as reflected by striatal DOPAC concentrations. Raclopride administration alone caused a 4-fold increase in striatal DA metabolism. Tyrosine supplementation in raclopride-treated mice further increased striatal DA metabolism compared to mice treated with raclopride alone. As depicted in Figure 7-3 (B), tyrosine administration alone slightly increased basal levels of striatal DA storage, as reflected by concentrations of DA. Raclopride administration decreased striatal DA storage by approximately 25% in normal and tyrosine supplemented mice. As depicted in Figure 7-3 (C), tyrosine administration had no effect on NSDA activity, as reflected by the DOPAC to DA ratio. Raclopride administration alone caused a 5-fold increase in NSDA activity and tyrosine supplementation caused a further 30% increase in the DOPAC to DA ratio over mice treated with raclopride alone.

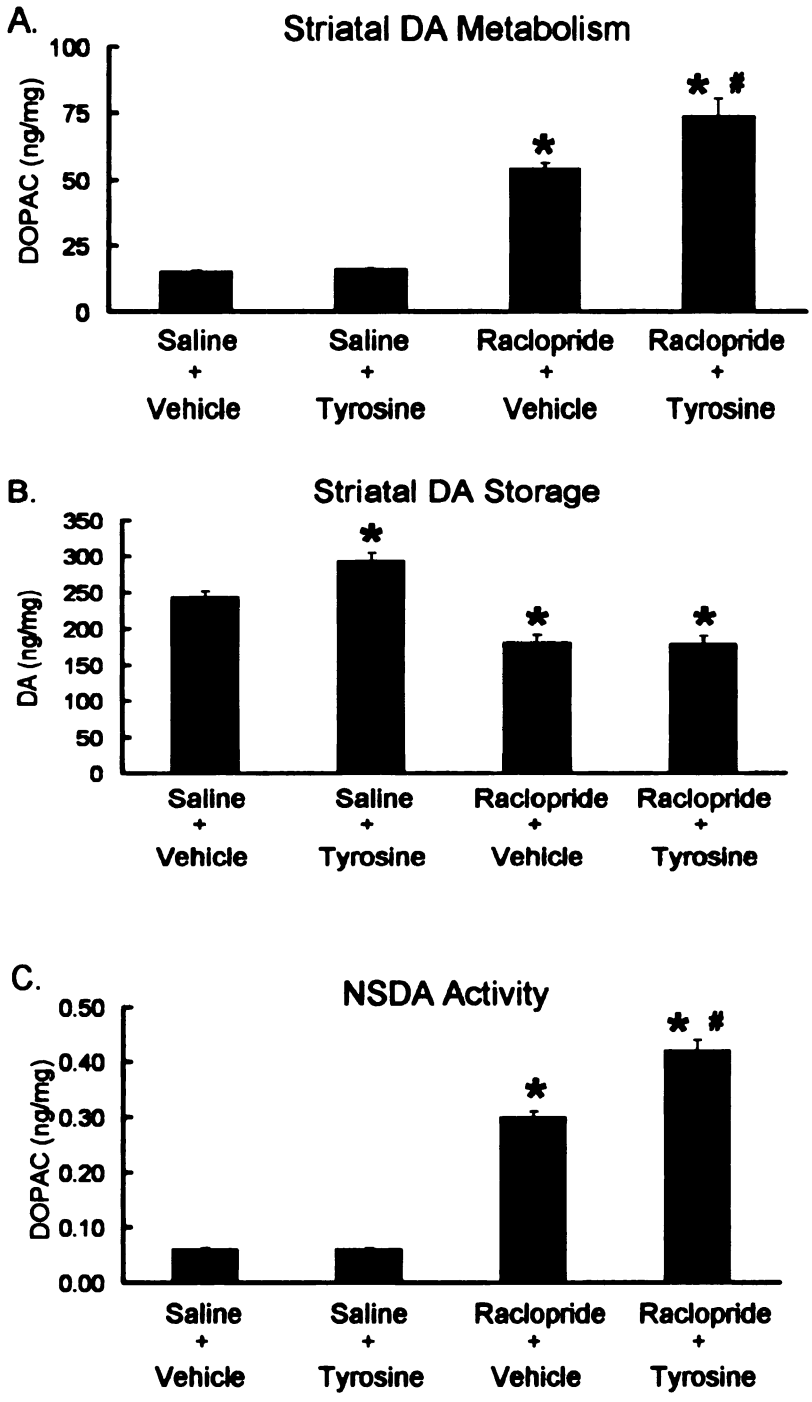

Figure 7-3. Concentrations of DOPAC (A), and DA (B), and the DOPAC/DA ratio (C) in the striatum of α-synuclein knock-out mice 60 min after administration of either saline (1 ml/kg, i.p.) + vehicle (saline 1 ml/kg, i.p.), saline + tyrosine (100 mg/kg, i.p.), raclopride (1.0 mg/kg, i.p.) + vehicle, or raclopride + tyrosine. Columns represent means of groups ± S.E.M. of seven mice per group. (*) Values significantly different from saline treated controls. # Values significantly different from raclopride + vehicle-treated mice. $p \leq 0.05$.

The Effect of Acute Raclopride Administration on TH Phosphorylation State in α-Synuclein Knock-out Mice

As depicted in Figure 7-4 (A), tyrosine administration alone had no effect on basal levels of serine-19 phosphorylated TH. Raclopride administration alone produced an approximately 1.5-fold increase in serine-19 phosphorylated TH levels. Tyrosine plus raclopride administration did not further increase serine-19 phosphorylated TH levels over mice treated with raclopride alone. As depicted in Figure 7-4 (B), tyrosine administration alone did not change basal levels of serine-31 phosphorylated TH. Raclopride administration alone produced an approximately 1.5-fold increase in serine-31 phosphorylated TH levels. Tyrosine supplementation in raclopride-treated mice did not affect serine-31 phosphorylated TH levels compared with raclopride treatment alone. As depicted in Figure 7-4 (C), tyrosine administration alone had no effect on basal levels of serine-40 phosphorylated TH. Raclopride administration alone produced an approximately 6-fold increase in serine-40 phosphorylated TH. Tyrosine plus raclopride administration did not further increase serine-40 phosphorylated TH levels over raclopride treatment alone.

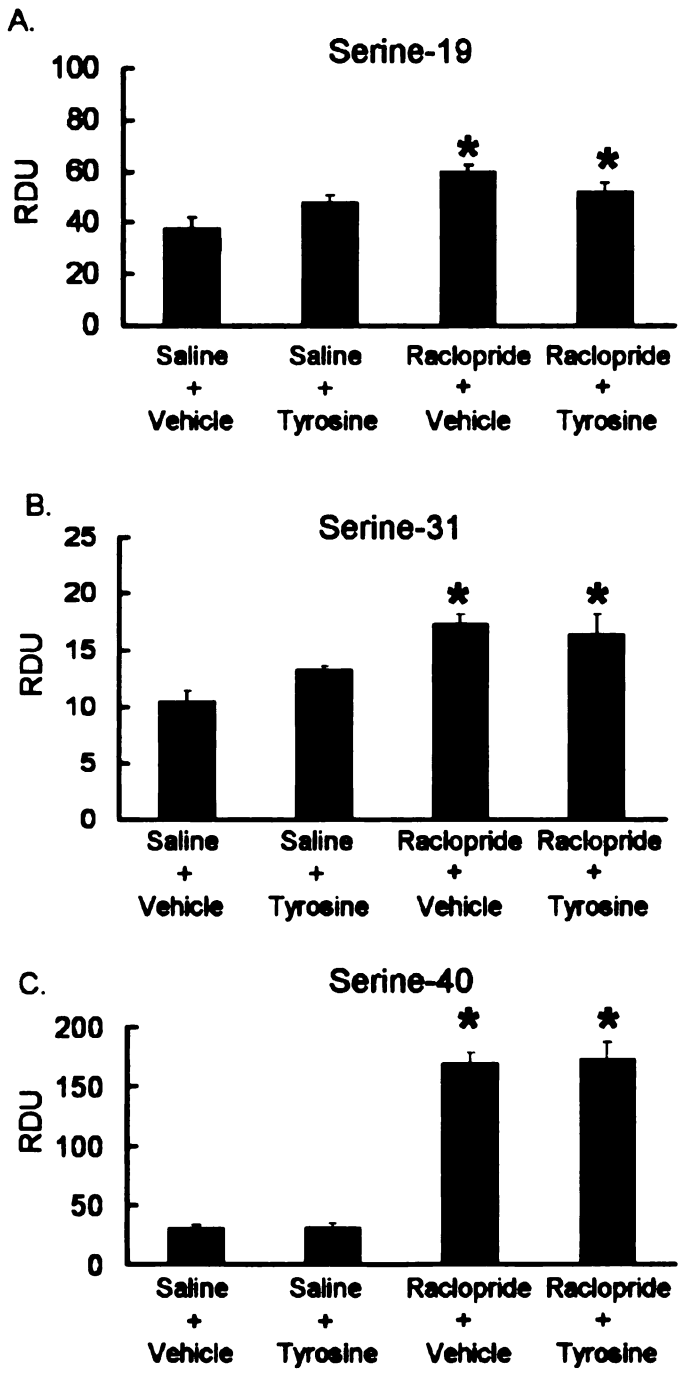

Figure 7-4. Serine-19 (A), serine-31 (B) and serine-40 (C) phosphorylated TH levels in the striatum of α-synuclein knock-out mice treated with either saline (1 ml/kg, i.p.) + vehicle (1 ml/kg, i.p.), saline + tyrosine (100 mg/kg, i.p.), raclopride (1.0 mg/kg, i.p.) + vehicle, or raclopride + tyrosine. Mice were killed 1 hr after drug administration. Columns represent means of groups ± S.E.M. of seven mice/group. * indicate a significant difference from saline + vehicle-treated mice. $p \leq 0.05$.

The Effect of Acute Raclopride Administration on TH Enzymatic Activity and Protein Expression

As depicted in Figure 7-5, tyrosine administration alone did not change basal TH catalytic activity, as reflected by striatal DOPA concentrations. Raclopride administration alone produced an approximately 3-fold increase in TH catalytic activity and tyrosine supplementation did not further increase TH catalytic activity compared to mice treated with raclopride alone. As depicted in Table 7-1, levels of total TH did not vary in response to any treatment condition.

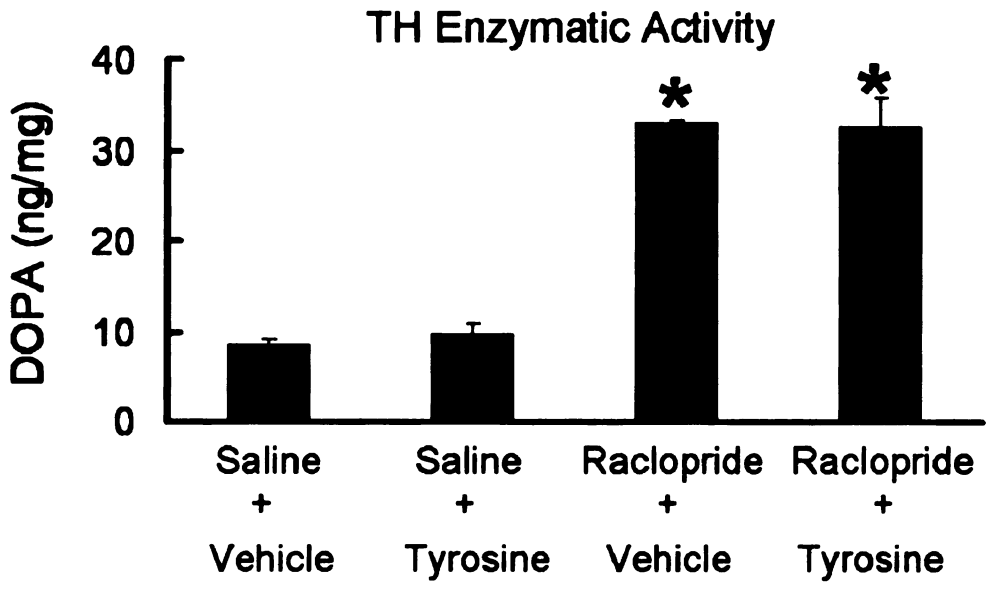

Figure 7-5. Concentrations of DOPA in the striatum of α-synuclein knock-out mice after administration of either saline (1 ml/kg, i.p.) + vehicle (saline, 1 ml/kg, i.p.), saline + tyrosine (100 mg/kg, i.p.), raclopride (1.0 mg/kg, i.p.) + vehicle, or raclopride + tyrosine. All mice received an injection of NSD-1015 (100 mg/kg, i.p.) 30 minutes prior to decapitation. Columns represent means of groups ± S.E.M of seven mice per group. (*) Values significantly different from saline treated controls. $p \leq 0.05$.

	Saline + Vehicle	Saline + Tyrosine	Raclopride + Vehicle	Raclopride + Tyrosine
TH Protein (RDU)	31 ± 4	39 ± 4	29 ± 4	31 ± 3

Table 7-1. Total TH levels measured in relative density units (RDU) in the striatum of α-synuclein knock-out mice after administration of either saline (1 ml/kg, i.p.) + vehicle (saline, 1 ml/kg, i.p.), saline + tyrosine (100 mg/kg, i.p.), raclopride (1.0 mg/kg, i.p.) + vehicle, or raclopride + tyrosine. Values represent means of groups ± S.E.M of seven mice per group.

Regulation of TH Activity in α-Synuclein Knock-out Mice Following Sub-Chronic MPTP Administration

To determine if α-synuclein plays a role in regulating DA synthesis in NSDA axon terminals activated in response to MPTP administration, α-synuclein knock-out mice were treated with saline (1 ml/kg, s.c.) or MPTP (25 mg/kg, s.c.) once a day for 5 consecutive days. Mice were sacrificed 3 days after the last injection. NSDA activity was measured by determining striatal DOPAC and DA concentrations, and the DOPAC to DA ratio. In a separate experiment, mice were injected with either saline or MPTP as described above and 30 min prior to sacrifice mice were injected with NSD-1015 (100 mg/kg, i.p.). The rate of DA synthesis as well as TH phosphorylation state, enzymatic activity and protein expression were measured in the striatum as described above. To determine if α-synuclein plays a role in regulating the sub-cellular distribution of TH at the axon terminal, a subsequent experiment was conducted in which α-synuclein knock-out mice were injected with either saline (1 ml/kg, s.c.) or MPTP (25 mg/kg, s.c.) once a day for 5 consecutive days. Mice were killed 3 days after the last injection. The striatum was freshly dissected and prepared for sub-cellular fractionation as described previously in Chapter 5. Striatal protein was separated into cytoplasmic, early endosomal, synaptic vesicle and plasma membrane fractions using differential centrifugation. TH protein located in each fraction was determined using Western blot analysis.

Effects of Sub-Chronic MPTP Administration on NSDA Axon terminals in α-Synuclein Knock-out Mice

In α-synuclein knock-out mice sub-chronic MPTP administration caused a 75% loss of NSDA axon terminals, as reflected by striatal DA concentrations (Figure 7-6, A). MPTP also caused a 65% decrease in striatal DA metabolism, as reflected by striatal DOPAC concentrations (Figure 7-6, B). There was a slight increase in the activity of NSDA neurons in the striatum following MPTP administration, as reflected by the DOPAC to DA ratio (Figure 7-6, C).

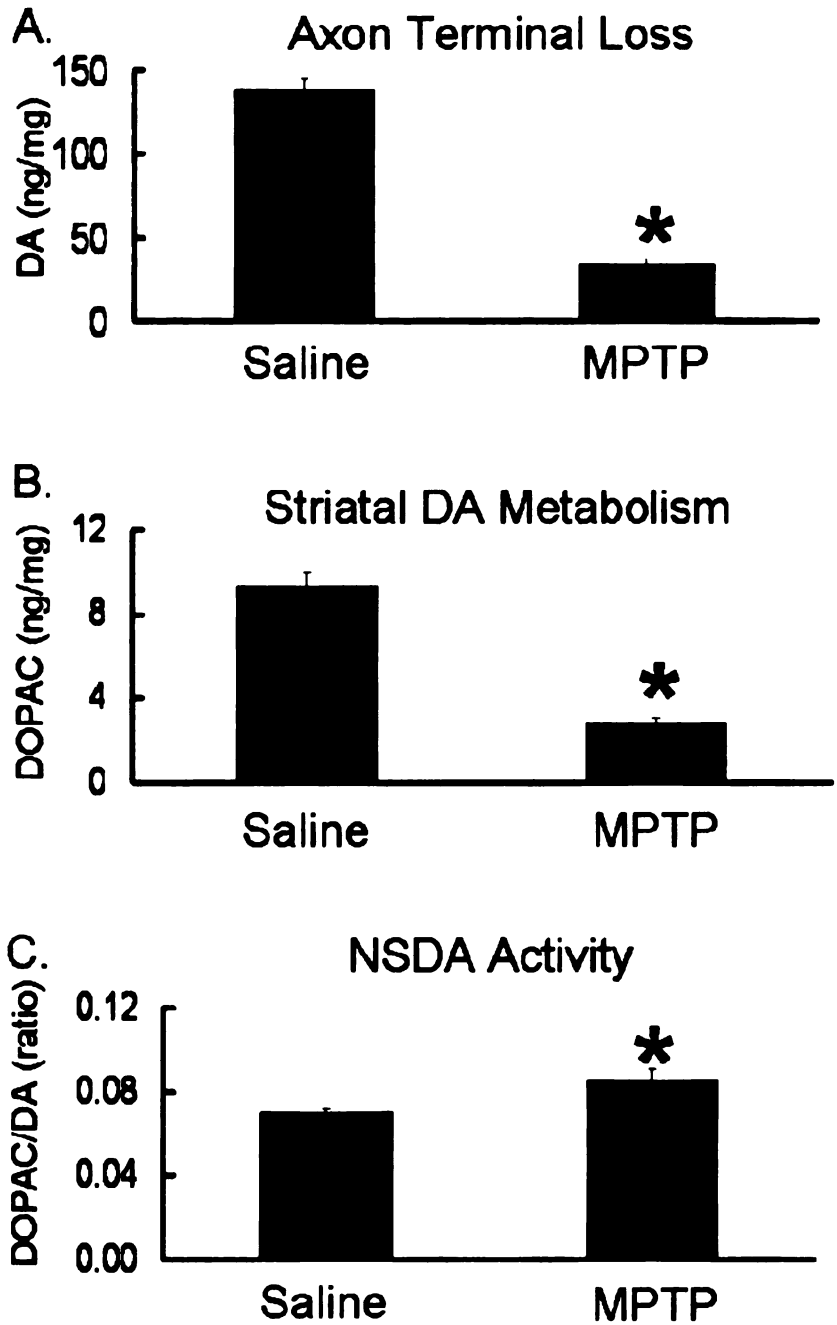

Figure 7-6. Effects of sub-chronic MPTP administration on striatal DA (A) and DOPAC (B) concentrations and DOPAC/DA ratios (C) in α-synuclein knock-out mice. Mice were treated with saline (1.0 ml/kg, s.c.) or MPTP (25 mg/kg, s.c.) once a day for five consecutive days and killed by decapitation three days following the last injection. Columns represent means of groups ± S.E.M. of six to eight determinants. (*) indicate a significant difference from saline treatment group. ($P \leq 0.05$).

The Rate of Striatal DA Synthesis under Basal and Activated Conditions

Sub-chronic MPTP administration caused a decrease in striatal DOPA (Figure 7-7, A) and DA concentrations (Figure 7-7, B). However, the loss of striatal DA concentrations was much more severe than the loss of DOPA concentrations. As such, MPTP caused a robust increase in the ratio of DOPA to DA in the striatum of mice treated with MPTP (Figure 7-7, C).

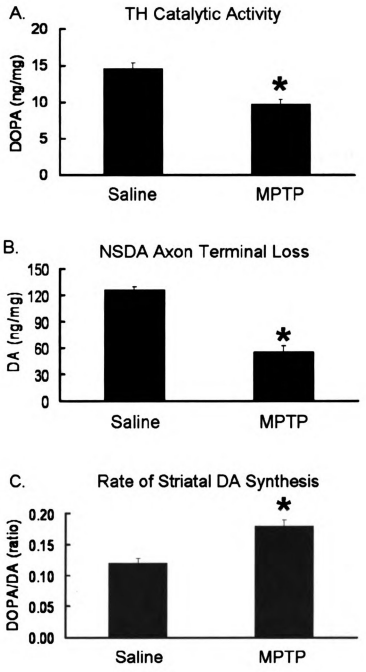

Figure 7-7. Striatal DOPA (A) and DA (B) concentrations, and the DOPA to DA ratio in α-synuclein knock-out mice injected with either saline (1.0 ml/kg, s.c.) or MPTP (25 mg/kg, s.c.) once a day for 5 consecutive days and killed by decapitation 3 days following the last injection. DOPA concentrations were determined 30 min after injection with NSD-1015 (100 mg/kg, i.p.). Columns represent means of groups ± S.E.M. of seven determinants. (*) indicate a significant difference from saline treatment group. ($P \leq 0.05$).

Effects of MPTP Administration on TH Phosphorylation State in α-Synuclein Knock-out Mice

Sub-chronic MPTP administration caused a differential loss of serine-19, serine-31, and serine-40 phosphorylated TH (Table 7-2). MPTP caused a 50% decrease in serine-19 and serine-31 phosphorylated TH levels. However, there was no change in serine-40 phosphorylated TH levels in the striatum of mice treated with MPTP as compared to saline-treated mice. Phosphorylated serine-19, serine-31, or serine-40 TH levels were normalized to total TH protein levels in the striatum (Table 7-3), as an index of the relative proportion of TH phosphorylated at each residue (Figure 7-8). MPTP decreased the proportion of TH phosphorylated at serine-19 and serine-31 by approximately 40%. MPTP had no effect on the proportion of serine-40 phosphorylated TH in NSDA axon terminals of α-synuclein knock-out mice treated with MPTP.

	Serine-19 (RDU)	Serine-31 (RDU)	Serine-40 (RDU)
Saline	11.8 ± 0.3	6.1 ± 0.7	2.8 ± 0.1
MPTP	6.4 ± 0.3*	3.1 ± 0.5*	1.8 ± 0.3

Table 7-2. Quantification of the effect of either saline (1 ml/kg, s.c.) or MPTP (25 mg/kg, i.p.) on serine-19, serine-31, or serine-40 phosphorylated TH in the striatum of α-synuclein knock-out mice. Columns represent mean ± S.E.M. of seven mice/group. * indicates a significant decrease from saline-treated controls. $p \leq 0.05$.

	Striatal TH Protein (RDU)
Saline	49 ± 4
MPTP	33 ± 2 *

Table 7-3. Quantification of the effect of either saline (1 ml/kg, s.c.) or MPTP (25 mg/kg, i.p.) on striatal TH protein levels in α-synuclein knock-out mice. Columns represent mean ± S.E.M. of seven mice/group. * indicates a significant decrease from saline-treated controls. $p \leq 0.05$.

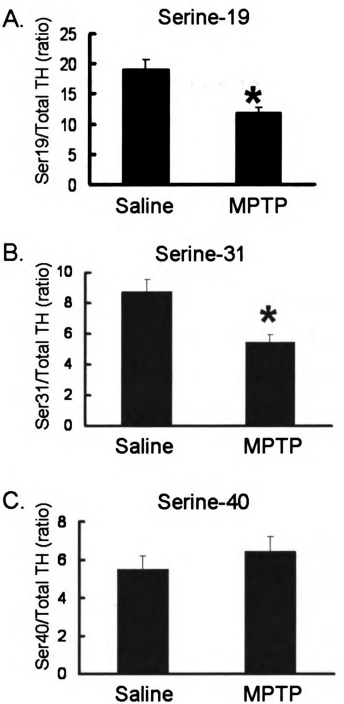

Figure 7-8. Quantification of the effect of MPTP (25 mg/kg, s.c.) on the relative proportion of serine-19 (A), serine-31 (B), or serine-40 (C) phosphorylated TH compared to total TH in the striatum. Phosphorylated serine-19, 31, or 40 phosphorylated TH relative density units were normalized to total TH relative density units. Columns represent mean ± S.E.M. of seven mice/group. * indicates a significant decrease from saline-treated controls. $p \leq 0.05$.

Effects of MPTP Administration on TH Catalytic Activity and Protein Expression in α-Synuclein Knock-out Mice

Sub-chronic MPTP administration caused a decrease in striatal DOPA concentrations (Figure 7-7, A) and TH protein expression (Table 7-3). The decrease in DOPA concentrations paralleled that of TH protein. As such, MPTP administration did not alter the catalytic activity of TH, as reflected by the ratio of DOPA to TH protein (Figure 7-9, LEFT PANEL).

MPTP caused a decrease in striatal TH protein (Table 7-3) however the decrease in TH protein expression was not as robust as the loss of striatal DA concentrations (Figure 7-7, B). As such, sub-chronic MPTP administration caused a marked increase in TH protein expression in surviving axon terminals, as reflected by the ratio of TH to DA (Figure 7-9, RIGHT PANEL).

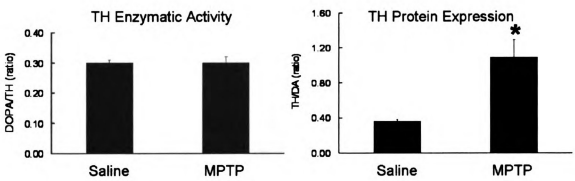

Figure 7-9. LEFT PANEL: TH enzymatic activity in the striatum of α-synuclein knock-out mice treated with either saline (1 ml/kg, s.c.) or MPTP (25 mg/kg, s.c.). TH enzymatic activity was determined by normalizing striatal DOPA concentrations, determined through neurochemical analysis to striatal TH protein content, determined through Western blot analysis. Striatal DOPA accumulation was measured 30 minutes following injection of NSD-1015 (100 mg/kg, i.p.). RIGHT PANEL: TH protein content in the striatum of mice treated with either saline or MPTP. TH protein content was determined by normalizing striatal TH protein levels, determined through Western blot analysis, to striatal DA concentrations, determined through neurochemical analysis. Columns represent means ± S.E.M. of seven mice/group. * indicate a significant difference from saline treated mice. $p \leq 0.05$.

Effects of Tyrosine Administration on TH Catalytic Activity in α-Synuclein Knock-out Mice Pre-Treated Under Basal and Activated Conditions

As depicted in Figure 7-10, tyrosine administration 60 min prior to decapitation had no effect on the enzymatic activity of TH in mice pre-treated with either saline or MPTP, as reflected by the ratio of striatal DOPA concentrations to total TH.

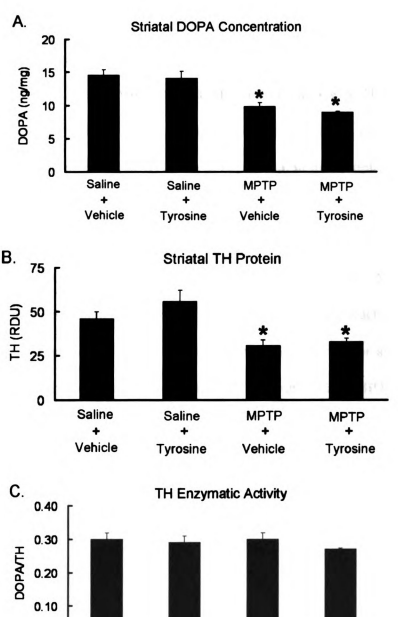

Figure 7-10. The effects of vehicle (1.0 ml/kg, i.p.) or tyrosine (100 mg/kg, i.p.) on striatal DOPA concentrations (A), TH protein (B) and the DOPA to TH ratio in α-synuclein knock-out mice treated with either saline (1 ml/kg, s.c.) or MPTP (25 mg/kg, s.c.) once a day for 5 consecutive days and killed by decapitation 3 days after the last injection. Striatal DOPA concentrations were measured 30 min following NSD-1015 administration (100 mg/kg, i.p.). Columns represent means ± S.E.M. of seven mice/group. * indicate a significant difference from saline vehicle treated control mice. $p \leq 0.05$.

The Effects of MPTP Administration on the Sub-Cellular Localization of TH at the Axon Terminal of α-Synuclein Knock-out Mice

Sub-chronic MPTP administration caused a differential loss of TH protein in the striatum depending on which sub-cellular compartment the enzyme was associated with (Table 7-4). MPTP had no effect on TH protein expression in the cytoplasmic fraction. However, it caused a 23% decrease in TH protein associated with the early endosomal fraction, and a 25% decrease in TH associated with the synaptic vesicle fraction. The loss of TH associated with plasma membrane fraction was more severe. MPTP caused a 60% decrease in TH associated with the plasma membrane enriched fraction. To quantify the relative change in TH localization relative to total TH at the axon terminal, TH in each fraction was normalized to total striatal TH. Sub-chronic MPTP increased the proportion of TH associated with the cytoplasmic fraction, but had no effect on TH associated with the early endosomal or synaptic vesicle fractions. MPTP caused a decreased in TH associated with the plasma membrane enriched fraction (Figure 7-11).

	Cytoplasmic (RDU)	Endosomal (RDU)	Synaptic Vesicle (RDU)	Plasma Membrane (RDU)
Saline	15 ± 2	62 ± 8	16 ± 2	20 ± 2
MPTP	13 ± 1	48 ± 2*	12 ± 1*	8 ± 1*

Table 7-4. Quantification of the TH protein distribution in the striatum of α-synuclein knock-out mice treated with either saline (1 ml/kg, s.c.) or MPTP (25 mg/kg, s.c.). Differential centrifugation was used to isolate TH associated with sub-cellular fractions enriched in either cytosolic, early endosomal vesicles, synaptic vesicles, or plasma membrane protein. TH associated with each compartment was normalized to proteins enriched in each fraction β-III tubulin, early endosome antigen 1 (EEA1), synaptophysin, or Snap-25, respectively to control for variations in loading. Values represent means ± S.E.M. of four samples per group. * indicate a significant difference from saline treated mice. $p \leq 0.05$.

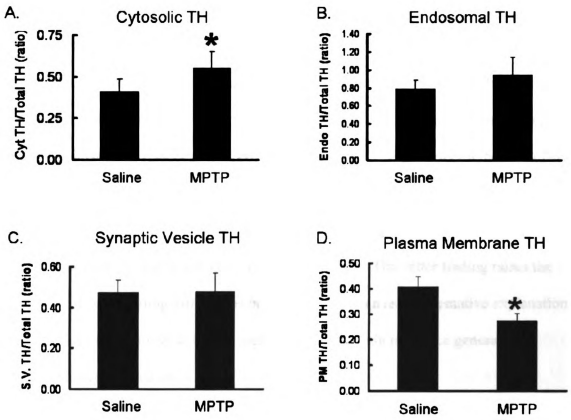

Figure 7-11. The effects of MPTP (25 mg/kg, s.c.) on the proportion of TH associated with sub-cellular fractions enriched in either cytoplasmic (A), early endosomal vesicles (B), synaptic vesicles (C) or plasma membrane (D) protein in the striatum of α-synuclein knock-out mice. The relative amount of TH protein associated with each sub-cellular fraction was determined by normalizing TH in each fraction to total striatal TH. Columns represent means ± S.E.M. of four samples per group. * indicate a significant difference from saline treated mice. $p \leq 0.05$.

D. Discussion

Prolonged-Chronic MPTP Toxicity in α-Synuclein Knock-out Mice

Specific deletion of the α-synuclein gene by homologous recombination attenuates the destruction of nigrostriatal DA neurons following acute and sub-chronic MPTP administration (Dauer et al., 2002; Schluter et al., 2003). However, Schlüter et al. (2003) also reported that mice with a spontaneous deletion of a 2 cM region surrounding the native α-synuclein gene have decreases in striatal DA concentrations following a single dose of MPTP that is similar to wild-type controls. This latter finding raises the possibility of confounding differences in background strain as an alternative explanation for the attenuated response to MPTP seen in the α-synuclein null mice generated by homologous recombination.

The results of this study provide evidence that mice lacking α-synuclein have an attenuated response to prolonged, chronic MPTP administration. Axon terminal integrity, as reflected by striatal DA concentrations, demonstrate that α-synuclein knock-out mice have attenuated responses to prolonged, chronic systemic MPTP exposure when compared to wild-type control mice. Using a MPTP administration protocol that more closely mimics the chronic time course of neurodegeneration neurodegeneration seen in PD, our findings are in agreement with previous studies suggesting that selective deletion of α-synuclein gene expression from either insertion of a stop codon prior to a start codon, or the deletion of the α-synuclein gene with targeting vectors confers resistance to either acute, sub-chronic and now prolonged-chronic MPTP administration (Dauer et al., 2002; Schluter et al., 2003).

Despite supporting the hypothesis that α-synuclein is involved in MPTP-induced toxicity, the present study does not provide an explanation why mice with a spontaneous 2 cM genomic deletion in a region containing the α-synuclein gene have a similar response to MPTP as wild-type mice. The present study alone cannot exclude the possibility of an unknown variation in background strain between the wild-type and α-synuclein knock-out mice as an alternative explanation for the differential response to MPTP described herein.

An attenuated response to MPTP however, has now been replicated independently in three unique strains of mice with absent α-synuclein expression. Taken together, it is more plausible that the resistance to MPTP is directly related to the loss of α-synuclein and less likely due to an unaccounted variation in background strain coincidentally occurring in three independent strains of α-synuclein knock-out mice. Nevertheless, the fact that the spontaneous deletion of a segment of the genome containing the α-synuclein gene does not result in altered sensitivity to acute MPTP exposure is an important finding and might suggest the presence of an adjacent modifying gene that could also influence the response to MPTP or interact with α-synuclein.

The activity of DA neurons in α-synuclein knock-out mice was assessed using the ratio of DOPAC to DA in the striatum. Following treatment with doses of MPTP that sufficiently deplete striatal DA levels, wild-type mice have an increase in the DOPAC/DA ratio (Chapter 3). The increase in the ratio of DOPAC to DA observed in wild-type mice following MPTP exposure reflects increased metabolism of newly synthesized DA due to the dysfunctional regulation of DA synthesis. Interestingly, α-synuclein knock-out mice do not have an increase in the DOPAC/DA ratio following a

loss of greater than 50% of striatal DA innervation. One potential explanation is that following MPTP there is a similar deficit in regulating DA synthesis in α-synuclein knock-out mice however, the newly synthesized DA does not have access to the mitochondria, where it is metabolized by MAO to DOPAC. This could also account for the attenuated response to MPTP.

Similar to DA, there may be an inability of MPP^+ to reach mitochondrial complex I, its primary site of neurotoxic action (Dauer et al., 2002). However, this is not the case since following MPTP administration to wild-type and α-synuclein knock-out mice, mitochondrial complex I activity is inhibited to the same extent (Fornai et al., 2005). A more likely explanation for the lack of a compensatory increase in NSDA activity is that following MPTP the rate of DA synthesis remains coupled with vesicular storage capability. Thus, in α-synuclein knock-out mice, there may not be an over-activation of DA synthesis, or there is an enhanced ability to package the increase in newly synthesized DA.

Despite a significant loss of DA concentrations, mice lacking α-synuclein do not have a loss of VMAT-2 protein in the striatum. Using VMAT-2 as an indicator of DA vesicular storage capacity, there is a discrepancy between DA and VMAT-2 concentrations in α-synuclein knockout mice following MPTP. Therefore, it is possible that the lack of a compensatory increase in NSDA activity in α-synuclein knock-out mice is due to an increased storage capability for newly synthesized DA in these mice. However, it is unclear whether VMAT-2 protein levels reflect actual activity of the transporter and storage capability *in vivo.* The lack of a compensatory increase in NSDA

activity following MPTP could also be explained by an inability to increase the rate of DA synthesis.

The Regulation of NSDA Activity in α-Synuclein Knock-out Mice

α-Synuclein interacts with numerous proteins that play a role in medating the compensatory activation of NSDA neurons. For example, α-synuclein inhibits the activity of phospholipase D2, which may regulate monoaminergic vesicle content and axon terminal DA storage (Jenco et al., 1998; Lotharius and Brundin, 2002). α-Synuclein expression also alters DAT-mediated uptake of synaptic DA, suggesting a role in terminating DA neurotransmission (Sidhu et al., 2004). Finally, α-synuclein regulates the catalytic activity of TH, the rate-limiting enzyme in DA synthesis (Perez et al., 2002). Taken together, there is ample evidence that α-synuclein may play a critical role in mediating the uncoupling between DA synthesis and storage capacity that occurs following MPTP administration.

To determine if α-synuclein plays a role in regulating DA synthesis, TH phosphorylation state, catalytic activity and protein expression were assessed in the striatum of α-synuclein knockout mice under basal conditions and during accelerated neuronal activity. Mice were injected with raclopride, which increases DA neuronal firing and stimulates DA synthesis, by decreasing D2 receptor-mediated long- and short-loop feedback inhibition (Chapter 6). Supplemental tyrosine was administered to prevent substrate limitations on TH activity in activated NSDA neurons (Sved and Fernstrom, 1981).

Under basal conditions, DA storage, release, reuptake and metabolism were similar in NSDA neurons of α-synuclein knock-out mice as in wild-type mice (Chapter 6). Therefore, it appears that α-synuclein does not affect DA release, reuptake and metabolism or DA storage in NSDA neurons under basal conditions.

Raclopride increases NSDA neuronal activity through a loss of long and short-loop feedback inhibition. The loss of feedback inhibition increases NSDA cell firing, bursts of action potentials and DA release at the axon terminal (Andersson et al., 1994; Andersson et al., 1995; Millan et al., 1998). In the present study, raclopride increased NSDA neuronal activity in α-synuclein knockout mice to a similar extent as wild-type mice (Chapter 6), as demonstrated by an increase in the ratio of DOPAC to DA. These results suggest both long and short-loop feedback mechanisms are not affected by α-synuclein. This finding is consistent with previous work demonstrating that there is no difference in DA neurotransmission between wild-type and α-synuclein knockout mice in response to either single-pulse or train electrical stimulation of NSDA axon terminals (Abeliovich et al., 2000). There is an increased recovery time from a paired-pulse depression paradigm in α-synuclein knockout mice, suggesting that α-synuclein may play a role in the refilling of the readily releasable pool of synaptic vesicles. Although this has implications for the present study, the differences in the time frame of sample collection and methodological considerations in determination of DA release prevent direct comparison of the paired-pulse depression electrical stimulation paradigm.

The Regulation of DA Synthesis in α-Synuclein Knock-out Mice

Under basal conditions, levels of serine-19, serine-31 and serine-40 as well as TH enzymatic activity were similar in α-synuclein knock-out mice as in wild-type mice (Chapter 6). This is in contrast to a previous report that α-synuclein inhibits the phosphorylation and consequently the activity of TH in immortalized MN9D cells under basal conditions (Perez et al., 2002). The discrepancy in findings may stem from the ability of α-synuclein to bind to TH. The initial report demonstrated a clear deficit in TH phosphorylation and activity when either wild-type or mutant (A53T) α-synuclein was over-expressed in MN9D cells. Over-expression of the protein corresponded with a dramatic increase in TH and α-synuclein co-immunoprecipitation. Therefore, over-expression of wild-type or mutant α-synuclein may have resulted in non-physiological protein–protein interactions that could have prevented kinase access to proper phosphorylation sites, resulting in decreased enzyme phosphorylation and consequently catalytic activity. In addition, *in vitro* studies may lack key microenvironmental factors or long-loop neuronal feedback mechanisms that are physiologically relevant. Regardless, in the present study there was no difference between wild-type and α-synuclein knockout mice in NSDA neuronal phosphorylated TH levels or enzyme catalytic activity *in vivo* under normal physiological conditions. This suggests that α-synuclein does not play a role in regulating the phosphorylation state or catalytic activity of TH under basal levels of neuronal activity.

TH activation occurs predominantly through phosphorylation of the serine-40 residue (Kumer and Vrana, 1996), which serves to couple neuronal activity with DA synthesis. Consistent with this, in the present study, acceleration of NSDA neuronal

activity increased serine-19, serine-31, and serine-40 phosphorylated TH levels, and TH catalytic activity in α-synuclein knock-out mice. There was no difference between wild-type and α-synuclein knock-out mice in phosphorylated TH levels or TH catalytic activity in response to raclopride, suggesting that feedback mechanisms that couple neuronal activity and D2 autoreceptors to TH phosphorylation state are not affected by α-synuclein. Accordingly, α-synuclein does not appear play a role in activity-dependent or D2 autoreceptor-dependent TH activation.

The Ability of Tyrosine to Enhance Phosphorylated TH is Dependent on α-Synuclein

The present study reveals that α-synuclein plays a role in the ability of tyrosine to enhance phosphorylated TH levels and TH catalytic activity in activated NSDA neurons. In wild-type mice, tyrosine supplementation enhances phosphorylated TH levels and enzymatic activity in raclopride-treated mice (Chapter 6). In contrast, tyrosine supplementation does not further increase phosphorylated TH levels or enzyme catalytic activity in activated NSDA neurons in α-synuclein knock-out mice. Tyrosine likely stabilizes phosphorylated TH preventing it from de-activation through destabilization, and this phenomenon is dependent on the presence of α-synuclein. Taken together, these findings suggest that α-synuclein plays a critical role in regulating TH phosphorylation state in an activity and substrate-dependent manner. The net result of this proposed function for α-synuclein would be to allow DA synthesis to remain elevated in NSDA neurons during prolonged periods of accelerated neuronal activity.

The results from the present study are congruent with the molecular chaperone hypothesis for α-synuclein function. The activity-dependent molecular chaperone

hypothesis for α-synuclein is strengthened by two observations. First, α-synuclein shares structural homology with the 14-3-3 family of molecular chaperone proteins that can bind to phospho-serine residues on proteins and stabilize their active conformation (Tzivion et al., 1998; Ostrerova et al., 1999). Secondly, α-synuclein expression is regulated throughout development; i.e., during periods of accelerated neuronal activity and plasticity, α-synuclein expression is up-regulated (George et al., 1995; Petersen et al., 1999).

Taken together, the results from the experiments described have demonstrated that α-synuclein knock-out mice have are less susceptible to the toxic effects of prolonged, chronic MPTP administration and there is no increase in DA metabolism in surviving NSDA neurons. While further experiments are necessary to determine a cause and effect relationship, the present studies suggest that preventing excessive DA metabolism may protect NSDA neurons from the toxic effects of MPTP. However, it is clear that α-synuclein knock-out mice do not have a deficit in regulating TH phosphorylation state or catalytic activity under basal or activated conditions induced by a loss of long and short-loop feedback inhibition. As such, the lack of an increase in DA metabolism in surviving NSDA neurons in α-synuclein knock-out mice may not reflect a deficit in accelerating DA synthesis. However, as described in Chapter 6, there are critical differences between the compensatory activation of NSDA neurons in response to MPTP administration and the chronic activation of NSDA neurons induced by the loss of D2 receptor-mediated feedback inhibiton. The possibility that α-synuclein knock-out mice have a deficit in accelerating DA synthesis following MPTP administration cannot be excluded.

The Regulation of DA Synthesis in α-Synuclein Knock-out Mice Following MPTP Administration

To determine if α-synuclein knock-out mice have a deficit in regulating DA synthesis following MPTP administration, mice were treated with sub-chronic MPTP and the rate of striatal DA synthesis and TH phosphorylation state, enzymatic activity, protein expression and sub-cellular distribution were assessed in the striatum. Sub-chronic MPTP administration caused a 75% loss of NSDA axon terminals and a 65% decrease in striatal DA metabolism. Interestingly, sub-chronic MPTP administration caused a slight increase in the activity of surviving axon terminals (unlike following prolonged-chronic administration). However, the loss of axon terminals in this study was more severe than following prolonged, chronic MPTP administration, suggesting that NSDA neurons in α-synuclein knock-out mice may be activated in response to more a pronounced loss of axon terminals. Thus, α-synuclein knock-out mice may have a higher threshold of axon terminal loss required for the compensatory activation of NSDA neuron than wild-type mice.

The increase in DA metabolism following MPTP administration is due to an uncoupling between DA synthesis and storage, such that synthesis is accelerated beyond storage capability. It is clear that mice lacking α-synuclein are more capable of maintaining the balance between synthesis and storage capability than wild-type mice. This may be due to a less robust activation of DA synthesis or enhanced storage capability following MPTP administration. To determine if this is the case, the rate of striatal DA synthesis was determined in the striatum following MPTP administration.

Results demonstrated that there is a robust acceleration in the rate of DA synthesis following MPTP administration that was similar in magnitude to wild-type mice. Also similar to wild-type mice, the accelerated rate of DA synthesis was the result of an increase in TH protein expression in surviving axon terminals, rather than an increase in the catalytic activity of individual TH molecules. These findings demonstrate that the primary response of NSDA neurons to axon terminal loss (i.e., up-regulation of TH expression in surviving neurons and acceleration of DA synthesis) is not affected by the loss of α-synuclein protein.

Sub-chronic MPTP administration also caused a differential loss of TH protein depending on whether it was phosphorylated at serine-19, serine-31, or serine-40. Following MPTP, there was a 50% decrease in TH phosphorylated at serine-19 and serine-31, but no loss of serine-40 phosphorylated TH. The amount of TH phosphorylated at each residue was compared to the amount of total TH at the axon terminal to reflect the relative change in TH phosphorylation state. Similar to wild-type mice, MPTP caused a decrease in proportion of TH phosphorylated at serine-19 and seirne-31. However, in contrast to wild-type mice, there was no increase in TH phosphorylated at serine-40 (relative to total TH levels). The lack of effect on serine-40 was likely due to the attenuated MPTP-induced lesion since the preservation of serine-40 phosphorylated TH was consistent with what was observed in wild-type mice. Thus, it is unlikely that the α-synuclein protein plays a role in regulating TH phosphorylation state in the axon terminals of NSDA neurons following MPTP administration.

Regulation of TH sub-cellular compartmentalization is also conserved in α-synuclein knock-out mice. Under basal conditions, there were no differences between in

wild-type and α-synuclein knock-out mice in TH associated with the cytoplasmic, endosomal, synaptic vesicle, or plasma membrane sub-cellular fractions. Thus, it does not appear that α-synuclein performs a molecular chaperone-like function in trafficking proteins within sub-cellular compartments under basal conditions. Following MPTP administration, there was a differential loss of TH depending on which sub-cellular compartment the enzyme was associated with. MPTP administration had no effect on TH associated with the cytoplasmic fraction. When normalized to total TH at the axon terminal prior to sub-cellular fractionation, there was an increase in TH associated with the cytosolic fraction. This was consistent with wild-type mice and suggests increased TH expression in surviving axon terminals following MPTP results in an increase in cytoplasmic TH, where the enzyme is primarily active and can contribute to the accelerated rate of DA synthesis.

In contrast to the cytoplasmic fraction, there was a robust loss of TH associated with the plasma membrane fraction. Similar to wild-type mice, the loss of plasma membrane associated TH was more severe than the loss of total striatal TH and as such, there was a decrease in the proportion of total enzyme located in this sub-cellular compartment. This may reflect either protein translocation to the cytosolic fraction or a loss of compartmentalization capability in axon terminals that survive MPTP administration.

In contrast to wild-type mice, MPTP administration caused a 25% decrease in TH associated with the early endosomal vesicle and synaptic vesicle enriched fractions. The loss of TH associated with these sub-cellular compartments was similar to the loss of total TH, and as such, there was no change in the proportion of the enzyme located within

these sub-cellular compartments. In wild-type mice, there is an increase in the amount of TH associated with the early endosomal vesicle fraction and a robust decrease in TH associated with the synaptic vesicle fraction. These results could suggest that α-synuclein plays a role in regulating the sub-cellular distribution of TH between early endosomal and synaptic vesicles. Further experiments comparing the regulation of TH sub-cellular compartmentalization in α-synuclein knock-out mice to wild-type mice (following equivalent neurotoxic lesions) are required to determine if these mice have a deficit in regulating TH compartmentalization. Another possibility is that the differential effect of MPTP on endosomal and synaptic vesicle TH in wild-type versus α-synuclein knock-out mice is due to the attenuated lesion in α-synuclein knock-out mice treated with MPTP. In this case, the sub-cellular distribution of TH in MPTP-treated α-synuclein knock-out mice may reflect the distribution of the enzyme in wild-type mice at a time point when the lesion was less severe.

Thus, these findings suggest the initial changes in TH distribution following MPTP are increased cytosolic TH and decreased plasma membrane TH. It is still unclear whether these events reflect protein translocation from reserve pools of TH to the active cytosolic fraction or an increase in *de novo* TH synthesis coupled with decreased enzyme compartmentalization at the axon terminal. As the lesion becomes more severe, the amount of TH associated with the endosome is increased and TH associated with synaptic vesicles is decreased. In wild-type mice the increase in endosomal TH is associated with increased serine-40 phosphorylated TH without an increase in enzyme catalytic activity, indicative of an increased amount of destabilized enzyme at the axon terminal. The fact that there is no increase in endosomal TH in α-synuclein knock-out

mice is consistent with a lack of an increase in serine-40 phosphorylated TH. Thus, the increase in destabilized TH may occur later in the neurodegenerative process.

The loss of synaptic vesicle-associated TH may contribute to the uncoupling between DA synthesis and storage capability. The localization of the rate limiting enzyme in DA synthesis near the site of vesicular packaging is likely a mechanism used to couple DA synthesis to storage capability which prevents the metabolism of newly synthesized DA. In this case, the fact that synthesis-storage coupling does not occur in α-synuclein knock-out mice is consistent with the lack of an increase in DA metabolism following prolonged-chronic MPTP and an attenutated increase following sub-chronic MPTP administration.

Taken together, it is clear that there is no difference between wild-type and α-synuclein knock-out mice in the activation of DA synthesis following MPTP administration. The fact that there is a lack of an increase in the metabolism of newly synthesized DA in axon terminals that survive MPTP administration likely reflects enhanced vesicular packaging capability in these mice, which may reflect enhanced TH and synaptic vesicle association or increased VMAT-2 activity and/or expression, or both. Several lines of evidence support this conclusion. There is no loss of VMAT-2 protein expression in the striatum, a marker of vesicular packaging capacity, despite the loss of over 50% of striatal DA concentrations. While further experiments are required that directly measure VMAT-2 activity and storage capability following MPTP, enhanced VMAT-2 protein in α-synuclein knock-out mice would be consistent with the proposed role for the protein in inhibiting the activity of phospholipase D2 which stimulates monoaminergic vesicle formation (Lotharius and Brundin, 2002). Alternatively, the lack

of an increase in the metabolism of newly synthesized DA may be due to sparing of synaptic vesicle associated TH. Further biochemical experiments that isolate and quantify the activity of synaptic vesicle associated TH as well as further characterize the mechanisms that govern sub-cellular compartmentalization are required to determine if the association of TH with synaptic vesicles couples synthesis to vesicular packaging. These experiments may define an important role for this coupling in the pathogenesis of PD and finally determine what role α-synuclein plays in this process.

Summary

The findings from the studies described in this Chapter highlight the importance of α-synuclein protein expression in mediating the toxic effects of MPTP and the compensatory activation of surviving NSDA neurons. Results point towards a molecular chaperone like function for α-synuclein that mediates the ability of tyrosine to stablize phosphorylated TH. However, using two distinct models of NSDA activation it is clear that α-synuclein does not play a role in the regulation of NSDA activity or DA synthesis under basal or activated conditions. Yet, decreasing the expression of this protein may protect NSDA neurons from the oxidative damage induced by toxic byproducts of DA metabolism due to an enhanced ability to generate synaptic vesicles to package newly synthesized DA.

Chapter 8. Concluding Remarks

PD places a tremendous burden on the American society. Greater than one-million Americans currently suffer from PD and when primary caregivers are accounted for, the number of people adversely affected by the disease drastically increases. The estimated cost of health care treatment for PD patients is over 6 billion dollars per year (Whetten-Goldstein et al., 1997), placing a tremendous economic burden on the American society as well. These statistics draw enormous emphasis towards the discovery of therapeutic strategies for curing the disease. The primary drawback to this approach is that PD is not identified until significant pathological damage has already occurred. A logical approach to treating PD therefore, is to slow or halt disease progression once it is identified. This would drastically improve the quality of life for both patients and primary caregivers and reduce the associated economic burden of treating late-stage PD. A major roadblock that prevents accomplishing this task is the mechanisms that underlie PD progression are still unknown.

The gradual decline in the quality of life for PD patients is due to the progressive worsening of the cardinal motor symptoms. The manifestation and gradual worsening of symptoms is due to the progressive loss of NSDA neurons. Preventing the progressive loss of NSDA neurons should halt the worsening of motor symptoms. The primary goal of the research conducted in this dissertation was to identify detrimental mechanisms that may contribute to the progressive degeneration of NSDA neurons. The strategy employed was to use a neurotoxin to induce NSDA cell death similar to PD. Pharmacological manipulation combined with neurochemical and immunohistochemical

techniques were then used to identify detrimental mechanisms that may cause degeneration of the neurons that survive the initial neurotoxic insult.

One of the primary findings of this dissertation research is that following a neurotoxic lesion there is an increase in the activity of surviving NSDA neurons. This compensatory increase is similar to PD, where there is an increase in the activity of the 50% of NSDA neurons that have not yet degenerated. The activation of NSDA neurons following neurotoxic insult is a compensatory mechanism that increases the amount of DA release from surviving neurons to continue to activate post-synaptic DA receptors involved in basal ganglia function. The sustained increase in surviving neuron activity likely increases ROS exposure derived from accelerated DA metabolism and may cause NSDA cell death. Oxidative damage in the striatum of post-mortem PD brains supports this hypothesis. The compensatory activation of NSDA neurons may, therefore, contribute to the progressive loss of NSDA neurons which underlies the progressive nature of PD.

NSDA firing rate and DA release are regulated by feedback inhibition from D2 receptors, suggesting that the compensatory activation that occurs in response to neurotoxicity is due to a loss of this feedback inhibition. Consistent with this, studies demonstrated that acute D2 receptor blockade increases NSDA neuronal activity and DA metabolism in axon terminals. Chronic D2 receptor blockade however, does not activate NSDA neurons in a similar manner. Prolonged activation of NSDA neurons does not result in a prolonged increase in DA metabolism and thus is not detrimental to neuronal survival. These findings suggest compensatory activation of NSDA neurons, following D2 receptor blockade, permits prolonged accelerated neuronal activity without increasing

DA metabolism. This is in stark contrast to the compensatory activation of NSDA neurons where the chronic increase in NSDA activity does cause a chronic increase in DA metabolism.

The finding that NSDA neurons are differentially activated in response to axon terminal loss as compared with blockade of D2 receptors highlights the importance and potentially detrimental nature of the compensatory activation of NSDA neurons in PD. An important task of future research will be to 1) determine the mechanisms in NSDA neurons that permit prolonged accelerated neuronal activity without increased DA metabolism and 2) determine if these mechanisms are dysfunctional following a neurotoxic lesion. Accomplishing these tasks will provide critical insight into PD pathogenesis and potential pathways that can be manipulated to protect NSDA neurons.

A key finding from this dissertation research is that the primary source of excessive DA metabolism during NSDA compensatory activation is the DA biosynthetic pathway. As described in Figure 8-1 (A, B) the increased metabolism of newly synthesized DA is due to an accelerated rate of DA synthesis. Accelerated DA synthesis is due to increased expression of the rate limiting enzyme TH. Increasing the rate of DA synthesis could benefit surviving neurons by boosting the amount of neurotransmitter available for release (Figure 8-1C). This is not the case however, since the newly synthesized DA is primarily metabolized. These findings highlight the therapeutic potential of enhancing DA vesicular storage in preventing exposure to ROS-derived from DA metabolism and augmenting the function of surviving NSDA neurons.

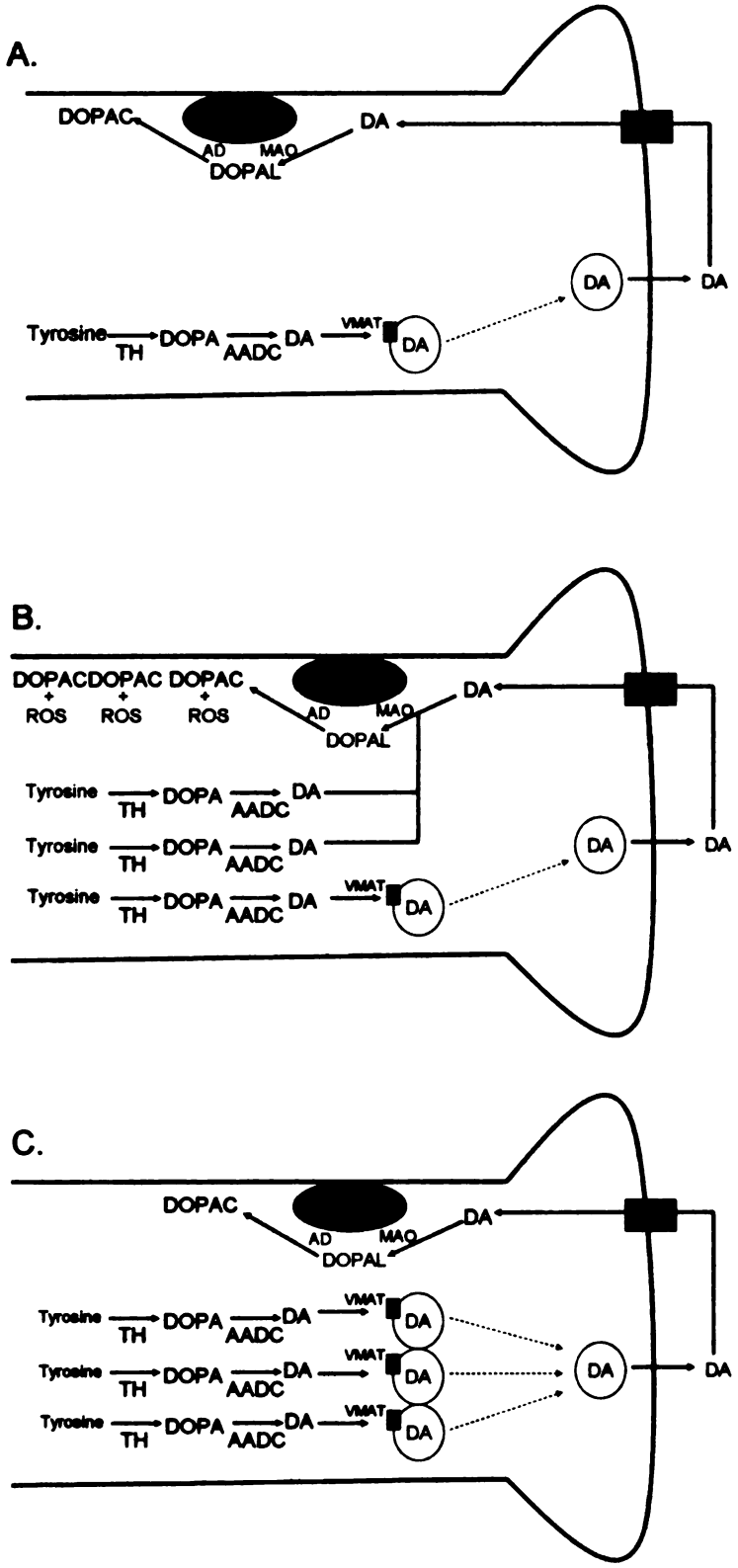

Figure 8-1. (A) NSDA axon terminal neurochemistry under basal conditions. Normally, newly synthesized DA is coupled to vesicular storage, such that metabolism of newly synthesized DA is minimal. (B) NSDA axon terminal neurochemistry following compensatory activation. There is an increase in the expression of TH protein in surviving axon terminals which accelerates the rate of DA synthesis. The newly synthesized DA is not packaged into synaptic vesicles and is metabolized as a consequence, increasing ROS production. (C) Enhancing DA storage can decrease the metabolism of newly synthesized DA following compensatory activation and increase the amount of vesicular DA available for release

Studies also identified mechanisms that may be responsible for the inability to package the newly synthesized DA. The uncoupling between DA synthesis and vesicular packaging may be due to decreased expression or activity of the vesicular transporter VMAT-2, or both. Additionally, decreased association of TH with synaptic vesicles may cause DA to be synthesized at a location distant from the site of vesicular storage and thus increase the metabolism of newly synthesized DA. To this end, a major goal of future research will be to determine the mechanisms that regulate VMAT-2 expression and activity and TH-synaptic vesicle compartmentalization. These mechanisms may be primary therapeutic target that can be manipulated to inhibit DA metabolism and enhance DA release in NSDA axon terminals following compensatory activation.

The hypothesis that enhancing the association between TH and synaptic vesicles could be neuroprotective is strengthened by another primary finding of this dissertation research. Blocking the expression of α-synuclein, a protein that plays a primary role in PD pathogenesis, prevents increased DA metabolism following compensatory activation and attenuates the neurotoxin-induced lesion. Accelerated DA synthesis however, still occurs in the absence of α-synuclein, suggesting the loss of this protein enhances vesicular storage. These findings provide evidence that promoting DA vesicular storage can prevent excessive DA metabolism following a neurotoxic lesion and may protect NSDA neurons from oxidative damage. It is still unclear if enhanced vesicular storage is due to increased VMAT-2 expression and activity, preservation of TH-synaptic vesicle compartmentalization, or both. A goal of future research will be to determine how expression of the α-synuclein protein affects these mechanisms. Accomplishing these

goals will increase the current knowledge of α-synuclein function and provide pathways that can be exploited to treat PD.

To summarize, the research described in this dissertation was conducted under the premise that identifying mechanisms responsible for progressive NSDA cell death will lead to therapeutic approaches to slow or halt the gradual worsening of motor symptoms in PD. Studies have identified and characterized dysfunctional regulation of a key pathway in NSDA neurons that may predispose these neurons to oxidative damage and cell death. Additionally, studies have clarified the role that a genetic factor, extensively linked to PD pathogenesis, plays in mediating NSDA neuronal death. Moreover, a number of potential therapeutic targets have been identified that may prevent the progressive demise of NSDA neurons in PD, ultimately slowing or halting the progressive nature of the disease.

References

Abeliovich A, Schmitz Y, Farinas I, Choi-Lundberg D, Ho WH, Castillo PE, Shinsky N, Verdugo JM, Armanini M, Ryan A, Hynes M, Phillips H, Sulzer D, Rosenthal A (2000) Mice lacking alpha-synuclein display functional deficits in the nigrostriatal dopamine system. Neuron 25:239-252.

Ahlenius S, Ericson E, Hillegaart V, Nilsson LB, Salmi P, Wijkstrom A (1997) In vivo effects of remoxipride and aromatic ring metabolites in the rat. J Pharmacol Exp Ther 283:1356-1366.

Albert KA, Helmer-Matyjek E, Nairn AC, Muller TH, Haycock JW, Greene LA, Goldstein M, Greengard P (1984) Calcium/phospholipid-dependent protein kinase (protein kinase C) phosphorylates and activates tyrosine hydroxylase. Proc Natl Acad Sci U S A 81:7713-7717.

Alvord E, Forno, LS (1987) Handbook of Parkinson's disease.209.

Anden N, Carlsson, A, Dahlstrom A, Fuxe, K, Hillarp, NA, Larsson, K (1964) Life Sciences 3:523.

Andersson JL, Marcus M, Nomikos GG, Svensson TH (1994) Prazosin modulates the changes in firing pattern and transmitter release induced by raclopride in the mesolimbic, but not in the nigrostriatal dopaminergic system. Naunyn Schmiedebergs Arch Pharmacol 349:236-243.

Andersson JL, Nomikos GG, Marcus M, Hertel P, Mathe JM, Svensson TH (1995) Ritanserin potentiates the stimulatory effects of raclopride on neuronal activity and dopamine release selectivity in the mesolimbic dopaminergic system. Naunyn Schmiedebergs Arch Pharmacol 352:374-385.

Andersson KK, Cox DD, Que L, Jr., Flatmark T, Haavik J (1988) Resonance Raman studies on the blue-green-colored bovine adrenal tyrosine 3-monooxygenase (tyrosine hydroxylase). Evidence that the feedback inhibitors adrenaline and noradrenaline are coordinated to iron. J Biol Chem 263:18621-18626.

Anglade P, Vyas S, Javoy-Agid F, Herrero MT, Michel PP, Marquez J, Mouatt-Prigent A, Ruberg M, Hirsch EC, Agid Y (1997) Apoptosis and autophagy in nigral neurons of patients with Parkinson's disease. Histol Histopathol 12:25-31.

Annunziato L, Leblanc P, Kordon C, Weiner RI (1980) Differences in the kinetics of dopamine uptake in synaptosome preparations of the median eminence relative to other dopaminergically inervated brain regions. Neuroendocrinology 31:316-320.

Arbuthnott GW, Fairbrother IS, Butcher SP (1990) Brain microdialysis studies on the control of dopamine release and metabolism in vivo. J Neurosci Methods 34:73-81.

Au WL, Adams JR, Troiano AR, Stoessl AJ (2005) Parkinson's disease: in vivo assessment of disease progression using positron emission tomography. Brain Res Mol Brain Res 134:24-33.

Barrio JR, Huang SC, Melega WP, Yu DC, Hoffman JM, Schneider JS, Satyamurthy N, Mazziotta JC, Phelps ME (1990) 6-[18F]fluoro-L-dopa probes dopamine turnover rates in central dopaminergic structures. J Neurosci Res 27:487-493.

Ben-Jonathan N (1985) Dopamine: a prolactin-inhibiting hormone. Endocr Rev 6:564-589.

Bergman H, Feingold, A, Nini, A, Raz, A, Slovin, H, Abeles, M, Vaadia, E (1998) Physiological Aspects of Information Processing in the Basal Ganglia of Normal and Parkinsonism Primates. TINS 21:32.

Bergman H, Wichmann, T, Karmon, B, Delong, MR (1994) The Primate Subthalamic Nucleus. II. Neuronal Activity in the MPTP Model of Parkinsonism. Journal of Neurophysiology 72:507.

Bernheimer H, Birkmayer W, Hornykiewicz O, Jellinger K, Seitelberger F (1973) Brain dopamine and the syndromes of Parkinson and Huntington. Clinical, morphological and neurochemical correlations. J Neurol Sci 20:415-455.

Bertler A, Rosengren, E (1959a) Physiologica Scandinavica 47:350.

Bertler A, Rosengren, E (1959b) Experientia 15:10.

Betarbet R, Sherer TB, Greenamyre JT (2002) Animal models of Parkinson's disease. Bioessays 24:308-318.

Betarbet R, Sherer TB, MacKenzie G, Garcia-Osuna M, Panov AV, Greenamyre JT (2000) Chronic systemic pesticide exposure reproduces features of Parkinson's disease. Nat Neurosci 3:1301-1306.

Bettini E, Ceci A, Spinelli R, Samanin R (1987) Neuroleptic-like effects of the l-isomer of fenfluramine on striatal dopamine release in freely moving rats. Biochem Pharmacol 36:2387-2391.

Bezard E, Dovero S, Bioulac B, Gross C (1997) Effects of different schedules of MPTP administration on dopaminergic neurodegeneration in mice. Exp Neurol 148:288-292.

Bezard E, Dovero S, Imbert C, Boraud T, Gross CE (2000) Spontaneous long-term compensatory dopaminergic sprouting in MPTP-treated mice. Synapse 38:363-368.

Biggs C, Starr M, Fowler L, Whitton P (1996a) Effects of glutamate antagonists on nigral dopamine release in the reserpine-treated rat. Biochem Soc Trans 24:173-177.

Biggs CS, Fowler LJ, Whitton PS, Starr MS (1996b) NMDA receptor antagonists increase the release of dopamine in the substantia nigra of reserpine-treated rats. Eur J Pharmacol 299:83-91.

Birkmayer W, Ambrozi, L, Neumayer, E, Riederer, P (1974) Longevity in Parkinson's disease Treated with L-DOPA. Clinical Neurology Neurosurgery 1:15-19.

Blum D, Torch S, Lambeng N, Nissou M, Benabid AL, Sadoul R, Verna JM (2001) Molecular pathways involved in the neurotoxicity of 6-OHDA, dopamine and MPTP: contribution to the apoptotic theory in Parkinson's disease. Prog Neurobiol 65:135-172.

Bongiovanni R, Yamamoto BK, Simpson C, Jaskiw GE (2003) Pharmacokinetics of systemically administered tyrosine: a comparison of serum, brain tissue and in vivo microdialysate levels in the rat. J Neurochem 87:310-317.

Borek LL, Amick MM, Friedman JH (2006) Non-motor aspects of Parkinson's disease. CNS Spectr 11:541-554.

Bower JH, Maraganore DM, McDonnell SK, Rocca WA (1999) Incidence and distribution of parkinsonism in Olmsted County, Minnesota, 1976-1990. Neurology 52:1214-1220.

Braak H, Braak E (2000) Pathoanatomy of Parkinson's disease. J Neurol 247 Suppl 2:II3-10.

Brown P, Oliviero, A, Mazzone, P, Insola, A, Tonali, P, Di Lazzaro, V (2001) Dopamine Dependency of Oscillations between Subthalamic Nucleus and Pallidum in Parkinson's Disease. Journal of Neuroscience 21:1033-1038.

Burchiel KJ, Anderson VC, Favre J, Hammerstad JP (1999) Comparison of pallidal and subthalamic nucleus deep brain stimulation for advanced Parkinson's disease: results of a randomized, blinded pilot study. Neurosurgery 45:1375-1382; discussion 1382-1374.

Burke WJ, Li SW, Chung HD, Ruggiero DA, Kristal BS, Johnson EM, Lampe P, Kumar VB, Franko M, Williams EA, Zahm DS (2004) Neurotoxicity of MAO metabolites of catecholamine neurotransmitters: role in neurodegenerative diseases. Neurotoxicology 25:101-115.

Camarero J, Sanchez V, O'Shea E, Green AR, Colado MI (2002) Studies, using in vivo microdialysis, on the effect of the dopamine uptake inhibitor GBR 12909 on 3,4-methylenedioxymethamphetamine ('ecstasy')-induced dopamine release and free radical formation in the mouse striatum. J Neurochem 81:961-972.

Campbell DG, Hardie DG, Vulliet PR (1986) Identification of four phosphorylation sites in the N-terminal region of tyrosine hydroxylase. J Biol Chem 261:10489-10492.

Carboni E, Tanda G, Di Chiara G (1992) Extracellular striatal concentrations of endogenous 3,4-dihydroxyphenylalanine in the absence of a decarboxylase inhibitor: a dynamic index of dopamine synthesis in vivo. J Neurochem 59:2230-2236.

Carlsson A (1959) Pharmacological Reviews 11:490.

Carlsson A (1975) Monoamine-depleting drugs. Pharmacol Ther [B] 1:393-400.

Carlsson A, Davis JN, Kehr W, Lindqvist M, Atack CV (1972) Simultaneous measurement of tyrosine and tryptophan hydroxylase activities in brain in vivo using an inhibitor of the aromatic amino acid decarboxylase. Naunyn Schmiedebergs Arch Pharmacol 275:153-168.

Chen RC, Chang SF, Su CL, Chen TH, Yen MF, Wu HM, Chen ZY, Liou HH (2001) Prevalence, incidence, and mortality of PD: a door-to-door survey in Ilan county, Taiwan. Neurology 57:1679-1686.

Chiueh CC, Burns RS, Markey SP, Jacobowitz DM, Kopin IJ (1985) Primate model of parkinsonism: selective lesion of nigrostriatal neurons by 1-methyl-4-phenyl-1,2,3,6-tetrahydropyridine produces an extrapyramidal syndrome in rhesus monkeys. Life Sci 36:213-218.

Christiansen J, Squires RF (1974) Antagonistic effects of apomorphine and haloperidol on rat striatal synaptosomal tyrosine hydroxylase. J Pharm Pharmacol 26:367-369.

Cooper AJ, Kristal BS (1997) Multiple roles of glutathione in the central nervous system. Biol Chem 378:793-802.

Cuello AC, Iversen LL (1973) Localization of tritiated dopamine in the median eminence of the rat hypothalamus by electron microscope autoradiography. Brain Res 63:474-478.

Cumming P, Brown E, Damsma G, Fibiger H (1992) Formation and clearance of interstitial metabolites of dopamine and serotonin in the rat striatum: an in vivo microdialysis study. J Neurochem 59:1905-1914.

Dahlstrom A, Fuxe K (1964) Localization of monoamines in the lower brain stem. Experientia 20:398-399.

Daubner SC, Lauriano C, Haycock JW, Fitzpatrick PF (1992) Site-directed mutagenesis of serine 40 of rat tyrosine hydroxylase. Effects of dopamine and cAMP-dependent phosphorylation on enzyme activity. J Biol Chem 267:12639-12646.

Dauer W, Przedborski S (2003) Parkinson's disease: mechanisms and models. Neuron 39:889-909.

Dauer W, Kholodilov N, Vila M, Trillat AC, Goodchild R, Larsen KE, Staal R, Tieu K, Schmitz Y, Yuan CA, Rocha M, Jackson-Lewis V, Hersch S, Sulzer D, Przedborski S, Burke R, Hen R (2002) Resistance of alpha -synuclein null mice to the parkinsonian neurotoxin MPTP. Proc Natl Acad Sci U S A 99:14524-14529.

Davey GP, Clark JB (1996) Threshold effects and control of oxidative phosphorylation in nonsynaptic rat brain mitochondria. J Neurochem 66:1617-1624.

Davidson WS, Jonas A, Clayton DF, George JM (1998) Stabilization of alpha-synuclein secondary structure upon binding to synthetic membranes. J Biol Chem 273:9443-9449.

Day BJ, Patel M, Calavetta L, Chang LY, Stamler JS (1999) A mechanism of paraquat toxicity involving nitric oxide synthase. Proc Natl Acad Sci U S A 96:12760-12765.

Dearry A, Gingrich JA, Falardeau P, Fremeau RT, Jr., Bates MD, Caron MG (1990) Molecular cloning and expression of the gene for a human D1 dopamine receptor. Nature 347:72-76.

Demarest KT, Moore KE (1979a) Lack of a high affinity transport system for dopamine in the median eminence and posterior pituitary. Brain Res 171:545-551.

Demarest KT, Moore KE (1979b) Comparison of dopamine synthesis regulation in the terminals of nigrostriatal, mesolimbic, tuberoinfundibular and tuberohypophyseal neurons. J Neural Transm 46:263-277.

DeMaria JE, Lerant AA, Freeman ME (1999) Prolactin activates all three populations of hypothalamic neuroendocrine dopaminergic neurons in ovariectomized rats. Brain Res 837:236-241.

Dexter DT, Carter CJ, Wells FR, Javoy-Agid F, Agid Y, Lees A, Jenner P, Marsden CD (1989) Basal lipid peroxidation in substantia nigra is increased in Parkinson's disease. J Neurochem 52:381-389.

Dexter DT, Holley AE, Flitter WD, Slater TF, Wells FR, Daniel SE, Lees AJ, Jenner P, Marsden CD (1994) Increased levels of lipid hydroperoxides in the parkinsonian substantia nigra: an HPLC and ESR study. Mov Disord 9:92-97.

Di Chiara G, Tanda G, Carboni E (1996) Estimation of in-vivo neurotransmitter release by brain microdialysis: the issue of validity. Behav Pharmacol 7:640-657.

Di Monte DA, Tokar I, Langston JW (1999) Impaired glutamate clearance as a consequence of energy failure caused by MPP(+) in astrocytic cultures. Toxicol Appl Pharmacol 158:296-302.

Dicker E, Cederbaum AI (1991) NADH-dependent generation of reactive oxygen species by microsomes in the presence of iron and redox cycling agents. Biochem Pharmacol 42:529-535.

Dringen R, Gutterer JM, Hirrlinger J (2000) Glutathione metabolism in brain metabolic interaction between astrocytes and neurons in the defense against reactive oxygen species. Eur J Biochem 267:4912-4916.

Drolet RE, Behrouz B, Lookingland KJ, Goudreau JL (2004) Mice lacking alpha-synuclein have an attenuated loss of striatal dopamine following prolonged chronic MPTP administration. Neurotoxicology 25:761-769.

Dunkley PR, Bobrovskaya L, Graham ME, von Nagy-Felsobuki EI, Dickson PW (2004) Tyrosine hydroxylase phosphorylation: regulation and consequences. J Neurochem 91:1025-1043.

Eaton MJ, Tian Y, Lookingland KJ, Moore KE (1992) Comparison of the effects of remoxipride and raclopride on nigrostriatal and mesolimbic dopaminergic neuronal activity and on the secretion of prolactin and alpha-melanocyte-stimulating hormone. Neuropsychopharmacology 7:205-211.

Ebadi M, Sharma SK, Ghafourifar P, Brown-Borg H, El Refaey H (2005) Peroxynitrite in the pathogenesis of Parkinson's disease and the neuroprotective role of metallothioneins. Methods Enzymol 396:276-298.

Ehringer H, Hornykiewicz, O (1960) Klin Wschr 38:1236.

Fairbrother IS, Arbuthnott GW, Kelly JS, Butcher SP (1990a) In vivo mechanisms underlying dopamine release from rat nigrostriatal terminals: I. Studies using veratrine and ouabain. J Neurochem 54:1834-1843.

Fairbrother IS, Arbuthnott GW, Kelly JS, Butcher SP (1990b) In vivo mechanisms underlying dopamine release from rat nigrostriatal terminals: II. Studies using potassium and tyramine. J Neurochem 54:1844-1851.

Fall PA, Axelson O, Fredriksson M, Hansson G, Lindvall B, Olsson JE, Granerus AK (1996) Age-standardized incidence and prevalence of Parkinson's disease in a Swedish community. J Clin Epidemiol 49:637-641.

Feany MB, Bender WW (2000) A Drosophila model of Parkinson's disease. Nature 404:394-398.

Fearnley JM, Lees AJ (1991) Ageing and Parkinson's disease: substantia nigra regional selectivity. Brain 114 (Pt 5):2283-2301.

Felten DL, Felten SY, Fuller RW, Romano TD, Smalstig EB, Wong DT, Clemens JA (1992) Chronic dietary pergolide preserves nigrostriatal neuronal integrity in aged-Fischer-344 rats. Neurobiol Aging 13:339-351.

Fornai F, Schluter OM, Lenzi P, Gesi M, Ruffoli R, Ferrucci M, Lazzeri G, Busceti CL, Pontarelli F, Battaglia G, Pellegrini A, Nicoletti F, Ruggieri S, Paparelli A, Sudhof TC (2005) Parkinson-like syndrome induced by continuous MPTP infusion: convergent roles of the ubiquitin-proteasome system and alpha-synuclein. Proc Natl Acad Sci U S A 102:3413-3418.

Freed C, Revay R, Vaughan RA, Kriek E, Grant S, Uhl GR, Kuhar MJ (1995) Dopamine transporter immunoreactivity in rat brain. J Comp Neurol 359:340-349.

Frielingsdorf H, Schwarz K, Brundin P, Mohapel P (2004) No evidence for new dopaminergic neurons in the adult mammalian substantia nigra. Proc Natl Acad Sci U S A 101:10177-10182.

Gahn LG, Roskoski R, Jr. (1995) Thermal stability and CD analysis of rat tyrosine hydroxylase. Biochemistry 34:252-256.

George JM, Jin H, Woods WS, Clayton DF (1995) Characterization of a novel protein regulated during the critical period for song learning in the zebra finch. Neuron 15:361-372.

German DC, Manaye K, Smith WK, Woodward DJ, Saper CB (1989) Midbrain dopaminergic cell loss in Parkinson's disease: computer visualization. Ann Neurol 26:507-514.

Giasson BI, Duda JE, Quinn SM, Zhang B, Trojanowski JQ, Lee VM (2002) Neuronal alpha-synucleinopathy with severe movement disorder in mice expressing A53T human alpha-synuclein. Neuron 34:521-533.

Goldberg MS, Pisani A, Haburcak M, Vortherms TA, Kitada T, Costa C, Tong Y, Martella G, Tscherter A, Martins A, Bernardi G, Roth BL, Pothos EN, Calabresi P, Shen J (2005) Nigrostriatal dopaminergic deficits and hypokinesia caused by inactivation of the familial Parkinsonism-linked gene DJ-1. Neuron 45:489-496.

Gopalan C, Tian Y, Moore KE, Lookingland KJ (1993) Neurochemical evidence that the inhibitory effect of galanin on tuberoinfundibular dopamine neurons is activity dependent. Neuroendocrinology 58:287-293.

Graham DG (1978) Oxidative pathways for catecholamines in the genesis of neuromelanin and cytotoxic quinones. Mol Pharmacol 14:633-643.

Graham DG, Tiffany SM, Bell WR, Jr., Gutknecht WF (1978) Autoxidation versus covalent binding of quinones as the mechanism of toxicity of dopamine, 6-hydroxydopamine, and related compounds toward C1300 neuroblastoma cells in vitro. Mol Pharmacol 14:644-653.

Greene JC, Whitworth AJ, Kuo I, Andrews LA, Feany MB, Pallanck LJ (2003) Mitochondrial pathology and apoptotic muscle degeneration in Drosophila parkin mutants. Proc Natl Acad Sci U S A 100:4078-4083.

Gudelsky GA, Moore EK (1976) Differential drug effects on dopamine concentrations and rates of turnover in the median eminence, olfactory tubercle and corpus striatum. J Neural Transm 38:95-105.

Haavik J, Martinez A, Flatmark T (1990) pH-dependent release of catecholamines from tyrosine hydroxylase and the effect of phosphorylation of Ser-40. FEBS Lett 262:363-365.

Haavik J, Le Bourdelles B, Martinez A, Flatmark T, Mallet J (1991) Recombinant human tyrosine hydroxylase isozymes. Reconstitution with iron and inhibitory effect of other metal ions. Eur J Biochem 199:371-378.

Haavik J, Schelling DL, Campbell DG, Andersson KK, Flatmark T, Cohen P (1989) Identification of protein phosphatase 2A as the major tyrosine hydroxylase phosphatase in adrenal medulla and corpus striatum: evidence from the effects of okadaic acid. FEBS Lett 251:36-42.

Hall H, Kohler C, Gawell L, Farde L, Sedvall G (1988) Raclopride, a new selective ligand for the dopamine-D2 receptors. Prog Neuropsychopharmacol Biol Psychiatry 12:559-568.

Halloran SM, Vulliet PR (1994) Microtubule-associated protein kinase-2 phosphorylates and activates tyrosine hydroxylase following depolarization of bovine adrenal chromaffin cells. J Biol Chem 269:30960-30965.

Haycock JW (1990) Phosphorylation of tyrosine hydroxylase in situ at serine 8, 19, 31, and 40. J Biol Chem 265:11682-11691.

Haycock JW, Ahn NG, Cobb MH, Krebs EG (1992) ERK1 and ERK2, two microtubule-associated protein 2 kinases, mediate the phosphorylation of tyrosine hydroxylase at serine-31 in situ. Proc Natl Acad Sci U S A 89:2365-2369.

Heikkila RE, Cohen G (1973) 6-Hydroxydopamine: evidence for superoxide radical as an oxidative intermediate. Science 181:456-457.

Herrero MT, Barcia C, Navarro JM (2002) Functional anatomy of thalamus and basal ganglia. Childs Nerv Syst 18:386-404.

Herve D, Levi-Strauss M, Marey-Semper I, Verney C, Tassin JP, Glowinski J, Girault JA (1993) G(olf) and Gs in rat basal ganglia: possible involvement of G(olf) in the coupling of dopamine D1 receptor with adenylyl cyclase. J Neurosci 13:2237-2248.

Hilker R, Schweitzer K, Coburger S, Ghaemi M, Weisenbach S, Jacobs AH, Rudolf J, Herholz K, Heiss WD (2005) Nonlinear progression of Parkinson disease as determined by serial positron emission tomographic imaging of striatal fluorodopa F 18 activity. Arch Neurol 62:378-382.

Hoglinger GU, Feger J, Prigent A, Michel PP, Parain K, Champy P, Ruberg M, Oertel WH, Hirsch EC (2003) Chronic systemic complex I inhibition induces a hypokinetic multisystem degeneration in rats. J Neurochem 84:491-502.

Hornykiewicz O (1963) Wien lin Wsch 75:309.

Hornykiewicz O (1972) Research Publication of the Association for Research in Nervous and Mental Disease 50:390.

Hornykiewicz O (1975) Brain monoamines and parkinsonism. Natl Inst Drug Abuse Res Monogr Ser:13-21.

Hornykiewicz O (1998) Biochemical aspects of Parkinson's disease. Neurology 51:S2-9.

Howard SG, Feigenbaum JJ (1997) Effect of gamma-hydroxybutyrate on central dopamine release in vivo. A microdialysis study in awake and anesthetized animals. Biochem Pharmacol 53:103-110.

Imperato A, Di Chiara G (1988) Effects of locally applied D-1 and D-2 receptor agonists and antagonists studied with brain dialysis. Eur J Pharmacol 156:385-393.

Imperato A, Mulas A, Di Chiara G (1987) The D-1 antagonist SCH 23390 stimulates while the D-1 agonist SKF 38393 fails to affect dopamine release in the dorsal caudate of freely moving rats. Eur J Pharmacol 142:177-181.

Jackson-Lewis V, Jakowec M, Burke RE, Przedborski S (1995) Time course and morphology of dopaminergic neuronal death caused by the neurotoxin 1-methyl-4-phenyl-1,2,3,6-tetrahydropyridine. Neurodegeneration 4:257-269.

Jackson DM, Westlind-Danielsson A (1994) Dopamine receptors: molecular biology, biochemistry and behavioural aspects. Pharmacol Ther 64:291-370.

Jackson DM, Johansson C, Lindgren LM, Bengtsson A (1994) Dopamine receptor antagonists block amphetamine and phencyclidine-induced motor stimulation in rats. Pharmacol Biochem Behav 48:465-471.

Jakes R, Spillantini MG, Goedert M (1994) Identification of two distinct synucleins from human brain. FEBS Lett 345:27-32.

Jakowec MW, Nixon K, Hogg E, McNeill T, Petzinger GM (2004) Tyrosine hydroxylase and dopamine transporter expression following 1-methyl-4-phenyl-1,2,3,6-tetrahydropyridine-induced neurodegeneration of the mouse nigrostriatal pathway. J Neurosci Res 76:539-550.

Jenco JM, Rawlingson A, Daniels B, Morris AJ (1998) Regulation of phospholipase D2: selective inhibition of mammalian phospholipase D isoenzymes by alpha- and beta-synucleins. Biochemistry 37:4901-4909.

Jenner P, Olanow CW (1996) Oxidative stress and the pathogenesis of Parkinson's disease. Neurology 47:S161-170.

Jeon BS, Jackson-Lewis V, Burke RE (1995) 6-Hydroxydopamine lesion of the rat substantia nigra: time course and morphology of cell death. Neurodegeneration 4:131-137.

Jo E, McLaurin J, Yip CM, St George-Hyslop P, Fraser PE (2000) alpha-Synuclein membrane interactions and lipid specificity. J Biol Chem 275:34328-34334.

Joh TH, Park DH, Reis DJ (1978) Direct phosphorylation of brain tyrosine hydroxylase by cyclic AMP-dependent protein kinase: mechanism of enzyme activation. Proc Natl Acad Sci U S A 75:4744-4748.

Johannessen JN, Sobotka TJ, Weise VK, Markey SP (1991) Prolonged alterations in canine striatal dopamine metabolism following subtoxic doses of 1-methyl-4-phenyl-1,2,3,6-tetrahydropyridine (MPTP) and 4'-amino-MPTP are linked to the persistence of pyridinium metabolites. J Neurochem 57:981-990.

Kaji R (2001) Basal ganglia as a sensory gating devise for motor control. J Med Invest 48:142-146.

Kandel E, Schwartz, JH, Jessell, TM (1991) Principles of Neural Science.542-543.

Kehr W, Carlsson A, Lindqvist M, Magnusson T, Atack C (1972) Evidence for a receptor-mediated feedback control of striatal tyrosine hydroxylase activity. J Pharm Pharmacol 24:744-747.

Kilbourn MR, Kuszpit K, Sherman P (2000) Rapid and differential losses of in vivo dopamine transporter (DAT) and vesicular monoamine transporter (VMAT2) radioligand binding in MPTP-treated mice. Synapse 35:250-255.

Kilty JE, Lorang D, Amara SG (1991) Cloning and expression of a cocaine-sensitive rat dopamine transporter. Science 254:578-579.

Kimmel HL, Joyce AR, Carroll FI, Kuhar MJ (2001) Dopamine D1 and D2 receptors influence dopamine transporter synthesis and degradation in the rat. J Pharmacol Exp Ther 298:129-140.

Kitada T, Asakawa S, Hattori N, Matsumine H, Yamamura Y, Minoshima S, Yokochi M, Mizuno Y, Shimizu N (1998) Mutations in the parkin gene cause autosomal recessive juvenile parkinsonism. Nature 392:605-608.

Knoll J (1986) The pharmacology of (-)deprenyl. J Neural Transm Suppl 22:75-89.

Koeltzow TE, Xu M, Cooper DC, Hu XT, Tonegawa S, Wolf ME, White FJ (1998) Alterations in dopamine release but not dopamine autoreceptor function in dopamine D3 receptor mutant mice. J Neurosci 18:2231-2238.

Krack P, Benazzouz A, Pollak P, Limousin P, Piallat B, Hoffmann D, Xie J, Benabid AL (1998) Treatment of tremor in Parkinson's disease by subthalamic nucleus stimulation. Mov Disord 13:907-914.

Kruger R, Kuhn W, Muller T, Woitalla D, Graeber M, Kosel S, Przuntek H, Epplen JT, Schols L, Riess O (1998) Ala30Pro mutation in the gene encoding alpha-synuclein in Parkinson's disease. Nat Genet 18:106-108.

Kumer SC, Vrana KE (1996) Intricate regulation of tyrosine hydroxylase activity and gene expression. J Neurochem 67:443-462.

Lamensdorf I, Eisenhofer G, Harvey-White J, Hayakawa Y, Kirk K, Kopin IJ (2000) Metabolic stress in PC12 cells induces the formation of the endogenous dopaminergic neurotoxin, 3,4-dihydroxyphenylacetaldehyde. J Neurosci Res 60:552-558.

Lange KW, Rausch WD, Gsell W, Naumann M, Oestreicher E, Riederer P (1994) Neuroprotection by dopamine agonists. J Neural Transm Suppl 43:183-201.

Langston JW, Forno LS (1978) The hypothalamus in Parkinson disease. Ann Neurol 3:129-133.

Langston JW, Ballard P, Tetrud JW, Irwin I (1983) Chronic Parkinsonism in humans due to a product of meperidine-analog synthesis. Science 219:979-980.

Lau YS, Trobough KL, Crampton JM, Wilson JA (1990) Effects of probenecid on striatal dopamine depletion in acute and long-term 1-methyl-4-phenyl-1,2,3,6-tetrahydropyridine (MPTP)-treated mice. Gen Pharmacol 21:181-187.

Lavoie B, Smith Y, Parent A (1989) Dopaminergic innervation of the basal ganglia in the squirrel monkey as revealed by tyrosine hydroxylase immunohistochemistry. J Comp Neurol 289:36-52.

LaVoie MJ, Hastings TG (1999a) Peroxynitrite- and nitrite-induced oxidation of dopamine: implications for nitric oxide in dopaminergic cell loss. J Neurochem 73:2546-2554.

LaVoie MJ, Hastings TG (1999b) Dopamine quinone formation and protein modification associated with the striatal neurotoxicity of methamphetamine: evidence against a role for extracellular dopamine. J Neurosci 19:1484-1491.

Lazar MA, Truscott RJ, Raese JD, Barchas JD (1981) Thermal denaturation of native striatal tyrosine hydroxylase: increased thermolability of the phosphorylated form of the enzyme. J Neurochem 36:677-682.

Lee MK, Stirling W, Xu Y, Xu X, Qui D, Mandir AS, Dawson TM, Copeland NG, Jenkins NA, Price DL (2002) Human alpha-synuclein-harboring familial Parkinson's disease-linked Ala-53 --> Thr mutation causes neurodegenerative disease with alpha-synuclein aggregation in transgenic mice. Proc Natl Acad Sci U S A 99:8968-8973.

Legros H, Dingeval MG, Janin F, Costentin J, Bonnet JJ (2004) Toxicity of a treatment associating dopamine and disulfiram for catecholaminergic neuroblastoma SH-SY5Y cells: relationships with 3,4-dihydroxyphenylacetaldehyde formation. Neurotoxicology 25:365-375.

Leng Y, Chase TN, Bennett MC (2001) Muscarinic receptor stimulation induces translocation of an alpha-synuclein oligomer from plasma membrane to a light vesicle fraction in cytoplasm. J Biol Chem 276:28212-28218.

Leviel V, Guibert B, Mallet J, Faucon-Biguet N (1991) Induction of tyrosine hydroxylase in the rat substantia nigra by local injection of forskolin. J Neurosci Res 30:427-432.

Levitt M, Spector S, Sjoerdsma A, Udenfriend S (1965) Elucidation Of The Rate-Limiting Step In Norepinephrine Biosynthesis In The Perfused Guinea-Pig Heart. J Pharmacol Exp Ther 148:1-8.

Lindley SE, Gunnet JW, Lookingland KJ, Moore KE (1990) 3,4-Dihydroxyphenylacetic acid concentrations in the intermediate lobe and neural lobe of the posterior pituitary gland as an index of tuberohypophysial dopaminergic neuronal activity. Brain Res 506:133-138.

Liochev SI, Fridovich I (1994) Paraquat diaphorases in Escherichia coli. Free Radic Biol Med 16:555-559.

Liochev SI, Hausladen A, Beyer WF, Jr., Fridovich I (1994) NADPH: ferredoxin oxidoreductase acts as a paraquat diaphorase and is a member of the soxRS regulon. Proc Natl Acad Sci U S A 91:1328-1331.

Liou HH, Tsai MC, Chen CJ, Jeng JS, Chang YC, Chen SY, Chen RC (1997) Environmental risk factors and Parkinson's disease: a case-control study in Taiwan. Neurology 48:1583-1588.

Lloyd KG, Davidson L, Hornykiewicz O (1975) The neurochemistry of Parkinson's disease: effect of L-dopa therapy. J Pharmacol Exp Ther 195:453-464.

Lookingland KJ, Moore KE (1984) Dopamine receptor-mediated regulation of incertohypothalamic dopaminergic neurons in the male rat. Brain Res 304:329-338.

Lee MK, Shining W, Xu Y, Xu X, Qui D, Mandir AS, Dawson TM. Copeland NG, Jenkins NA, Price DL (2002) Human alpha-synuclein-harboring familial Parkinson's disease-linked Ala-53 --> Thr mutation causes neurodegenerative disease with alpha-synuclein aggregation in transgenic mice. Proc Natl Acad Sci U S A 99:8968-8973.

Lepore H, Dingeval MG, Jurin P, Costentin J, Bonnet JJ (2001) Toxicity of a treatment associating dopamine and disulfiram for catecholaminergic neuroblastoma SH-SY5Y cells: relationships with 3,4-dihydroxyphenylacetaldehyde formation. Neurotoxicology 22:365-375.

Leng Y, Chase TN, Bennett MC (2001) Muscarinic receptor stimulation induces translocation of an alpha-synuclein oligomer from plasma membrane to a light vesicle fraction in cytoplasm. J Biol Chem 276:28212-28218.

Levivier V, Guiben B, Mallet J, Passon-Bigeat N (1991) Induction of tyrosine hydroxylase in the rat substantia nigra by local injection of forskolin. J Neurosci Res 30:127-132.

Levitt M, Spector S, Sjoerdsma A, Udenfriend S (1965) Elucidation Of The Rate-Limiting Step In Norepinephrine Biosynthesis In The Perfused Guinea-Pig Heart. J Pharmacol Exp Ther 148:1-8.

Lindley SE, Ouatas TW, Lookingland KJ, Moore KE (1999) 3,4-Dihydroxyphenylacetic acid concentrations in the intermediate lobe and neural lobe of the posterior pituitary gland as an index of tuberohypophysial dopaminergic neuronal activity. Brain Res 806:133-138.

Locsher SJ, Fridovich I (1994) Paraquat diaphorases in Escherichia coli. Free Radic Biol Med 16:555-559.

Locsher SJ, Hunsaker A, Beyer WF, Jr., Fridovich I (1994) NADPH: flavodoxin oxidoreductase acts as a paraquat diaphorase and is a member of the soxRS regulon. Proc Natl Acad Sci U S A 91:1328-1331.

Lou HH, Tsai MC, Chen CJ, Jeng JS, Chang YC, Chen SY, Chen RC (1997) Environmental risk factors and Parkinson's disease: a case-control study in Taiwan. Neurology 48:1583-1588.

Lloyd KG, Davidson L, Hornykiewicz O (1975) The neurochemistry of Parkinson's disease: effect of L-dopa therapy. J Pharmacol Exp Ther 195:453-464.

Lookingland KJ, Moore KE (1984) Dopamine receptor-mediated regulation of incerhohypothalamic dopaminergic neurons in the male rat. Brain Res 304:329-338.

Lookingland KJ, Moore K.E. (2005) Functional neuroanatomy of hypothalamic dopaminergic neuroendocrine systems. In: Handbook of Chemical Neuroanatomy. Dunnett SB, Bentivoglio M, Björklund A, Hökfelt T:p.433-521.

Lorang D, Amara SG, Simerly RB (1994) Cell-type-specific expression of catecholamine transporters in the rat brain. J Neurosci 14:4903-4914.

Lotharius J, O'Malley KL (2000) The parkinsonism-inducing drug 1-methyl-4-phenylpyridinium triggers intracellular dopamine oxidation. A novel mechanism of toxicity. J Biol Chem 275:38581-38588.

Lotharius J, Brundin P (2002) Impaired dopamine storage resulting from alpha-synuclein mutations may contribute to the pathogenesis of Parkinson's disease. Hum Mol Genet 11:2395-2407.

Lovenberg W, Bruckwick EA (1975) Molecular mechanisms in the receptor-mediated regulation of tyrosine hydroxylase. Psychopharmacol Bull 11:11-12.

Lowry OH, Rosebrough NJ, Farr AL, Randall RJ (1951) Protein measurement with the Folin phenol reagent. J Biol Chem 193:265-275.

Lozano AM, Lang AE, Galvez-Jimenez N, Miyasaki J, Duff J, Hutchinson WD, Dostrovsky JO (1995) Effect of GPi pallidotomy on motor function in Parkinson's disease. Lancet 346:1383-1387.

Luthman J, Fredriksson A, Sundstrom E, Jonsson G, Archer T (1989) Selective lesion of central dopamine or noradrenaline neuron systems in the neonatal rat: motor behavior and monoamine alterations at adult stage. Behav Brain Res 33:267-277.

Manning-Bog AB, McCormack AL, Li J, Uversky VN, Fink AL, Di Monte DA (2002) The herbicide paraquat causes up-regulation and aggregation of alpha-synuclein in mice: paraquat and alpha-synuclein. J Biol Chem 277:1641-1644.

Markey SP, Johannessen JN, Chiueh CC, Burns RS, Herkenham MA (1984) Intraneuronal generation of a pyridinium metabolite may cause drug-induced parkinsonism. Nature 311:464-467.

Masliah E, Rockenstein E, Veinbergs I, Mallory M, Hashimoto M, Takeda A, Sagara Y, Sisk A, Mucke L (2000) Dopaminergic loss and inclusion body formation in alpha-synuclein mice: implications for neurodegenerative disorders. Science 287:1265-1269.

Matsuoka Y, Vila M, Lincoln S, McCormack A, Picciano M, LaFrancois J, Yu X, Dickson D, Langston WJ, McGowan E, Farrer M, Hardy J, Duff K, Przedborski S, Di Monte DA (2001) Lack of nigral pathology in transgenic mice expressing human alpha-synuclein driven by the tyrosine hydroxylase promoter. Neurobiol Dis 8:535-539.

Mayeux R, Marder K, Cote LJ, Denaro J, Hemenegildo N, Mejia H, Tang MX, Lantigua R, Wilder D, Gurland B, et al. (1995) The frequency of idiopathic Parkinson's disease by age, ethnic group, and sex in northern Manhattan, 1988-1993. Am J Epidemiol 142:820-827.

McCallum SE, Parameswaran N, Perez XA, Bao S, McIntosh JM, Grady SR, Quik M (2006) Compensation in pre-synaptic dopaminergic function following nigrostriatal damage in primates. J Neurochem 96:960-972.

McCormack AL, Thiruchelvam M, Manning-Bog AB, Thiffault C, Langston JW, Cory-Slechta DA, Di Monte DA (2002) Environmental risk factors and Parkinson's disease: selective degeneration of nigral dopaminergic neurons caused by the herbicide paraquat. Neurobiol Dis 10:119-127.

McLean PJ, Ribich S, Hyman BT (2000) Subcellular localization of alpha-synuclein in primary neuronal cultures: effect of missense mutations. J Neural Transm Suppl:53-63.

Meiergerd SM, Patterson TA, Schenk JO (1993) D2 receptors may modulate the function of the striatal transporter for dopamine: kinetic evidence from studies in vitro and in vivo. J Neurochem 61:764-767.

Melamed E, Hefti F, Wurtman RJ (1980) Tyrosine administration increases striatal dopamine release in rats with partial nigrostriatal lesions. Proc Natl Acad Sci U S A 77:4305-4309.

Millan MJ, Newman-Tancredi A, Brocco M, Gobert A, Lejeune F, Audinot V, Rivet JM, Schreiber R, Dekeyne A, Spedding M, Nicolas JP, Peglion JL (1998) S 18126 ([2-[4-(2,3-dihydrobenzo[1,4]dioxin-6-yl)piperazin-1-yl methyl]indan-2-yl]), a potent, selective and competitive antagonist at dopamine D4 receptors: an in vitro and in vivo comparison with L 745,870 (3-(4-[4-chlorophenyl]piperazin-1-yl)methyl-1H-pyrrolo[2, 3b]pyridine) and raclopride. J Pharmacol Exp Ther 287:167-186.

Missale C, Nash SR, Robinson SW, Jaber M, Caron MG (1998) Dopamine receptors: from structure to function. Physiol Rev 78:189-225.

Mochizuki H, Goto K, Mori H, Mizuno Y (1996) Histochemical detection of apoptosis in Parkinson's disease. J Neurol Sci 137:120-123.

Monsma FJ, Jr., Mahan LC, McVittie LD, Gerfen CR, Sibley DR (1990) Molecular cloning and expression of a D1 dopamine receptor linked to adenylyl cyclase activation. Proc Natl Acad Sci U S A 87:6723-6727.

Moore KE, Demarest KT, Lookingland KJ (1987) Stress, prolactin and hypothalamic dopaminergic neurons. Neuropharmacology 26:801-808.

Morgan JI, Curran T (1989) Stimulus-transcription coupling in neurons: role of cellular immediate-early genes. Trends Neurosci 12:459-462.

Morrish PK, Rakshi JS, Bailey DL, Sawle GV, Brooks DJ (1998) Measuring the rate of progression and estimating the preclinical period of Parkinson's disease with [18F]dopa PET. J Neurol Neurosurg Psychiatry 64:314-319.

Nakajo S, Tsukada K, Omata K, Nakamura Y, Nakaya K (1993) A new brain-specific 14-kDa protein is a phosphoprotein. Its complete amino acid sequence and evidence for phosphorylation. Eur J Biochem 217:1057-1063.

Nicklas WJ, Vyas I, Heikkila RE (1985) Inhibition of NADH-linked oxidation in brain mitochondria by 1-methyl-4-phenyl-pyridine, a metabolite of the neurotoxin, 1-methyl-4-phenyl-1,2,5,6-tetrahydropyridine. Life Sci 36:2503-2508.

Novikova L, Garris BL, Garris DR, Lau YS (2006) Early signs of neuronal apoptosis in the substantia nigra pars compacta of the progressive neurodegenerative mouse 1-methyl-4-phenyl-1,2,3,6-tetrahydropyridine/probenecid model of Parkinson's disease. Neuroscience 140:67-76.

Okuno S, Fujisawa H (1985) A new mechanism for regulation of tyrosine 3-monooxygenase by end product and cyclic AMP-dependent protein kinase. J Biol Chem 260:2633-2635.

Oldendorf WH, Szabo J (1976) Amino acid assignment to one of three blood-brain barrier amino acid carriers. Am J Physiol 230:94-98.

Onali P, Olianas MC, Gessa GL (1985) Characterization of dopamine receptors mediating inhibition of adenylate cyclase activity in rat striatum. Mol Pharmacol 28:138-145.

Ostrerova N, Petrucelli L, Farrer M, Mehta N, Choi P, Hardy J, Wolozin B (1999) alpha-Synuclein shares physical and functional homology with 14-3-3 proteins. J Neurosci 19:5782-5791.

Otsuka M, Ichiya Y, Kuwabara Y, Hosokawa S, Sasaki M, Yoshida T, Fukumura T, Masuda K, Kato M (1996) Differences in the reduced 18F-Dopa uptakes of the caudate and the putamen in Parkinson's disease: correlations with the three main symptoms. J Neurol Sci 136:169-173.

Oxender DL, Christensen HN (1963) Distinct Mediating Systems For The Transport Of Neutral Amino Acids By The Ehrlich Cell. J Biol Chem 238:3686-3699.

Palacin M, Estevez R, Bertran J, Zorzano A (1998) Molecular biology of mammalian plasma membrane amino acid transporters. Physiol Rev 78:969-1054.

Palkovits M (1973) Isolated removal of hypothalamic or other brain nuclei of the rat. Brain Res 59:449-450.

Palkovits M (1978) Neurochemical anatomy of the neuroendocrine hypothalamus. Neurochemical anatomy of the hypothalamus. Bull Schweiz Akad Med Wiss 34:113-130.

Parent A, Hazrati LN (1993) Anatomical aspects of information processing in primate basal ganglia. Trends Neurosci 16:111-116.

Park J, Kim SY, Cha GH, Lee SB, Kim S, Chung J (2005) Drosophila DJ-1 mutants show oxidative stress-sensitive locomotive dysfunction. Gene 361:133-139.

Parkinson J (1817) An Essay on the Shaking Palsy. Medical Classics (1938) 2:10.

Pasinetti GM, Morgan DG, Johnson SA, Millar SL, Finch CE (1990) Tyrosine hydroxylase mRNA concentration in midbrain dopaminergic neurons is differentially regulated by reserpine. J Neurochem 55:1793-1799.

Pate BD, Kawamata T, Yamada T, McGeer EG, Hewitt KA, Snow BJ, Ruth TJ, Calne DB (1993) Correlation of striatal fluorodopa uptake in the MPTP monkey with dopaminergic indices. Ann Neurol 34:331-338.

Patlak CS, Blasberg RG, Fenstermacher JD (1983) Graphical evaluation of blood-to-brain transfer constants from multiple-time uptake data. J Cereb Blood Flow Metab 3:1-7.

Payami H, Zareparsi S (1998) Genetic epidemiology of Parkinson's disease. J Geriatr Psychiatry Neurol 11:98-106.

Perez RG, Hastings TG (2004) Could a loss of alpha-synuclein function put dopaminergic neurons at risk? J Neurochem 89:1318-1324.

Perez RG, Waymire JC, Lin E, Liu JJ, Guo F, Zigmond MJ (2002) A Role for alpha - Synuclein in the Regulation of Dopamine Biosynthesis. J Neurosci 22:3090-3099.

Pesah Y, Pham T, Burgess H, Middlebrooks B, Verstreken P, Zhou Y, Harding M, Bellen H, Mardon G (2004) Drosophila parkin mutants have decreased mass and cell size and increased sensitivity to oxygen radical stress. Development 131:2183-2194.

Petersen K, Olesen OF, Mikkelsen JD (1999) Developmental expression of alpha-synuclein in rat hippocampus and cerebral cortex. Neuroscience 91:651-659.

Petroske E, Meredith GE, Callen S, Totterdell S, Lau YS (2001) Mouse model of Parkinsonism: a comparison between subacute MPTP and chronic MPTP/probenecid treatment. Neuroscience 106:589-601.

Pirker W, Holler I, Gerschlager W, Asenbaum S, Zettinig G, Brucke T (2003) Measuring the rate of progression of Parkinson's disease over a 5-year period with beta-CIT SPECT. Mov Disord 18:1266-1272.

Polymeropoulos MH, Lavedan C, Leroy E, Ide SE, Dehejia A, Dutra A, Pike B, Root H, Rubenstein J, Boyer R, Stenroos ES, Chandrasekharappa S, Athanassiadou A, Papapetropoulos T, Johnson WG, Lazzarini AM, Duvoisin RC, Di Iorio G, Golbe LI, Nussbaum RL (1997) Mutation in the alpha-synuclein gene identified in families with Parkinson's disease. Science 276:2045-2047.

Przedborski S, Ischiropoulos H (2005) Reactive oxygen and nitrogen species: weapons of neuronal destruction in models of Parkinson's disease. Antioxid Redox Signal 7:685-693.

Przedborski S, Jackson-Lewis V, Naini AB, Jakowec M, Petzinger G, Miller R, Akram M (2001) The parkinsonian toxin 1-methyl-4-phenyl-1,2,3,6-tetrahydropyridine (MPTP): a technical review of its utility and safety. J Neurochem 76:1265-1274.

Ramsay RR, Krueger MJ, Youngster SK, Singer TP (1991) Evidence that the inhibition sites of the neurotoxic amine 1-methyl-4-phenylpyridinium (MPP+) and of the respiratory chain inhibitor piericidin A are the same. Biochem J 273(Pt 2):481-484.

Revay R, Vaughan R, Grant S, Kuhar MJ (1996) Dopamine transporter immunohistochemistry in median eminence, amygdala, and other areas of the rat brain. Synapse 22:93-99.

Reveron ME, Savelieva KV, Tillerson JL, McCormack AL, Di Monte DA, Miller GW (2002) L-DOPA does not cause neurotoxicity in VMAT2 heterozygote knockout mice. Neurotoxicology 23:611-619.

Ribeiro MJ, Vidailhet M, Loc'h C, Dupel C, Nguyen JP, Ponchant M, Dolle F, Peschanski M, Hantraye P, Cesaro P, Samson Y, Remy P (2002) Dopaminergic function and dopamine transporter binding assessed with positron emission tomography in Parkinson disease. Arch Neurol 59:580-586.

Richardson JR, Quan Y, Sherer TB, Greenamyre JT, Miller GW (2005) Paraquat neurotoxicity is distinct from that of MPTP and rotenone. Toxicol Sci 88:193-201.

Riederer P, Wuketich S (1976) Time course of nigrostriatal degeneration in parkinson's disease. A detailed study of influential factors in human brain amine analysis. J Neural Transm 38:277-301.

Rodriguez MC, Guridi OJ, Alvarez L, Mewes K, Macias R, Vitek J, DeLong MR, Obeso JA (1998) The subthalamic nucleus and tremor in Parkinson's disease. Mov Disord 13 Suppl 3:111-118.

Rosegay H (1944) Journal of Comparative Neurology 80:293.

Polymeropoulos MH, Lavedan C, Leroy E, Ide SE, Dehejia A, Dutra A, Pike B, Root H, Rubenstein J, Boyer R, Stenroos ES, Chandrasekharappa S, Athanassiadou A, Papapetropoulos T, Johnson WG, Lazzarini AM, Duvoisin RC, Di Iorio G, Golbe LI, Nussbaum RL (1997) Mutation in the alpha-synuclein gene identified in families with Parkinson's disease. Science 276:2045-2047.

Pramstaller P, Jackson-Lewis V, Naini AB, Jakowec M, Przedborski S, Miller R, Adams M (2001) The parkinsonian toxin 1-methyl-4-phenyl-1,2,3,6-tetrahydropyridine (MPTP): a technical review of its utility and safety. J Neurochem 76:1265-1274.

Ramsay RR, Kinemuchi MU, Youngster SK, Singer TP (1991) Evidence that the inhibition of the neurotoxic amine 1-methyl-4-phenylpyridinium (MPP+) and of the reversible chain inhibitor pirindolin A are the same. Biochim J 273(Pt 2):481-484.

Revuelta M, Solas M, Ramirez MJ, Matheu A (2015) Neuroprotective effects of the histamine H3 receptor antagonist DL76 in a mouse model of Alzheimer's disease. Neurobiol Aging 36:1-11.

Revuelta MP, Cadete-Leite A, Gerlach M, Hidalgo J, Zigmond MJ, Levin ED (1997) Neurochemical changes in striatum and hippocampus following 6-hydroxydopamine lesions of the substantia nigra in rats. Brain Res Bull 42:217-223.

Revuelta MP, Cadete-Leite A, Gerlach M, Hidalgo J, Zigmond MJ, Levin ED (1997) Neurochemical changes in striatum and hippocampus following 6-hydroxydopamine lesions of the substantia nigra in rats. Brain Res Bull 42:217-223.

Revuelta MP, Cadete-Leite A, Gerlach M, Hidalgo J, Zigmond MJ, Levin ED (1997) Neurochemical changes in striatum and hippocampus following 6-hydroxydopamine lesions of the substantia nigra in rats. Brain Res Bull 42:217-223.

Roskoski R, Jr., Wilgus H, Vrana KE (1990) Inactivation of tyrosine hydroxylase by pterin substrates following phosphorylation by cyclic AMP-dependent protein kinase. Mol Pharmacol 38:541-546.

Roth RH (1975) Gamma-hydroxybutyrate and control of dopaminergic neurons. Psychopharmacol Bull 11:57-58.

Schapira AH (2002) Neuroprotection and dopamine agonists. Neurology 58:S9-18.

Schapira AH, Cooper JM, Dexter D, Clark JB, Jenner P, Marsden CD (1990) Mitochondrial complex I deficiency in Parkinson's disease. J Neurochem 54:823-827.

Schluter OM, Fornai F, Alessandri MG, Takamori S, Geppert M, Jahn R, Sudhof TC (2003) Role of alpha-synuclein in 1-methyl-4-phenyl-1,2,3,6-tetrahydropyridine-induced parkinsonism in mice. Neuroscience 118:985-1002.

Schober A (2004) Classic toxin-induced animal models of Parkinson's disease: 6-OHDA and MPTP. Cell Tissue Res 318:215-224.

Sedelis M, Schwarting RK, Huston JP (2001) Behavioral phenotyping of the MPTP mouse model of Parkinson's disease. Behav Brain Res 125:109-125.

Shimada H, Hirai K, Simamura E, Pan J (1998) Mitochondrial NADH-quinone oxidoreductase of the outer membrane is responsible for paraquat cytotoxicity in rat livers. Arch Biochem Biophys 351:75-81.

Shimada S, Kitayama S, Walther D, Uhl G (1992) Dopamine transporter mRNA: dense expression in ventral midbrain neurons. Brain Res Mol Brain Res 13:359-362.

Shimizu K, Matsubara K, Ohtaki K, Shiono H (2003) Paraquat leads to dopaminergic neural vulnerability in organotypic midbrain culture. Neurosci Res 46:523-532.

Shimizu K, Ohtaki K, Matsubara K, Aoyama K, Uezono T, Saito O, Suno M, Ogawa K, Hayase N, Kimura K, Shiono H (2001) Carrier-mediated processes in blood--brain barrier penetration and neural uptake of paraquat. Brain Res 906:135-142.

Sian J, Dexter DT, Lees AJ, Daniel S, Jenner P, Marsden CD (1994) Glutathione-related enzymes in brain in Parkinson's disease. Ann Neurol 36:356-361.

Sibley DR (1999) New insights into dopaminergic receptor function using antisense and genetically altered animals. Annu Rev Pharmacol Toxicol 39:313-341.

Sidhu A, Wersinger C, Vernier P (2004) alpha-Synuclein regulation of the dopaminergic transporter: a possible role in the pathogenesis of Parkinson's disease. FEBS Lett 565:1-5.

Singleton AB, Farrer M, Johnson J, Singleton A, Hague S, Kachergus J, Hulihan M, Peuralinna T, Dutra A, Nussbaum R, Lincoln S, Crawley A, Hanson M, Maraganore D, Adler C, Cookson MR, Muenter M, Baptista M, Miller D, Blancato J, Hardy J, Gwinn-Hardy K (2003) alpha-Synuclein locus triplication causes Parkinson's disease. Science 302:841.

Slowiejko DM, McEwen EL, Ernst SA, Fisher SK (1996) Muscarinic receptor sequestration in SH-SY5Y neuroblastoma cells is inhibited when clathrin distribution is perturbed. J Neurochem 66:186-196.

Smeyne RJ, Jackson-Lewis V (2005) The MPTP model of Parkinson's disease. Brain Res Mol Brain Res 134:57-66.

Snyder GL, Keller RW, Jr., Zigmond MJ (1990) Dopamine efflux from striatal slices after intracerebral 6-hydroxydopamine: evidence for compensatory hyperactivity of residual terminals. J Pharmacol Exp Ther 253:867-876.

Sofic E, Lange KW, Jellinger K, Riederer P (1992) Reduced and oxidized glutathione in the substantia nigra of patients with Parkinson's disease. Neurosci Lett 142:128-130.

Sossi V, de la Fuente-Fernandez R, Holden JE, Schulzer M, Ruth TJ, Stoessl J (2004) Changes of dopamine turnover in the progression of Parkinson's disease as measured by positron emission tomography: their relation to disease-compensatory mechanisms. J Cereb Blood Flow Metab 24:869-876.

Sossi V, de La Fuente-Fernandez R, Holden JE, Doudet DJ, McKenzie J, Stoessl AJ, Ruth TJ (2002) Increase in dopamine turnover occurs early in Parkinson's disease: evidence from a new modeling approach to PET 18 F-fluorodopa data. J Cereb Blood Flow Metab 22:232-239.

Spillantini MG, Schmidt ML, Lee VM, Trojanowski JQ, Jakes R, Goedert M (1997) Alpha-synuclein in Lewy bodies. Nature 388:839-840.

Stachowiak MK, Keller RW, Jr., Stricker EM, Zigmond MJ (1987) Increased dopamine efflux from striatal slices during development and after nigrostriatal bundle damage. J Neurosci 7:1648-1654.

Sturtz F, Rollet D, Faucon Biguet N, Mallet J, Buda M (1994) Long-term alteration in tyrosine hydroxylase mRNA levels in rat locus coeruleus after intraventricular injection of 5,6-dihydroxytryptamine. Brain Res Mol Brain Res 22:107-112.

Sutherland C, Alterio J, Campbell DG, Le Bourdelles B, Mallet J, Haavik J, Cohen P (1993) Phosphorylation and activation of human tyrosine hydroxylase in vitro by mitogen-activated protein (MAP) kinase and MAP-kinase-activated kinases 1 and 2. Eur J Biochem 217:715-722.

Singleton AB, Farrer M, Johnson J, Singleton A, Hague S, Kachergus J, Hulihan M, Peuralinna T, Dutra A, Nussbaum R, Lincoln S, Crawley A, Hanson M, Maraganore D, Adler C, Cookson MR, Muenter M, Baptista M, Miller D, Blancato J, Hardy J, Gwinn-Hardy K (2003) alpha-Synuclein locus triplication causes Parkinson's disease. Science 302:841.

Slowikjo DM, Meßwen EI, Ernst SA, Fisher SK (1990) Muscarinic receptor sequestration in SH-SY5Y neuroblastoma cells is inhibited when chlorin diurethation is perturbed. J Neurochem 66:189-198.

Smeyne RJ, Jackson-Lewis V (2005) The MPTP model of Parkinson's disease. Brain Res Mol Brain Res 134:57-66.

Snyder GL, Keller RW, Jr., Zigmond MJ (1990) Dopamine efflux from striatal slices after intracerebral 6-hydroxydopamine: evidence for compensation by preserved of residual terminals. J Pharmacol Exp Ther 253:627-636.

Sohr E, Lange KW, Jellinger K, Riederer P (1990) Reduced and oxidized glutathione in the substantia nigra of patients with Parkinson's disease. Neurosci Lett 142:128-130.

Soni V, de la Fuente-Fernandez R, Holden JE, Sossi V, Ruth TJ, Stoessl J (2004) Changes of dopamine turnover in the progression of Parkinson's disease as measured by positron emission tomography: their relation to disease-compensatory mechanisms. J Cereb Blood Flow Metab 24:806-870.

Soni V, de La Fuente-Fernandez R, Holden JE, Fowler JE, McGeachy T, Stoessl AJ, Ruth TJ (2002) Increase in dopamine turnover occurs early in Parkinson's disease: evidence from a new modeling approach to PET 18 F-fluorodopa data. J Cereb Blood Flow Metab 22:232-239.

Spillantini MG, Schmidt ML, Lee VM, Trojanowski JQ, Jakes R, Goedert M (1997) Alpha-synuclein in Lewy bodies. Nature 388:839-840.

Stachowiak MK, Keller RW, Jr., Snyder EM, Zigmond MJ (1987) Increased dopamine efflux from striatal slices during development and after nigrostriatal bundle damage. J Neurosci 7:1648-1654.

Sturz F, Roller D, Benson Bignet N, Muller I, Bode M (1969) Long-term alteration in tyrosine hydroxylase mRNA levels in rat locus coeruleus after intraventricular injection of 5,6-dihydroxytryptamine. Brain Res Mol Brain Res 22:107-112.

Sutherland C, Alterio J, Campbell DG, Le Bourdellès B, Mallet J, Haavik J, Cohen P (1993) Phosphorylation and activation of human tyrosine hydroxylase in vitro by mitogen-activated protein (MAP) kinase and MAP-kinase-activated kinase 1 and 2. Eur J Biochem 217:715-722.

Sved A, Fernstrom J (1981) Tyrosine availability and dopamine synthesis in the striatum: studies with gamma-butyrolactone. Life Sci 29:743-748.

Sved AF, Fernstrom JD, Wurtman RJ (1979) Tyrosine administration decreases serum prolactin levels in chronically reserpinized rats. Life Sci 25:1293-1299.

Swerdlow RH, Parks JK, Miller SW, Tuttle JB, Trimmer PA, Sheehan JP, Bennett JP, Jr., Davis RE, Parker WD, Jr. (1996) Origin and functional consequences of the complex I defect in Parkinson's disease. Ann Neurol 40:663-671.

Takenouchi T, Hashimoto M, Hsu LJ, Mackowski B, Rockenstein E, Mallory M, Masliah E (2001) Reduced neuritic outgrowth and cell adhesion in neuronal cells transfected with human alpha-synuclein. Mol Cell Neurosci 17:141-150.

Talpade DJ, Greene JG, Higgins DS, Jr., Greenamyre JT (2000) In vivo labeling of mitochondrial complex I (NADH:ubiquinone oxidoreductase) in rat brain using [(3)H]dihydrorotenone. J Neurochem 75:2611-2621.

Tanner CM (1992) Occupational and environmental causes of parkinsonism. Occup Med 7:503-513.

Tatton NA, Kish SJ (1997) In situ detection of apoptotic nuclei in the substantia nigra compacta of 1-methyl-4-phenyl-1,2,3,6-tetrahydropyridine-treated mice using terminal deoxynucleotidyl transferase labelling and acridine orange staining. Neuroscience 77:1037-1048.

Thiffault C, Langston JW, Di Monte DA (2000) Increased striatal dopamine turnover following acute administration of rotenone to mice. Brain Res 885:283-288.

Thiruchelvam M, Brockel BJ, Richfield EK, Baggs RB, Cory-Slechta DA (2000) Potentiated and preferential effects of combined paraquat and maneb on nigrostriatal dopamine systems: environmental risk factors for Parkinson's disease? Brain Res 873:225-234.

Tzivion G, Luo Z, Avruch J (1998) A dimeric 14-3-3 protein is an essential cofactor for Raf kinase activity. Nature 394:88-92.

Ungerstedt U (1968) 6-Hydroxy-dopamine induced degeneration of central monoamine neurons. Eur J Pharmacol 5:107-110.

van der Putten H, Wiederhold KH, Probst A, Barbieri S, Mistl C, Danner S, Kauffmann S, Hofele K, Spooren WP, Ruegg MA, Lin S, Caroni P, Sommer B, Tolnay M, Bilbe G (2000) Neuropathology in mice expressing human alpha-synuclein. J Neurosci 20:6021-6029.

Vingerhoets FJ, Schulzer M, Ruth TJ, Holden JE, Snow BJ (1996) Reproducibility and discriminating ability of fluorine-18-6-fluoro-L-Dopa PET in Parkinson's disease. J Nucl Med 37:421-426.

Vingerhoets FJ, Snow BJ, Schulzer M, Morrison S, Ruth TJ, Holden JE, Cooper S, Calne DB (1994) Reproducibility of fluorine-18-6-fluorodopa positron emission tomography in normal human subjects. J Nucl Med 35:18-24.

Volkow ND, Wang GJ, Fowler JS, Logan J, Gatley SJ, MacGregor RR, Schlyer DJ, Hitzemann R, Wolf AP (1996) Measuring age-related changes in dopamine D2 receptors with 11C-raclopride and 18F-N-methylspiroperidol. Psychiatry Res 67:11-16.

Vrana KE, Roskoski R, Jr. (1983) Tyrosine hydroxylase inactivation following cAMP-dependent phosphorylation activation. J Neurochem 40:1692-1700.

Vrana KE, Allhiser CL, Roskoski R, Jr. (1981) Tyrosine hydroxylase activation and inactivation by protein phosphorylation conditions. J Neurochem 36:92-100.

Vulliet PR (1985) Direct activation of tyrosine hydroxylase by calmodulin. Proc West Pharmacol Soc 28:27-30.

Vulliet PR, Langan TA, Weiner N (1980) Tyrosine hydroxylase: a substrate of cyclic AMP-dependent protein kinase. Proc Natl Acad Sci U S A 77:92-96.

Vulliet PR, Woodgett JR, Cohen P (1984) Phosphorylation of tyrosine hydroxylase by calmodulin-dependent multiprotein kinase. J Biol Chem 259:13680-13683.

Westerink BH, Spaan SJ (1982) Simultaneous determination of the formation rate of dopamine and its metabolite 3,4-dihydroxyphenylacetic acid (DOPAC) in various rat brain areas. Brain Res 252:239-245.

Whetten-Goldstein K, Sloan F, Kulas E, Cutson T, Schenkman M (1997) The burden of Parkinson's disease on society, family, and the individual. J Am Geriatr Soc 45:844-849.

Widerlov E, Lewander T (1978) Inhibition of the in vivo biosynthesis and changes of catecholamine levels in rat brain after alpha-methyl-p-tyrosine; time- and dose-response relationships. Naunyn Schmiedebergs Arch Pharmacol 304:111-123.

Wilson JM, Kalasinsky KS, Levey AI, Bergeron C, Reiber G, Anthony RM, Schmunk GA, Shannak K, Haycock JW, Kish SJ (1996) Striatal dopamine nerve terminal markers in human, chronic methamphetamine users. Nat Med 2:699-703.

Wooten (1997) Functional anatomical and behavioral consequences of dopamine receptor stimulation. Ann N Y Acad Sci 835:153-156.

Yamauchi T, Fujisawa H (1979) In vitro phosphorylation of bovine adrenal tyrosine hydroxylase by adenosine 3':5'-monophosphate-dependent protein kinase. J Biol Chem 254:503-507.

Yamauchi T, Fujisawa H (1981) A calmodulin-dependent protein kinase that is involved in the activation of tryptophan 5-monooxygenase is specifically distributed in brain tissues. FEBS Lett 129:117-119.

Yee RE, Irwin I, Milonas C, Stout DB, Huang SC, Shoghi-Jadid K, Satyamurthy N, Delanney LE, Togasaki DM, Farahani KF, Delfani K, Janson AM, Phelps ME, Langston JW, Barrio JR (2001) Novel observations with FDOPA-PET imaging after early nigrostriatal damage. Mov Disord 16:838-848.

Yoritaka A, Hattori N, Uchida K, Tanaka M, Stadtman ER, Mizuno Y (1996) Immunohistochemical detection of 4-hydroxynonenal protein adducts in Parkinson disease. Proc Natl Acad Sci U S A 93:2696-2701.

Youdim MB, Gassen M, Gross A, Mandel S, Grunblatt E (2000) Iron chelating, antioxidant and cytoprotective properties of dopamine receptor agonist; apomorphine. J Neural Transm Suppl:83-96.

Zesiewicz TA, Hauser RA (2001) Phenomenology and treatment of tremor disorders. Neurol Clin 19:651-680, vii.

Zhou QY, Grandy DK, Thambi L, Kushner JA, Van Tol HH, Cone R, Pribnow D, Salon J, Bunzow JR, Civelli O (1990) Cloning and expression of human and rat D1 dopamine receptors. Nature 347:76-80.

Zigmond MJ (1997) Do compensatory processes underlie the preclinical phase of neurodegenerative disease? Insights from an animal model of parkinsonism. Neurobiol Dis 4:247-253.

Zigmond MJ, Stricker EM (1984) Parkinson's disease: studies with an animal model. Life Sci 35:5-18.

Zigmond MJ, Abercrombie ED, Stricker EM (1990) Partial damage to nigrostriatal bundle: compensatory changes and the action of L-dopa. J Neural Transm Suppl 29:217-232.

Zigmond MJ, Acheson AL, Stachowiak MK, Stricker EM (1984) Neurochemical compensation after nigrostriatal bundle injury in an animal model of preclinical parkinsonism. Arch Neurol 41:856-861.

MICHIGAN STATE UNIVERSITY LIBRARIES
3 1293 02845 5811